MAR 19990007: STEEPBANK RIVER

Received date: Mar 19, 1999

Public release date: Mar 20, 2000

DISCLAIMER
By accessing and using the Alberta Energy website to download or otherwise obtain a scanned mineral assessment report, you (“User”) agree to be bound by the following terms and conditions:

a) Each scanned mineral assessment report that is downloaded or otherwise obtained from Alberta Energy is provided “AS IS”, with no warranties or representations of any kind whatsoever from Her Majesty the Queen in Right of Alberta, as represented by the Minister of Energy (“Minister”), expressed or implied, including, but not limited to, no warranties or other representations from the Minister, regarding the content, accuracy, reliability, use or results from the use of or the integrity, completeness, quality or legibility of each such scanned mineral assessment report;
b) To the fullest extent permitted by applicable laws, the Minister hereby expressly disclaims, and is released from, liability and responsibility for all warranties and conditions, expressed or implied, in relation to each scanned mineral assessment report shown or displayed on the Alberta Energy website including but not limited to warranties as to the satisfactory quality of or the fitness of the scanned mineral assessment report for a particular purpose and warranties as to the non-infringement or other non-violation of the proprietary rights held by any third party in respect of the scanned mineral assessment report;
c) To the fullest extent permitted by applicable law, the Minister, and the Minister’s employees and agents, exclude and disclaim liability to the User for losses and damages of whatsoever nature and howsoever arising including, without limitation, any direct, indirect, special, consequential, punitive or incidental damages, loss of use, loss of data, loss caused by a virus, loss of income or profit, claims of third parties, even if Alberta Energy have been advised of the possibility of such damages or losses, arising out of or in connection with the use of the Alberta Energy website, including the accessing or downloading of the scanned mineral assessment report and the use for any purpose of the scanned mineral assessment report so downloaded or retrieved.
d) User agrees to indemnify and hold harmless the Minister, and the Minister’s employees and agents against and from any and all third party claims, losses, liabilities, demands, actions or proceedings related to the downloading, distribution, transmissions, storage, redistribution, reproduction or exploitation of each scanned mineral assessment report obtained by the User from Alberta Energy.

Alberta Mineral Assessment Reporting System

MIN9907
19990007

Steepbank River Permit

Permit no. #9396110048

ASSESSMENT REPORT

Authors:

Larry MacGougan
Debbie Puckett

March 10, 1998

19990007

Steepbank River Permit March 10, 1998

Table of Contents

Page

Page

Research Papers

INTRODUCTION

One Metallic and Industrial Mineral permit, totally 9216 hectares, land description of

4-08-090: 19-21; 28-33
4-08-091: 4-9; 16-21; 28-33
4-08-092: 4-9; 16-18

was staked in northeast Alberta for the purpose of prospecting. The permit was filed and registered on November 21, 1996 as Metallic Mineral Exploration Permit # 9396110048. Anniversary date is November 21, 1998 when renewal or downsizing is mandatory.

This regional land position was staked for surface collection, causing none to minimal surface distrubance in the course of recovery and work. Its location was ideal because of where it is situated within the Western Canada Sedimentary Basin (WCSB), its close proximity to the Suncor Mine, and the feasibility of shallow overburden in comparison to other areas where it is deep and encumbersome. The principal exploration objective was to find and record anomalous values of gold, silver, platinum, PGM's, and other metals in the overlying Clearwater shales, Cretaceous sands, and Devonian limestones. In order to better understand and deal with the mineralization, it was pertinent to examine the potential source rocks and investigate the complexities of why their metals can't be assayed, through geochemical study.

The regional geology and its history were studied by reading numerous reports, studies, scientific research from Geological Survey of Canada (GSC), so to continue work from what was learned from them. To date all exploration companies have had difficulties in assaying with the standard fire assay, were gold even could be impregnated into a sample, and then they could not get it back out. Until the assay problem is resolved an economical mineral deposit is controversial, so more work needed to be assessed towards mineralogy and its chemical makeup, than geology.

By processing and assaying samples certain minerals or metals can be lost or altered, and some persist through different treatments. In nature it is much the same, some chemical evolution, alternation, or geological mechanisms can change the environment and mineralization. In this area the mineralogy and the gold are predominatedly in native and/or salt form, and the metals have been enriched by some process to form a deposit. It is postulated low temperature saline brines flowed up along the fault systems precipitating out the mineral assemblage from solution when encountering an reducing environment. The reducing zones were in areas of high carbon content such as shales, bitumen-rich rocks, and in the overlying limestones. Working with the Au/Ag/Pt mineralization in the sedimentary rocks helped with the study in relationships between gold and discharging brines, gold brines and hydrocarbons.

Inconsistencies between assay methods are related to the presence of dispersed organic (hydrocarbons) material or bitumen in the rocks and the search for a reliable gold analysis of these organic-rich rocks has been a long and diligent hunt. With the salts vaporizing at about 600 degrees C, some of the gold, especially if it is in salt form, will vaporize during the fire assay process; and secondly when there is bitumen present and the samples are being crushed for assay, the gold could be selectively screened out or could vaporize with the bitumen, or even go into the slag, during the assay. So either way it explains why it could be lost.

Every mineral and metal being a chemical element, the use of chemicals was an essential and necessary tool in changing the composition of the ore, ridding certain unhomogeneous material by dissolving them, to make it more assayable. To further an attempt in understanding the chemistry of ore deposition carried out in nature, in determining the host mineralogy of the metals (sulphides, organic or clay?) or whatever rock or layer the fluids went through, in terms of alternation.

SUMMARY

In 1996 this Steepbank River permit was acquired for the purpose to collect and process samples for the potential of gold, platinum-group minerals, and for any other precious or base metal occurrences. This assessment report is mainly technical because of the many assay procedures involved, and the costs incurred are due to fieldwork, processing rocks, with follow-ups of extensive microinvestigative, analytical and mineral concentration testwork. The scope of fieldwork comprised of reconnaissance prospecting, stream sediment and glacier till sampling, orientation surveys of the land that has virtually been unexplored by mining companies and previous owners. Selective rock grabs of limestones with disseminated and veinlets of mineralization, bitumen-stained or sulfur-stained, and any other alternations were taken for leaching and roasting in the lab or interpretation. With many return visits to the area of primary interest for follow-up sampling and re-testing.

Stream sediments collected for panning showed no visible gold other than a few fine specks, with some specimens in the water floating, possibly gold coated with oil or carbon. The mineralization here doesn't seem to be as related to the faulting as it does to the carbons and hydrocarbons. Towards the north of the property there is more sulfurous (rusty) shale and green decalcified rock, and fewer pyrites.

The history of gold in the Fort McMurray and Athabasca area is it is found in microdisseminated, sediment-hosted deposits; and its gold grains can be scanned by a scanning electron microscope (SEM), but it can't be assayed. One of the biggest reasons gold doesn't assay properly is because it doesn't want to go into metallic form. The metal doesn't form into a metallic bead when certain other bonding elements are present, and in the instances were tellurium, sodium, sulfur, arsensic are involved the metal won't change unless they are removed. This is also complicated by the deterrence of carbon, iron and organic matter.

The interfering constituents have to be eliminated firstly either chemically and/or burned off prior to assaying. There are also probably many other metals besides them that could interfere, alter or hinder. Certain elements bond together and by being together it prevents a complete

recovery by conventional extraction techniques. With the gold and platinum, it was hard to get out of solution, it won't gather together and volatilizes easily. Native metals and complex alloys were commonly encountered. Another theory why the assaying is problematic is because gold is in a salt form or because it is finely disseminated in organic and carbonaceous material. Or just for the simple reason disseminated gold can't be assayed.

Extensive study, time and expense was allocated to the investigation of platinum and the platinum group, after Birch Mountain Mineral's impressive results of 2.21 and 4.94 grams per tonne over a 1.6 metre interval on Township 96, Range 10, W4. After many trips to the library searching for information regarding this precious metal, only scarce material would prove to be useful. Very little exploration and independent studies have been done strictly on platinum and the platinum group in Alberta, and the metal is usually found in placer deposits, not microdisseminated like the gold. When there are iron impurities present platinum can be weakly magnetic and it is almost always alloyed with iron, which poses the same problem of assaying as with the gold. When platinum is bonded with tellurium and sulfur it is not metallic and will not form into a lead bead. The reason for this is it might be in a salt form or perhaps it can't even go into metallic form. It inhibits the solid solution and in a complex solid solution high temperatures (in a hydrogen atmosphere) are needed to extract metal.

A standard lead fire assay is a method for collecting all the precious metals into a lead bead by oxidizing the base metals, semi-conductors and salts, etc. off, and then compelling and oxidizing the lead off without losing the metal. Platinum by itself could be assayed this way, but it can't be with the platinum group, and platinum always contains other members of its chemical group. All six metals (ruthenium, rhodium, palladium "light" specific gravities; osmium, iridium, platinum "heavy") with various molecules combined in the same metal act differently than platinum by itself. An example being rhodium and palladium alone join 1 to 1 with iron when firing, therefore the separation is hard. Not being fully separated, detection devices such as ICP and AA are distorted by the iron.

Unless the standard is changed platinum-group minerals are near impossible to assay accurately because of the many bonds they create with alternation. In assaying they either oxidize or volatile off; too much oxygen it either volatiles off or goes into the slag (it won't form a bead) PGM's need to break their bond, they're extremely easy to oxidize, readily more than gold and platinum by itself. When roasting to remove sulfur, arsenic, cerium, etc. PGM metals probably volitile off because their oxygen state changed or because of atmospheric conditions, or should of been done under reducing (direct flame) conditions and not oxidizing conditions (electric kiln). Over numerous chemical methods and metallurgical testwork by reducing organic matter the platinum was lost by roasting it too high, changing it to an oxide. Roasting samples over several hours resulted in increases in Au/Pt content due to breakdown, and likely to favorable atmospheric conditions. For the most part PGM's are chemically inert, have high electrical conductivity and serve as catalysts in many chemical reactions.

WORK PERFORMED

DATES

1996

Winter trips:

Dec 1-3;	3 days
Dec 7-9;	3 days

1997

Winter trips:

Jan 7-8;	2 days
Jan 18-20;	2 days
Feb 1-3;	3 days
Feb 16-18;	3 days
Mar 4-5;	2 days

Spring trips:

Mar 24-29;	6 days
April 2-4;	3 days
April 30-May 2;	3 days
May 5-9;	5 days
May 15-18;	4 days
May 23-28;	6 days
June 10-14;	5 days
Sept 7-9;	3 days

Summer trips:

June 25-30;	6 days
July 1-3;	3 days
July 9-12;	4 days
July 17-21;	5 days
Aug 1-7;	7 days

Fall trips:

Sept 23-26;	4 days
Oct 5-6;	2 days
Oct 11-14;	4 days
Nov 3-4;	2 days

In 1996 there was a total of 2 trips & 6 days to the field. All trips and days are divided in half for each permit.(Permit no.# 9396110048 with 1 trip/3 days. Permit no. #9396110050 with 1 trip/3 days.)

In 1997 there was a total of 22 trips & 84 days to the field.(Permit no. #9396110048 with 11 trips/24 days. Permit no. #9396110050 with 11 trips/24 days)

1998

Winter trips:

Feb 11-13; 3 days

Spring trips:

April 26-30; 5 days
May 5-8; 4 days
May 23-28; 6 days

Summer trips:

June 13-16; 4 days
June 21-27; 7 days
Aug 12-17; 6 days
Aug 20-25; 5 days
Aug 31-Sept 1; 2 days
Sept 12-15; 4 days

In 1998 there was a total of 10 trips & 46 days in the field.(Permit no. #9396110048 with 5 trips/ 23 days. Permit no. #9396110050 with 5 trips/23 days.)

1996 FIELDWORK

The first two trips to the area were to get an orientation to the geological setting; ground work for which areas held better potential for a mineral deposit. Initial exploratory work was mainly done by foot traverse and only a few samples were taken at this time.

1997 FIELDWORK

Winter & Spring Work:

The roads were passable for as long as the frost was in the ground and still freezing at night. Access was sometimes gained by skidoo. During this period sample collecting sites were chosen and an area reconnaissance was done on both permits. Also several regional surface samplings. Samples were obtained by either a shovel or a hand auger and anywhere there was an open pit or soil moved by a pipeline crossing.

Summer & Fall Work:

Roads weren't passable because of the muskeg. To get to the location of sites was either done by foot traverse or quad, depending on distance and weather conditions.

While in the field, rock samples and panned concentrates were collected. Those samples were later processed and assayed for gold and platinum. With the aid of a microscope, to detect mineralization of interest, it was important to examine and identify the accompanying heavy minerals. Samples of oddity, staining, mineralization and weight were all selectively chosen.

1998 FIELDWORK

Winter & Spring Work:

More trips were taken to the permits and surrounding areas to find rocks of the same type and texture. All rocks were put in a pail and tagged, smaller samples were bagged and labeled according to area and surface coordinates. Most of the work performed was surface soil sampling and collecting.

Summer Work:

Grab samples were taken from various spots along the rivers and streams. To evacuate deeper a hand auger (with an extension adjustment) was used, boring holes from six to sixteen feet deep depending on the density of the rock and soil beneath the vegetation and peat moss. Any oddity of land was sampled, in a search for outcroppings. Many of the rivers and streams were panned, their concentrates studied on a microscope, later dried and bottled.

LAB AND RESEARCH LABOUR

With 136 days (Nov 21/96 - Nov 21/98) in total in the field (68 days on permit no. #9396110048), the rest of the time was dedicated to lab work and research. A total of 190 days (95 days) was claimed for assessment.

After each trip to Fort McMurray and/or Fort McKay, the samples were taken back to Edmonton, where a small lab was sent up to process and test them. Many hours were spent on exploratory laboratory work, first with simple chemical tests to more complicated procedures, using various chemicals. Working on concentration and leaching equipments, searching for a method and answers to why the metals won't assay consistently, extreme care taken in not to expose samples to sources of metallic contamination prior to process, assay and examination.

A kiln was purchased to roast samples. Prior to that a torch was used.

Experimental and unexperimental samples were couriered to different labs to be assayed.

While results were awaited, time was utilized in the library (Alberta Energy) doing research or going to the university for assistance. Research information gathering consisted of map searches (faults,overburden,geology) theories on gold deposition, geochemistry of gold and platinum, Alberta Geological Survey material on Prairie-type sedimentary Au-Ag-Pt., etc.
At the University of Alberta instrumental analysis were performed.

STEEP BANK RIVER PERMIT

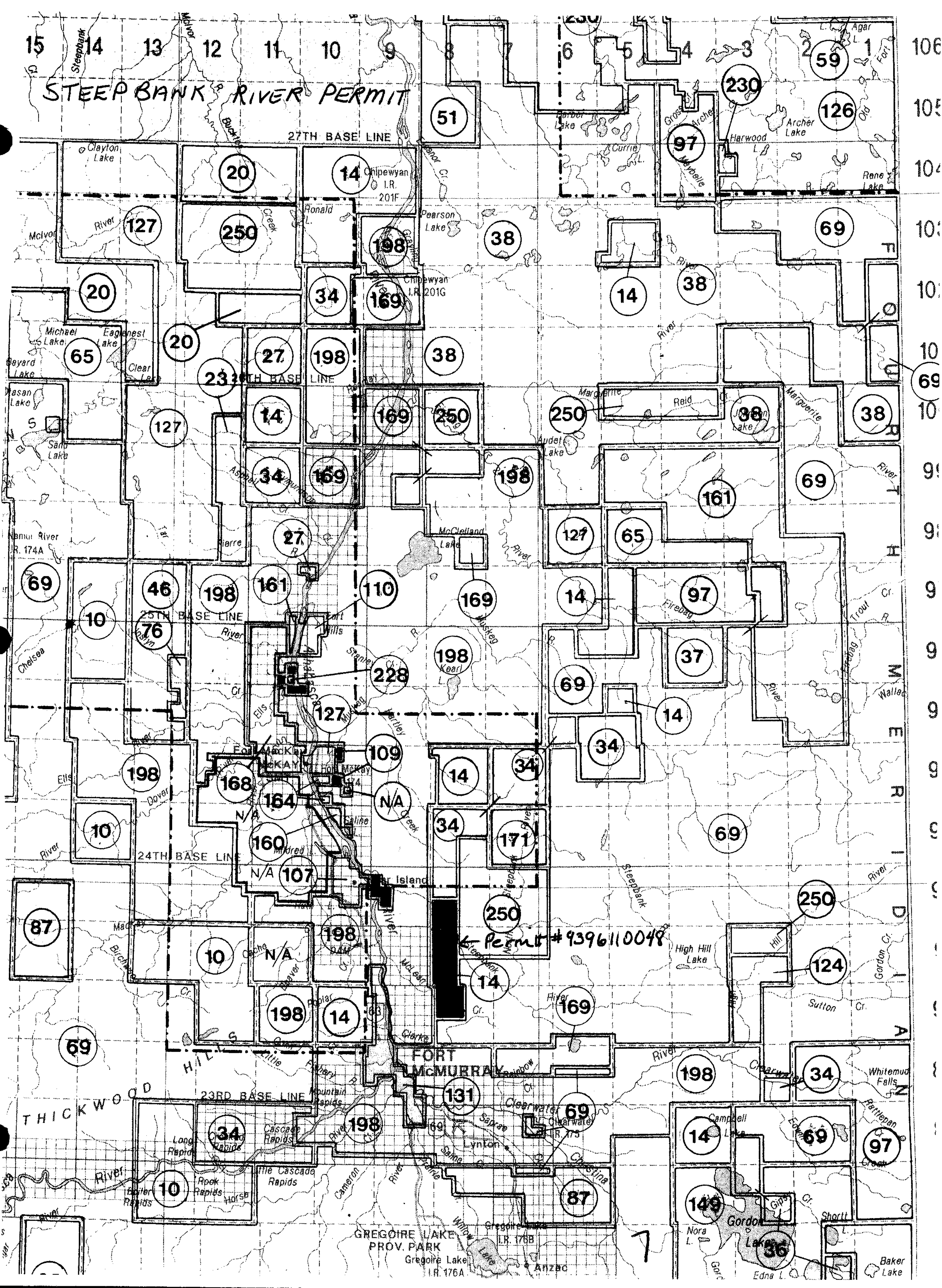

7

LOCATION

The Steepbank River permit, totalling an aggregrated area of 23,010 acres, portions on Townships 90-91-92, Range 8, West of the 4th, is bounded by a 56 latitude and 111 longitude. It is situated northeast of the town of Fort McMurray and Highway 63 by approximately six miles. There are several cutline and seismic trails throughout the property. The Steepbank River runs north and southwesternly through Township 91-92; and McLean Creek runs through a portion of Township 90, dipping south and east. The permit's one township is in the south portion of the Athabasca Basin and in the Alberta Oil Sands, and the Suncor Mine site overlaps the western portion of the permitted area.

GEOLOGY

TOPOGRAPHY AND DRIFT :

The land on this permit is mostly a low-lying region and is drained by the Athabasca River directly west of it. There are several intermittent streams and creeks. The rocks east of the Athabasca River are carbonaceous Devonian to lower Cretaceous. This particular area is also known for brinal activity proximal to bituminous coals.
Sample specimens contained:

i) reddish ironstone
ii) siliceous sand, partially clay
iii) limestone till
iv) green and blackish green shale
v) rusty clay and sand

There is allegedly a broad zone of northeasterly faulting; and structural distrubances overlying the mineralized sources. No bedrock exposure was found. The overburden deepness is very shallow, < 50 feet.

REGIONAL GEOLOGY:

The area of Fort McMurray contains a diversity of rock types, including exposures of Precambrian Shield, Paleozoic carbonates and Cretaceous claustic sedimentary rocks and is situated on the edge of a significant subsurface brine basin (AGS, Dufresne & Henderson). Most of the area is underlain by rocks of Devonian and Cretaceous ages.

Northeast Alberta is known for its bitumen reserves in the Lower Cretaceous Manniville Group, the development of the oil sands within the McMurray Formation. The discovery of a potential for precious metals such as gold, silver and platinum in the Devonian carbonates, which directly underlies the Cretaceous McMurray Formation, has put a new focus on the area. Between the Devonian and Cretaceous rocks there is the Beaver River sandstones (silica-rich) which outcrops in the Fort McMurray area. The McMurray Formation contains hydrocarbons, providing the necessary reducing environment.

The potential deposit types to explore for include:

(a) Brine - and/or hydrocarbon related gold deposits.
(b) Archean shear zone hosted gold deposits.
(c) Mississippi Valley type lead-zinc deposits.
(d) sediment hosted base metal deposits with one or more of zinc, lead, copper, nickel, silver and gold.
(e) granitoid-related uranium and/or rare earth element, precious metal or base metal deposits.
(f) sandstone-hosted or vein-type uranium deposits.
(g) diamondiferous kimberlite or lamproite diatremes.
(h) various types of placer or paleoplacer deposits, with the important metals/minerals being gold, diamonds, titanium or other heavy minerals. (AGS- Dufresne & Henderson)

EXPENDITURES

Currently two permits have reached the end of their 1st assessment period of November 21, 1998, and their assessment reports need to be submitted so the land can be kept for another two year term. One permit being no. #9396110048 on Township 90-91-92, Range 8, W4; the other being no. #9396110050 on Township 100, Range 11, W4. Their assessment work is general assaying, results from grab samples coming off both permits, including the expanse of area in between them. The samples assayed were rocks of the same rock type and texture, and their processing and assaying were done in duplicate, therefore the expenses will be divided equally between the two assessments.

Permit No. # 9396110048 - $1,893.80
9396110050 - $1,893.80

1996 EXPENDITURE STATEMENT
(Nov 21- Dec 31)

	Full Total	Half Total
Office	$15.00	$7.50
Food	$30.98	$15.49
Gas (Fort McMurray)	$49.60	$24.80
Travelling expenses (mileage*)	$1,200.00	$600.00
Fieldwork labour (6 days@ #300/per day)	$1,800.00	$900.00
Fuel (Edmonton)	$305.02	$152.51
Equipment (microscope)	$387.00	$193.50
Total expenses:	$3,787.60	$1,893.80

*Mileage - 1996 GMC 4x4: 2400 kms x $.50

A total of $69,592.52 was spent in 1997:
Permit no. #9396110048 - $34,796.26
#9396110050 - $34,796.26

1997 EXPENDITURE STATEMENT

	Full Total	Half Total
Office	$682.14	$341.07 R
Warranty (oxygen & acetylene)	$90.00	$45.00 P
Lodging	$1,544.38	$772.19 P
Food	$328.56	$164.28 P
Gas (Fort McMurray)	$536.64	$268.32 P
Travelling expenses (mileage*)	$13,200.00	$6,600.00 P
Fieldwork labour (46 days@ $300/per day)	$25,200.00	$12,600.00 ⑤
Transportation (plane)	$300.00	$150.00 P
Fuel (Edmonton)	$2,597.90	$1,298.95 P
Lab & Research labour (180 days @ $100/per day)	$18,000.00	$9,000.00 P
Lab chemicals & supplies	$4,000.52	$2,000.26 P
Courier services	$310.38	$155.19 R
Assaying	$1,659.00	$829.50 P
Camping supplies	$1,143.00	$571.50 P
Total Expenses:	$69,592.52	$34,796.26

* Mileage - 1996 GMC 4x4: 26,400 kms x $.50

A total of $59,545.36 was spent in 1998:

Permit no.#9396110048 - $29,772.68
#9396110050 - $29,772.68

1998 EXPENDITURE STATEMENT

	Full Total	Half Total
Office	$1648.08	$824.04 R
Warranty (oxygen & acetylene)	$90.00	$45.00 P
Lodging	$529.90	$264.95 P
Food	$802.66	$401.33 P
Gas (Fort McMurray)	$576.38	$288.19 P
Travelling expenses (mileage*)	$6,000.00	$3,000.00 P
Fieldwork labour (46 days @ $300/per day)	$13,800.00	$6,900.00 S
Fuel (Edmonton)	$1,549.08	$774.54 P
Lab & Research labour (200 days @ $100/per day)	$20,000.00	$10,000.00 P
Lab chemicals & supplies	$2,138.14	$1,069.07 A
Courier services	$277.48	$138.74 R
Assaying	$2,605.92	$1,302.96 A
Equip. purchases (kiln)	$2,009.22	$1,004.61 P.
Consulting fees	$2,500.00	$1,250.00 R
Computer lease	$2,018.50	$1.009.25 R
Assessment report preparation	$2,000.00	$1,000.00 A
Helper (5 days @ $200/per day)	$1,000.00	$500.00 R
Total Expenses:	$59,545.36	$29,772.68

*Mileage - 1996 GMC 4x4: 12,000 kms x .50

From the period, November 21, 1996 to November 21, 1998, a total of $132,925.48 was spent on expenditures. Claiming $66,462.74 on Permit no.# 9396110048
$66,462.74 on Permit no.# 9396110050

CONCLUSION

This report is a preliminary assessment of the potential for metallic mineral deposits in the tar sands and surrounding areas of N.E. Alberta. Although there has been extensive scientific research done on this area, there has been doubt and minimal exploration work done with the metallogeny of heavy oil in comparison to other parts of the world, such as Russia (Report on Metallogeny of Heavy Oils, Natural Bitumens & Oil Shales; Goldberg)

This compilation of assessment work summarizes the results of two years of research, by physically testing and assaying samples and rocks from beginning to end. By working with the mineralization of this nature it is quickly learned procedural and metallurgical problems first have to be addressed, and not ignored, before any assaying can be accurate or truthful to what actual values of minerals and metals exist.

In using various various experimental methods, and analytical work at the university and labs, the work performed was successful in identifying anomalous values of several precious and base metals, showing an increase of those values with a better process and leach. Example being #1 (raw) and #2 (pre-leach) in comparison to #3 (leach residue), all the same sample; assayed and resulting differently. All the assaying completed showed you first have to separate something, so you to develop the right leach, if you want to effectively record a higher value in a difficult-to-assay rock and metal such as platinum. The results show the gold and platinum are there. Assay problems will take due diligence, because the oddity in the complexes in the mineralization are yet to be all identified. Before there is any feasibility of extraction further research and time will need to be applied to solve and combat those complexities and by understanding the origins of the gold and PGE's the answers will undoubtedly follow.

RECOMMENDATIONS:

Further evaluation and assessment is warranted with pre-assaying samples and rocks, to better define mineralized trends, to subsequently pick out drill locations.

This area is structurally perfect for a discovery of metals or diamonds, because of the uplift of the Peace River Arch and its location to the Proterozoic Taltson Arc, a strong magnetic high.

A diamond indictor mineral analysis should be done in order to assess its potential for kimberlite and diamonds, also being found close by.

DECLARATION

I, Larry MacGougan, solemnly swear all expenditures claimed on this assessment are valid and were spent on assessing the mineralogy of this permit.

[redacted]

AUTHOR INFORMATION:

This report was prepared by Debbie Puckett. The work and results reported herein were carried out by and under the supervision of Larry MacGougan.

Larry MacGougan is the permit holder. He is a full-time prospector and files as such with Revenue Canada. He has over ten years of experience in prospecting and mining. He is also the vice- president of 374624 Alberta Limited.

Chris Puckett was his helper in 1998 on one expedition. He worked five days.

Addresses of the above:

Larry MacGougan
[redacted]

Debbie Puckett
[redacted]

Chris Puckett
[redacted]

REFERENCES

Abercrombie, H. & Feng R.; Disseminated Au-Ag-Cu Mineralization in the Western Canadian Sedimentary Basin, Fort McKay, NE Alberta, presented at C.I.M., Toronto, 1994.

Dufresne, M.B. & Henderson, B.A.; The Mineral Deposits Potential of the Marguerite River and Fort McKay Areas, Northeast Alberta, Alberta Research Council, 1994.

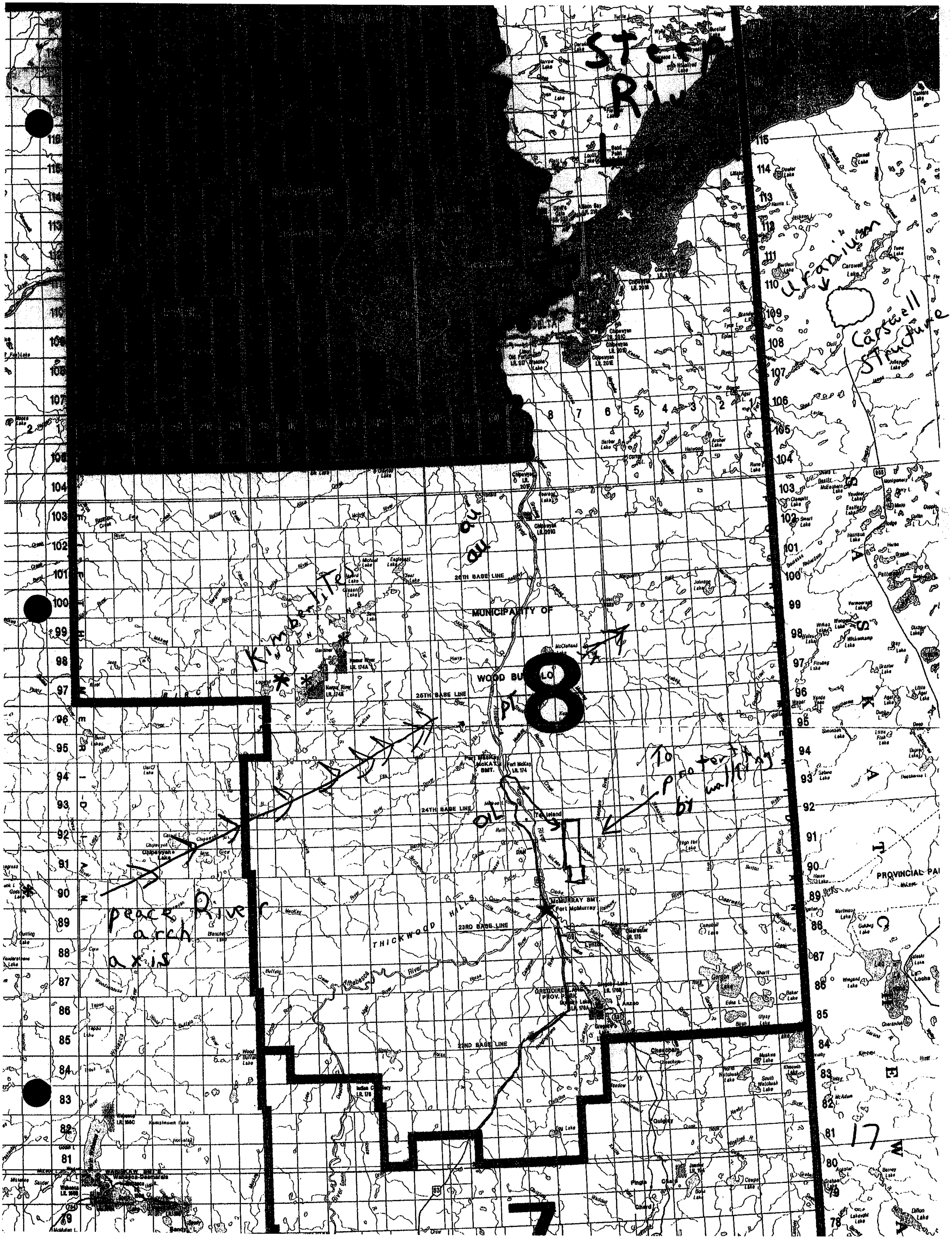
Steep River
L
uranium
Carswell Structure
au
Kimberlites
oil
pt
8
To protecting by walking
Peace River arch axis
17
7
MUNICIPALITY OF
WOOD BUFFALO
26TH BASE LINE
25TH BASE LINE
24TH BASE LINE
23RD BASE LINE
22ND BASE LINE
THICKWOOD HILLS
Athabasca River
Fort McKay
Fort McMurray
McMURRAY SMT.
Lynton
Anzac
GREGOIRE LAKE PROV. PARK
Chipewyan Lake
Wabasca
Carswell Lake
PROVINCIAL PA
SASKATCHEWAN

STeep Bank River Land

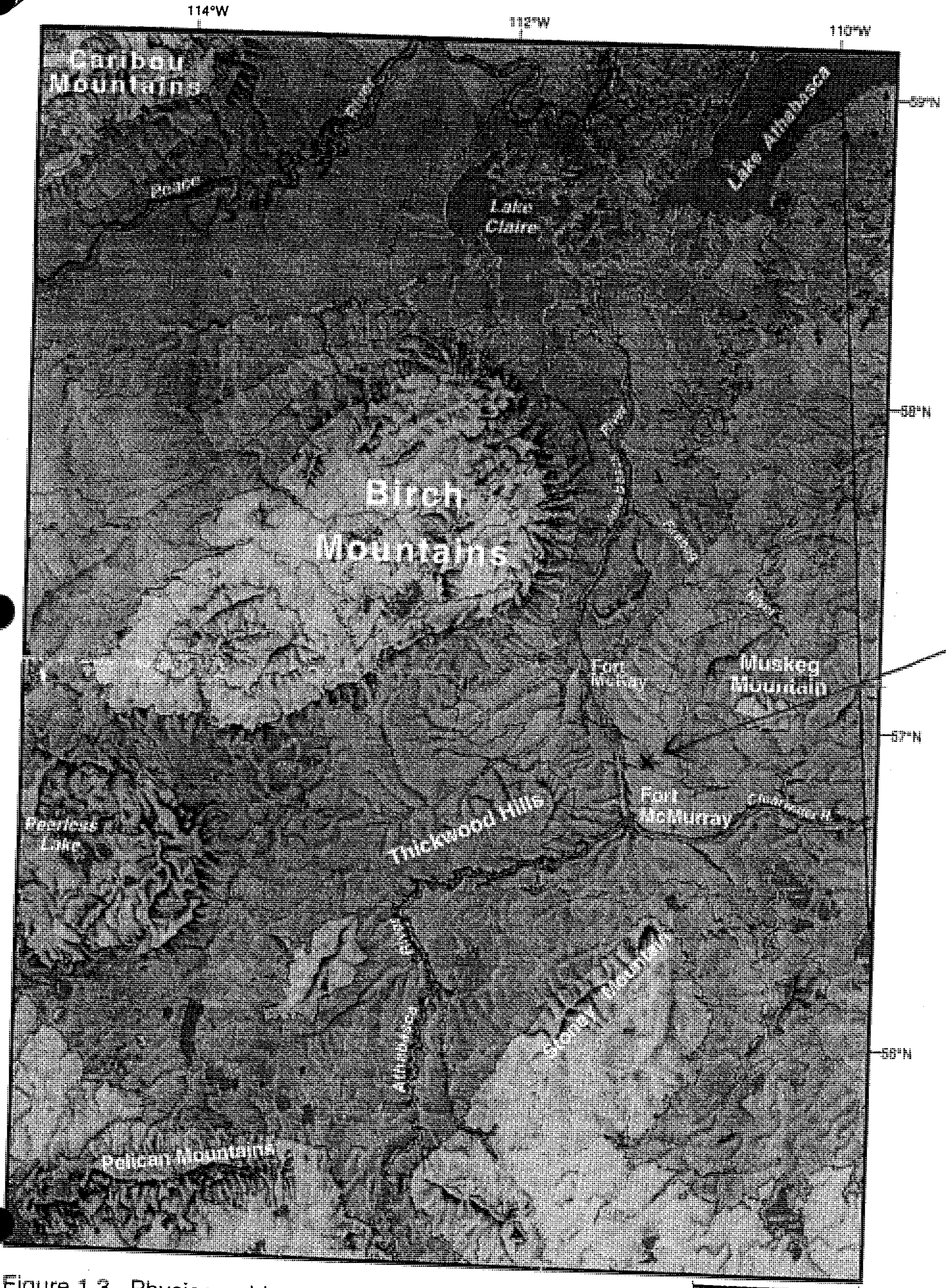

property

Figure 1.3. Physiographic map of northeastern Alberta showing location of major topographic features (from Alberta Transportation, 1978).

18

DriFT thickness

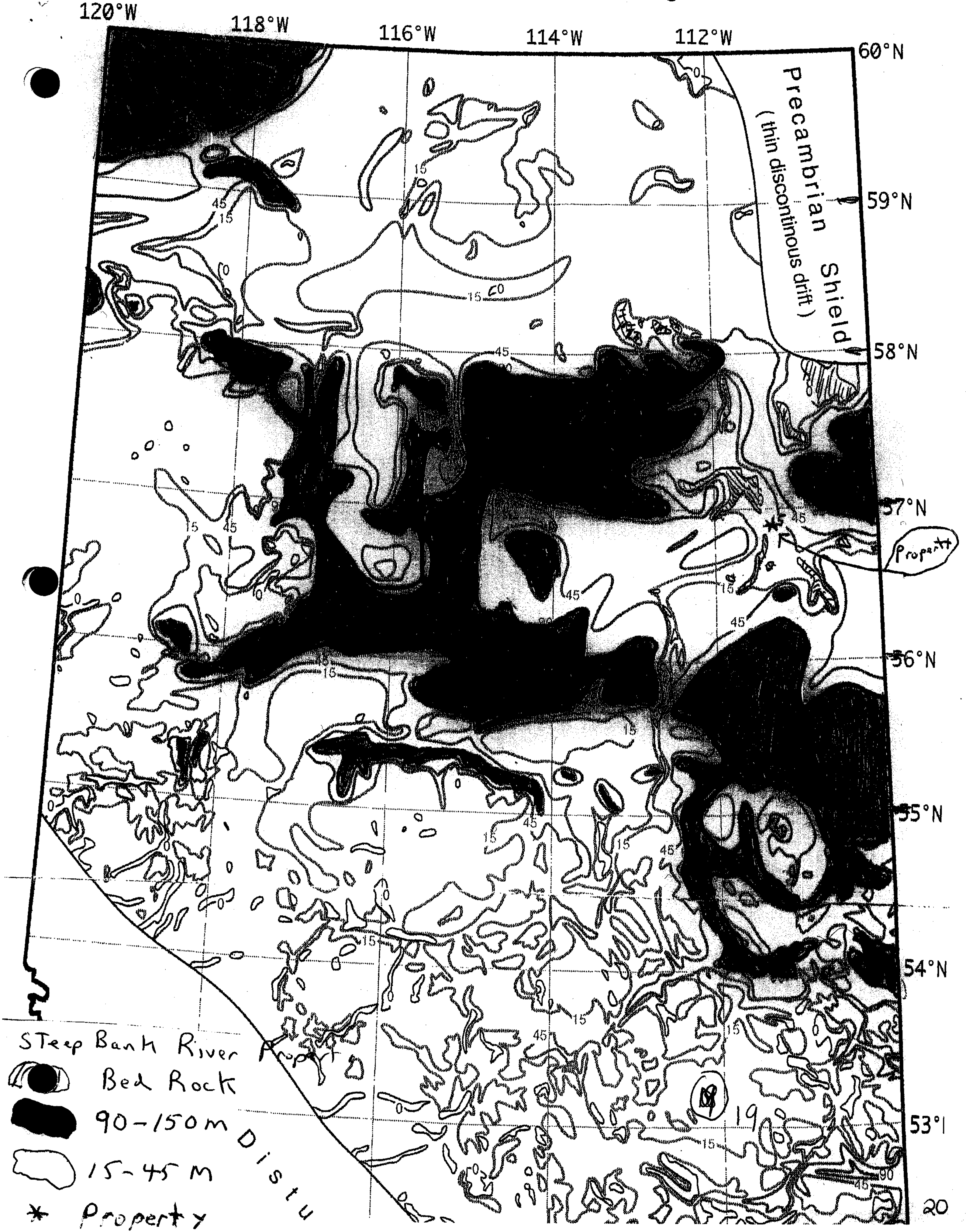

STeep Bank River Propert

● Bed Rock

■ 90-150m

○ 15-45 M

* Property

Precambrian Basement Tectonic Features

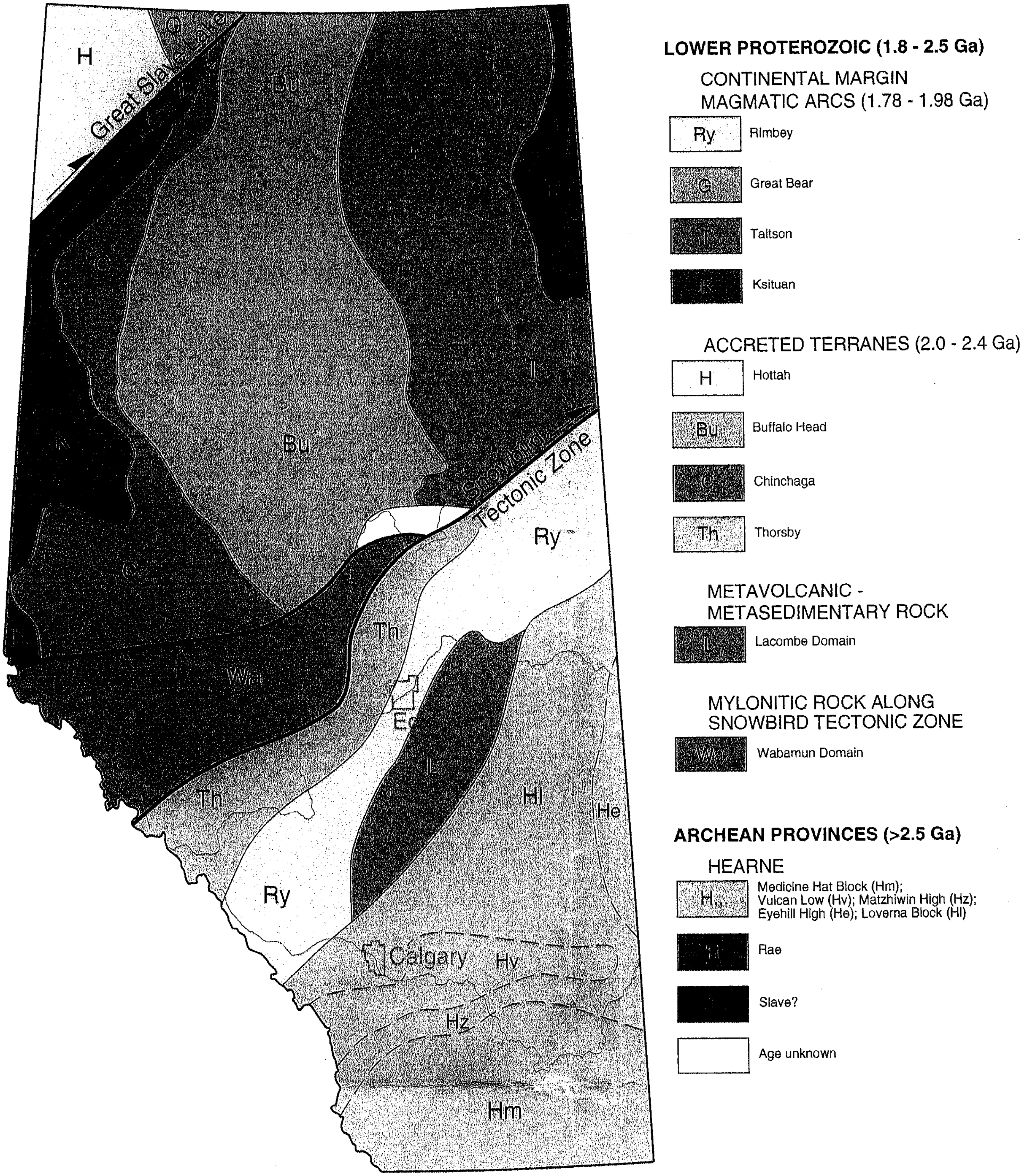

[illegible]

20

Regional Cross Secti

Steep Bank Land

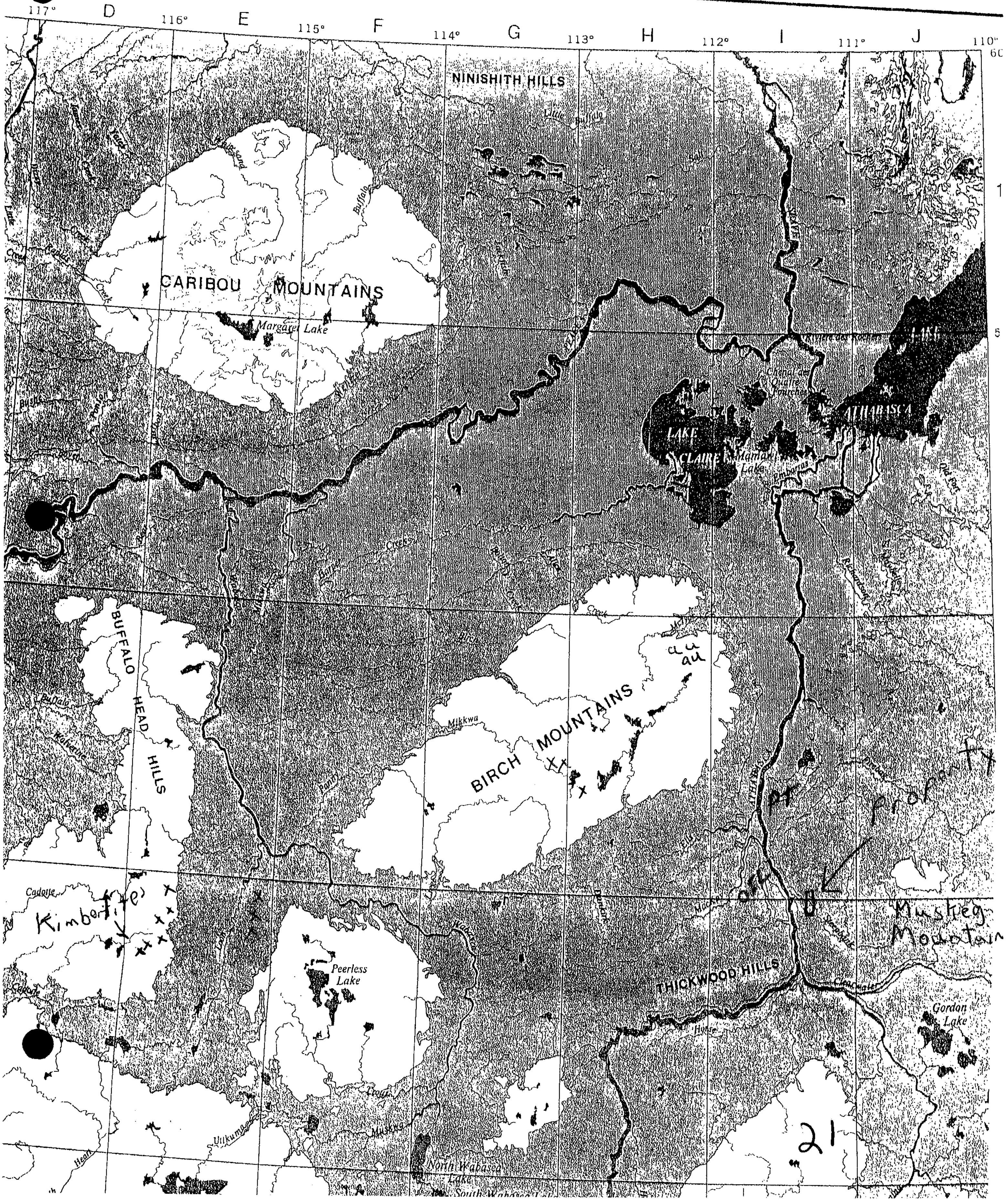

CRETACEOUS

UPPER AND LOWER CRETACEOUS

Klb	**LABICHE FORMATION:** dark grey shale and silty shale; ironstone partings and concretions; silty fish-scale bearing beds in lower part; marine

LOWER CRETACEOUS

Kpl	**PELICAN FORMATION:** fine-grained quartzose sandstone, silty and glauconitic in lower part; marine
Kj	**JOLI FOU FORMATION:** dark grey fossiliferous shale, silty interbeds in upper part; marine
Kg	**GRAND RAPIDS FORMATION:** fine-grained quartzose and feldspathic sandstone, laminated siltstone and silty shale; thin coal beds; shoreline complex
Kc	**CLEARWATER FORMATION:** dark grey, fossiliferous, silty shale; laminated siltstone and fine-grained cherty sandstone; glauconitic sandstone (**Wabiskaw Member**) near base; marine
Km	**McMURRAY FORMATION:** thick-bedded quartzose sandstone and siltstone; oil-impregnated; grey silty shale interbeds in upper part; nonmarine to deltaic

DEVONIAN

UPPER DEVONIAN

Dw	**WATERWAYS FORMATION:** grey and greenish grey shale and argillaceous limestone interbedded with grey and greyish brown, fine-grained to coarse clastic limestone; marine

MIDDLE DEVONIAN

Ds	**SLAVE POINT FORMATION:** grey and brown fine- to medium-grained limestone and dolomitic limestone; minor shale, gypsum; marine
Dfv	**FORT VERMILION FORMATION:** white and grey gypsum, argillaceous and dolomitic gypsum; minor anhydrite; some fine-grained limestone, dolomitic limestone and green shale; evaporitic
Dmg	**MUSKEG FORMATION:** white and grey gypsum, anhydrite; minor dolomite, salt and shale; evaporitic
Dk	**KEG RIVER FORMATION:** grey and brown fine- to medium-grained limestone, thin- to thick-bedded, locally richly fossiliferous and coarse grained; grey medium-grained dolomite, locally vuggy (upper member); fine-grained brown dolomite and laminated dolomite, locally vuggy; minor limestone; unit locally much brecciated and recemented (lower member); marine
Dch	**CHINCHAGA FORMATION:** white and grey gypsum, argillaceous and dolomitic gypsum and anhydrite; some dolomite, dolomitic limestone, red and green shale; some salt in subsurface; evaporitic
Df	**FITZGERALD FORMATION:** grey and brown fine- to medium-grained dolomite to sandy dolomite and dolomitic limestone, locally vuggy, grading down into sandstone, arkose and breccia (**La Loche Formation**); marine
DM	**MIDDLE DEVONIAN** (undivided): arkosic sandstone (**La Loche Formation**); grey-green and sandy shale, reddish shale; dolomite; minor anhydrite (**McLean River Formation**); br and buff, massive, porous dolomite; brown to grey thin-bedded dolomite; dolomitic limestor (**Methy Formation**); gypsum; anhydrite; grey-green silty and dolomitic shale; minor dolom (leached **Prairie Evaporite Formation**); marine to evaporitic Note: **McLean River, Methy** and **Prairie Evaporite Formations** are equivalents of **Chinct** **Keg River** and **Muskeg Formations** respectively, the Prairie Evaporite including a thick succession of salt beds in subsurface

HELIKIAN

ATHABASCA GROUP

HELIKIAN

ATHABASCA GROUP

Ho	**OTHERSIDE FORMATION:** sandstone with minor siltstone; nonmarine
Hl	**LOCKER LAKE FORMATION:** massively bedded pebbly sandstone and sandstone; nonmarine
Hwu Hwl	**WOLVERINE POINT FORMATION:** Hw-u: upper Wolverine Point – altered vitric and ash-flow tuffs, interbedded with medium-grained, clay-rich, friable sandstones; marine-pyroclastic Hw-l: lower Wolverine Point – medium-grained sandstone, with minor interbedded siltstone; nonmarine-marine
Hm	**MANITOU FALLS FORMATION:** medium-grained pebbly sandstone and sandstone; abundant clay intraclasts; nonmarine
Hfp	**FAIR POINT FORMATION:** coarse-grained, pebbly, clay-rich sandstone; conglomeratic at base; nonmarine

APHEBIAN

[illegible]	**LOW GRADE METASEDIMENTARY AND METAVOLCANIC ROCKS:** arkosic sandstones, felsic and mafic volcanics, turbidites, phyllite; locally ferruginous, gold bearing shear zones, with quartz-tourmaline veins (**Waugh Lake Group**); arkosic sandstone with pebble bands interbedded with subordinate phyllonitic chloritic argillite (**Burntwood Group**)
Ag	**GRANITOIDS:** reddish, medium- to coarse-grained, megacrystic, well foliated, feldspar-blue quartz-biotite granite (**Arch Lake Granitoid**); pink-spotted medium grey, medium-grained, megacrystic, massive granite (**Francis Granite**); red to pink, medium- to fine-grained, equigranular, massive to poorly foliated biotite granite (**Chipewyan Red Granite**); light grey to brownish grey, medium-grained, rarely megacrystic, massive to poorly foliated granodiorite (**La Butte Granodiorite**); dark greenish to brownish red, medium-grained, equigranular, massive to poorly foliated, feldspar-quartz-biotite granodiorite (**Wylie Lake Granitoids**); light grey to pink or reddish, medium- to fine-grained, equigranular, massive to foliated, alkali feldspar-quartz-plagioclase-biotite granite (possibly **K feldspar-enriched Wylie Lake Granitoid?**); grey, medium-grained, megacrystic, poorly foliated, feldspar-quartz-biotite quartz diorite (**Fishing Creek Quartz Diorite**); light to medium grey, medium-grained, equigranular, moderately foliated to massive, alkali feldspar-quartz-plagioclase-biotite granite (possibly **K feldspar-enriched Fishing Creek Quartz Diorite?**); light to medium grey, medium- to coarse-grained, megacrystic, well foliated, biotite-quartz-feldspar granite (**Colin Lake Granitoids**); dark grey, with red to pink megacrystic augen feldspars, medium-grained, foliated, blue grey quartz-biotite granite (**Thesis Lake Granite**); whitish grey, medium- to coarse-grained, locally megacrystic, massive to foliated, feldspar-quartz-biotite granodiorite (**Slave Granitoids**)
Ax	**MYLONITIC ROCKS:** dark grey to dark green, fine-grained, massive rock; light grey felsic varieties present locally; commonly chlorite epidote-rich; well-foliated with streaky patches of quartz and feldspar; includes protomylonites

ARCHEAN

[illegible]	**CHARLES LAKE GRANITOIDS:** subhedral feldspars in coarse-grained, massive to poorly foliated megacrystic granite; buff to grey with dark specks of hornblende and local feldspar megacrysts in fine- to medium-grained, massive to slightly foliated grey hornblende granite; equigranular, medium- to coarse-grained, massive to locally foliated leucocratic granite
Ahm	**HIGH-GRADE METASEDIMENTARY ROCKS:** typically dark greenish grey, fine-grained quartzite; interlayered with ferruginous and garnetiferous zones; minor amphibolite; locally fine- to medium-grained metamorphic quartzo-feldspathic phase; fine-grained retrograde phyllite and schist, and phyllonite
Agg	**GRANITE GNEISSES:** pink to reddish, fine- to medium-grained, equigranular to rarely megacrystic, well banded to foliated, granitic composition, quartz-feldspar bands interlayered with mafic-rich bands; predominantly biotite-rich but rarely hornblende; commonly migmatitic

STeep Bank River
First Bed Rock

For Map # 23


Birch
River
Richardson Lake
Kpl
Kl
Kch
Km
Kc
Kd
Kg
Dm
Ds
Dw
Ks
Birch Mountains
21 20 19 17 15 14 13 12 9 8 7 6 5 3 2 1
Namur Lake
McClelland Lake
Klb
Ells
Dover
Dover
Kj
River
63
Kpl
MacKay
River
Thickwood Hills
Fort McMurray
Clearwater
property
74D/14
Horse
River
Willow Lake
CNR
Gordon Lake
Gipsy Lake
Birch Lake
Gardon Lake
Kg
FOURTH MERIDIAN
108 107 106 105 104 103 102 101 100 99 98 97 96 95 94 93 92 91 90 89 88 87 86 85 84 83 82 81

Steep Bank River

Table 2. Generalized Stratigraphy For The Bitumount Area [1]

SYSTEM	GROUP	FORMATION	MEMBER	DOMINANT LITHOLOGY
Upper Cretaceous	La Biche north start	La Biche	[illegible]	Shale
		Dunvegan		Sandstone & siltstone
	steep bank	Shaftesbury		Shale, bentonites, fish-scale horizon
Lower Cretaceous	missing	Pelican		Sands
		Joli Fou		Shale
	Mannville	Grand Rapids		Lithic sands
	start south	Clearwater	✓	Shale & glauconitic sands
		McMurray		Quartzose sands, heavy oil
Jurassic?		Beaver River		Quartzose sandstone
Upper Devonian	Beaverhill Lk.	Waterways	Mildred	Argillaceous limestone
			Moberly	Limestone & shale
			Christina	Shale & limestone
			Calumet	Limestone & shale
			Firebag	Shale, minor limestone
Middle Devonian		Slave Point		Limestone, local breccia
	Upper Elk Point	Prairie Evapoite		Salt, anhydrite (gypsum), shale & dolomite
		Methy		Dolomite, minor reefs
	Lower Elk Point	McLean River		Shale, siltstone & dolomite
		Cold Lake		Salt, minor shale
		Ernestina		Shale, limestone & Anhydrite
		Lotsberg		Salt, minor shale
		LaLoche		Arkosic sand & conglomerate
Precambrian				Granitic basement

Start

---

[1] Modified after Carrigy (1959, 1973), Norris (1963, 1973) and Hamilton (1971).

Steep bank Property

Back in 1967, when Great Canadian Oil Sands Ltd. (one of the precursors to Suncor) invested $250 million to build the first commercial plant to extract bitumen from the oil sands and up-grade it to salable crude, the plant was designed to produce 45,000 barrels of product per day. Today, the operation cranks out 78,400 barrels a day and plans are in place to increase further to 105,000 barrels per day by the year 2000.

To get just one barrel of product, the operation mines one and a half tonnes of oil sand. So, to feed the expanded plant, the mine will have to be capable of supplying 72.6 million tonnes of oil sands per year compared with the current 48.9 million tonnes.

Key to the expansion plans is a wholesale change in the corporate culture at Suncor — essentially bringing the company out of its 1960s mindset and into the 1990s way of thinking, or, as Executive Vice President of the Oil Sands Group, Dee Parkinson prefers to state it: "creating economic value by doing things that make environmental sense."

"In the past, managers didn't under-

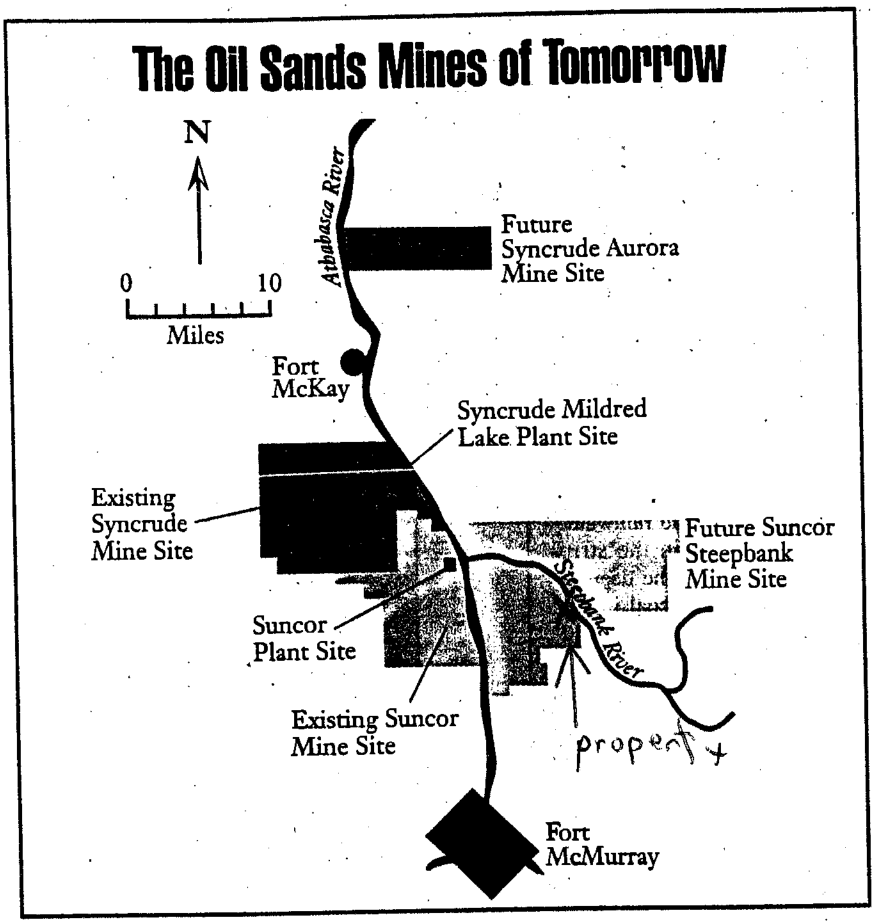

The Oil Sands Mines of Tomorrow

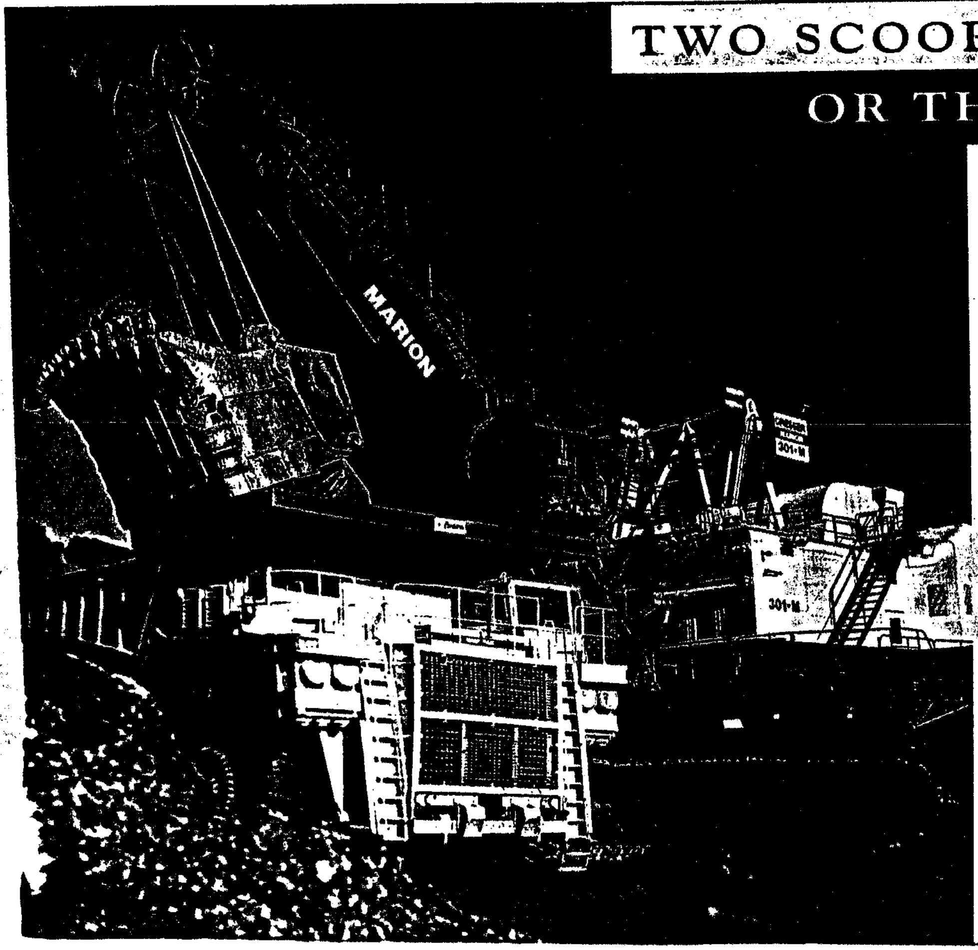

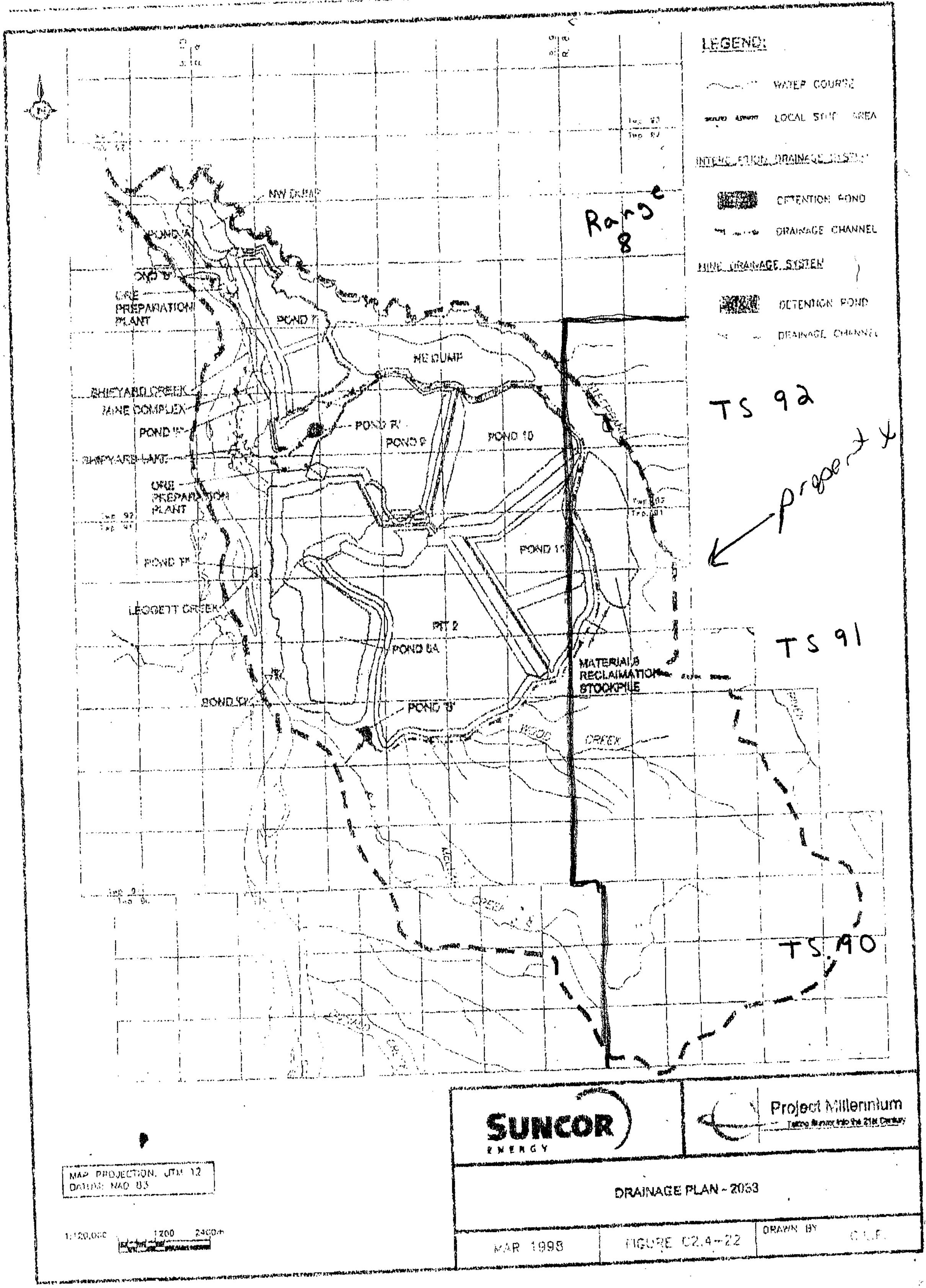

Figure C2.4-22 Drainage Plan - 2033

Steepbank River

26

GOLD AND PLATINUM GROUP ELEMENTS

ROCKPECKER TIP # 218 -- If your ore tests positive for GOLD, have it tested for PLATINUM GROUP METALS. If it tests positive for platinum & palladium, have the ore assayed for OSMIUM, RHODIUM, and RUTHENIUM. Two or more of these metals are usually alloyed together as PLATINUM GROUP METALS.

ROCKPECKER TIP # 219 - ASSAYS can pick up low GOLD values ranging to .008 oz. Au/ton with good repeatability and acceptable limits. With low gold values a check assay can be ordered where INQUARTS of gold are added to the sample. (This is a spiking procedure where an ore of known gold value is added to the sample.) For example: If you have 1 gold coin and place it in a glass of water, then add 2 more gold coins, you expect to count 3 coins.

THE ROCKPECKER TIP PROBLEM -- What if you only count 2 coins ?

IT HAS BEEN FOUND THAT CERTAIN NATURAL, PLATINUM GROUP ELEMENT ORES, WHEN COMBINED WITH GOLD, BARELY SHOW THE GOLD VALUE AND SOMETIMES NONE OF THE PLATINUM GROUP ELEMENTS. In fact, the more spiking or inquarting of gold into the sample, the lower the GOLD values reported. The reason for this strange behavior is unknown. It is as if the gold is being eaten without trace. Your tip-off to look more closely, will be a fire assay which produces a gold bead that looks unusual, oftentimes indicating the probable presence of other elements. THESE MAY BE PGM's. CHECK !

FOR THESE REASONS, GOLD TEST # 6 AND GOLD TEST # 7 ARE PRESENTED.

IF YOUR PRE-ASSAY TESTS INDICATE GOLD, PLATINUM, PALLADIUM AS PRESENT, AND THE FEE-ASSAY REPORT READS "NONE REPORTABLE", YOU MAY HAVE THIS STRANGE ORE.

If test # 6 GOLD SPOT TEST shows the presence of GOLD, you should retest for antimony, sulfides, and tellurium as combining elements in the GOLD ORE before ROASTING. Too high a roasting heat makes ores containing those elements REFRACTORY. (If you consider using the rosebud on your acetylene torch, you must be extremely careful in heating.) HEATING temperatures OVER 1000 C (1800 F) lock gold, platinum and palladium into a refractory so that chemical identity is retained in spite of high temperatures. THIS MEANS THE ORE SHOULD NEVER EXCEED "VERY DULL RED HEAT".

ROASTING ORE -- Ore is roasted to get rid of sulfides, tellurides, antinomides, and to reduce elements to the metallic state.

PROCEDURE -- The idea is to check for heavier elements in your crude ore. You'll need a few pounds of ore. Crush it, bring it to a dull red heat, stirring, until all the gases such as smoke and fumes are released. Then pulverize the sample. Pan it to concentrate the "heavies" and wash off the lighter material. Use a magnet to remove the magnetics. USE 1 SPOONFUL FOR TESTS.

GOLD,

MATERIALS NEEDED --

For Gold Spot Test

OTHER MATERIALS NEI
dishes, 4 cc's pure
(KI), alcohol lamp.

TEST #

TEST RESULT --- *TES*

TEST #

TEST RESULT --- *TES*

CONFIRM ROSE
solution, th
dish. RESUL

ducting the TEST AC
the solution turns
on the dish bottom
solution, the higher

STEEPBANK RIVER ASSAYS

SAMPLE LOCATION UTM N 6315100
E 482505

TILL SAMPLES 200 m RADIUS.

Lab
Report

(1)

CLIENT: MR. LARRY MACGOUGAN
REPORT: V97-01599.0 (COMPLETE)
DATE RECEIVED: 10-JUL-97
PROJECT: NONE GIVEN
DATE PRINTED: 30-JUL-97
PAGE 1 OF 2

SAMPLE NUMBER	ELEMENT UNITS	AU PPB	PT PPB	PD PPB
R2 3		3	<5	<1
R2 4		4	<5	<1

Steep Bank River

Green Shale - Drill hole
High Iron 15%
~~poor~~ - Likly Till Slab

Normal Assay

ITS Intertek Testing Services
Bondar Clegg

2

Geochemical
Lab
Report

CLIENT: MR. LARRY MACGOUGAN
PROJECT: NONE GIVEN
REPORT: V97-02342.0 (COMPLETE)
DATE RECEIVED: 04-SEP-97
DATE PRINTED: 22-SEP-97
PAGE 3 OF 3

SAMPLE NUMBER	ELEMENT UNITS	AU PPB	PT PPB	PD PPB
P12 1		10	<5	<1
Duplicate		42	<5	1

STeep Bank River

Rusty iron stone To Black
Till Sample

Normal assay

ITS Intertek Testing Services
Bondar Clegg

3

Geochemical Lab Report

CLIENT: MR. LARRY MACGOUGAN
PROJECT: NONE GIVEN
REPORT: V97-02018.0 (COMPLETE)
DATE RECEIVED: 12-AUG-97
DATE PRINTED: 25-AUG-97
PAGE 1 OF 2

SAMPLE NUMBER	ELEMENT UNITS	AU PPB	PT PPB	PD PPB
84 7		16	<5	1
84 8		11	<5	<1
84 9		15	<5	3

Steep Bank River

Sand stone Till

Normal Assay

Iron - Carbon Limestone 4

Steep Bank River

Purpose: To determine Au and Ag content by cyanidation of Sample #1, (460-012).

Procedure: The sample was pulverized to 100% passing 100 mesh, and then pulped with water to 33% solids in a 2.5 L bottle. Lime and NaCN were added and the leach carried out over 48 hours on rolls. At the end of the leach period the pulp was filtered and washed thoroughly with water. The pregnant/wash solution and the residue were submitted for gold and silver analyses.

Feed: 380 g of Sample # 1 (460-012)

Solution Volume: 770 mL

Pulp Density: 33 % solids

Sol'n Composition: 2 g/L NaCN

pH Range: 10.5 - 11.2 with $Ca(OH)_2$

Reagent Consumption (kg/t of cyanide feed) NaCN: 0.22 CaO: 1.86

Time	Added, Grams				Residual		Consumed		pH
	Actual		Equivalent		Grams		Grams		
hours	NaCN	$Ca(OH)_2$	NaCN	CaO	NaCN	CaO	NaCN	CaO	
0 - 4	1.61	0.41	1.53	0.31	1.46		0.07		11.0-9.9
4 - 22	0.08	0.28	0.08	0.21	1.50		0.04		11.1-10.5
22 - 30	0.04	0.08	0.04	0.06	1.54		0.00		11.1-10.6
30 - 48	0.00	0.17	0.00	0.13	1.56	0.02	-0.02	0.70	11.2-10.9
Total	1.73	0.95	1.65	0.72	1.56	0.02	0.08	0.70	

Results:

Product	Amount g, mL	Assays, mg/L, g/t Au	Ag	% Distribution Au	Ag
48 hour Preg\Wash	1359	0.025		> 81.9	
CN Residue	375.8	< 0.02	*	< 18.1	
Head	375.8	< 0.11		100.0	

* The residue Au assay was reported as less than the analytical detection limit of 0.02 g/t, therefore the 48 hour gold extraction is greater than 81.9%.

Normal NaCN Leach Test

⑤

To : **MR. LARRY MACGOUGAN**
Box 56
Coronation, Alberta
T0L 1C0

Certificate of Assay
Loring Laboratories Ltd.

Sample No.	OZ./TON GOLD	OZ./TON SILVER
<u>"Assay Analysis"</u>		
# 1B	0.010	<0.01

- 30g start
- iron Carbon Limestone
- Leach with Sulpharous Leach
- send Leach Residue To Loring
- Calculate Back To 30g
- Experimental Assay

I HEREBY CERTIFY that the above results are those assays made by me upon the herein described samples :

[redacted]

Assayer

Rejects and pulps are retained for one month unless specific arrangements are made in advance.

6

Geochemical Lab Report

NT: MR. LARRY MACGOUGAN
REPORT: V99-00011.0 (COMPLETE)
DATE RECEIVED: 05-JAN-99
PROJECT: NONE GIVEN
DATE PRINTED: 8-FEB-99
PAGE 1A(1/ 2)

SAMPLE NUMBER	ELEMENT UNITS	Au PPM	Pt PPM	Pd PPM	Au Wt1 GM	AU PPB	PT PPB	PD PPB	Au PPB	Pt PPB	Pd PPB	Rh PPB	Os PPB
P4 SAMPLE 1					15.10	9	7	10					
P4 SAMPLE 2					7.66	16	14	20					
P4 SAMPLE 3									4	<20	<20	<5	<10
84 SAMPLE 4		0.189	0.048	0.058									

<u>Normal Assay</u>

- ironstone <u>same Sample</u>

Steep Bank River

7

To : MR. LARRY MACGOUGAN
Box 56
Coronation, Alberta
T0L 1C0

File No : 38866
Date : February 14, 1997
Samples :
Project :
P.O.#

Certificate of Assay

Loring Laboratories Ltd.

629 Beaverdam Road, NE Calgary Alberta
Tel: (403)274-2777 Fax: (403)275-0541

Sample No.	OZ./TON GOLD	OZ./TON SILVER	OZ./TON PLATINUM
1	0.001	<0.01	<0.001
2	0.016	<0.01	<0.001
3	<0.001	<0.01	<0.001

1# and 3# Normal assay

2# Leach Residue Fired
Experimental assay

I HEREBY CERTIFY that the above results are those assays made by me upon the herein described samples :

[redacted]
Assayer

Rejects and pulps are retained for one month unless specific arrangements are made in advance.

8

To : **MR. LARRY MACGOUGAN**
Box 56
Coronation, Alberta
T0C 1C0

Certificate of Assay
Loring Laboratories Ltd.

629 Beaverdam Road, NE Calgary Alberta
Tel: (403)274-2777 Fax: (403)275-0541

File No : **38872**
Date : February 24, 1997
Samples : Filters
Project :
P.O.#

Sample No.	PPB Au	PPM Ag	PPB Pt
"Assay Analysis"			
1	<5	<0.1	<10
2	<5	<0.1	<10
3	<5	<0.1	<10
4	<5	<0.1	<10

Steep Bank
Grab Samples Assay
Normal Assays

I HEREBY CERTIFY that the above results are those assays made by me upon the herein described samples :

[redacted]
Assayer

Rejects and pulps are retained for one month unless specific arrangements are made in advance.

35

9

To : **MR. LARRY MACGOUGAN**
Box 56
Coronation, Alberta
T0L 1C0

File No : 40438
Date : September 17, 1998
Samples :
Project :
P.O.#

Certificate of Assay

Loring Laboratories Ltd.

629 Beaverdam Road, NE Calgary Alberta
Tel: (403)274-2777 Fax: (403)275-0541

Sample No.	Au oz/ton	Ag oz/ton
"Assay Analysis"		
# 1	< 0.001	< 0.01
# 2	< 0.001	< 0.01
# 3	< 0.001	< 0.01

Steep Bank
- iron stone Light Color

Normal assay

I HEREBY CERTIFY that the above results are those assays made by me upon the herein described samples :

[redacted]
Assayer

Rejects and pulps are retained for one month unless specific arrangements are made in advance.

To : MR. LARRY MACGOUGAN
Box 56
Coronation, Alberta
T0L 1C0

File No : 39435 10
Date : August 25, 1997
Samples :
Project :
P.O.#

Certificate of Assay
Loring Laboratories Ltd.

629 Beaverdam Road, NE Calgary Alberta
Tel: (403)274-2777 Fax: (403)275-0541

Sample No.	ppb Au	ppb Pt	oz/ton Ag
"Geochemical Analysis"			
# 4	< 5	---	< 0.01
# 4B	< 5	< 5	< 0.01

Steep Bank
Normal assay

#4B Sample Rock as page 5#
Leach

I HEREBY CERTIFY that the above results are those assays made by me upon the herein described samples :

[redacted]
Assayer

Rejects and pulps are retained for one month unless specific arrangements are made in advance.

(11)

ITS Intertek Testing Services
Bondar Clegg

Geochemical Lab Report

CLIENT: MR. LARRY MACGOUGAN
REPORT: V98-01591.4 (COMPLETE)

PROJECT: NONE GIVEN
DATE RECEIVED: 01-SEP-98 DATE PRINTED: 14-SEP-98 PAGE 1A(1/ 4)

SAMPLE NUMBER	ELEMENT UNITS	AU PPB	PT PPB	PD PPB	Au PPM	Ag PPM	Ag PPM	Cu PPM	Pb PPM	Zn PPM	Mo PPM	Ni PPM	Co PPM	Cd PPM	Bi PPM	As PPM	Sb PPM
SAMPLE 4		5	<5	2													
SAMPLE 1		15	<5	34													
SAMPLE 2							1.8	35	20	17	19	29	12	<.2	<5	<5	<5
SAMPLE 3					<.03	1.4											

SAMPLE NUMBER	Fe PCT	FeOL PCT	Mn PPM	Te PPM	Ba PPM	Cr PPM	V PPM	Sn PPM	W PPM	La PPM	Al PCT	Mg PCT	Ca PCT	Na PCT	K PCT	Sr PPM	Y PPM	Ga PPM	Li PPM	Nb PPM	Sc PPM	Ta PPM	Ti PCT
SAMPLE 4																							
SAMPLE 1																							
SAMPLE 2	>10.00	>30.0	57	<10	<1	12	<1	<20	23	<1	<.01	<.01	<.01	0.02	0.08	7	2	<2	<1	19	<5	<10	<.01
SAMPLE 3																							

Till Sample
Steep Bank
- iron Stone
Normal assay

=

38

ITS Intertek Testing Services
Bondar Clegg

12

Geochemical
Lab
Report

CLIENT: MR. LARRY MACGOUGAN
REPORT: V98-01591.4 (COMPLETE)

PROJECT: NONE GIVEN
DATE RECEIVED: 01-SEP-98 DATE PRINTED: 14-SEP-98 PAGE 1B(2/ 4)

SAMPLE NUMBER	ELEMENT UNITS	Zr PPM
SAMPLE 4		
SAMPLE 1		
SAMPLE 2		6
SAMPLE 3		

Till sampl
Iron Stone
Steep Bank
Normal assay

-2

(13)

Enzyme Leach Job #: 9966 Report#: 9911 Customer: Larry Machougan Customer's Job #: ----

Trace Element Values Are in Parts Per Billion. Negative Values Equal Not Detected at That Lower Limit.

Values = 999999 are greater than working range of instrument. S.Q.=That element is determined SEMIQUANTITATIVELY.

Sample ID:	S.Q.Li	S.Q.Be	S.Q.Cl	S.Q.Sc	S.Q.Ti	V	Mn	Co	Ni	Cu	Zn	Ga	Ge	As	Se	Br	Rb	Sr	Y	Zr	Nb	Mo	Ru
Sample #1	389	-20	4415575	36	322	1369	696	5	33	21	-10	-1	-1	20	-30	1861	94	6168	2	3	-1	66	-1

- lime stone Till

Step Bank

Normal Assay

Same Sample

page 13 - 14 - 15

13

40

Enzyme Leach J
Trace Element V
Values = 99999

Sample ID:	Rh	Pd	Ag	Cd	In	Sn	Sb	Te	I	Cs	Ba	La	Ce	Pr	Nd	Sm	Eu	Gd	Tb	Dy	Ho	Er	Tm	Yb	Lu	Hf	Ta	W	Re	Os	Ir	Pt	Au
Sample #1	-1	-1	-0.2	0.7	-0.2	3	3	-1	28	1	164	3	5	1	2	-1	-1	-1	-1	-1	-1	-1	-1	-1	-1	-1	-1	1	-0.1	-1	-1	-1	-0.1

14

15

Enzyme Leach J
Trace Element V
Values = 99999

Sample ID:	S.Q.Hg	Tl	Pb	Bi	Th	U
Sample #1	-1.0	-1	1	-1	2	9

15

4a

Experimental Assay #1

All same sample:

Page 1- 2- 3

- All the same rock
- Limestone, Ironstone (Fort McKay)

MUSKEG RIVER.

UTM N 6332420
E 464110

Fire Assays
Mackay

Saskatchewan
Research Council

①

RE: **Beads and Roasted/Unroasted Ores As Per Your Letter**

Bead #	Dore Wt mg	Au ppm*	Residual Au Bead**	mg Ag by ICP	mg Pb by ICP	µg Au in bead
1	1.95	0.01	No	1.90	–	<0.03
2	2.07	1.82	Yes	2.04	–	5.46
3	2.05	0.12	Yes	1.95	–	0.36
4	0.35	0.06	Yes	0.40	–	0.18
***5	5.05	0.02	Yes	3.09	1.85	0.06

* Au ppm in the original 3g ore sample by AA.
**Residual Au beads left after parting were too small to weigh. We confirmed they were gold by microscopic examination. Bead #1 produced no visible residual Au bead after parting.
***Bead #5 was unusual in appearance. It was dull, flat and very rough. All other beads were typical.

?

In all cases except Bead # 5 the wt in mg of the dore correlated with the mg of Ag determined by ICP on the parting solutions. We analyzed the Bead #5 parting solution for Pb, Pt, and Pd to determine it's composition and account for the high dore weight. No Pt or Pd were detected, however, the equivalent of 1.85 mg of Pb was found. The presence of Pb accounts for 97.8% of the original dore #5.

- 3gram assays
- Lime stone Mud stone Brigde by Ft mckay
- Scorification assay
- 30gr Lead 2grm Flour only

Experimental assay

ITS Intertek Testing Services
Bondar Clegg

2

Geochemical Lab Report

ENT: MR. LARRY MACGOUGAN
REPORT: V97-01600.0 (COMPLETE)
PROJECT: NONE GIVEN
DATE RECEIVED: 11-JUL-97
DATE PRINTED: 18-AUG-97
PAGE 3 OF 3

SAMPLE NUMBER	ELEMENT UNITS	AU PPB	PT PPB	PD PPB	Ag PPM
1		17	8	10	<0.1
Duplicate					<0.1

No Pre Leach

R2-2

Same Rock as
2248 PPB Gold

- Iron stone Shale
- Normal assay

Intertek Testing Services
Bondar Clegg

3

Geochemical Lab Report

CLIENT: MR. LARRY MACGOUGAN
REPORT: V97-01600.0 (COMPLETE)
PROJECT: NONE GIVEN
DATE RECEIVED: 11-JUL-97
DATE PRINTED: 18-AUG-97
PAGE 1 OF 3

SAMPLE NUMBER	ELEMENT UNITS	AU PPB	PT PPB	PD PPB	Ag PPM
R2 1		17	8	10	<0.1
R2 2		2248	115	18	<0.1

- Iron stone

1# Normal assay

2# (A) Leach 30gram ore
(B) Send Leach Residue To Bondar Clegg
Experimental assay
Calculated Back To 30gram start

45

EXPERIMENTAL ASSAY #3

Same Sample:

Page 1-7;	SEM of Leach Residual
Page 8;	Fire Leach Residue

SAME AS EXPERIMENTAL ASSAY #1

UTM N 6332420
E 464110

MUSKEG RIVER.

ARC
Alberta Research Council Analytical Services

250 Karl Clark Road
Edmonton, Alberta T6N1E4
Tel. (403) 450-5429
Fax. (403) 450-5477

sample ??

1

[illegible]ate : 08/06/98
Time : 2:48:33PM

Spectrum: 10a Folder: MacGOUGAN

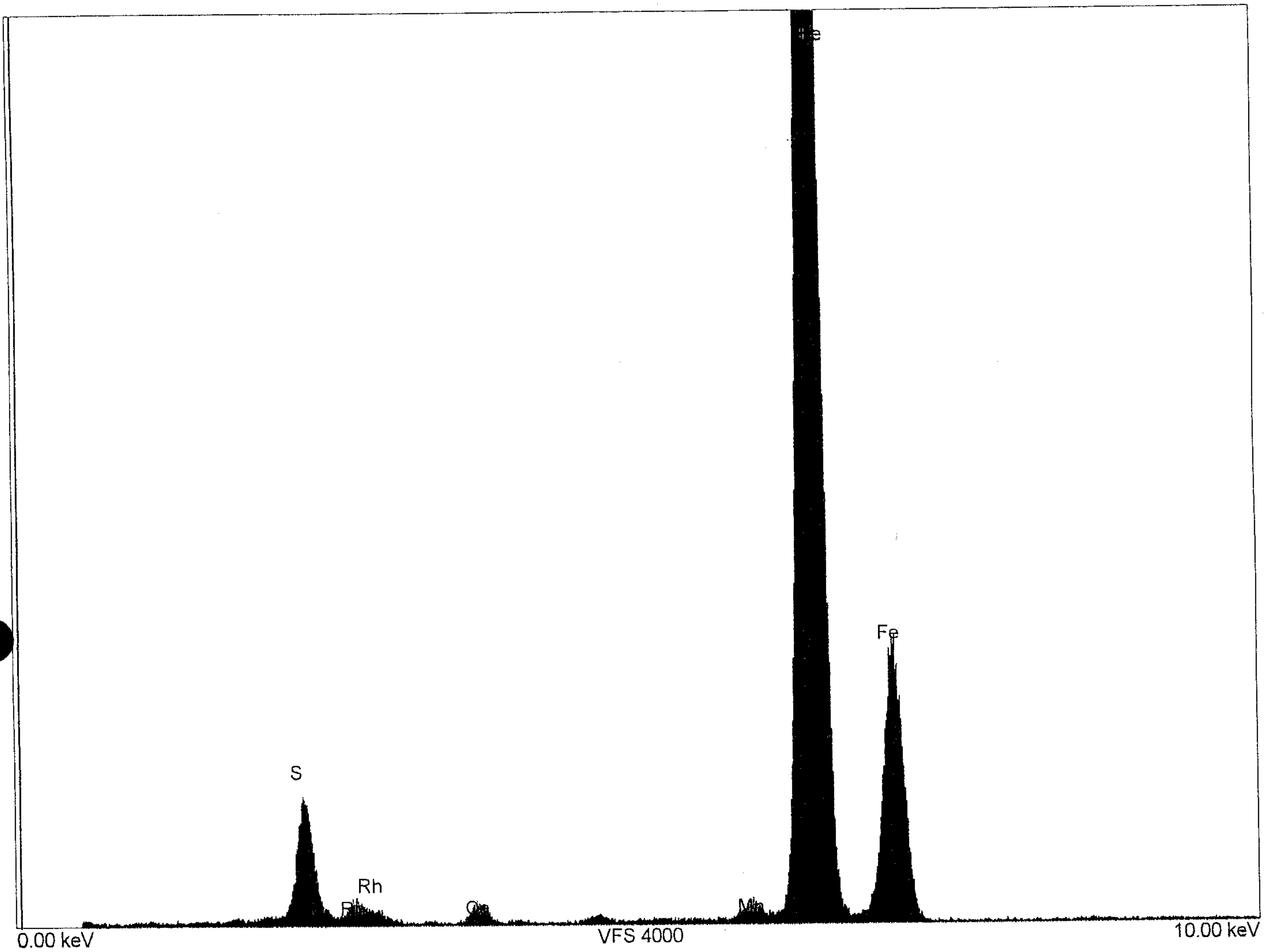

Acquisition parameters

Current	20 µA
Voltage	38 kV
Filter	1 - --
Station	2
Range	20 keV
L.Time	50 sec
CPS	4918
D.Time	44 %
Tube	Direct
Collimator	4
Througput	Low
Atmosphere	Vacuum
Date	08/06/98
Time	2:44:30PM

ROI information
Not defined

Overlap information

No overlaps

Acquisition status

Current proc.
Current batch

Voltage	0.0 kV
Emission curr.	1.0 µA
Filament curr.	4.6 A
Zero DAC	108
Zero Shift	-1
Zero Width	101
Gain DAC	120
Temperature	27 °C
Vacuum level	1539
Nitrogen level	30 %

Cursor information
Position: 0.04 keV Counts: 0

9A 7

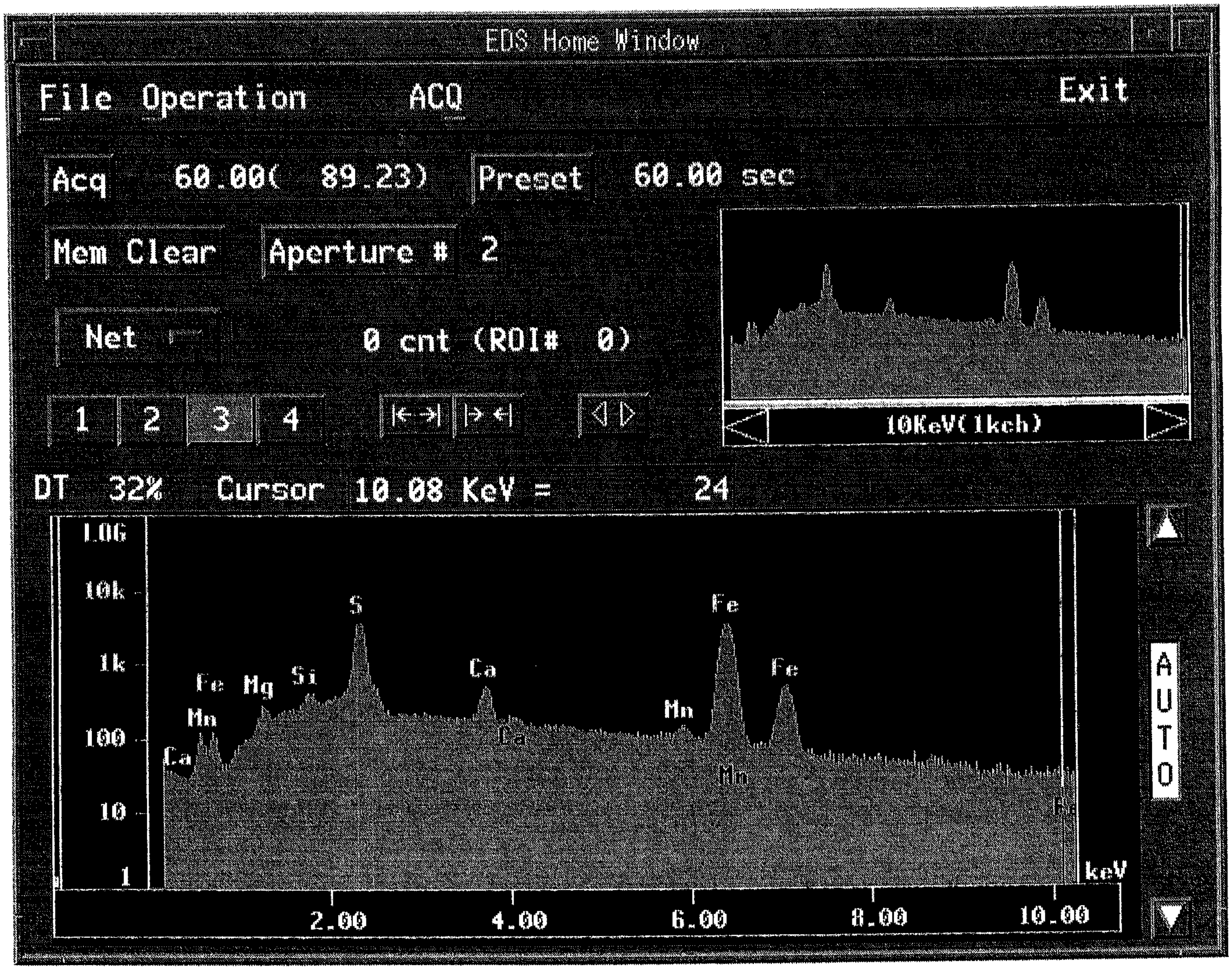

Acq 60.00(89.23) Preset 60.00 sec

Aperture # 2

0 cnt (ROI# 0)

DT 32% Cursor 10.08 KeV = 24

9A 3

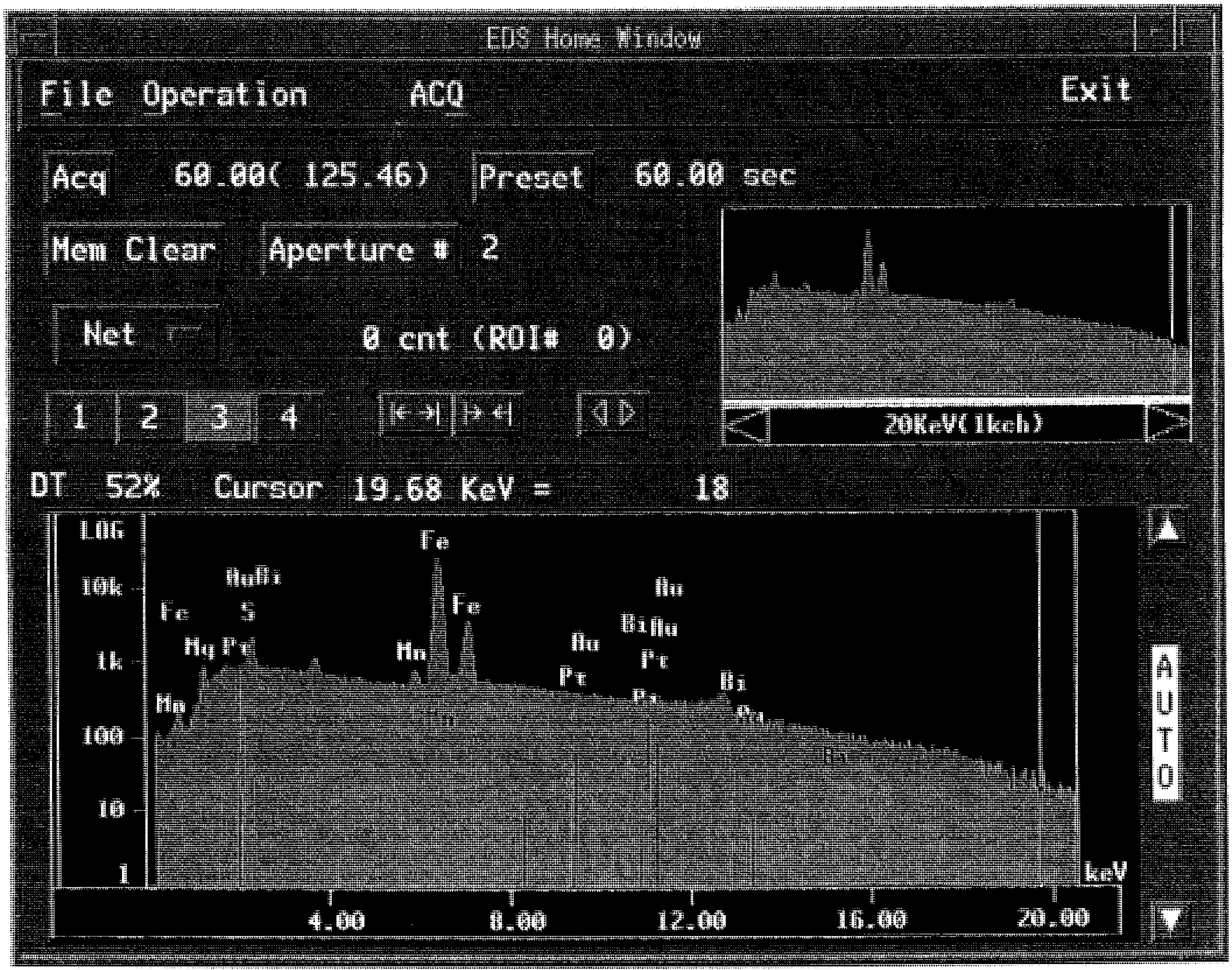

Acq 60.00(125.46) Preset 60.00 sec

Aperture # 2

0 cnt (ROI# 0)

DT 52% Cursor 19.68 KeV = 18

9A 4

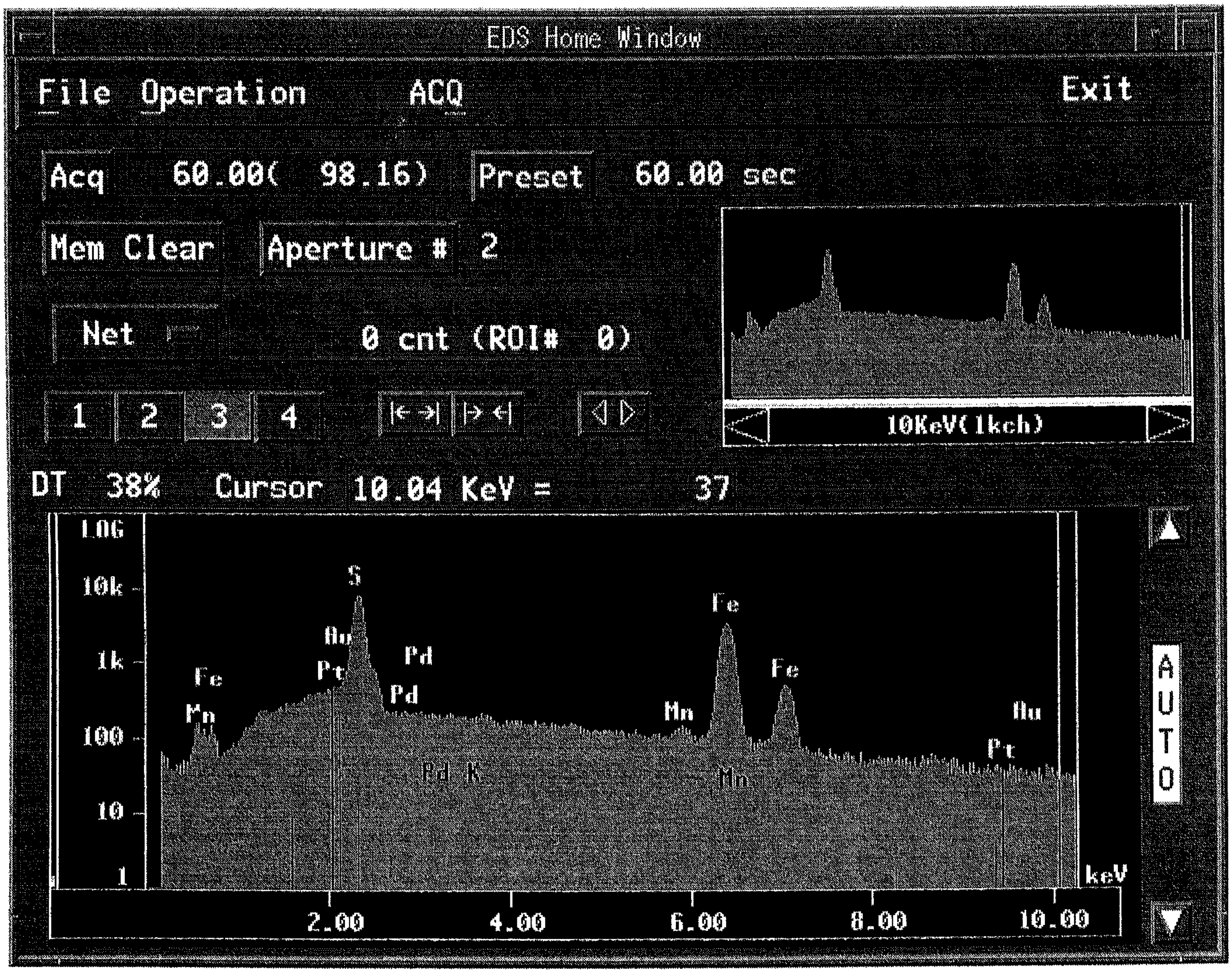

EDS Home Window

Acq 60.00(98.16)

Preset 60.00 sec

Aperture # 2

Net 0 cnt (ROI# 0)

DT 38% Cursor 10.04 KeV = 37

5

9A

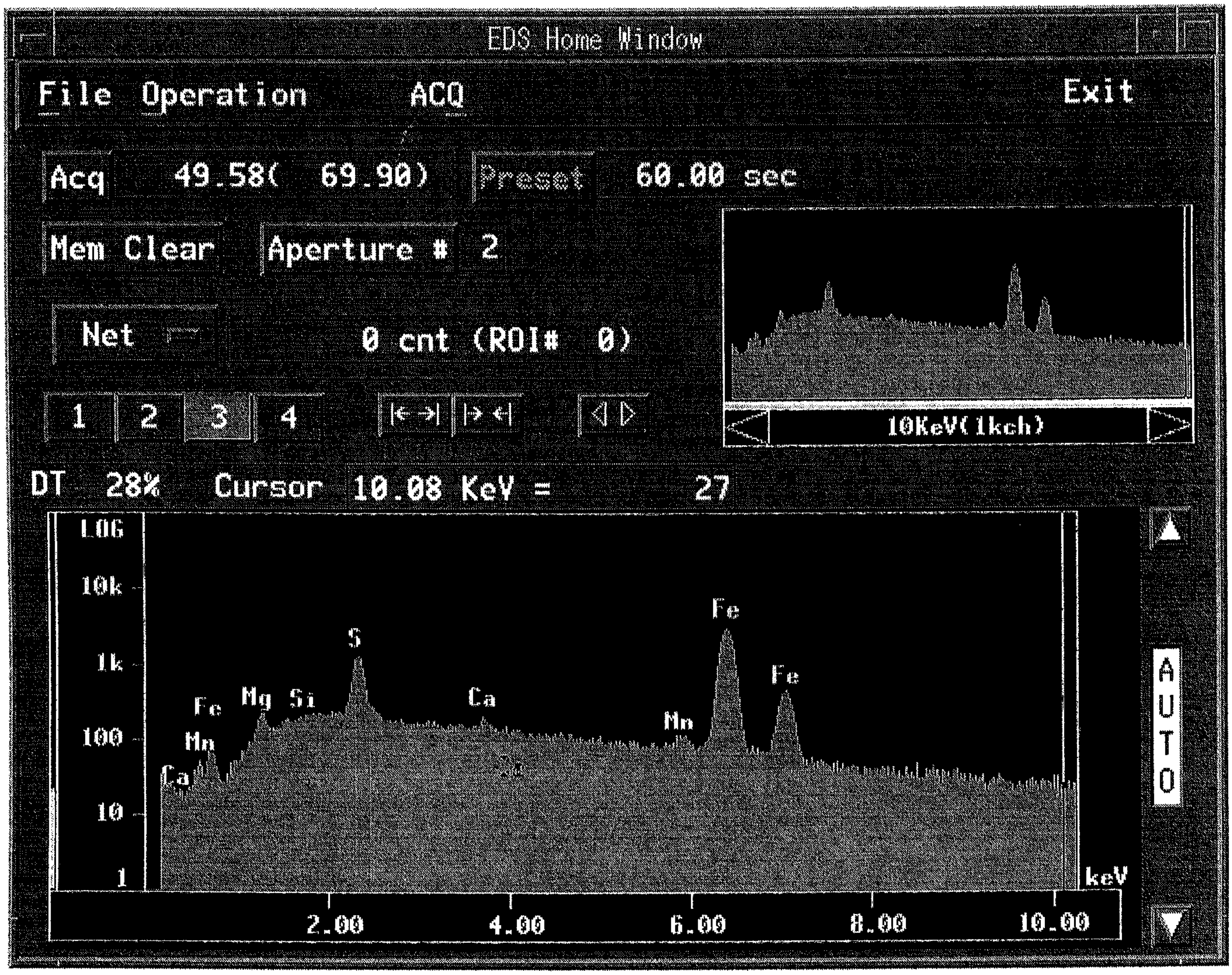

Acq 49.58(69.90) Preset 60.00 sec

Aperture # 2

0 cnt (ROI# 0)

DT 28% Cursor 10.08 KeV = 27

6 9A

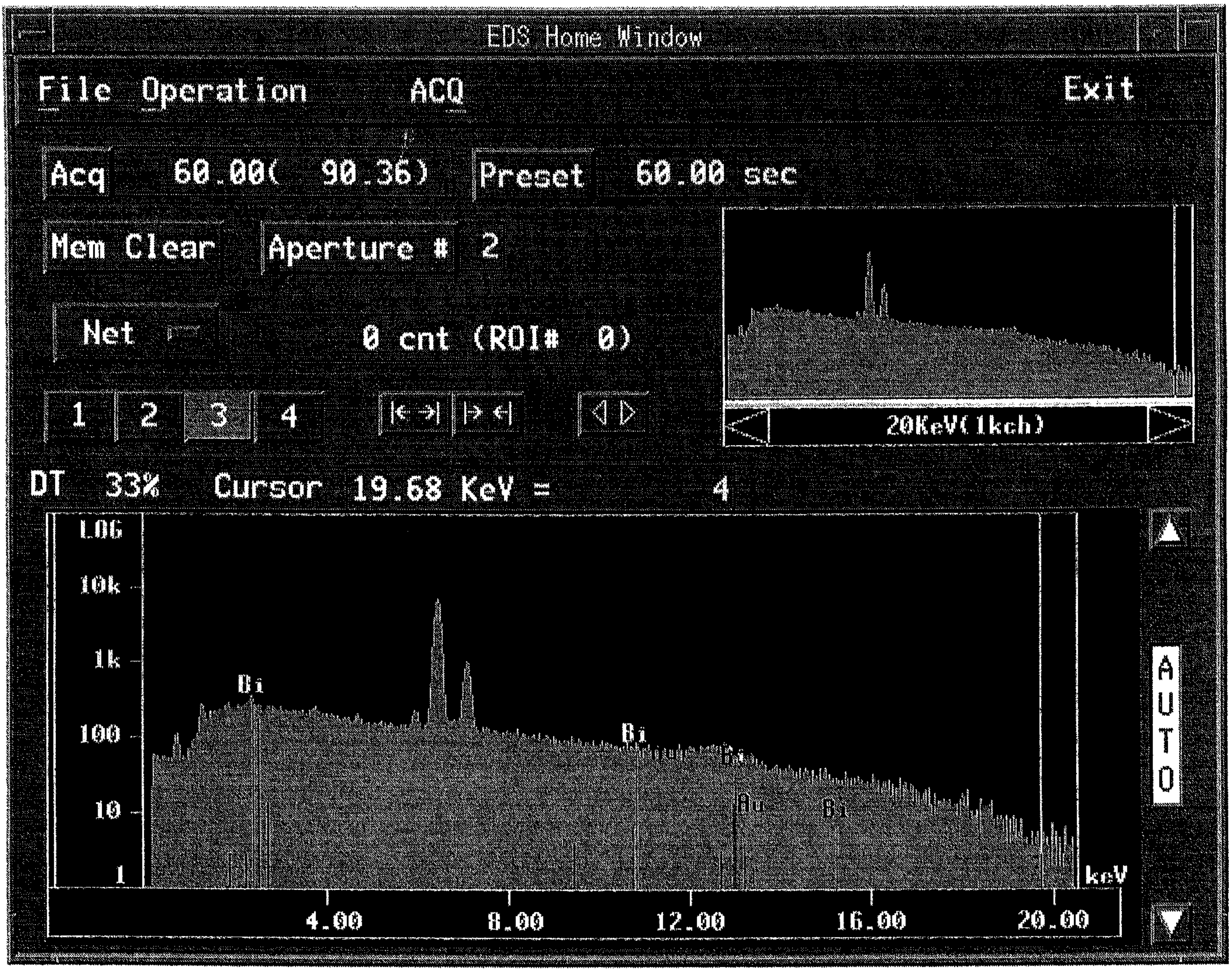

Acq 60.00(90.36) Preset 60.00 sec

Aperture # 2

Net 0 cnt (ROI# 0)

DT 33% Cursor 19.68 KeV = 4

7

9A

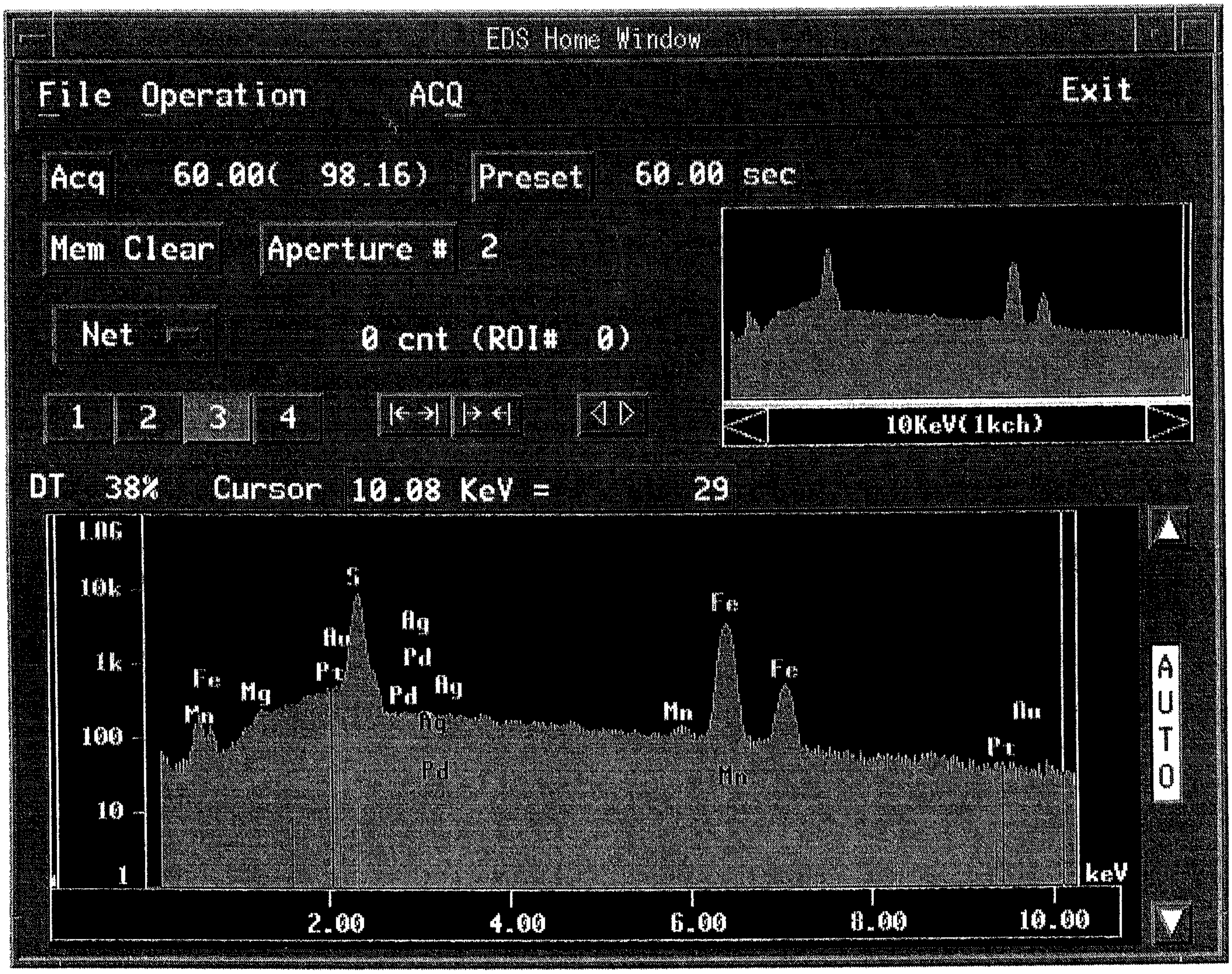

Acq 60.00(98.16) Preset 60.00 sec

Aperture # 2

0 cnt (ROI# 0)

DT 38% Cursor 10.08 KeV = 29

8

Saskatchewan Research Council Geoanalytical Services
125-15 Innovation Blvd., Saskatoon, SK., S7N 2X8
Phone:306-933-5426 Fax:306-933-5656

M273 MACGOUGAN JUNE 25/98 (3)

1 Au ppb ICP
2 Pt ppb ICP
3 Pd ppb ICP
4 Pd ppm AA
5
6
7
8
9

* = NI SULFIDE FUSION
** = NORMAL FIRE ASSAY

	Au	Pt	Pd	Pd
* 11A	<10	30	4200	<0.05
* 13A	<10	30	4150	<0.05
** LARRY 1	<1	3	<1	<0.05

Pre

EXPERIMENTAL ASSAY #5

Same Samples:

Page 1-2-3;	Roasted Beads
Page 4-5-6;	Roasted Beads
Page 7-8-9;	Roasted Beads
Page 10-11-12;	Roasted Beads
Page 13;	Roasted Beads
Page 14;	Roasted Beads
Page 15-16;	Roasted Beads
Page 17-18;	Roasted Beads
Page 19-20;	Roasted Beads
Page 21-22;	Roasted Beads
Page 23;	Roasted Beads
Page 24;	Roasted Beads
Page 25;	Roasted Beads
pages 26-28	Roasted Beads

UTM N 6315100
E 482505

```
Spectrum file : ILM30
#1.                                         LIVETIME(spec.)=   200
 ENERGY     RES      AREA
     7.4   71.96   103100
 OTAL AREA=   856943
...
Peak at    .36 keV omitted?
Peak at    .92 keV omitted?
Peak at   5.40 keV omitted?
FIT INDEX= 3.07

ELMT        APP.CONC    ERROR(WT%)
P K : 0      4.079        .070
SiK : 1       .183        .029
S K : 3      1.250        .038
PbM : 1      -.336        .094* < 2 Sigma*Not used for quantitation
PbL : 1      1.924        .481
FeK : 1     34.251        .179
NiK : 1      4.396        .120
CuK : 1     69.330        .345

ZAF CALCULATIONS


...[ 3 iterations]

20.00 kV  TILT =    .00 ELEV = 35.00 AZIM =    .00 COSINE = 1.000

Spectrum: #1                                        CHEM.&MATERIALS ENG.

 ll elmts analysed,NORMALISED

ELMT   ZAF Ratio %ELMT          Error          ATOM.%
P K : 0  .824    4.201 +-      .072            7.953
SiK : 1  .515     .302 +-      .048             .630
S K : 3  .825    1.285 +-      .039            2.351
PbL : 1  .697    2.343 +-      .585             .663
FeK : 1 1.104   26.316 +-      .138           27.627
NiK : 1  .991    3.765 +-      .103            3.760
CuK : 1  .952   61.789 +-      .307           57.016
TOTAL          100.000                       100.000
---------------------------------------------------------------------------
```

1

3 Beads
B. Pen

001 HCL
Si Breakdown

2

```
Spectrum file : ILM30
#1                                         LIVETIME(spec.)=   200
 ENERGY     RES      AREA
     7.4   71.96   103100
  TAL AREA=    856943
...
Peak at     .36 keV omitted?
Peak at     .92 keV omitted?
Peak at    5.40 keV omitted?
FIT INDEX= 3.00

ELMT         APP.CONC    ERROR(WT%)
P K : 0      4.079        .070
SiK : 1       .183        .029
S K : 3      1.250        .038
PbM : 1     -.336         .094* < 2 Sigma*Not used for quantitation
PbL : 1      1.928        .481
FeK : 1     34.251        .179
NiK : 1      4.397        .120
CuK : 1     69.328        .345
AuL : 1       .237        .319* < 2 Sigma*
PtL : 1       .008        .343* < 2 Sigma*

ZAF CALCULATIONS


...[ 3 iterations]

20.00 kV  TILT =    .00 ELEV = 35.00 AZIM =    .00 COSINE = 1.000

  ectrum: #1                                    CHEM.&MATERIALS ENG.

All elmts analysed,NORMALISED

ELMT    ZAF Ratio %ELMT         Error          ATOM.%
P K : 0   .825     4.184 +-     .072             7.945
SiK : 1   .516      .301 +-     .048              .629
S K : 3   .824     1.284 +-     .039             2.355
PbL : 1   .697     2.340 +-     .583              .664
FeK : 1 1.104     26.259 +-     .137            27.648
NiK : 1   .991     3.753 +-     .103             3.759
CuK : 1   .952    61.589 +-     .306            57.000
AuL : 1   .711      .282 +-     .379 <1 sd , below confidence limit
PtL : 1   .709      .009 +-     .409 <1 sd , below confidence limit
TOTAL             99.709                       100.000
-----------------------------------------------------------------------------
```

3

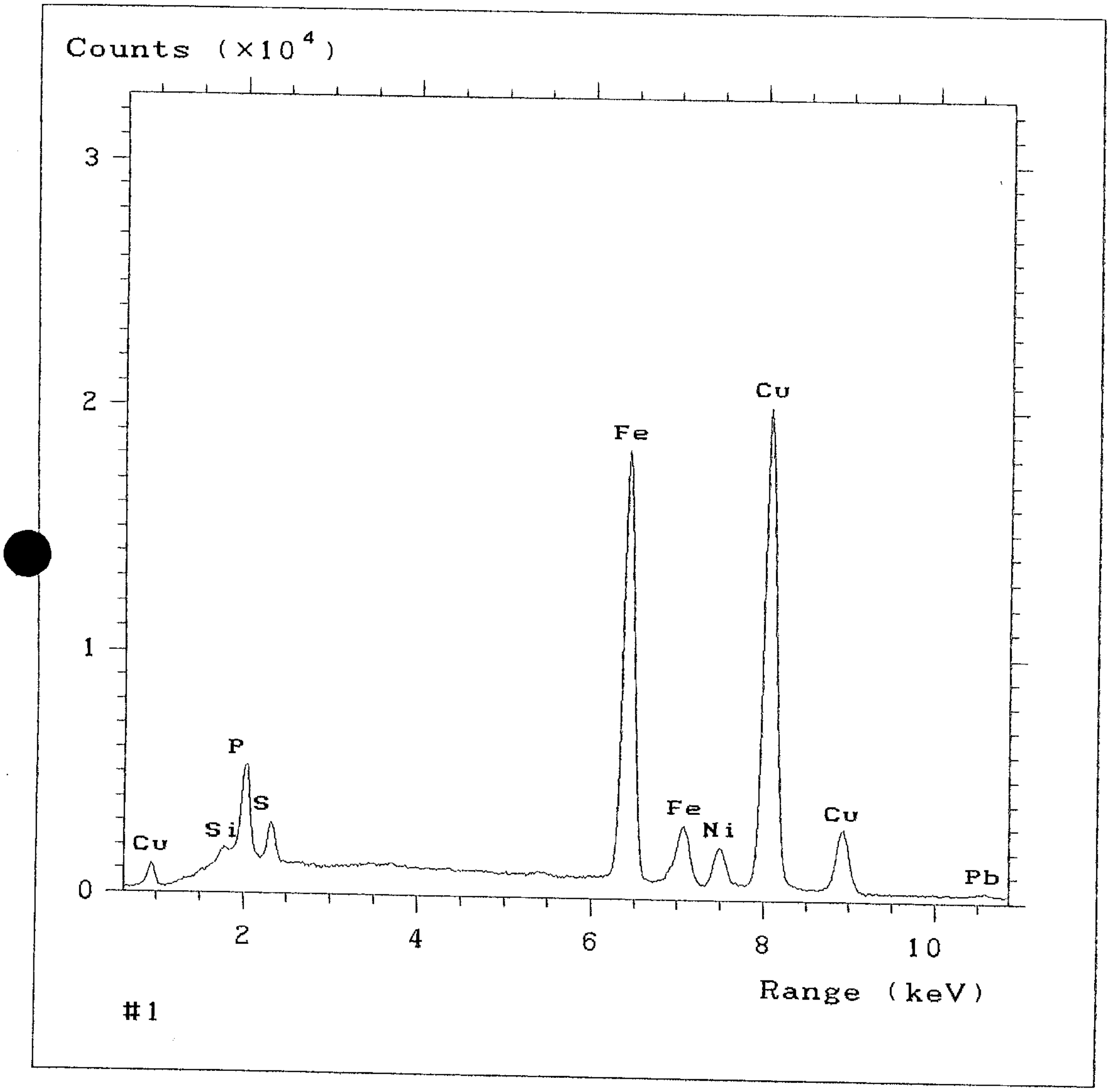

4

```
Spectrum file : ILM31
#2                                        LIVETIME(spec.)=   200
 ENERGY     RES      AREA
    7.5    71.77     97780
TOTAL AREA=    826514
...
Peak at     .38 keV omitted?
Peak at    5.40 keV omitted?
FIT INDEX= 3.52

ELMT         APP.CONC    ERROR(WT%)
P K  :  0       .177      .048
AlK  :  1      1.034      .034
SiK  :  1      6.357      .047
TiK  :  1       .214      .040
FeK  :  1     77.853      .251
CuK  :  1       .169      .087* < 2 Sigma*

ZAF CALCULATIONS


...[ 3 iterations]

20.00 kV  TILT =    .00 ELEV = 35.00 AZIM =    .00 COSINE = 1.000

Spectrum: #2                                   CHEM.&MATERIALS ENG.

All elmts analysed,NORMALISED

[illegible]MT   ZAF Ratio %ELMT          Error         ATOM.%
P K  :  0   .819      .229 +-      .062              .362
AlK  :  1   .446     2.455 +-      .080             4.443
SiK  :  1   .576    11.692 +-      .087            20.324
TiK  :  1  1.023      .222 +-      .042              .226
FeK  :  1   .968    85.192 +-      .275            74.484
CuK  :  1   .854      .210 +-      .108 <2 sd        .161
TOTAL             100.000                         100.000
--------------------------------------------------------------------------
```

001 14A

5

```
Spectrum file : ILM31
#2                                              LIVETIME(spec.)=    200
 ENERGY     RES       AREA
-   7.5    71.77     97780
TOTAL AREA=    826514
...
Peak at     .38 keV omitted?
Peak at    5.40 keV omitted?
FIT INDEX= 1.96

ELMT          APP.CONC     ERROR(WT%)
P  K  : 0       .177        .048
AlK   : 1      1.034        .034
SiK   : 1      6.357        .047
TiK   : 1       .214        .040
FeK   : 1     77.853        .251
CuK   : 1       .170        .087*  <  2 Sigma*
PtL   : 1       .004        .327*  <  2 Sigma*
AuL   : 1      -.296        .296*  <  2 Sigma*

ZAF CALCULATIONS


...[ 3 iterations]

20.00 kV   TILT =     .00 ELEV = 35.00 AZIM =    .00 COSINE = 1.000

Spectrum: #2
                                                   CHEM.&MATERIALS ENG.

All elmts analysed,NORMALISED

ELMT    ZAF Ratio  %ELMT           Error           ATOM.%
P K  : 0   .819       .229  +-    .062              .362
AlK  : 1   .446      2.455  +-    .080             4.443
SiK  : 1   .576     11.691  +-    .087            20.324
TiK  : 1  1.023       .222  +-    .042              .226
FeK  : 1   .968     85.186  +-    .275            74.484
CuK  : 1   .854       .210  +-    .108  <2 sd       .162
PtL  : 1   .685       .006  +-    .506  <1 sd  , below confidence limit
AuL  : 1   .686      -.431  +-    .431  <2 sd  , warning -ve conc. not in totals
TOTAL               99.994                        100.000
-------------------------------------------------------------------------------
```

6

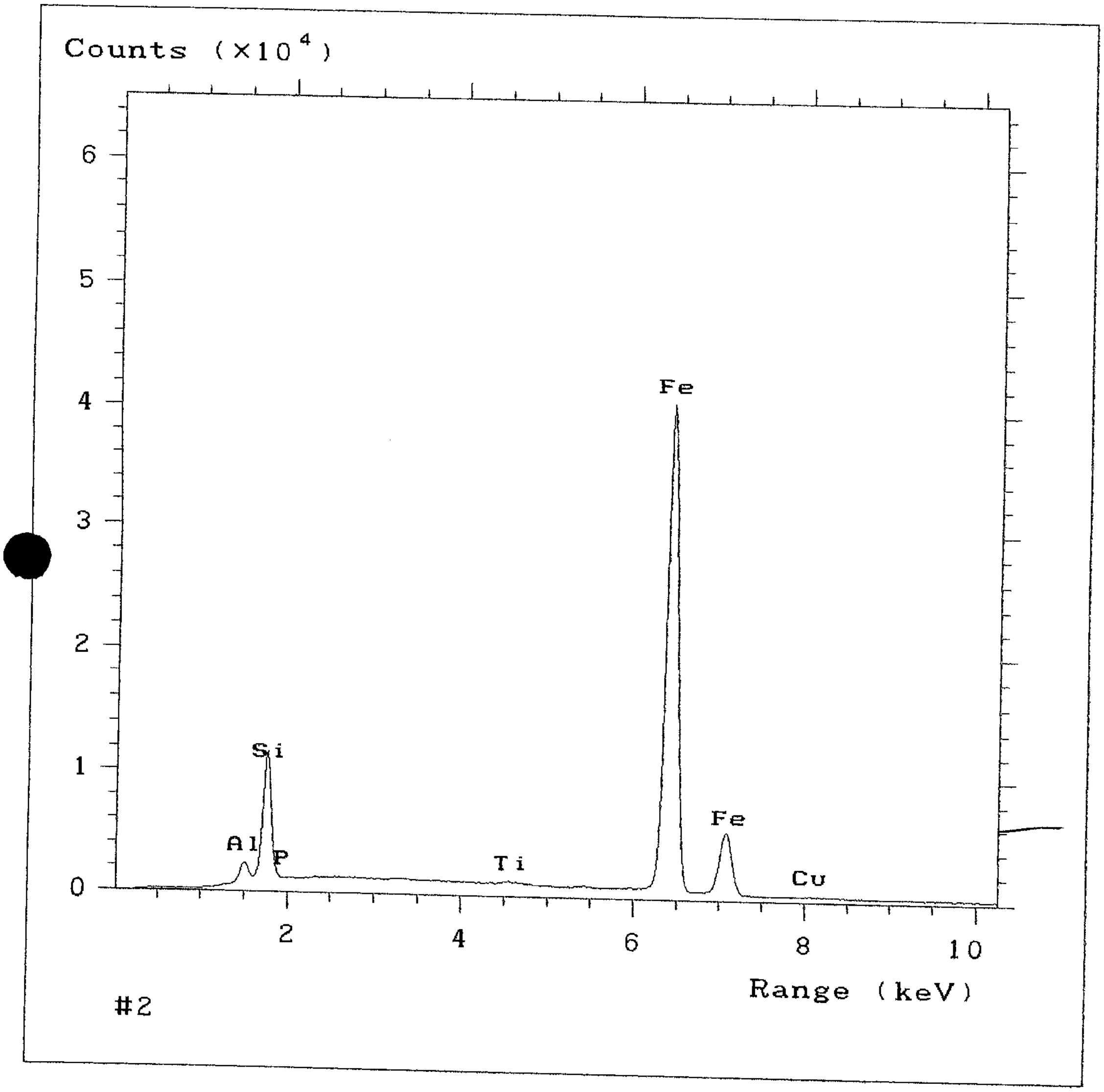

```
Spectrum file : ILM33                                                    7
#4                                 LIVETIME(spec.)=    200
 ENERGY       RES       AREA
    7.5     72.02     124954
 OTAL AREA=   1011410
...
Peak at      .36 keV omitted?
Peak at      .92 keV omitted?
FIT INDEX=11.79

ELMT         APP.CONC     ERROR(WT%)
P K : 0       7.260         .090
S K : 3       3.241         .049
FeK : 1      87.498         .266
CuK : 1      15.688         .189

ZAF CALCULATIONS


...[ 3 iterations]

20.00 kV   TILT =     .00 ELEV = 35.00 AZIM =     .00 COSINE = 1.000

Spectrum: #4                                      CHEM.&MATERIALS ENG.

All elmts analysed,NORMALISED

ELMT     ZAF Ratio  %ELMT           Error          ATOM.%
P K : 0   .890      6.941 +-        .086           11.794
S K : 3   .856      3.222 +-        .048            5.288
FeK : 1   .998     74.647 +-        .227           70.337
CuK : 1   .879     15.191 +-        .183           12.581
TOTAL             100.000                         100.000
---------------------------------------------------------------------------
```

001 - Sur P
- Carbon B

Bic Pen
2 Burn

8

```
Spectrum file : ILM33
#4                                      LIVETIME(spec.)=    200
 ENERGY      RES       AREA
-   7.5     72.02     124954
[illegible]TAL AREA=   1011410
...
Peak at      .36 keV omitted?
Peak at      .92 keV omitted?
FIT INDEX= 5.68

ELMT         APP.CONC     ERROR(WT%)
P K  :  0     7.260        .090
S K  :  3     3.241        .049
FeK  :  1    87.498        .266
CuK  :  1    15.687        .189
PtL  :  1     -.284        .351* < 2 Sigma*
AuL  :  1     -.130        .322* < 2 Sigma*

ZAF CALCULATIONS


...[ 3 iterations]

20.00 kV  TILT =    .00 ELEV = 35.00 AZIM =    .00 COSINE = 1.000

Spectrum: #4                                 CHEM.&MATERIALS ENG.

All elmts analysed,NORMALISED

E[illegible]T    ZAF Ratio  %ELMT          Error          ATOM.%
[illegible] :  0   .890      6.941 +-     .086           11.794
S K  :  3   .856      3.222 +-     .048            5.288
FeK  :  1   .998     74.648 +-     .227           70.337
CuK  :  1   .879     15.190 +-     .183           12.581
PtL  :  1   .694      -.409 +-     .506 <1 sd , warning -ve conc. not in totals
AuL  :  1   .695      -.188 +-     .463 <1 sd , warning -ve conc. not in totals
TOTAL                100.000                     100.000
---------------------------------------------------------------------------------
```

9

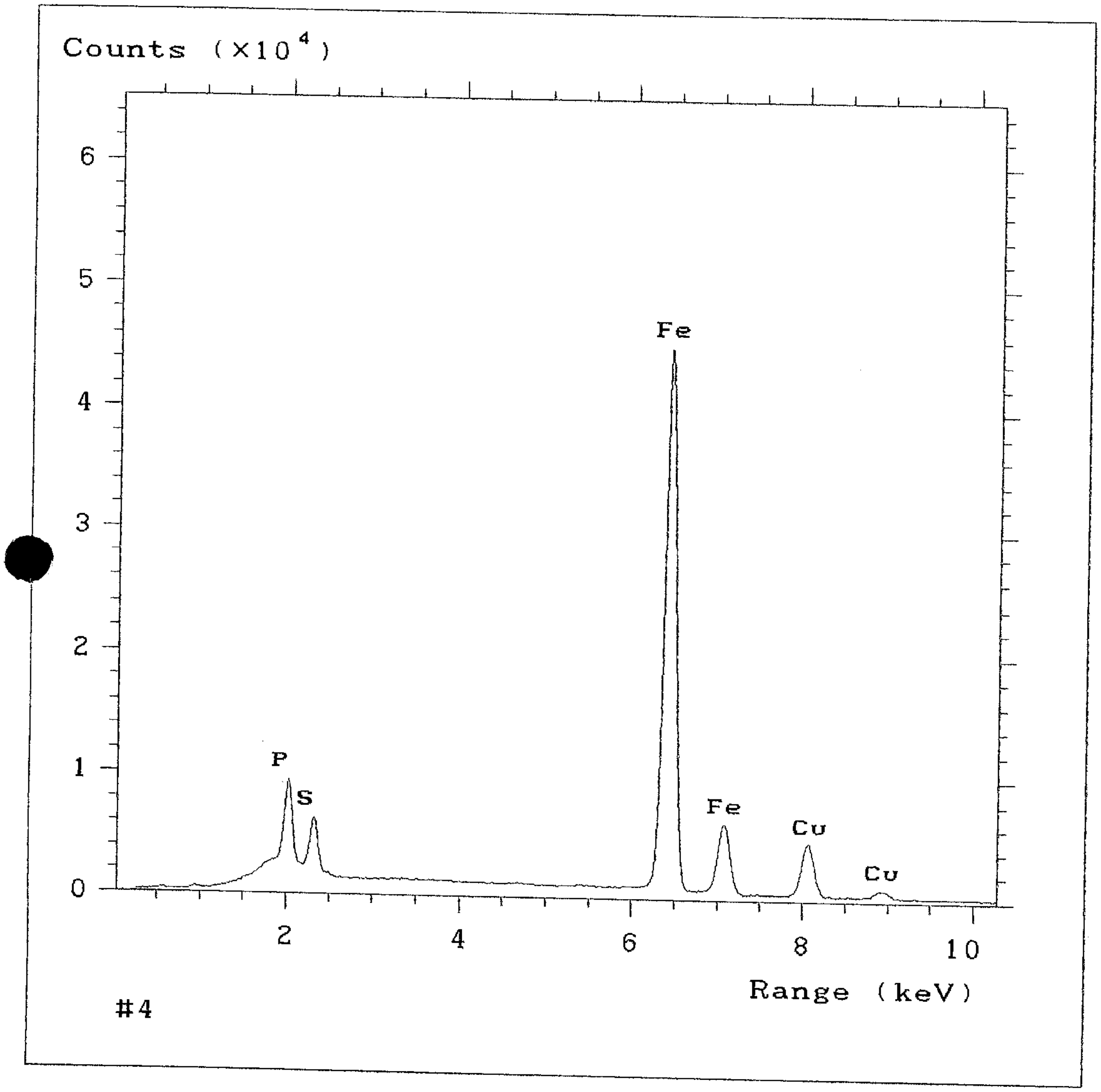

10

```
Spectrum file : ILM34
#5                                         LIVETIME(spec.)=    200
 ENERGY      RES       AREA
    7.6    72.71     131297
TOTAL AREA=   1085944
...
Peak at     .36 keV omitted?
Peak at    2.32 keV omitted?
Peak at    3.64 keV omitted?
Peak at    5.42 keV omitted?
Peak at   12.78 keV omitted?
FIT INDEX= 7.79

ELMT         APP.CONC    ERROR(WT%)
SiK : 1        .359       .022
FeK : 1   130.730         .288

ZAF CALCULATIONS


...[ 3 iterations]

20.00 kV   TILT =     .00 ELEV = 35.00 AZIM =    .00 COSINE = 1.000

Spectrum: #5                                    CHEM.&MATERIALS ENG.

All elmts analysed,NORMALISED

ELMT    ZAF Ratio %ELMT         Error          ATOM.%
 iK : 1   .561       .486 +-    .029              .962
FeK : 1   .999     99.514 +-    .219            99.038
TOTAL             100.000                      100.000
----------------------------------------------------------------------------
```

Nit -

11

```
Spectrum file : ILM34
#5                                      LIVETIME(spec.)=   200
 ENERGY     RES      AREA
-   7.6   72.71   131297
TOTAL AREA=  1085944
...
Peak at    .36 keV omitted?
Peak at   2.32 keV omitted?
Peak at   3.64 keV omitted?
Peak at   5.42 keV omitted?
FIT INDEX= 2.54

ELMT        APP.CONC    ERROR(WT%)
SiK : 1       .359       .022
FeK : 1   130.731       .288
PtL : 1       .173       .316* < 2 Sigma*
AuL : 1      -.028       .297* < 2 Sigma*

ZAF CALCULATIONS


..[ 2 iterations]

20.00 kV  TILT =    .00 ELEV = 35.00 AZIM =    .00 COSINE = 1.000

Spectrum: #5                                    CHEM.&MATERIALS ENG.

All elmts analysed,NORMALISED

ELMT    ZAF Ratio %ELMT          Error        ATOM.%
SiK : 1  .562      .485 +-     .029            .962
FeK : 1  .999    99.233 +-     .219          99.038
PtL : 1  .701      .187 +-     .342 <1 sd , below confidence limit
AuL : 1  .702     -.040 +-     .423 <1 sd , warning -ve conc. not in totals
TOTAL            99.718                      100.000
----------------------------------------------------------------------------
```

12

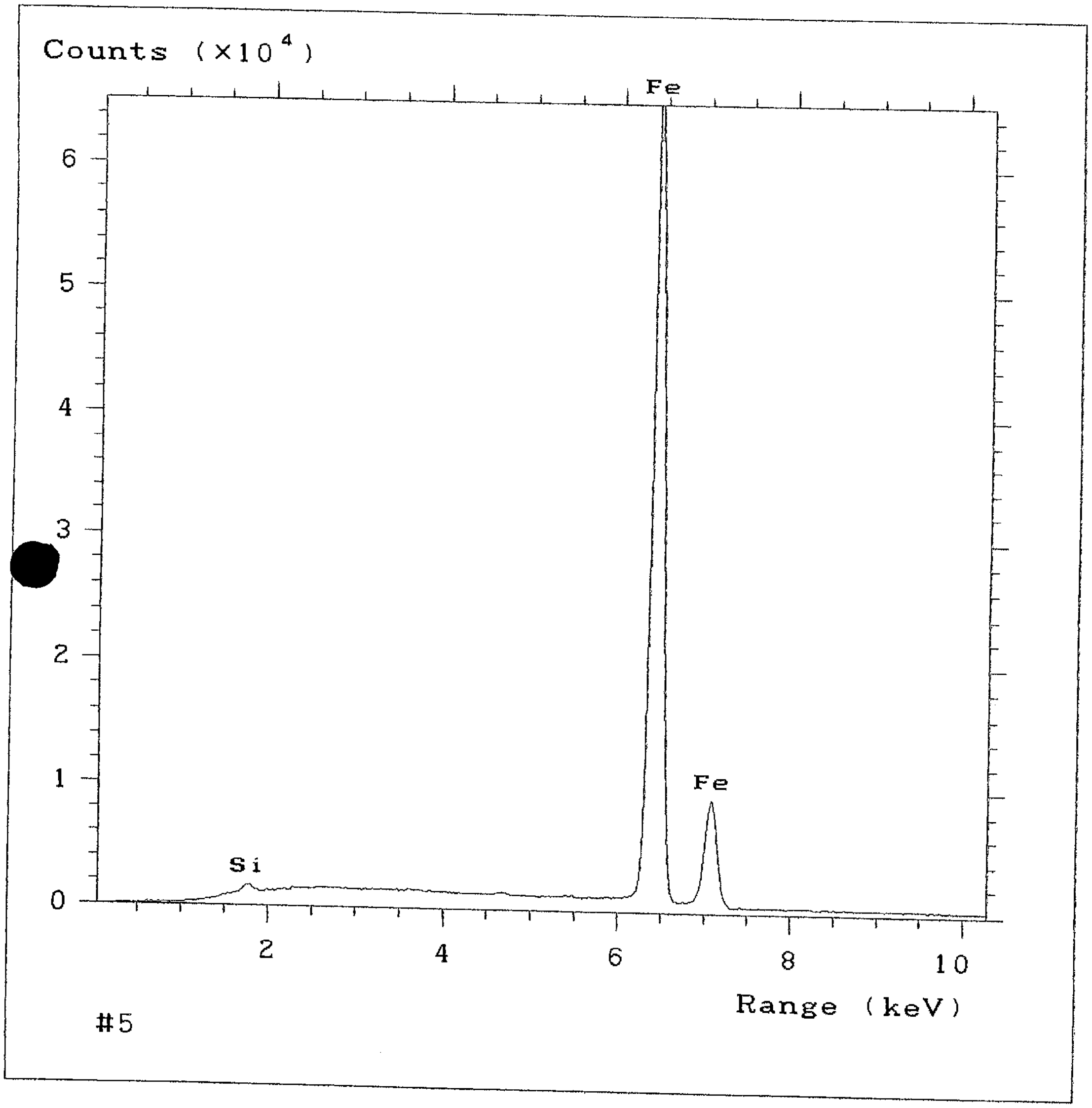

13

```
Spectrum file : ILM50
#3                                        LIVETIME(spec.)=    200
 ENERGY      RES       AREA
    7.5     71.67      94833
TOTAL AREA=    785814
...
Peak at     .14 keV omitted?
Peak at     .38 keV omitted?
Peak at    3.68 keV omitted?
FIT INDEX=16.89

ELMT         APP.CONC    ERROR(WT%)
P K : 0      11.785        .093
FeK : 1      77.518        .248
NiK : 1        .181        .070
CuK : 1        .210        .079

ZAF CALCULATIONS


..[ 2 iterations]

20.00 kV  TILT =    .00 ELEV = 35.00 AZIM =    .00 COSINE = 1.000

Spectrum: #3                                   CHEM.&MATERIALS ENG.

All elmts analysed,NORMALISED

ELMT    ZAF Ratio %ELMT          Error           ATOM.%
  K : 0   .921    13.792 +-     .109             22.399
FeK : 1   .974    85.726 +-     .275             77.203
NiK : 1   .883      .221 +-     .085 <3 sd         .189
CuK : 1   .860      .263 +-     .099 <3 sd         .208
TOTAL            100.002                        100.000
-----------------------------------------------------------------------------------
```

001
HCL
carbon
Blue

14

```
Spectrum file : ILM51
#4                                            LIVETIME(spec.)=   200
 ENERGY     RES      AREA
    7.5   71.82    102853
TOTAL AREA=    853198
...
Peak at    .16 keV omitted?
Peak at    .38 keV omitted?
FIT INDEX= 2.55

ELMT        APP.CONC    ERROR(WT%)
P K  :  0    2.395       .059
AlK  :  1     .094       .024
SiK  :  1     .332       .028
CaK  :  3     .445       .037
CrK  :  1     .628       .053
MnK  :  1     .193       .061
FeK  :  1   95.198       .275
CuK  :  1     .116       .083* < 2 Sigma*

ZAF CALCULATIONS


..[ 2 iterations]

20.00 kV  TILT =    .00 ELEV = 35.00 AZIM =    .00 COSINE = 1.000

Spectrum: #4                                      CHEM.&MATERIALS ENG.

All elmts analysed,NORMALISED

ELMT    ZAF Ratio  %ELMT          Error          ATOM.%
P K  :  0   .890    2.671  +-     .066            4.671
AlK  :  1   .425     .220  +-     .055             .441
SiK  :  1   .567     .581  +-     .049            1.121
CaK  :  3 1.188      .372  +-     .031             .503
CrK  :  1 1.243      .501  +-     .042             .522
MnK  :  1   .969     .198  +-     .062             .195
FeK  :  1   .991   95.325  +-     .275           92.434
CuK  :  1   .866     .133  +-     .095  <2 sd      .114
TOTAL              100.001                       100.000
-------------------------------------------------------------------------------
```

008
nothing

15

```
Spectrum file : ILM41
#4                                   LIVETIME(spec.)=   500
 ENERGY     RES      AREA
-     7.4   71.68   243697
TOTAL AREA=  2004489
...
Peak at    .38 keV omitted?
FIT INDEX=15.41

ELMT        APP.CONC     ERROR(WT%)
SiK : 1     15.087        .035
TiK : 1      2.288        .027
CrK : 1       .412        .027
FeK : 1     67.211        .132

ZAF CALCULATIONS


...[ 3 iterations]

20.00 kV  TILT =    .00 ELEV = 35.00 AZIM =    .00 COSINE = 1.000

Spectrum: #4                                       CHEM.&MATERIALS ENG.

All elmts analysed,NORMALISED

ELMT    ZAF Ratio %ELMT         Error         ATOM.%
SiK : 1  .617     24.788 +-     .057          39.452
TiK : 1  .976      2.379 +-     .028           2.221
CrK : 1 1.085       .385 +-     .025            .331
FeK : 1  .941     72.448 +-     .143          57.995
TOTAL            100.000                     100.000
----------------------------------------------------------------------------
```

16

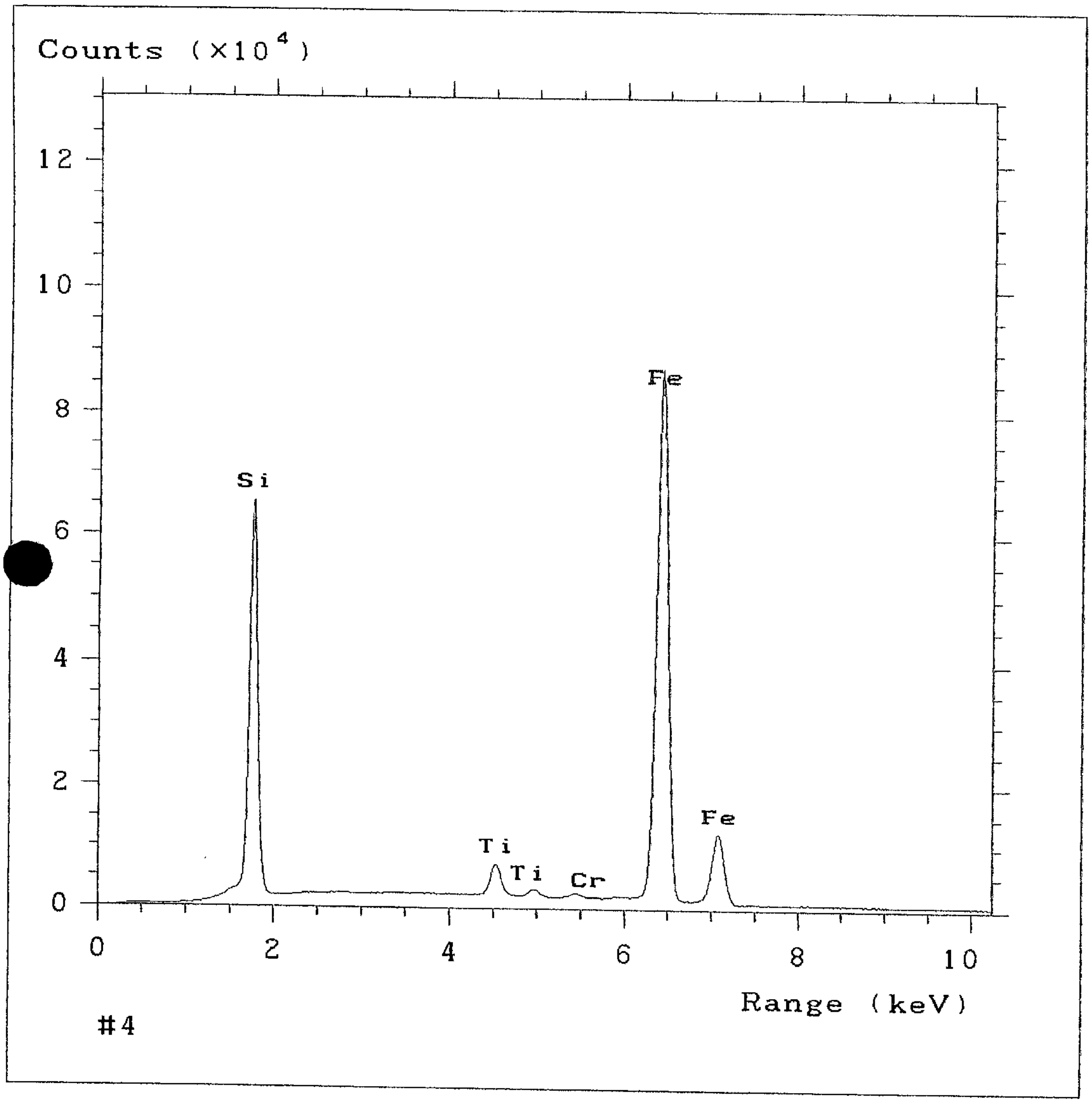

```
Spectrum file : ILM20
Black Powder                              LIVETIME(spec.)=   300
 ENERGY     RES       AREA
-   7.7    72.22    163121
TOTAL AREA=   1334273
...
Peak at     .36 keV omitted?
Peak at     .56 keV omitted?
FIT INDEX=**.**

ELMT         APP.CONC    ERROR(WT%)
SrL  : 0       .264       .082
S  K : 3     34.591       .095
CrK  : 1       .226       .033
FeK  : 1      7.685       .078
NiK  : 1     19.490       .139

ZAF CALCULATIONS


..[ 2 iterations]

20.00 kV  TILT =    .00 ELEV = 35.00 AZIM =    .00 COSINE = 1.000

Spectrum: Black Powder                                CHEM.&MATERIALS ENG.

All elmts analysed,NORMALISED

ELMT    ZAF Ratio %ELMT          Error        ATOM.%
SrL  : 0  .730       .539  +-    .167           .248
S K  : 3  .949     54.306  +-    .149         68.284
 rK  : 1  .898       .375  +-    .055           .291
FeK  : 1  .939     12.200  +-    .124          8.806
NiK  : 1  .892     32.580  +-    .233         22.371
TOTAL             100.000                    100.000
--------------------------------------------------------------------------------
```

17

Sans Re

Black

Ni Sn

Ni S Cl Take away

Residue

18

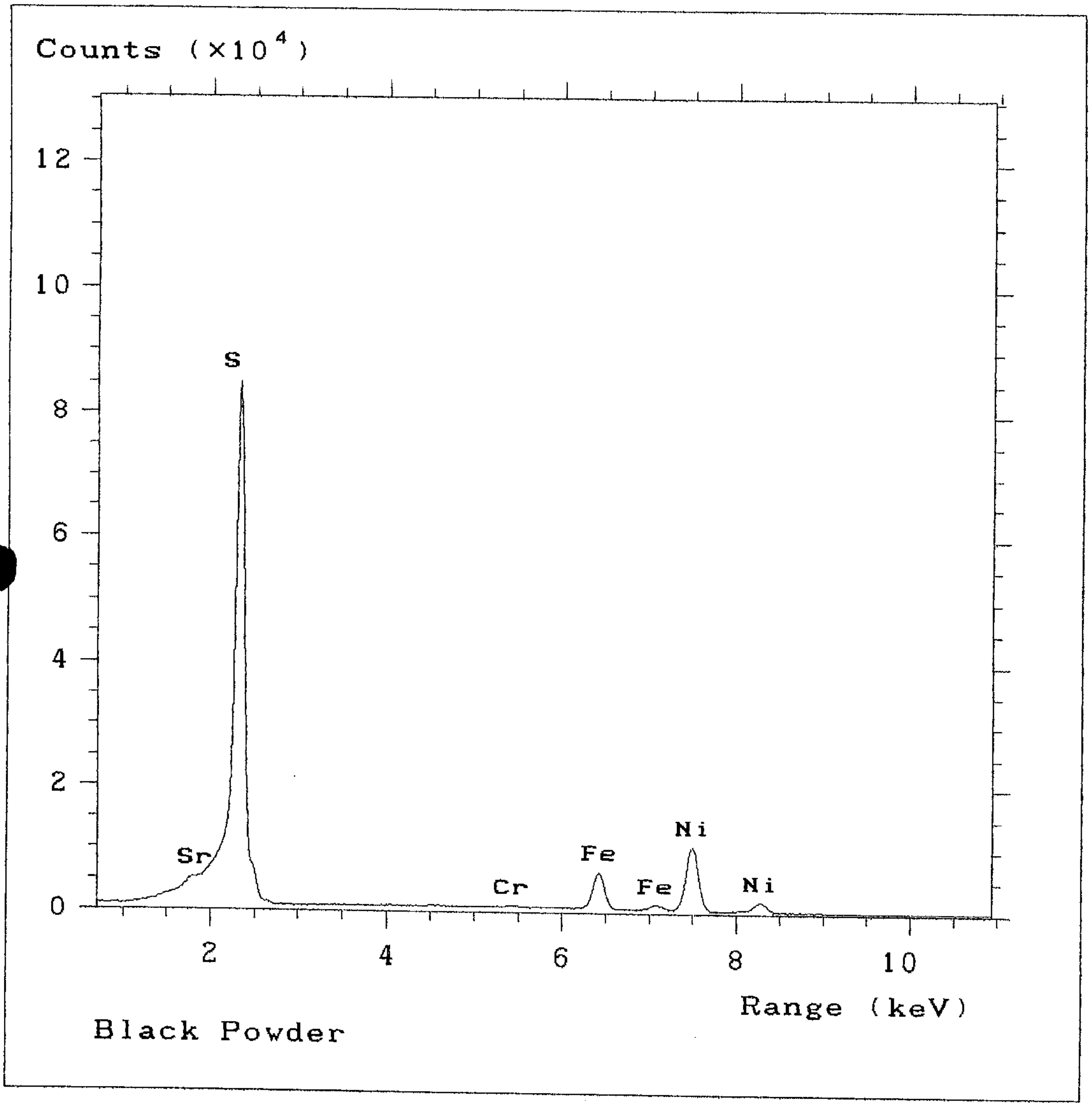
Counts (×10⁴)
12
10
8
6
4
2
0
S
Sr
Cr
Fe
Fe
Ni
Ni
2
4
6
8
10
Range (keV)
Black Powder

14

```
Spectrum file : ILM40
#1                                        LIVETIME(spec.)=    500
 ENERGY      RES      AREA
-     7.6   72.48    271799
TOTAL AREA=   2237506
...
Peak at     .40 keV omitted?
Peak at   12.80 keV omitted?
FIT INDEX= 3.97

ELMT         APP.CONC    ERROR(WT%)
P K  :  0      .127       .027
SiK  :  1      .156       .014
SnL  :  1     4.882       .068
CrK  :  1      .170       .032
FeK  :  1    99.532       .177

ZAF CALCULATIONS


..[ 2 iterations]

20.00 kV  TILT =    .00 ELEV = 35.00 AZIM =    .00 COSINE = 1.000

Spectrum: #1
                                                 CHEM.&MATERIALS ENG.

All elmts analysed,NORMALISED

ELMT    ZAF Ratio %ELMT           Error         ATOM.%
P K  :  0   .894      .134 +-     .028            .247
SiK  :  1   .567      .259 +-     .024            .528
SnL  :  1   .876     5.263 +-     .073           2.538
CrK  :  1 1.200      .134 +-     .026            .147
FeK  :  1   .997    94.211 +-     .168          96.540
TOTAL              100.000                     100.000
----------------------------------------------------------------------------
```

001
8.2g mat

N, T

H_2O_2 Boil

20

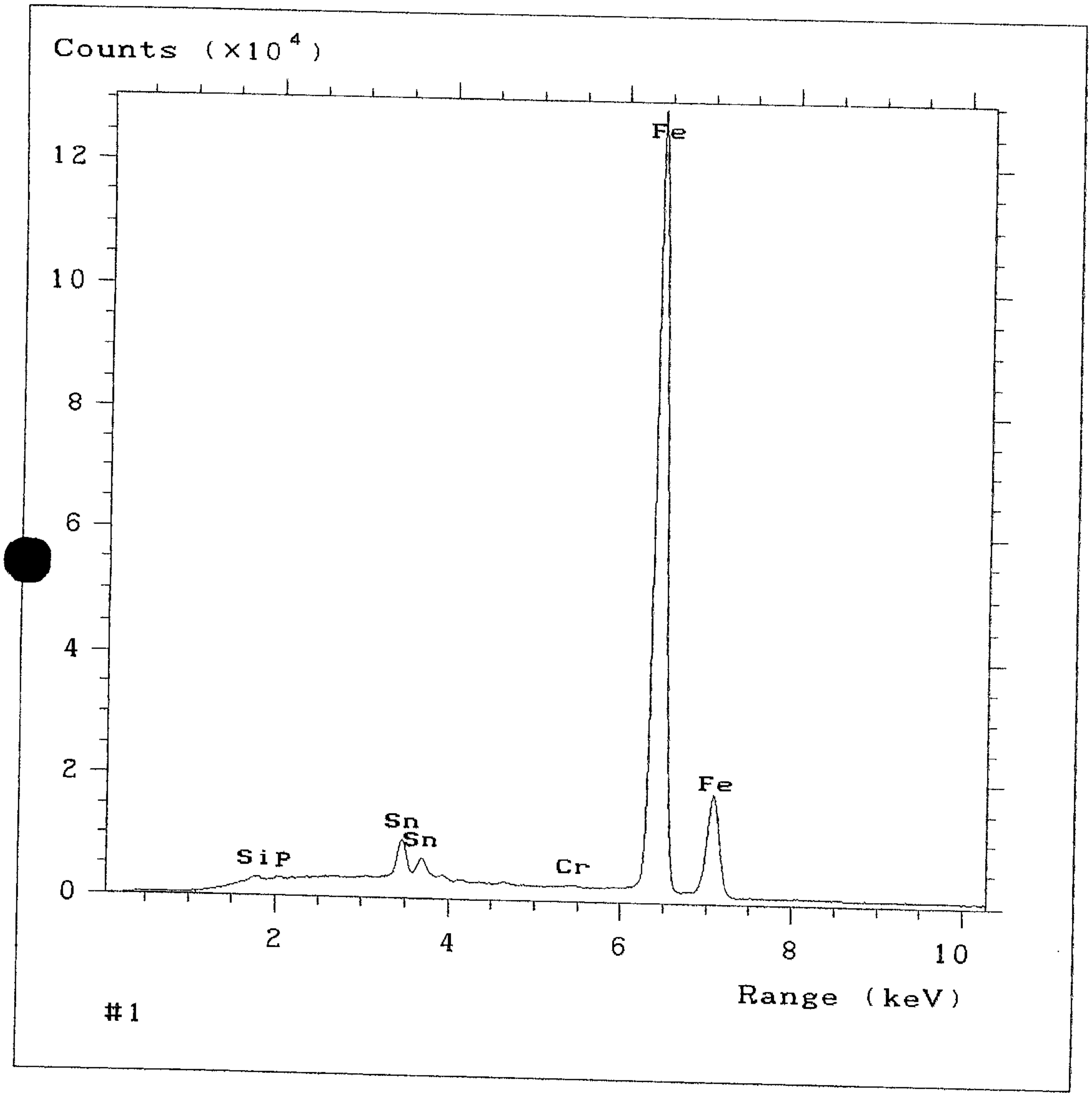

21

```
Spectrum file : ILM21
Metallic Sphere                              LIVETIME(spec.)=   500
 ENERGY     RES      AREA
    7.5    71.36   229891
TOTAL AREA=   1848605
...
Peak at     .38 keV omitted?
FIT INDEX=22.90

ELMT         APP.CONC    ERROR(WT%)
NaK  :  0      .177       .035
MgK  :  1      .100       .018
AlK  :  1      .085       .016
SiK  :  1     5.307       .026
CaK  :  3      .925       .023
TiK  :  1     1.874       .030
V  K :  0      .761       .033
FeK  :  1    74.556       .155
P  K :  0      .223       .025
S  K :  3      .118       .015

ZAF CALCULATIONS


...[ 3 iterations]

20.00 kV  TILT =    .00 ELEV = 35.00 AZIM =    .00 COSINE = 1.000

Spectrum: Metallic Sphere                       CHEM.&MATERIALS ENG.

All elmts analysed,NORMALISED

ELMT    ZAF Ratio %ELMT         Error         ATOM.%
NaK  :  0   .378     .517 +-    .102          1.117
MgK  :  1   .333     .330 +-    .061           .675
AlK  :  1   .441     .211 +-    .039           .389
SiK  :  1   .583   10.016 +-    .049         17.719
CaK  :  3 1.155     .882 +-    .022          1.094
TiK  :  1 1.023    2.016 +-    .032          2.092
V  K :  0 1.065     .787 +-    .034           .768
FeK  :  1   .968   84.796 +-    .176         75.444
P  K :  0   .839     .292 +-    .033           .469
S  K :  3   .857     .151 +-    .019           .234
TOTAL             100.000                   100.000
-----------------------------------------------------------------------------
```

22

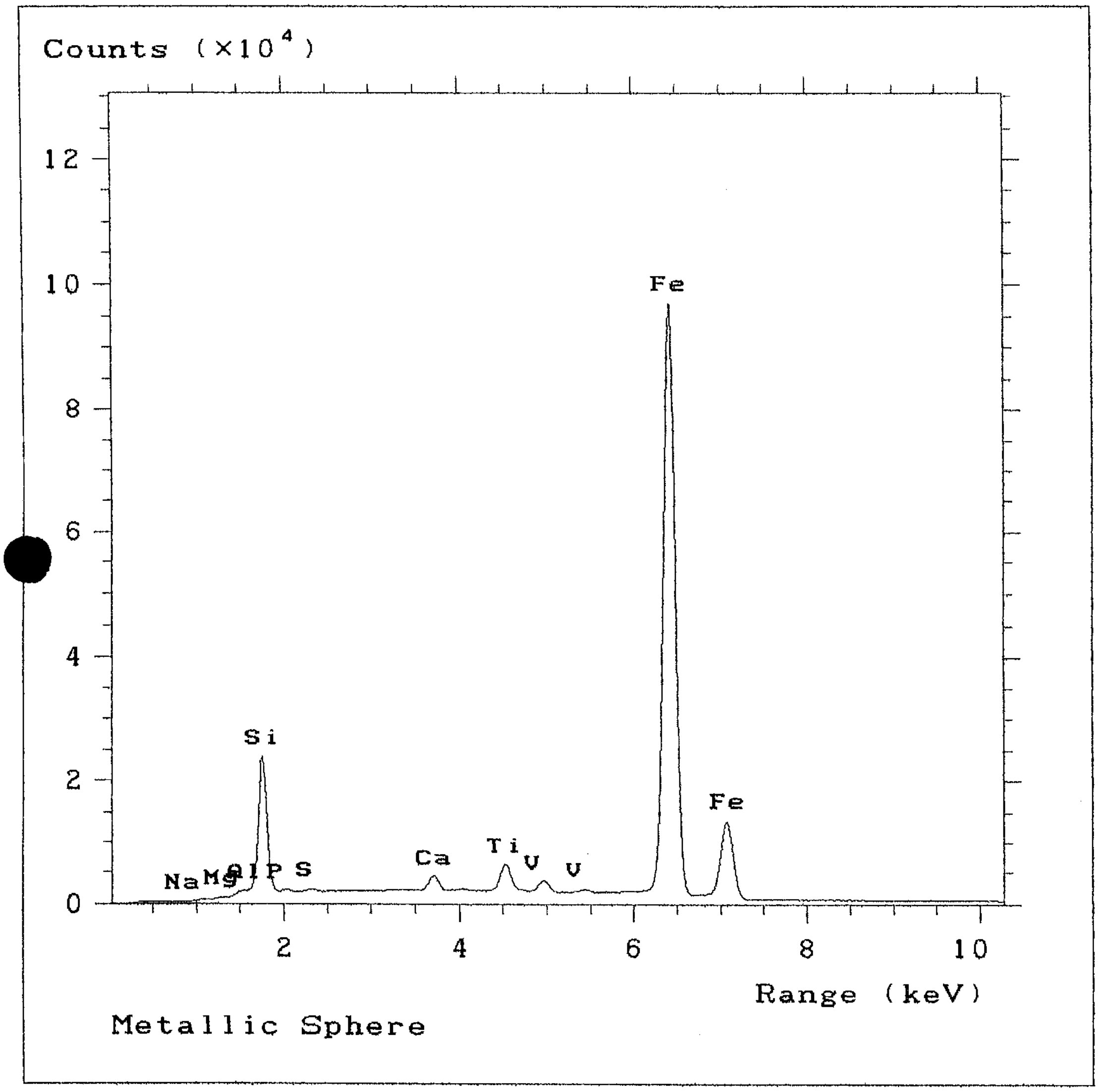

Metallic Sphere

23

Gold Bead From MacKay

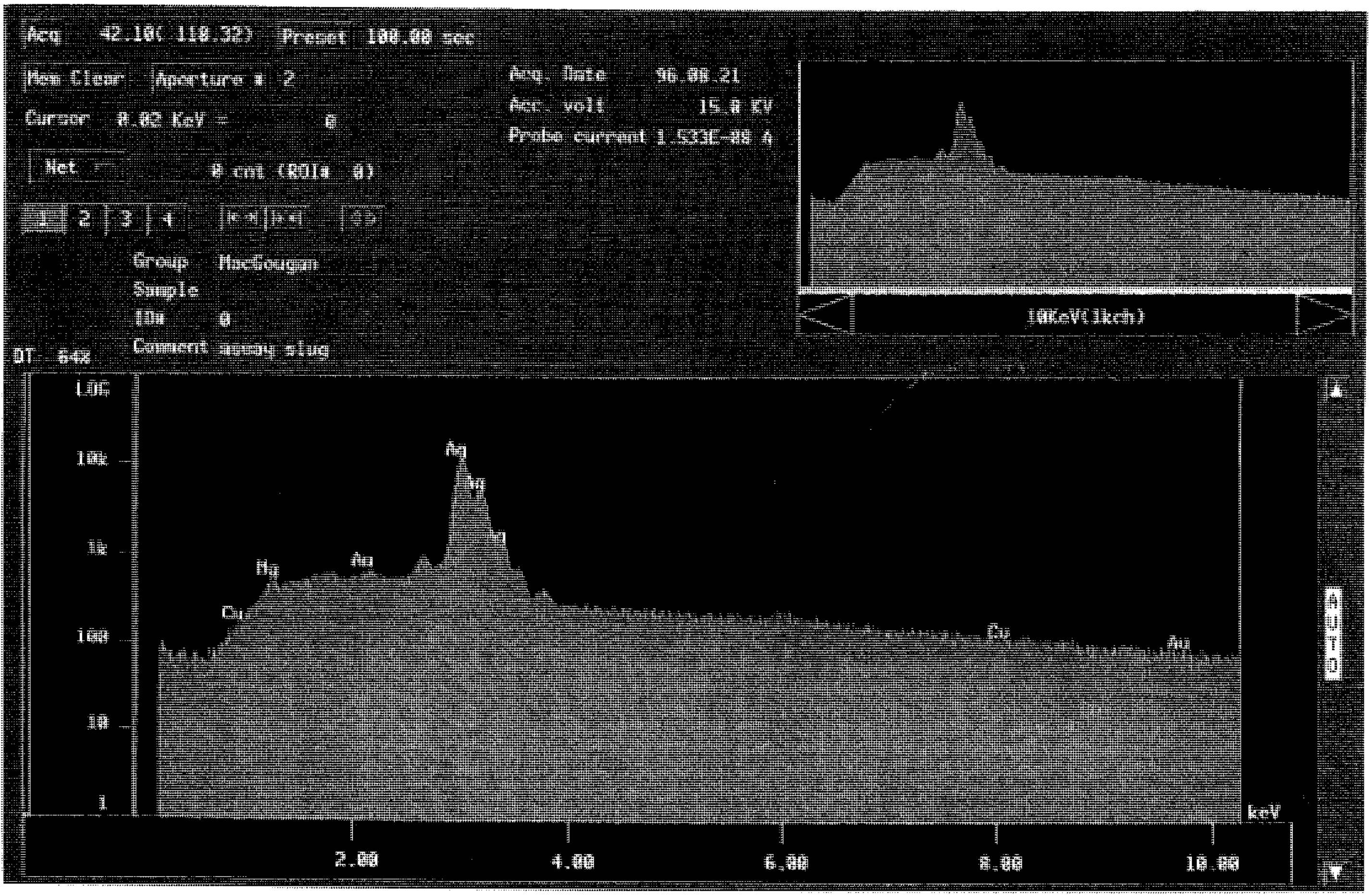

Acq 42.10(110.32) Preset 100.00 sec

Mem Clear Aperture # 2

Cursor 0.02 KeV = 0

Net 0 cnt (ROI# 0)

Group MacGougan

Sample

ID# 0

Comment assay slug

DT 64%

Acq. Date 96.08.21

Acc. volt 15.0 KV

Probe current 1.533E-08 A

24

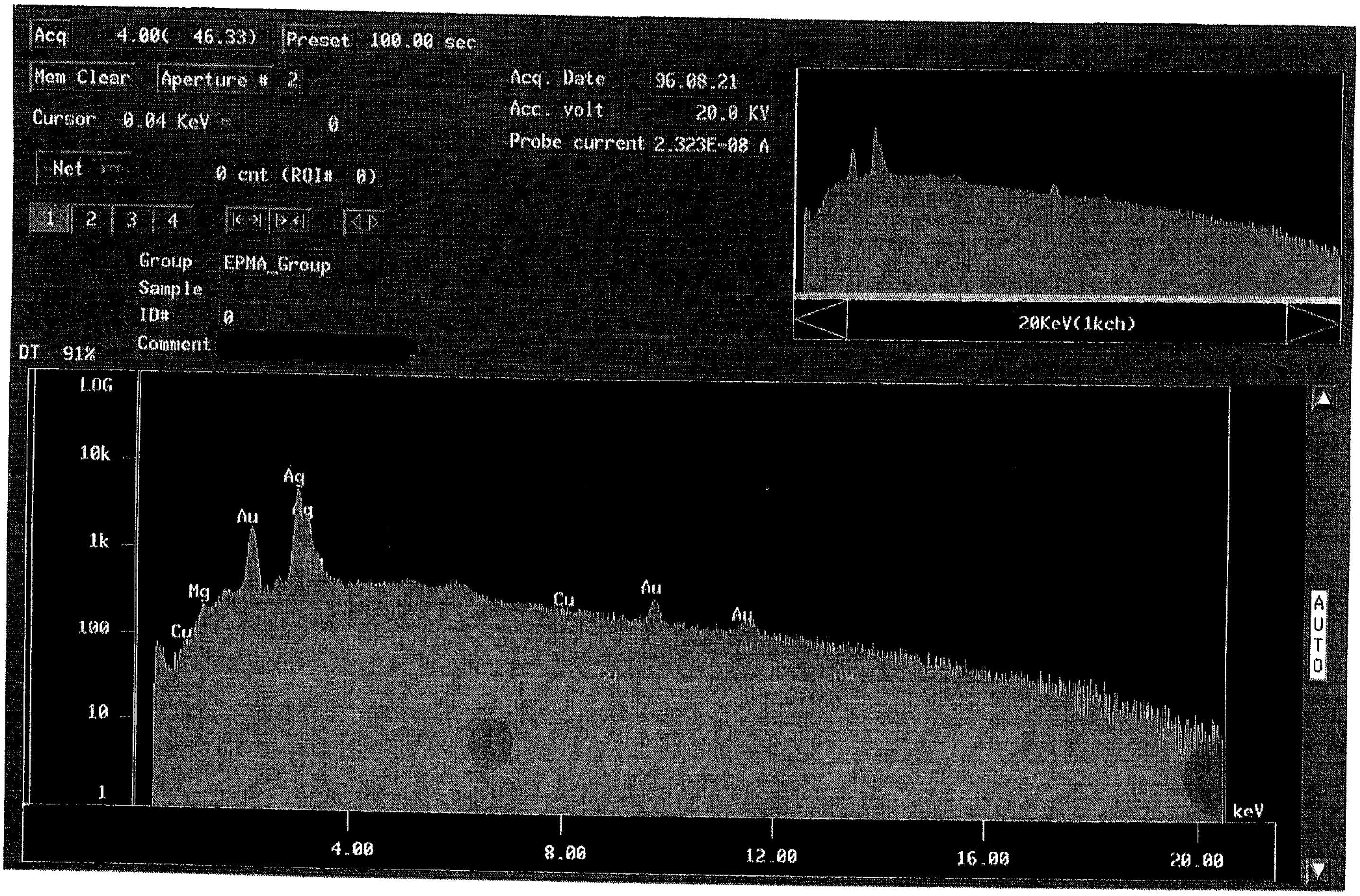

Acq 4.00(46.33) Preset 100.00 sec

Aperture # 2

Cursor 0.04 KeV = 0

0 cnt (ROI# 0)

Acq. Date 96.08.21

Acc. volt 20.0 KV

Probe current 2.323E-08 A

Group EPMA_Group

Sample

ID# 0

Comment [redacted]

DT 91%

20KeV(1kch)

25

1A

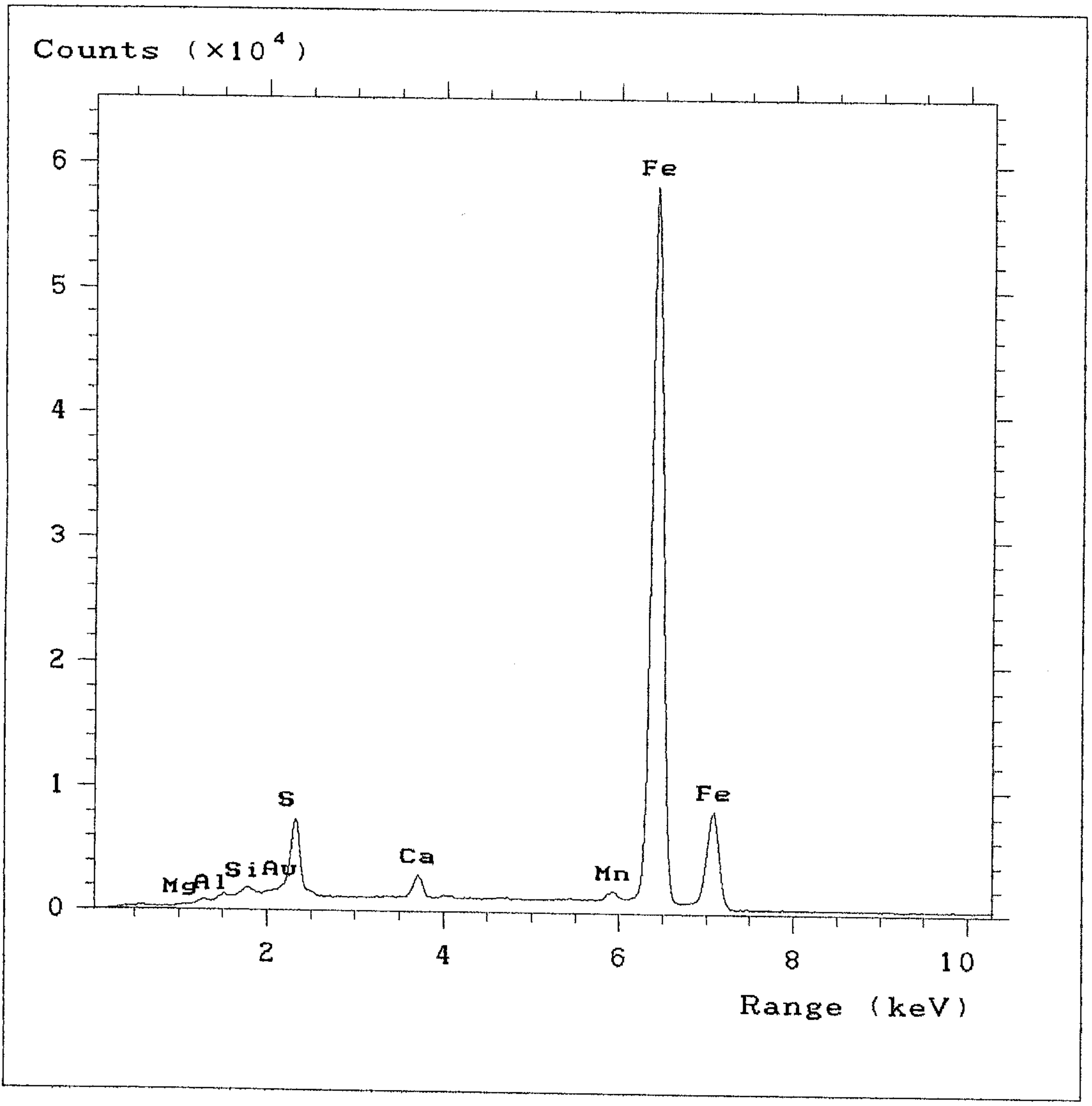

B 26

```
Spectrum file : ILM32
#3                                       LIVETIME(spec.)=    200
 ENERGY      RES       AREA
      7.5    72.58    106395
TOTAL AREA=    884630
...
Peak at     .38 keV omitted?
Peak at    1.28 keV omitted?
Peak at    2.32 keV omitted?
Peak at    3.68 keV omitted?
Peak at    5.44 keV omitted?
FIT INDEX= 2.85

ELMT          APP.CONC    ERROR(WT%)
SiK  :  1       .287       .020
PbL  :  1      1.260       .404
FeK  :  1    102.620       .256
CuK  :  1      1.351       .089

ZAF CALCULATIONS


..[ 2 iterations]

20.00 kV  TILT =    .00 ELEV = 35.00 AZIM =    .00 COSINE = 1.000

Spectrum: #3                                        CHEM.&MATERIALS ENG.

All elmts analysed,NORMALISED

ELMT    ZAF Ratio  %ELMT          Error          ATOM.%
SiK  : 1   .563      .480  +-     .034             .963
PbL  : 1   .690     1.718  +-     .550             .468
FeK  : 1 1.002     96.349  +-     .240           97.279
CuK  : 1   .874     1.453  +-     .096            1.290
TOTAL             100.000                        100.000
--------------------------------------------------------------------------------
```

Cap
HCL
— Cupel iron

#27

```
Spectrum file : ILM32
#3                                          LIVETIME(spec.)=    200
 ENERGY     RES      AREA
    7.5   72.58   106395
TOTAL AREA=    884630
...
Peak at    .38 keV omitted?
Peak at   1.28 keV omitted?
Peak at   2.32 keV omitted?
Peak at   3.68 keV omitted?
Peak at   5.44 keV omitted?
FIT INDEX= 2.69

ELMT       APP.CONC    ERROR(WT%)
SiK : 1      .287       .020
PbL : 1     1.261       .404
FeK : 1   102.620       .256
CuK : 1     1.351       .089
PtL : 1      .092       .293* < 2 Sigma*
AuL : 1      .103       .271* < 2 Sigma*

ZAF CALCULATIONS


..[ 2 iterations]

20.00 kV  TILT =    .00 ELEV = 35.00 AZIM =    .00 COSINE = 1.000

Spectrum: #3                                     CHEM.&MATERIALS ENG.

All elmts analysed,NORMALISED

ELMT   ZAF Ratio %ELMT         Error        ATOM.%
SiK : 1  .564      .478 +-    .033           .962
PbL : 1  .690     1.715 +-    .549           .468
FeK : 1 1.002    96.100 +-    .240         97.281
CuK : 1  .875     1.449 +-    .096          1.289
PtL : 1  .705      .122 +-    .390 <1 sd , below confidence limit
AuL : 1  .706      .137 +-    .360 <1 sd , below confidence limit
TOTAL            99.741                   100.000
-----------------------------------------------------------------------------
```

928

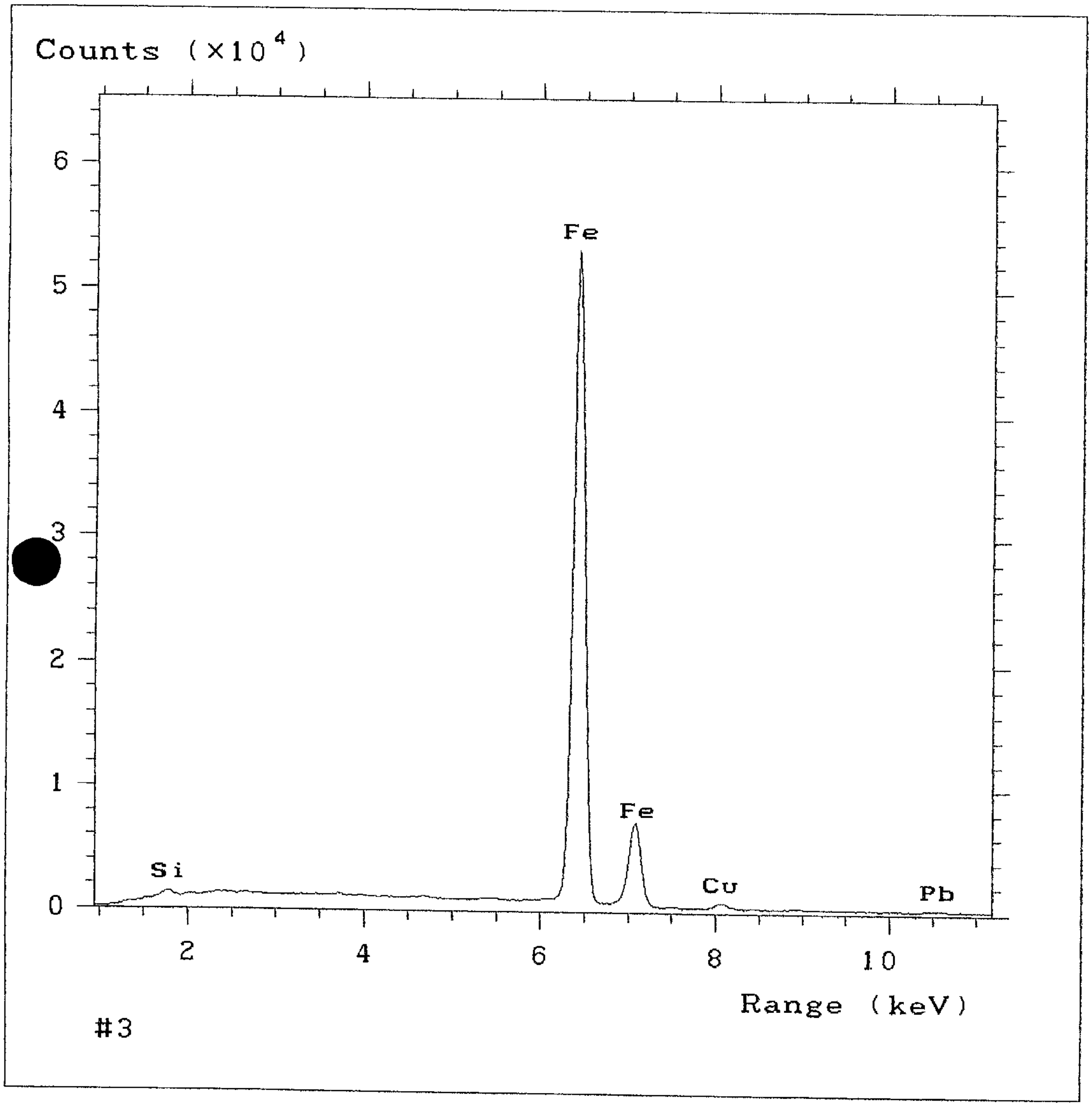

THE TRANSPORTATION OF DEPOSITION

OF

GOLD IN NATURE

:tion of gold
er i[illegible]f, not
: been made
ent parts of
he different
tion of gold
ı the ton) is
:ion, by the
lifficulty of
ent, there is
-solution of
state. This
ɛe influence
, in a paper
n sea-water.
s, oxidation
ıg power of
ıe excess of
;et free, and

to follow the lead
tions of the gold
:incipally for the
nous reparations
l much less gold
variations in the
va[illegible] of causes,
ıloroauric ion, in
matter. In recent
ı water, based on
shown that the
.at of silver about

ıd the mode of its
rable study since
l migrates in true
oth concepts are

ansport of gold in
er, Skey, Egleston,
narized by F. W.
at gold migrated
rs) that included
rbonate, alkaline

:arch and that of
:ure and provide
7 is a summary of

8-7: THE TRANSPORTATION AND DEPOSITION OF GOLD IN NATURE

Victor Lenher

Reprinted from *Econ. Geology* 7:744-750 (1912).

Of all the factors which play an important part in the genesis of ore deposits, the agency of solution is perhaps the most fundamental for it is by solution that the chemist is able to study and to attempt to imitate the chemistry of ore deposition as carried out in nature. Any information that will throw light on the character of possible ore-bearing solutions may be expected to aid in studying the many problems incident to the solution, transportation, and deposition of the metallic ores.

In connection with some recent chemical studies which have been made with gold, certain solutions have been worked with, the deportment of which toward various reagents as well as with certain minerals, indicates a degree of stability which appears to be of geological significance. Indeed certain gold solutions possess a stability from the purely chemical standpoint which one would not be likely to expect from our general knowledge of the ease with which gold is deposited out of most of its solutions by even the mildest reducing agents.

How gold is dissolved and transported in underground waters has not been clearly shown. The suggestive work of Stokes (ECONOMIC GEOLOGY, I., p. 650, 1906) on the solubility of gold in cupric chloride or in ferric chloride solutions at 200° with the redeposition of metallic gold on cooling, appears to afford a possible means of transportation of gold solutions at elevated temperatures with the subsequest deposition of the gold by lowering of the temperature. The work of Emmons on "The Agency of Manganese in the Superficial Alteration and Secondary Enrichment of Gold-Deposits in the United States" (*Trans. Amer. Inst. Min. Eng.*, 1910, 767) together with the work of McCaughey (*Jr. Amer. Chem. Soc.*, 31, 1,263, 1909), and Brokaw (*Jr. of*

Geol., Vol. 18, 321, 1910), as well as the earlier work of Pearce (*Trans. Amer. Inst. Min. Eng.*, 22, 739, 1893), Rickard (*Trans. Amer. Inst. Min. Eng.*, 26, 978, 1896), McIlhiney (*Amer. Jr. Sci.*, 1896, 293), and Don (*Trans. Amer. Inst. Min. Eng.*, 27, 599, 1897), apparently require that free chlorine is the solvent for the gold in the first instance, or if not free chlorine, a solvent whose powers are practically equivalent to that of free chlorine. When the chloride solution of gold is the transporting solution, it seems obvious that the gold is subsequently deposited as metal by a reducing agent. The agency of manganese in the solution of gold and its transportation is consistent in many gold deposits with the accompanying manganese deposits and throws considerable light on the superficial transportation of gold.

The solubility of gold in such media as the alkaline cyanides can hardly be deemed of material importance from the viewpoint of a natural transporting solution. The action of concentrated sulphuric acid or strong phosphoric acid in the presence of oxidizing agents on gold will cause solution (Lenher, *Jr. Amer. Chem. Soc.*, 26, 550, 1904) but this solvent action requires a higher concentration of acid than can be expected in nature. Similarly though hydrochloric acid under pressure (Lenher, ECON. GEOL., 4, 562, 1909) and nitric acid (Dewey, *Jr. Amer. Chem. Soc.*, 32, 318, 1910) at atmospheric pressure dissolve gold, the solution occurs only in concentrated acids, and the facts are of no importance in seeking for natural solvents for gold.

From all of these acid solutions the precipitation of the gold is usually assumed to take place by ferrous sulphate, metallic sulphides such as pyrites, or, in the case of Stokes' experiments, by lowering of the temperature.

The alkaline solutions which can dissolve and carry gold have not as a rule received as serious consideration as transporting media as the better known chloride solutions. Indeed the literature on alkaline gold solutions is very meager. This is particularly true in regard to the alkaline sulphide solutions.

That gold can be brought into solution by means of the alkaline sulphides has long been known, but it is doubtful if the geolog-

---

ical signif
ciated.
Probab
that gold
Stahl in t
Medicæ"
so sugges
alkali and
In mor
382, 187
suggests
medium t
Inst. Mi
of gold
soluble i
33, 207,
Pacific c
phide.
erable a
they wer
double s
New So
the orig
solubility
These
tory and
solutions
appears
line sul
As is
many ki
tion of
tions co
cipitate
solution
dition t

ical significance of the resulting solutions has been fully appreciated.

Probably at least as early as the time of Glauber it was known that gold can be rendered soluble by fusion with liver of sulphur. Stahl in the seventeenth century ("Observations Chymico-Physica Medicæ") is the first to bring out the fact clearly, and in doing so suggests that Moses burned the golden calf with sulphur and alkali and gave the solution to the children of Israel to drink.

In more recent times, Skey (*Trans. New Zealand Institute,* 5, 382, 1872) in studying the formation of gold nuggets in drift suggests the solution of gold in the alkaline sulphides as the medium by which gold can be carried. Eggleston (*Trans. Amer. Inst. Min. Eng.,* 9, 640, 1880–1881) in studying the formation of gold nuggets and placer deposits found spongy gold to be soluble in the alkaline sulphides. Becker (*Amer. Jr. Sci.* (3), 33, 207, 1887), in his studies on the mercury deposits of the Pacific coast, has shown that gold dust dissolves in sodium sulphide. He believed that some of the gold veins bear so considerable a resemblance to the quicksilver deposits that like the latter they were formed by precipitation from solutions of the soluble double sulphides. Liversidge (*Journal of the Royal Society of New South Wales,* 27, 303, 1893), in studying the question of the origin of gold nuggets, reviews the earlier work on the solubility of gold and finds it to be soluble in sodium sulphide.

These solubility experiments have been repeated in our laboratory and the fact corroborated that metallic gold is soluble in solutions of the alkaline sulphides. More significant, however, appears the fact that from these solutions of gold in the alkaline sulphides, iron pyrites will not throw out the gold.

As is well known, the metals, the metallic sulphides, and even many kinds of organic matter will precipitate gold from the solution of gold chloride. In the case of the alkaline sulphide solutions containing gold, neither pyrites nor metallic iron will precipitate the gold, but on the other hand, gold deposits out of these solutions by exposure of the solution to the air, under which condition the sulphide oxidizes.

3

The sulphide solutions of gold are permanent stable solutions to the ordinary reducing agents, that is, to such reducing agents as precipitate gold from the chloride solution. These alkaline sulphide solutions deposit their gold content by contact with acid or by exposure to oxidation. Not only are the alkaline sulphide solutions of gold stable to the metallic sulphides, but experiments made in sealed tubes have demonstrated that sodium, potassium, ammonium, or calcium sulphide solutions will dissolve gold leaf in the presence of pyrites without any deposition whatever of gold on the pyrites.

It is therefore obvious that through the agency of the alkaline sulphides it is possible for gold to be transported in alkaline sulphide solution through a bed of pyrites without deposition of metallic gold, and indeed it is possible to think of such a water passing through a bed of gold-bearing pyrites actually enriching itself by solution of the gold from the pyrites. To follow such a solution farther, it can be conceived that gold can be carried through a reduced zone and later the gold can be deposited by meeting acid in the reduced zone, or in absence of acid can be carried indefinitely until it reaches a zone of oxidation when the metal would be deposited.

When sodium thiosulphate is allowed to act on gold in the presence of oxygen, the double thiosulphate of gold and sodium is formed. This double thiosulphate is also formed when auric chloride and sodium thiosulphate are brought together in solution. This salt possesses remarkable stability in that the dilute acids, hydrochloric or sulphuric, do not at once decompose it, nor does ferrous sulphate or oxalic acid, two of the most common precipitating agents for gold, reduce it to metallic gold at once. All of these reagents do in time or in stronger solutions precipitate the gold from this thiosulphate compound. The extraction of metallic gold from silver ores in the thiosulphate extraction process depends on the formation of the double thiosulphate (Stetefeldt, "The Lixiviation of Silver Ores with Hyposulphite Solutions," pp. 15, 38).

These thiosulphate solutions are reasonably stable to iron pyrites, but on standing, metallic gold slowly deposits on the pyrites.

The sulphite sol
in which gold can
the double sulphit
the double gold s
Von Haase (C
double sulphite
ammoniacal solut
out of solution.
has been made ar
rites and to meta
been preserved f
from time to tim
metallic gold is
phite solutions v
metallic iron dep
Both the sodi
scribed by Haa
than the corresp
well as the pota
rites by a few
the potassium o
gold sulphite sc
latter toward re
a small quantit
ammonium salt
tically as readil
This tendency
stability of the
indicate that th
of transportati
in most natura
while ammoniu
ammoniacal sc
The alkaline
gold, namely t
ena when con
gold.

4

The sulphite solutions of gold are another example of a means in which gold can be held in alkaline solution. Curiously enough the double sulphite of gold and ammonium is quite stable, while the double gold sulphites of the alkalis are not nearly so stable. Von Haase (*Chemiker Zeitung,* 535, 1869) has studied the double sulphite of gold and ammonium. Haase worked in ammoniacal solution and was able to crystallize the double salt out of solution. The ammoniacal solution as prepared by Haase has been made and has been found to be quite stable to iron pyrites and to metallic iron. Ammoniacal sulphite solutions have been preserved for months in stoppered flasks and when tested from time to time by withdrawing small portions and acidifying, metallic gold is instantly precipitated. These ammoniacal sulphite solutions when sealed in tubes with iron pyrites or with metallic iron deposited no gold in months.

Both the sodium and potassium gold sulphites have been described by Haase. In solution, these salts are more unstable than the corresponding ammonium compound. The sodium as well as the potassium gold sulphite solutions yield gold to pyrites by a few minutes' contact. In reality a small quantity of the potassium or sodium gold sulphite added to the ammonium gold sulphite solution increases very much the instability of the latter toward reducing agents; indeed it is only necessary to add a small quantity of the sodium or potassium compound to the ammonium salt to cause the latter to lose its gold to pyrites practically as readily as though no ammonium salt had been present. This tendency on the part of the fixed alkalis to increase the instability of the ammonium gold sulphite solutions would seem to indicate that the sulphite solutions are not so plausible a means of transportation of gold in underground waters, inasmuch as in most natural waters sodium and potassium salts are present, while ammonium salts are found only in traces. Indeed natural ammoniacal solutions free from the alkalis are quite unknown.

The alkaline solutions of gold in the lower form of valence of gold, namely the aurous state, present some interesting phenomena when considered from the viewpoint of transportation of gold.

5

The aurous state of gold is produced when the ordinary or auric salts are reduced in a certain definite manner. The agencies by which this lower state of oxidation of gold can be produced are limited.

Aurous chloride and bromide are produced by the action of a moderate heat on the ordinary auric chloride or bromide. Experiments made recently in this laboratory show that by proper control sulphur dioxide, one of the best laboratory reducing agents and one of the common reagents used to precipitate gold from solution, can be used to effect the reduction of gold from the auric to the aurous state.

When sulphurous acid is added to a neutral or acid solution of gold without having present some other salt, it is very difficult to stop the reduction of the auric form of gold at the aurous state, the tendency being to produce complete reduction with the precipitation of metallic gold. If, however, a large excess of any of the alkaline chlorides, calcium, magnesium or zinc chlorides, be present, the reduction of the auric form of gold to the aurous state by means of sulphurous acid can be readily controlled. When an ordinary auric chloride solution is treated with a large excess of one of the above mentioned chlorides, and the solution then treated with a solution of sulphurous acid, the amber yellow color of the auric chloride gradually fades until the solution is rendered completely colorless. This colorless stage represents the existence of the aurous form of the gold, and the gold exists in this solution in all probability as a double aurous chloride.

Solutions of gold prepared in the manner indicated are far more stable under certain conditions than the ordinary auric chloride solutions. These conditions in which marked stability has been observed are somewhat curious. When such a solution is kept out of air contact and when no free acid or at most very little free acid is present, the solutions are fairly stable; if, however, the solution is exposed to the air, gold begins slowly to deposit. As far as the experiments have gone on this line, it seems as though the precipitation of metallic gold from this par-

tially reduced s
duction to met
The partially
far more stable
Here again is
gold is concern
Of the vario
which have bee
phide solution
of gold deposi
not lose its go
alkaline sulphi
solvents, and
solutions poss
nature would

6

tially reduced solution when exposed to the air is due to autoreduction to metallic gold by the oxygen of the air.

The partially reduced or aurous solution out of air contact is far more stable to pyrites than the ordinary or auric compounds. Here again is a suggestive solution so far as transportation of gold is concerned.

Of the various means of solution and transportation of gold which have been observed, it would appear that the alkaline sulphide solution may with study solve some at least of the problems of gold deposits. At all events, a solution is known which will not lose its gold to pyrites and yet will transport gold. The alkaline sulphides can easily be conceived as important natural solvents, and while other alkaline solutions such as the aurous solutions possess considerable stability, yet their formation in nature would not appear to be so likely as the sulphide solution.

In the paper entitled *Further Studies on the Deposition of Gold in Nature,* Lenher (1918, pp. 161-163, 183-184) gives data on the solubility of gold hydroxide at elevated temperatures 100°C-200+°C and discusses the behavior of gold chlorides toward calcite and magnesite under the action of heat and pressure. The introduction and observations of this paper are of considerable interest.

Introduction

> The various explanations which have been offered for the deposition of gold in nature have accounted in a satisfactory manner for the formation of certain deposits. Unquestionably, the alkaline sulphides play a very important part in the transportation of gold. The alkaline sulphides can, however, transport gold only in a zone free from oxidizing agents, since the oxidizing agents as well as the acids precipitate metallic gold from its sulphide solution. From the sulphide solutions gold is not deposited by the common reducing agents, but on the contrary, its precipitation takes place either by oxidation or by acidification.
>
> Presumably a large proportion of the gold which has been transported and deposited in the zone of oxidation has been carried in solution as the chloride or double chloride. From such a solution the gold is in a large measure deposited by reducing agents as pyrites or some other sulphide, by a ferrous mineral or by an organic reducing agent. Reduction from the chloride solution or from alkaline solutions is also accomplished in the zone of oxidation by the oxidized ores of manganese or by such oxidizing agents as will deposit gold by the phenomenon of autoreduction.
>
> Some of the more important gold deposits, however, cannot be explained by the theories proposed. For example, the low-grade gold ores in quartz commonly consist of a vein or bed of quartz containing very finely divided gold disseminated through it. This gold may appear in particles which are sufficiently large that they can be observed with the naked eye, but for the most part the gold particles are usually so small that they are indistinguishable. Moreover, the low-grade gold ores are usually remarkably uniform so far as their gold content is concerned; that is to say, their precious metal content varies comparatively little, and, expressed in actual percentage of gold present, the variation is insignificant.
>
> Again, the various theories offered for the transportation and deposition of gold fail to account for the general presence of silver with the gold. For example, the alkaline sulphide solutions, which are so important in the transportation of gold, do not appear to deport themselves similarly with silver. Silver sulphide is according to our experiments quite insoluble in the alkaline sulphide solutions and in the sulphaurate solutions. Hence the transportation of gold by the alkaline sulphides cannot explain the transportation of silver, nor can this method of transportation of gold in the light of our present knowledge be reconciled by the presence of silver in gold deposits. Up to the present time the presence of silver in gold is usually accounted for by the general principle that metallic silver will precipitate metallic gold from a gold solution as the two metals

---

stand in that
commonly ev
by means of
Experimen
quite anothe
gold is rather
well known, l
easily into m
moderate deg
bly stable un
tures, when i
The fact that
posed by suffi
oxide of gold
considerable

From our exp
more resistan
by the expan
The action
are plentiful
dissolved in t
when they co
then if the te
sure which ste
mately 100 at
It should b
hydroxide tak
in contact wi
hydroxide do
occurs in nat
to the stabilit
its stability is
gold are the n
of any of the
The action
sodium chlor
while the acti
ency to preve
Inasmuch
for silver chl
native gold m
data are lack
procedure, ye
magnesium c
carbonate, wl
150° is comp
The above

8

stand in that order in the electrochemical series, a fact which is so commonly evidenced in photography in the "toning" of a silver print by means of a gold solution.

Experiments recently conducted in our laboratory have shown quite another side to the deposition of gold in nature. The oxide of gold is rather remarkable for its stability. The oxide of silver, as is well known, like many of the silver compounds, breaks down rather easily into metallic silver and oxygen, under the action of only a moderate degree of heat. Gold oxide, on the other hand, is remarkably stable under the action of heat up to moderately high temperatures, when it gradually dissociates into metallic gold and oxygen. The fact that the oxide of silver and the oxide of gold are decomposed by sufficient elevation of the temperature and the fact that the oxide of gold can be formed so readily in nature, probably are of considerable importance in the formation of certain gold deposits.

Observations

From our experiments it is evident that the compounds of gold are more resistant to high temperatures when the pressure is that exerted by the expansion of steam, than they are at atmospheric pressures.

The action of calcium carbonate or magnesium carbonate, which are plentiful in nature both in the form of carbonate rocks and dissolved in the natural waters, is to first precipitate auric hydroxide when they come in contact with a water containing gold chloride; then if the temperature becomes higher than 310° under the pressure which steam would exert at those temperatures, which is approximately 100 atmospheres, crystals of metallic gold are produced.

It should be borne in mind that while the precipitation of auric hydroxide takes place readily when a gold chloride solution comes in contact with the alkaline earth carbonates, auric oxide or auric hydroxide do not occur in nature. No oxidized gold compound occurs in nature, and although we have repeatedly called attention to the stability of gold oxide, it must be distinctly borne in mind that its stability is only relative, and that in general the compounds of gold are the most easily broken down into metal of the compounds of any of the metals.

The action of various salts, such as magnesium chloride and sodium chloride, is to somewhat lower the decomposition point while the action of calcium chloride appears to have a slight tendency to prevent this decomposition.

Inasmuch as the alkaline chlorides are solvents to a slight degree for silver chloride, it is possible that the existence of silver in the native gold may be accounted for in this way. While experimental data are lacking on the coprecipitation of gold and silver by this procedure, yet we have ample evidence that calcium carbonate or magnesium carbonate in all of their natural forms precipitate silver carbonate, which at the boiling point of water or in the autoclave at 150° is completely reduced to metal.

9

The above experiments, in which an attempt has been made to imitate as closely as possible the conditions existing in nature, appear to be sufficiently suggestive to be offered as an explanation of at least how it is possible that certain gold deposits have been produced.

Transport of gold in hypogene (hydrothermal) solutions as chloride complexes has appealed to a number of investigators, particularly Ogryzlo (1935), Krauskopf (1951), and Helgeson and Garrels (1968). Ogryzlo (1935) examined the solubility of gold in water containing a number of components including chlorides, sodium carbonate, sodium sulfide and sodium bisulfide. The summary and conclusions from his paper *Hydrothermal Experiments with Gold,* (pp. 423-424) follow:

Summary and Conclusions

1. 20 per cent. hydrochloric acid vapor in a dynamic system has no action on gold between 250° and 600°C.
2. When chlorine and steam are passed over gold, $AuCl_3$ is formed. The volatilization of $AuCl_3$ in the presence of chlorine and steam begins below 125°C, increases rapidly to a maximum at 200°C, and then decreases rapidly to almost nothing at 400°C. The decrease in the amount of volatilization above 200°C is due to the fact that around this temperature the dissociation pressure of the $AuCl_3$ increases much more rapidly than the vapor pressure. It is possible that the presence of water vapor may have an effect on the temperature at which maximum volatilization takes place. Pressure would tend to prevent dissociation and would, therefore, affect the temperature of maximum volatilization.
3. Gold dissolves in weak hydrochloric acid at high temperatures and pressures. The amount dissolved increases with the concentration of the acid and the temperature and pressure. Pressure is an important factor in causing solution. Larger quantites of gold are dissolved in the presence of air than in the presence of carbon dioxide or nitrogen.
4. The writer did not find that aqueous solutions of alkali chlorides have an appreciable solvent action on gold in the presence of air or nitrogen and under high temperature and pressure conditions, although Lenher reports that they have.
5. Sodium carbonate was not found to have solvent action on gold at high temperatures and pressures. This is not in agreement with Doelter's work.
6. Stokes found that gold dissolves in hydrochloric acid solutions of ferric chloride at high temperatures and pressures and in the absence of oxygen. This was confirmed by the writer.
7. The writer found that Na_2S solutions dissolved only traces of gold at high temperatures and pressures, and none at room temperature. These results do not agree with those of Becker, Egleston, and Lenher.
8. On the other hand, considerable quantities of gold are dissolved by solutions of NaHS at high temperatures and pressures. Some gold is also dissolved by NaHS at room temperature.

In this inves
possible the c
dence shows t
alkaline aqueo
acid solutions,
from chloride
contact with
nature. In hot
ried as a doubl
acidification o
In a closed s
tion products w
tion of the chlo
under high tem
not carried in
pressure condit
tion with the e
phase as $AuCl$
which volatiliz
factor is uncert

Krauskopf (1951)
and free energy data
results reported in th
Gold, (pp. 869-870)

1. Solubilities
reasonably well
2. In acid solu
provided that r
an acid solutior
fairly strong ox
pressures the hy
ing agent; at lov
Cu^{++} must be pr
agent be presen
bly means that
at low temperat
agents like H_2S
tation of gold in
gene movement
3. The solubilit
which do not c
10
4. Gold may b
dilute solutions
as the very stabl
5. Gold may be
of mechanisms,
91 cated than a fall

> In this investigation an attempt was made to imitate as closely as possible the conditions existing in nature. The experimental evidence shows that gold may be transported either in acid or slightly alkaline aqueous solutions and also in the vapor phase as $AuCl_3$. In acid solutions, gold is probably carried as a chloride. Precipitation from chloride solutions would result when the solutions come in contact with one of the many reducing agents which occur in nature. In hot alkali hydrosulphide solutions, gold is probably carried as a double sulphide of the alkali metal and gold. Oxidation or acidification of the solution would cause precipitation.
>
> In a closed system, the partial pressures of $AuCl_3$ and its dissociation products would tend to prevent both volatilization and dissociation of the chloride after an equilibrium has been reached. Therefore, under high temperature and pressure conditions $AuCl_3$ is probably not carried in the vapor state. However, under somewhat reduced pressure conditions when the solutions and gases are in communication with the earth's surface, gold may be transported in the vapor phase as $AuCl_3$. It is difficult to place limits on the temperature at which volatilization would take place in Nature, as the pressure factor is uncertain.

Krauskopf (1951) calculated the solubilities of gold from electrode potential and free energy data and found results that agreed well with the experimental results reported in the literature. The summary from his paper *The Solubility of Gold,* (pp. 869-870) follows.

> **Summary**
>
> 1. Solubilities of gold calculated from thermodynamic data agree reasonably well with experimental results.
> 2. In acid solutions gold may be transported as the ion $AuCl_4^-$, provided that reducing agents are absent. The metal is dissolved by an acid solution provided that the solution contains Cl^- and that a fairly strong oxidizing agent is present. At high temperatures and pressures the hydrogen ion of the acid is a sufficiently strong oxidizing agent; at low temperatures a substance like MnO_2, O_2, Fe^{+++}, or Cu^{++} must be present in addition. The requirement that an oxidizing agent be present, or at least that a reducing agent be absent, probably means that gold would not be transported in acid vein solutions at low temperatures, since such solutions would contain reducing agents like H_2S and Fe^{++}. On the other hand, solution and transportation of gold in acid solution is probably the mechanism of supergene movement of gold.
> 3. The solubility of gold in naturally-occurring alkaline solutions which do not contain sulfide is negligible.
> 4. Gold may be transported in alkaline sulfide solutions, even in dilute solutions near the neutral point. The gold is probably present as the very stable ion AuS^-.
> 5. Gold may be precipitated from solution by any one of a number of mechanisms, but there is no need to call on one more complicated than a fall in temperature or pressure or both.

11

6. If a solution of gold at high temperature and pressure is cooled, part of the metal may be forced out of solution but may appear as a sol rather than as a precipitate. In this form it may remain in suspension down to low temperatures.
7. Because gold may be transported in solutions of various compositions, the presence of gold in a vein deposit gives little information as to the character of the vein fluids.
8. In sea water gold is probably present as both AuO_2^- and $AuCl_4^-$. A limit to the amount dissolved may be set by the formation of these ions from metallic gold with the aid of dissolved oxygen.

Helgeson and Garrels (1968) also applied thermodynamic calculations to the solubility, hydrothermal transport, and deposition of gold. They concluded that sufficient gold can be carried in solution as aurous chloride complexes to account for hydrothermal gold ore deposits precipated above 175°C. The concluding section of their paper *Hydrothermal Transport and Deposition of Gold* follows.

Concluding Remarks

> The solubility of gold has been the subject of repeated alchemical, experimental, theoretical, economic, industrial, and geologic investigation for thousands of years. Despite all of this attention, the origin of hydrothermal gold deposits is still poorly understood. Most theories of hydrothermal gold deposition fail to account for the geologic characteristics of gold ore deposits. Much of the pertinent experimental work has been semi-quantitative at best, and the fugacity of oxygen and pH are rarely controlled and/or monitored in such experiments. As a result, high-temperature gold solubilities predicted from thermodynamic data cannot be checked adequately against experimental results reported in the literature. As least for the present, the credibility of thermodynamic predictions of gold solubilities at high temperatures rests with the extent to which such predictions agree with the geologic occurrence of gold. In this respect, and from a thermodynamic and chemical standpoint, the geochemical model of gold deposition presented above appears to be realistic.
>
> It has been demonstrated that gold can be dispersed in significant concentrations in aqueous solutions as a stable colloid, [Frondel, C., 1938. Stability of colloidal gold under hydrothermal conditions, *Econ. Geology* **33:**1-20.] as alkali thioaurate or gold sulfide complexes in alkali sulfide solutions [Krauskopf, K. B., 1951. The solubility of gold, *Econ. Geology* **46:**858-870; Smith, F. G., 1943. The alkali sulphide theory of gold deposition, *Econ. Geology* **38:**561-590.] and as $AuCl_4^-$ in highly oxidizing acid solutions [Cloke, P. L., and W. C. Kelly, 1964. Solubility of gold under inorganic supergene conditions, *Econ. Geology* **59:**259-270; Kelly, W. C., and P. L. Cloke, 1961. The solubility of gold in near-surface environments, *Mich. Acad. Sci., Arts, and Letters Papers* **46:**19-30; Krauskopf, K. B., 1951. The solubility of gold, *Econ. Geology* **46:**858-870.]. The results of this study suggest that none of these is a requirement for the hydrother-

---

mal transport
tions indicate
in the aurous
0.02 ppm gol
ore deposits.
The order
formation of
few simple c
1,000 feet hig
ture profile f
10^9ft^3 of solu
gold along c
(predicted fr
ure 10], 4.25
precipitated
ounce of go
body. Even a
would take r
flow velocity
Hydrothe
transfer that
deposits at h
mathematic
tions to a gi
geochemica
positions an
of gangue, c
ore deposits

12

mal transport and deposition of gold. Thermodynamic considerations indicate that gold is carried in hydrothermal solutions primarily in the aurous state and geologic observations suggest that less than 0.02 ppm gold in solution is sufficient to account for major gold ore deposits.

The order of magnitude of the mass transfer involved in the formation of major gold deposits can be determined by making a few simple calculations. For example, to precipitate a quartz vein 1,000 feet high, 1,000 feet long, and one foot wide over a temperature profile from 300° to 200°C requires 2.3×10^8 short tons or $7.6 \times 10^9 \text{ft}^3$ of solution. Assuming the solution is saturated with respect to gold along curve *a* (based on geologic consideration) or curve *g* (predicted from thermodynamic calculations) in Figure 9 [and Figure 10], 4.25 short tons of gold and 13,000 tons of pyrite would be precipitated from solution along with the quartz. At $35.00 per troy ounce of gold, the quartz vein would constitute a $4,400,000 ore body. Even assuming a conservative flow rate of 10,000 $\text{ft}^3 \text{ day}^{-1}$, it would take no more than 2,000 years to form this ore body, and the flow velocity in the vein would only be 0.2 cm minute^{-1}.

Hydrothermal ore deposition is an irreversible process of mass transfer that can be evaluated quantitatively for most types of ore deposits at high temperatures from a thermodynamic, chemical and mathematical standpoint. Geologic application of such calculations to a given ore deposit is hindered primarily by the lack of key geochemical data. These data are, specifically, fluid inclusion compositions and temperatures of filling, compositions and mass ratios of gangue, ore, and alteration minerals, and mineral associations in ore deposits and altered wall rocks adjoining veins (p. 634).

Figure 9. (Top). Computed solubility of gold at elevated temperatures. Curve *a* corresponds to curve *a* in Figure 2, which is based on geologic considerations. Curves *g* and *h* represent solubilities computed from thermodynamic data and mass transfer calculations for cooling hydrothermal solutions with different initial compositions at 300°C (see text). All three curves are for a solution in equilibrium with quartz, pyrite, and gold.

Figure 10. (Bottom). Schematic illustration of the gold-quartz vein precipitated along curve *g* in Figure 9. The relative proportions of quartz and pyrite are indicated by the hatched and clear areas, respectively. The gold values given above are based on a gold price of $35.00 per troy ounce and the vein width corresponds to the stoping width of ore.

(See over for figures.)

13

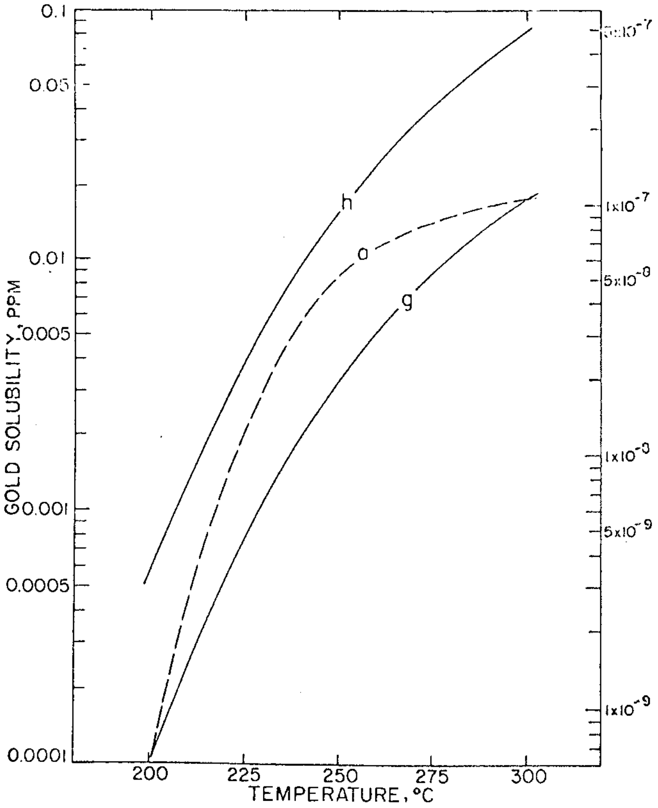

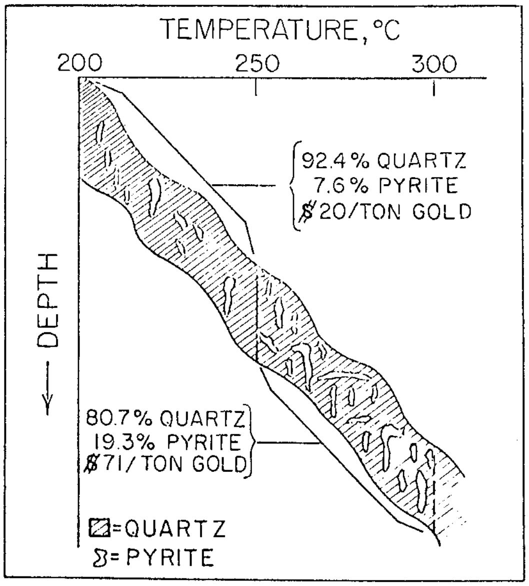

Boyle (1969
from a numbe
present in gold
of the wall ro
percentages o
general presen
from highly ac
presently prec
of gold unde
Rytuba and I
experimentall
gold in the B
[AuS]⁻ compl
these near-ne
One canno
both past an
Excepting co
thermal gold
probable, ho
sulfide or sul
Alkali sulfi
in hydrothern
wall rock alte
soluble in al
and that gold
excess at low
trated alkali
complex ion
present in t
solubility of
a pyrite-pyrr
kbar. Maxim
concluded th
predominate
and [Au(HS
first two co
suggesting t
transport of
The sulfi
tions betwe
stable to me
spring wate
alteration s
fide comple
nism for go
Smith (1
series of ex
tellurium i
gold is solu
other com

14

Boyle (1969) has criticized this proposed acid-chloride transport mechanism from a number of angles, pointing to the general low content of chloride now present in gold veins and their wall rock alteration zones, the alkaline character of the wall rock alteration associated with gold deposition, the low transfer percentages of alumina in alteration zones associated with gold deposits, the general presence in gold deposits of carbonates that are difficult to precipitate from highly acid solutions, and the general alkaline nature of hot spring waters presently precipitating gold. Others have also criticized the chloride transport of gold under hydrothermal conditions, among whom may be mentioned Rytuba and Dickson (1977) and Weissberg (1970), the latter having shown experimentally and by examination of thermal waters presently precipitating gold in the Broadlands, Ohaki and Waiotapu areas, New Zealand, that the $[AuS]^-$ complex is more than adequate to account for the transport of gold in these near-neutral low-salinity hydrothermal solutions.

One cannot doubt that gold is solubilized as a chloride complex, as proven by both past and more recent data (Vilor and Shkarupa, 1971; Henley, 1973). Excepting conditions where minerals such as alunite are precipitated in hydrothermal gold deposits, an indication of relatively high acidity, it appears more probable, however, that gold is transported under hydrothermal conditions as a sulfide or sulfide-arsenide-antimonide complex.

Alkali sulfide, bisulfide, sulfide-arsenide-antimonide, and telluride complexing in hydrothermal solutions seems most probable considering the mineralogy and wall rock alteration effects in gold deposits. It has long been known that gold is soluble in alkali hydrogen sulfide (e.g., NaHS) solutions at low temperatures, and that gold sulfide is soluble in solutions of alkali sulfide and polysulfide in excess at low temperatures. At high temperatures gold is also soluble in concentrated alkali sulfide solutions. There is some agreement that the principal complex ion in such solutions is $[AuS]^-$, although some $[AuS_2]^-$ may also be present in the systems. In a recent paper Seward (1973), determined the solubility of gold in aqueous sulfide solutions from pH4 to 9.5 in the presence of a pyrite-pyrrhotite redox buffer at temperatures from 160°C to 300°C and 1 kbar. Maximum solubilities were obtained in the neutral region of pH. It was concluded that three gold complexes contributed to the solubility: $[Au_2(HS)_2S]^{2-}$ predominated in alkaline solution, $[Au(HS)_2]^-$ in the near neutral pH region, and $[Au(HS)]^0$ with less certainty in the acid pH region. The stabilities of the first two complexes are much greater than chloroaurate (I) species, a feature suggesting that the chloride complexes play only a subsidiary part in the transport of gold in neutral and alkaline hydrothermal solutions.

The sulfide and polysulfide complexes of gold are stable in aqueous solutions between a pH of 6 and at least 10. The $[AuS]^-$ complex is also relatively stable to metallic sulfides and a number of other reductants. Because many hot spring waters are alkaline, and other effects such as certain types of wall rock alteration suggest alkaline solutions, transport of gold as soluble alkaline sulfide complexes has appealed to a number of investigators as a transport mechanism for gold during the formation of hypogene deposits.

Smith (1943, p. 582-589) reviewed the literature and carried out an extensive series of experiments involving the solution and transport of gold, silver, and tellurium in alkali sulfide solutions. He was able to show experimentally that gold is soluble in, and can be crystallized from, such solutions, and that two other common gold minerals, electrum (Au, Ag) and calaverite ($AuTe_2$), can be

15

96

similarly synthesized. The discussion and conclusion on the transport and deposition of gold, silver, and tellurium in his classic paper *The Alkali Sulphide Theory of Gold Deposition* deserve special attention because of their probable importance in the formation of hypogene gold ores (Paper 8-8).

(Text continues on page 173.)

8-8: THE
OF G

F. G. S

Copyright
from pages

The solubility
sulphide has bee
concentration. T
are considerably
of sodium sulphi
metallic sulphid
of sodium thiom
rather than their
postulated that
geological condi
concentration s
The factors i
tion of ore-beari
ones may be dis
ore-bearing solu
considered to b
types of ore dep
regions of near-
sulphide has bee
hot springs in su
probably greate
action of the or
There are three
One, not so co
sulphate ion by
noticed at Kewe
S. Burbank, et a
Prof. Paper 144,
solutions circul
was simultaneo
probably due to
oxidation maki
and doubtless t
wallrock to sul
of the wallrock
pyrite is usually
altered rock. T
aluminum min

16

8-10: THE TRANSPORTATION OF GOLD BY ORGANIC UNDERGROUND SOLUTIONS

Fred W. Freise

from *Econ. Geology* **26**:421-431 (1931).

ALL mining companies or individual miners who have worked alluvial gold deposits in Brazil realize that gold placers thoroughly exhausted may after a period of years once more be panned and yield a profitable amount of newly accumulated gold. The native gold digger maintains that every gold placer within ten years is again valuable enough to be worked over once more and that the *pinta que paga, i.e.* the "paying spark" reappears the sooner if the exhausted gold field has been hidden from the sun by vegetation or other means.

The author worked gold placers at the eastern boundary of the State of Minas Geraes in the districts of Palma and Muriahé in 1908 and 1909 and for the second time in 1926; the first time monazitic sands were the principal object of the mining work, but the gold contents of the gravel (8.5 grams per ton) were recovered, since they almost defrayed the pay roll. But when, in 1926, the same places were opened again, an average of 4.85 grams of gold per ton was realized near the bottom rock, the metal being quite different from the original gold, both in color, purity, coarseness, and affinity to mercury. The nature of the territory and the sequence of the strata precludes the hypothesis of mechanical transfer from a higher point; the occurrence suggested that this gold had been brought to its place by chemical transportation.[1]

In the eastern part of the State of Rio, the author opened up some gold placers in 1912; the gold content of the gravel was 11.6 grams per ton, and the average yield was 10.85 grams. When, in 1926, the old diggings, quite overgrown with "caapœira"

---

[1] Details concerning the above-mentioned gold and monazitic deposits were published by the writer in *Zeit. f. d. Berg-, Huetten- u. Salinenwesen i. Preuss. Staate*, vol. LVII., pp. 47–64, 1910.

(second g
above the
greenish v
ferently f
gold.

Finally,
undergrou
had occasi
an importa
These taili
in certain
much as 3
more the
recovery
hardly be
attributed

These c
of the age
its origin
properties
called, wer
means of
observed
toughness
gold were
see wheth
one, the
inches, co
action of
weighed
exposed t
for many
intervals
these tests

(second growth), were reopened, the lowest layers immediately above the granitic bed rock yielded 4.66 grams per ton, of a greenish variety of gold which chemically behaved quite differently from the commonly known allotropic modifications of gold.

Finally, an opportunity to see gold transported chemically by underground solutions was given to the writer in 1927, when he had occasion to examine the large tailing heaps accumulated by an important gold mining company in the center of Minas Geraes. These tailings generally showed 0.48 grams of gold per ton, but in certain parts overgrown by shrubberies there was found as much as 3.69 grams per ton. Since for the last twenty years or more the average ore treated assayed 9.5 to 10.2 grams and the recovery was 9.0 to 9.5, this high content in the tailings can hardly be ascribed to losses in milling and treatment, but must be attributed to accumulation after the tailings had been dumped.

These observations suggested an investigation into the nature of the agents that might have caused the transport of gold from its original point to lower levels. The physical and chemical properties of the original gold and the " new gold," as it may be called, were investigated. The specific gravity was determined by means of the specific-gravity bottle; the color and the surface were observed under the microscope; differences in hardness or in toughness could not be investigated since the particles of the new gold were too small. To examine the affinity to mercury, *i.e.* to see whether the new gold is a " free milling " or a " refractory " one, the gold samples were passed over copper plates of 4 to 6 inches, coated with a thin film of mercury. To determine the action of cyanide solutions on the two varieties of metal, carefully weighed portions of gold of the same degree of fineness were exposed to solutions of cyanide of potassium of various strengths for many days. The gold in solution was determined at equal intervals for both kinds of gold under treatment. The results of these tests are shown in Table I.

2

TABLE I.

PHYSICAL AND CHEMICAL PROPERTIES OF THE DIFFERENT KINDS OF GOLD OBSERVED.

Kind of Gold.	Spec. Gravity.	Color.	Surface.	% Metal Caught on Mercury.	% Gold Dissolved in KCN-solution of . . . % .5 When in Contact during . . . Hours		1.0		2.5	
					24	144	24	144	24	144
Common placer gold, 98.3% Au, 1.7% Cu	19,562	Yellow	Scarred	66.45	16.2	33.5	22.4	55.7	43.7	88.8
"New" gold, 100% Au	19,222	Greenish	Plain	18.38	3.5	11.8	10.1	48.2	21.4	44.5
"Black" gold, after crust was taken off. 100% Au	19,217	Greenish	Plain	16.66	2.9	11.5	9.9	40.4	19.7	43.9

It will be noted that the new gold is very refractory against mercury but is relatively more soluble in cyanide solutions.

It is remarkable that the physical and chemical properties of the new gold are, even in minute details, identical with those of the so-called "black gold" (*ouro preto*) found in Brazil at many places near the ancient State capital of Minas Geraes, which drew its name from the numerous deposits of "black gold" in its vicinity. These were worked out by the first discoverers in the districts of Itabirito, Diamantina, Sabará, Santa Barbara, São Gonçalo do Sapucahy, Carangola, all in Minas. Black gold is also commonly found in the districts of Rio Verde, Formosa, Santa Luzia in the State of Goyaz, and in the district of Santa Rita do Araguaya in Matto Grosso. The native prospector generally inadvertently throws it away with the heavy residuals in the pan, such as titanite, black garnet, magnetite, rutile, wolframite, and tourmaline; only by chance is it detected in the pan when the surface of the gold is given thorough attention. Black gold, as it is found at these places, is gold covered with a dark brown to dull black coating of 2 to 25μ in thickness; where larger grains of metal are found, they prove to be composed of several smaller individuals each of which preserves its own coating. A washing with a 5 per cent. solution of K_2CO_3 at a temperature of 35°–45° is sufficient in most cases to make the coating disappear;

where the
required, v
acid. The
moved by
to the met
dark varie
Fe_2O_3 and
In so far
whether th
brown one
(humate o

The abo
the " black
acids form
sponsible
levels. To
first with
coal found
ward with
of humific

The bro
ash, 36.28
matter, an
substances
by Simek
stance whi
vacuum at
4.98 per c
ash, of w
P_2O_5. Se
this raw p
solutions i

In order
pensions th
ties of go
exposed to

2 See *Bren*

3

where the coating is thicker, a cautious heating to 300°–330° is required, which is followed by a washing with dilute sulphuric acid. The sulphate of iron which is then formed has to be removed by washing before cyanide or other agents can be applied to the metal, which then shows its customary yellow color. The dark varieties of "black gold" show 0.22 to 0.35 per cent. of Fe_2O_3 and the browner ones, 2.85 to 3.5 per cent., in the coating. In so far as the writer's investigations go, it cannot be said whether there is only one kind of coating or several kinds; the brown one which was investigated can be considered as $C_2O_7H_{12}Fe$ (humate of iron).

The above considerations as to the character of the coating of the "black gold" flakes suggest that waters charged with organic acids formed by the decomposition of vegetable matter were responsible for the transportation of gold from higher to lower levels. To check this idea, several series of tests were made, first with an artificial product prepared from bituminous brown coal found in the vicinity of Carangola, Minas Geraes, and afterward with "black water" generated in virgin forests from centers of humification of decayed vegetation.

The brown coal contained 21.33 per cent. water, 15.62 per cent. ash, 36.28 per cent. fixed carbon, and 26.77 per cent. of volatile matter, and held in its combustible matter about 68 per cent. of substances soluble in alkali. According to the process indicated by Simek [2] this raw product was used to isolate a dark brown substance which, after a long period of drying, first in air, then in vacuum at 55° C., showed upon analysis 67.21 per cent. carbon, 4.98 per cent. hydrogen, 1.23 per cent. nitrogen, and 7 per cent. ash, of which the most important constituents were Fe_2O_3 and P_2O_5. Separation by solubility of the different components of this raw product was not tried; for the experiments described, solutions in water were used.

In order to determine the minimum concentration of such suspensions that would act upon free gold, carefully weighed quantities of gold in the form of plates of uniform granulation were exposed to solutions of known concentration contained in glass

---

[2] See *Brennstoff Chemie,* vol. 9, 1, 12, p. 381, 1928.

TABLE II. REACTIONS OF HUMIC ACIDS ON GOLD UNDER DIFFERENT CONDITIONS.

Strength of Solution.	Kind of Water.	Gold Experimented on.		Conditions.	Duration of Experiment. Hours.	Dissolved.	
		Shape.	Fineness.			Mg.	%
% .10	Rain water, airless	Plate, .01″	850/1000	No Motion	24	8.354	.05
					48	15.228	.91
		Dust, .01″	850/1000	"	24	11.182	1.14
					48	23.075	2.35
					72	25.553	2.59
.50	Rain water, airless	Plate, .01″	1000/1000	Constant Motion	24	2.134	.005
					48	2.664	.0062
	Rain water, aerated	Dust, .005″	1000/1000	"	24	Traces	0
					48	Traces	0
2.50	Dist. water, airless	Dust, .005–.1 mm.	900/1000	No Motion	24	32.551	3.68
					48	65.001	7.21
					72	97.161	11.08
4.00	Rain water, airless	Same material as before		Slow Motion	24	27.101	3.11
					96	111.402	12.50
					192	168.249	19.28
					300	175.455	20.21
10.00	Rain water	Dust, .002–.08 mm.	600/1000–975/1000	Slow Motion + air	24	23.450	1.56
					48	42.761	2.84
					72	70.111	4.66
					240	166.369	11.00
5.00	Dist. water	Gold precipitated by $FeSO_4$		No Motion	48	Traces	
					96	Little more	
10.00	Dist. water with 1 % of K_2CO_3	Plate, .01″	900/1000	"	24	Traces	
					30	Reaction stopped	
10.00	Dist. water with 1 % of K_2CO_3, 1 % of $NaHCO_3$	Same material and same conditions of experiment			Suspension without effect		
10.00	Aq. dist. with .5 % KNO_2, .5 % KNO_3, .5 % NaCl	Same material and same conditions of test			After 12 h. without any effect		
10.00	Water with .5 % Na_2SO_4, .5 % $CaHCO_3$	Identical material, under same conditions			Merely traces dissolved; after a few hours no effect whatever		

bottles that wei
stances distillec
access to the a
was conducted
was carried on
the same conc
shown in Table
The data of
1. Gold is at
character, prov
cluded. Oxyge
may readily be
brown to chestr
suspensions are
per cent. solutic
2. Distilled
ganic acid solut
rain water is c
different minera
acids; e.g. the
destroy the hur
sulphates, and
the stability of
determined wh
varies with diffe
ducted at field
3. The finen
fluence the solu
copper, and pal
cerned. Differ
of the acids on
In the latter ca
used; metal pre
rapidly attacked
of these differe
different precipi

bottles that were kept in slow, continuous motion. In some instances distilled water free from air was used; in others, free access to the air was allowed. Another series of experiments was conducted under free admission of carbonic acid, and a third was carried on with water mineralized with one or more salts in the same concentration as in subsoil water. The results are shown in Table II.

The data of Table II. allow of the following conclusions:

1. Gold is attacked by humic acids, even those of a very dilute character, provided sufficient time is allowed and oxygen is excluded. Oxygen rapidly destroys the organic combination, as may readily be seen by the clarifying of the water from dark brown to chestnut and reddish yellow to gold yellow; clear brown suspensions are absolutely innocuous to gold metal, even in 20 per cent. solutions.

2. Distilled water and water freed from air maintain the organic acid solutions in their full activity for a considerable time; rain water is only slightly inferior. With natural waters, the different minerals contained in them act differently on the organic acids; e.g. the carbonates and bicarbonates are the first salts to destroy the humic acids in the water, then follow sulphates, bisulphates, and nitrates; chlorides seem to have but little effect on the stability of the organic acids. The writer has not as yet determined whether the susceptibility of the metal to solution varies with different temperatures; all experiments have been conducted at field temperatures.

3. The fineness of the original metal does not appear to influence the solubility in the humic acids, at least so far as silver, copper, and palladium, as constituents of the gold ore, are concerned. Differences can be noted, however, between the reactions of the acids on natural gold and on gold produced by precipitation. In the latter case, solubilities vary according to the precipitant used; metal precipitated by ferrous sulphate, for example, is less rapidly attacked than gold precipitated by oxalic acid. The causes of these differences have not yet been investigated; probably the different precipitates are different allotropic varieties of gold.

6

Following these investigations more elaborate experiments were made, utilizing moor water or black water from the Serra dos Aymorés, the divide between the States of Minas Geraes and Espirito Santo and one of the thickest virgin forest districts of the whole country.[3]

Observation shows that these waters, which are dark yellow to brown or black in color, absolutely clear and transparent, low in oxygen or free from it, and of a strong acid reaction, quickly attack all the easily soluble components of the rocks such as the combinations of K_2O, Na_2O, CaO, and MgO. A relative concentration of the iron and manganese hydroxides and oxides is followed by the destruction of these constituents; the alumina and phosphoric anhydride combinations, if not destroyed and transported, are at least affected. Finally there remains merely silicic acid free from any metallic accessories except oxides of tin, tungsten, titanium, and zirconium. Gold, silver, and palladium disappear among the first constituents destroyed.

There can be no doubt that the black waters transport metallic combinations in the form of definite chemical compounds and not by adsorption; formulas can be established for the majority of metals, *i.e.* iron, copper, and manganese, for their combination with humic acids, and this is true of gold also.

After the black water has dissolved the metals, contact with the open air is sufficient to oxidize the metals and to cause them to form a scum on the water surface, in the case of iron, copper, and manganese (and probably of some other common metals also). In the case of gold, however, other conditions are necessary to bring about its reappearance. Simple contact with the atmosphere is not sufficient to separate it, since oxygen does not act

---

[3] Under normal conditions, an acre of ground produces in this region about 3,500 cubic feet of timber, 8 to 11 per cent. of which decays annually (about 7.5 to 10.8 tons); 80 per cent. of this raw material disappears by quick fermentation which leaves only 5 per cent. or even less, equal to one eighth inch, as humus on the ground, while 20 per cent. suffers transformation under water, giving origin to the so-called black waters (*rios negros* or *rios pretos*) commonly noted on geographical maps of the tropics. Although these black waters are not so extensive in this part of Brazil as in the Amazon districts, or in Sumatra or Borneo, they carry annually thousands and thousands of tons of rock material in suspended colloidal form to the ocean or to deeper levels alongside the Rio Doce.

---

intensely enou
precipitation o
circulation mee
sulphate waters
While invest
side valleys of
Doce on the le
dos Aymorés, t
ments the proc
that go on in
purpose a wood
long, was built
flume was fille
washed sand of
clay, or with p
III. The fillin
jets. The upp
sand and clay,
but in this secti
of gold dust of
at once if pann
a constant stre
that carried fr
black water wa
flume was cov
water allowed t
measured at th
passed through
permitted samp
the sand or oth
With each fil

4 The conglomera
head) in Minas Ge
by gold that origina
It is highly probabl
State of Minas are
black waters which

7

intensely enough on the gold humate; it is indispensable for the precipitation of gold that the gold humate in its underground circulation meet strongly mineralized waters such as carbonate or sulphate waters.[4]

While investigating a small placer gold deposit in one of the side valleys of the Rio Pancas, one of the affluents of the Rio Doce on the left which comes down from the center of the Serra dos Aymorés, the writer verified in an extensive series of experiments the processes of gold solution, transport, and redeposition that go on in nature in the manner described above. For this purpose a wooden flume six feet wide, four feet deep, and 50 feet long, was built with an inclination of one inch in three feet; this flume was filled for nine-tenths of its length with thoroughly washed sand of determined fineness, or with mixtures of sand and clay, or with pure kaolin, according to the details shown in Table III. The filling was evenly packed each time by means of water jets. The upper tenth of the flume was finally filled with sand, sand and clay, or pure kaolin, as in the longer part of the flume, but in this section there was admixed a carefully weighed amount of gold dust of known fineness and grain that could be recognized at once if panned out. Into this end of the flume was delivered a constant stream of black water derived from a nearby rivulet that carried from 6 to 10 per cent. of raw humus. Before the black water was introduced into the head of the flume, the whole flume was covered with water-tight boards. The amount of water allowed to sink into and pass through the flume filling was measured at the lower end by means of a tank fed by a pipe that passed through the bottom boards of the flume. This tank also permitted samples to be taken of the water that sank through the sand or other filling.

With each filling, one experiment lasted sixty days; at ten-day

---

[4] The conglomerates known by the name of *tapanhoancanga* or *canga* (nigger head) in Minas Geraes, famous for their gold and diamonds, are partly cemented by gold that originally circulated in solutions formed in the manner here described. It is highly probable that the deposits of lignite known and partly explored in the State of Minas are the remainders of those virgin forests that gave origin to the black waters which transported the gold solutions mentioned here.

8

pp. 55–62

Phanerozoic Analogues for Carbonaceous Matter in Witwatersrand Ore Deposits

J. PARNELL

Department of Geology, Queen's University, Belfast BT7 1NN, United Kingdom

Abstract

Thoriferous bitumen nodules in quartz-pebble conglomerates and pebbly sandstones of Phanerozoic age in the British Isles are analogues for the uraniferous bitumen nodules (flyspeck) in the Archean Witwatersrand gold-uranium deposits. They are comparable in morphology, relationship to bedding planes, replacive behavior toward quartz, mineralogy, fragmentation, and displacement of inclusions. In each case the quartz-rich sedimentary host rocks represent regionally important transgressive deposits.

The contrast in dominant radioelement (thorium or uranium) probably reflects differences in mobility of the elements as a function of variable Eh conditions. The Phanerozoic thoriferous nodules occur only in pale (low Eh) beds which lack uranium deposits, but in the Archean Witwatersrand deposits fractionation of uranium and thorium may not have been as marked.

In the Phanerozoic examples there is good evidence for migration of hydrocarbons through the host rocks and the bitumen nodules can confidently be attributed a hydrocarbon origin. By analogy, this supports proponents of a hydrocarbon origin for the Witwatersrand carbon, rather than a microbial origin.

THE GENESIS of mineralization in the Witwatersrand gold fields of South Africa has long been a matter for debate. In particular, two basic aspects of the mineralization have been subject to fundamentally different interpretations. The metalliferous phases in the Archean quartz-pebble conglomerates of the Witwatersrand have been attributed to either detrital or authigenic origins (Simpson and Bowles, 1977; Smits, 1984; Phillips and Myers, 1989; Reimer and Mossman, 1990; Robb and Meyer, 1991); and carbonaceous matter with which gold and other metals are closely associated has been widely interpreted as representing cyanobacterial or other microbial kerogen (Snyman, 1965; Hallbauer, 1975, 1986; Zumberge et al., 1978; Dyer et al., 1988; Ebert et al., 1990; Smits, 1992), but alternatively as the residue of migrating hydrocarbons (Schidlowski, 1981; Robb and Meyer, 1991). The understanding of the origin of the carbon is very important, as it constrains both the timing and mechanism of metal uptake by the carbon, and the prediction of carbon distribution in support of gold exploration. The resolution of the origin of the carbon in these Early Proterozoic rocks is hindered by the highly indurated state of the rocks and the advanced degree of maturation of the carbon. An apparent absence of younger analogues has also limited our understanding of the mineralization. Here I report a comparable style of mineralization involving carbonaceous matter in quartz-pebble conglomerates and pebbly sandstones of Paleozoic age in the British Isles. In this case the nature of the carbon is better understood, and by analogy may aid the understanding of the Witwatersrand carbon.

The Witwatersrand quartz-pebble conglomerates contain seams of carbon and widespread nodules of carbon (flyspeck) which are highly enriched in uranium and also other elements including gold. Conglomerates-pebbly sandstones in two regions of the British Isles have been studied in detail for their content of similar nodules of carbon which are highly enriched in thorium. The nodule-bearing sequences are in the Carboniferous North West Irish basin (Parnell and Monson, 1990) and in the Welsh borderland in rocks of Silurian age (Parnell et al., 1991). Nodule-bearing quartz-pebble conglomerates are particularly prominent in the Llandovery Folly Sandstone of Powys, Wales.

Carbonaceous Matter in Precambrian Deposits

Precambrian quartz-pebble conglomerates mineralised by gold and/or uranium include the deposits of the Witwatersrand basin; the Blind River-Elliot Lake district, Ontario; the Jacobina district, Bahia, and the Gandarela syncline, Minas Gerais, Brazil; and the Francevillian basin, Gabon. The Canadian, Brazilian and Gabon deposits are in Lower Proterozoic sediments, and the Witwatersrand deposits are Archean hosted (Robb et al., 1990). The nature of this type of mineralization is reviewed by Pretorius (1981). A fundamental aspect of the Witwatersrand deposits is the occurrence of seams and nodules of carbonaceous matter, mineralised by gold and uranium and therefore used as an exploration guide. The Canadian deposits similarly contain both seams and discrete globules, and also fracture fillings (Willingham et al., 1985; Mossman, 1987). In Brazil, the Moeda Formation of the Gandarela syncline also includes carbon seams and granules (Renger and Minter, 1986), and some uranium in the Jacobina deposits is located within carbon granules (Horscroft, 1986). The Francevillian basin includes uranium concentrations so rich that they gave rise to several natural fission reactors at Oklo, some of which show a very close relationship to carbonaceous matter, including fracture fillings, vug fillings and intergranular reservoir bitumens (Gauthier-Lafaye and Weber, 1989; Cortial et al., 1990). Clearly, carbonaceous matter is a consistent component of this type of ore deposit, and it is important to understand its origin. Samples from Brazil and Gabon as well as from the Witwatersrand are used in this comparison with Phanerozoic carbonaceous matter.

Phanerozoic Analogues

Nodule-bearing sequences

Detailed accounts of the distribution of thoriferous bitumen nodules in the Welsh borderland and northwest Irish basin are given by Parnell and Eakin (1989) and Parnell and

0361-0128/96/1802/55-8$5.00

106

Monson (1990), respectively. The following is a summary of pertinent aspects.

Welsh borderland: Bitumen nodules occur widely distributed in the Llandovery Folly Sandstone near the town of Presteigne, in pebbly sandstones and microconglomerates. The nodules are up to 1 mm in diameter and are replacive, particularly toward quartz grains and pebbles. The nodules contain numerous inclusions of thorite and thorianite. Ten kilometers to the northeast, similar-sized nodules occur in the Wenlockian Letton grits, and also in the Longmyndian (Upper Proterozoic) Brampton grits which also consist of conglomerates and pebbly sandstones (locations figured in Parnell et al., 1991). The Letton grits nodules contain inclusions of monazite; the Brampton grits nodules contain lesser amounts of carbon and consist predominantly of titanium and iron oxides. The latter nodules are concentrated in seams and show some coalescence. The nodules in Silurian rocks are generally isolated, but preferably may occur concentrated along certain layers. The nodule-bearing sequences all lie upon a Late Proterozoic basement. The Silurian rocks are characterized by shallow-marine faunas.

Northwest Irish basin: Submillimeter bitumen nodules occur in siliciclastic units of lower Carboniferous age over a region of 1,500 km^2 in North West Ireland. The sandstones are predominantly fluviodeltaic, with some marginal marine influence. The Carboniferous onlaps a crystalline basement surface of Caledonian granite and metasedimentary rocks. Nodules occur in sandstones and, near to the basement surface, in conglomerates and pebbly sandstones. The nodules are most abundant in the coarser marginal rocks nearest to an outcrop of radioelement-rich granite. The nodules are replacive and contain inclusions of thorite and a mixed thorium phosphate-silicate phase (Monson, 1993). It has been possible to place hydrocarbon migration within the diagenetic sequence for the sandstones (Fig. 1).

Comparison with Witwatersrand sequences

The carbonaceous matter in the Phanerozoic rocks shows many similarities with that in the Witwatersrand conglomerates and similar Archean-Proterozoic rocks elsewhere. The comparison includes nodular form, relationship to bedding planes, multiple carbon phases, aggressive behavior toward quartz, mineralogy of inclusions, and fragmentation and displacement of inclusions, as well as a similarity in petrography and paleoenvironment of the host rocks. The analogy is itemized as follows:

1. The major host to the mineralized carbonaceous matter is a quartz-pebble conglomerate-pebbly sandstone in each case. The Witwatersrand and Huronian conglomerates are well described (Roscoe, 1981) and represent major transgressive deposits. In the Welsh borderland, the thoriferous bitumen nodules occur particularly in conglomerates of the Folly Sandstone, deposited during a regionally important Llandovery transgression upon Precambrian rocks (Ziegler et al., 1968). In the North West Irish basin, nodules occur mostly in sandstones, but are best developed in a pebbly facies deposited where Carboniferous sedimentation transgressed the margin of a plutonic-metamorphic topographic high.

2. The carbon in the Witwatersrand occurs in two prominant forms: seams of carbon up to a few centimeters thick which (1) pass between, or (2) are moulded around, quartz pebbles (Schidlowski, 1981). The relationship between these forms is described below. In addition to the seam morphology, flyspeck nodules may be concentrated along certain layers. The thoriferous carbon nodules in the Welsh borderland and northwest Ireland are very similar to the flyspeck nodules, all up to 1 mm diam (Parnell et al., 1990). They are similarly concentrated on certain bedding planes (Fig. 2A), which probably reflects an anisotropy in permeability and access to mineralizing fluids. Where the nodules are most abundant, they are seen to be partially coalesced together along layers parallel to the bedding (Fig. 2B).

3. There is evidence for the introduction of carbon in more than one phase. Petrographic studies of the Witwatersrand rocks show that there are uraniferous and nonuraniferous carbon phases, which may be in contact with each other (Landais et al., 1990; Smits, 1992). There are similarly uraniferous and nonuraniferous carbon phases in close proximity in the

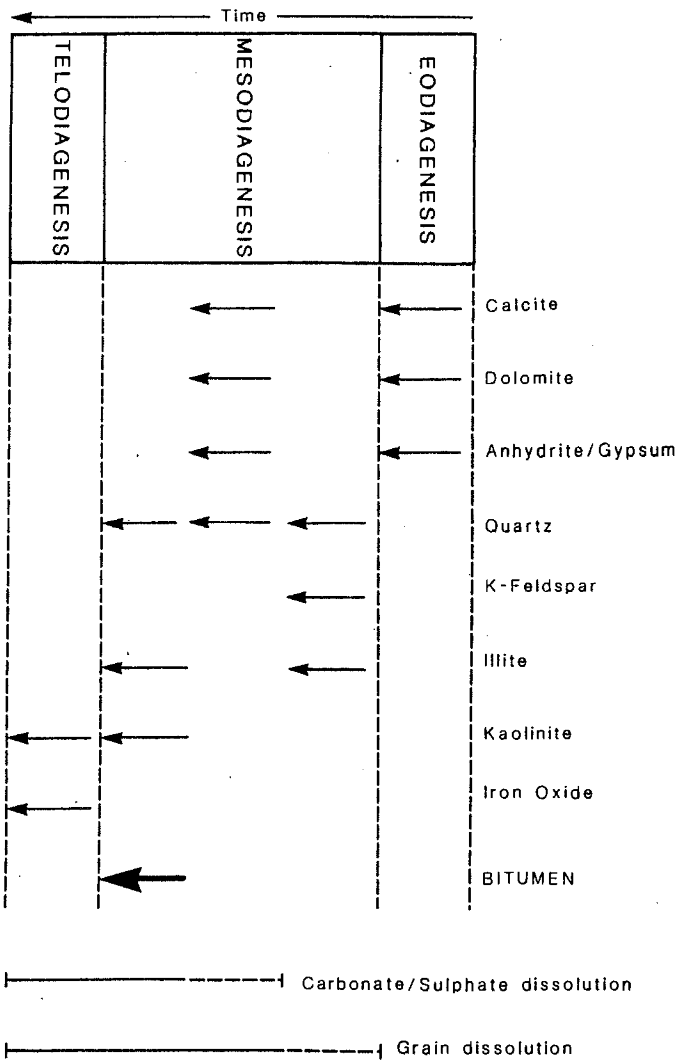

FIG. 1. Diagenetic sequence for host sandstones to thoriferous bitumen nodules, northwest Irish basin, showing that bitumen is paragenetically late. Maximum temperature of mesodiagenesis reached 140°C.

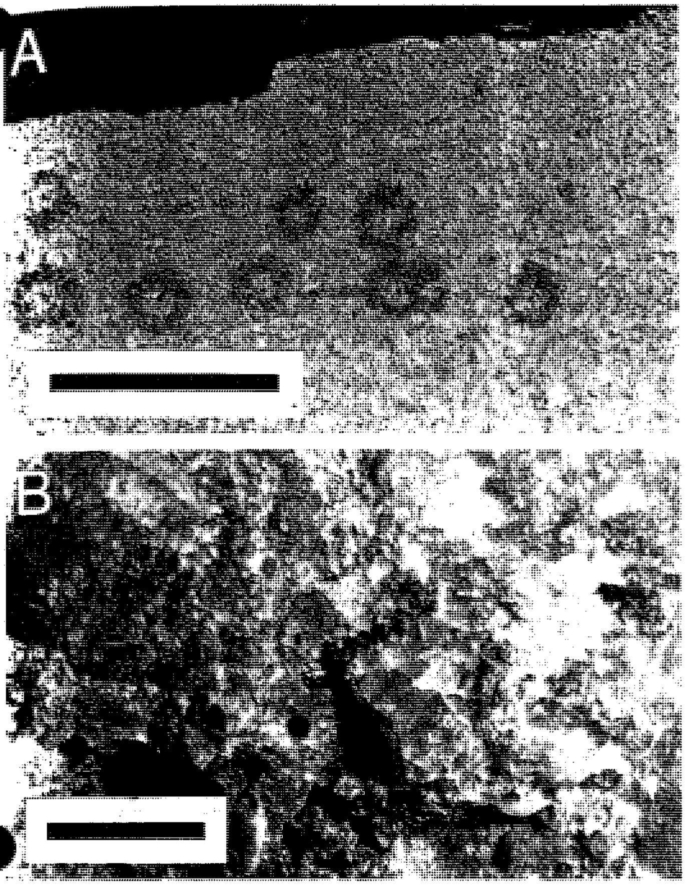

FIG. 2. Bedding plane siting of thoriferous bitumen nodules. A. Cross section of sandstone bed, northwest Irish basin, showing two horizons of nodules (encircled). B. Plan view of sandstone bed, Welsh borderland Silurian, showing partial coalescence of nodules. Scales: A = 2 cm, B = 1 mm.

Huronian Supergroup (Mossman, 1987). In the Welsh borderland, the thoriferous bitumen nodules in Llandovery sandstones are closely associated with nonthoriferous fracture-bound bitumens in the sandstones and superjacent Wenlockian limestones. The nodules themselves can show a network of nonthoriferous veinlets which appear to postdate the thoriferous phase (Fig. 3A), a feature which is similar to the sequence in the Witwatersrand.

A texture seen in some cases consists of a distinctive composition of bitumen around uraninite-thorite crystals, evinced in backscattered images (Fig. 4 compares this texture in the Proterozoic of Oklo and the Silurian of the Welsh borderland). The crystal coatings probably have compositions distinct from the background bitumen due to the effects of radiation.

4. The carbon in both cases has replaced the outer parts of quartz pebbles and other clasts. Carbonaceous nodules exhibit scalloped margins penetrating into the quartz pebbles; this is almost ubiquitous in Witwatersrand samples and samples from the Welsh borderland, and common in the Irish samples. Nodules are also found wholly isolated within quartz pebbles in each case: it is assumed that carbon entered the pebbles through microfractures in the quartz and then grew replacively. Many nodules occur at pebble contacts, where they penetrate two or more pebbles, precluding the possibility of mechanical transport with the pebbles. Some clasts have attracted many adhering nodules, partially coalesced to form a semicontinuous coating: examples are seen in both Phanerozoic (see fig. 1c of Parnell et al., 1990) and Proterozoic cases.

5. The detailed petrography of the nodules is similar. In addition to their replacive behavior toward siliciclastic grains, they exhibit patterns of mineral inclusions which appear to represent disintegration and displacement (Fig. 5). Examples exist showing a zonation in inclusion mineral composition, and the effects of irradiation from the radioactive minerals are evident in the immediately adjacent rock. I have drawn attention elsewhere to the radioactive blasting halos which occur around thoriferous bitumen nodules and to their marked similarity to those previously documented from the Witwatersrand (Parnell et al., 1990). Nodules embedded in

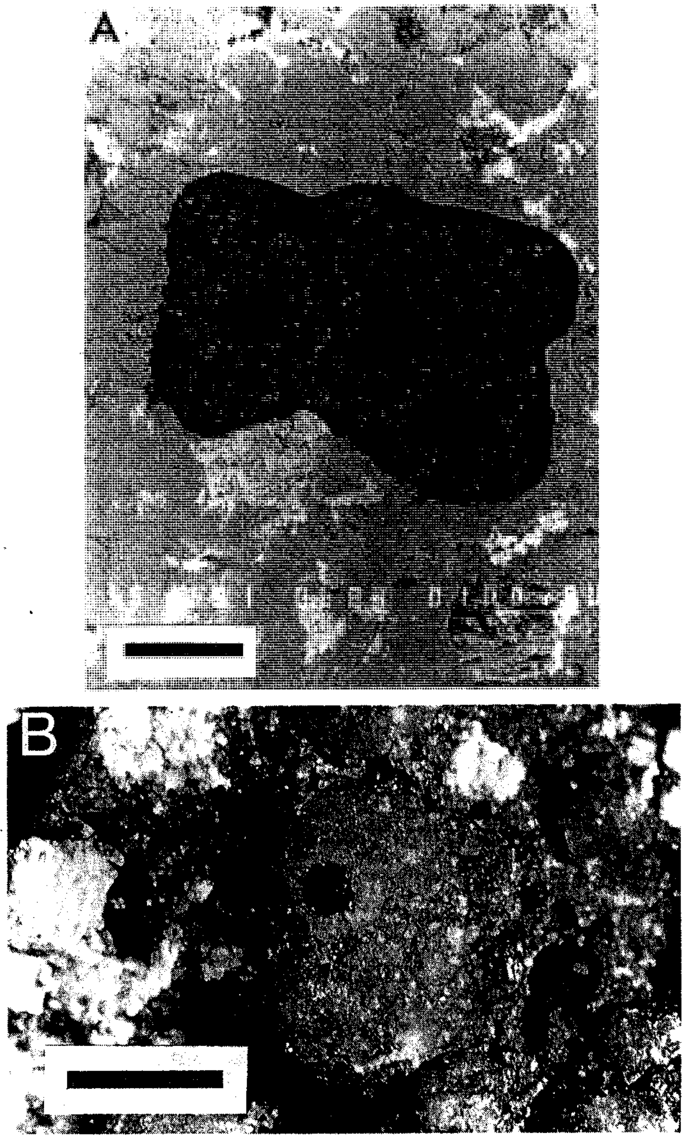

FIG. 3. Thoriferous bitumen nodules, Welsh borderland Silurian. A. Backscattered electron micrograph showing inclusions of thorite-thorianite (bright spots) and veining by nonthoriferous (inclusion-free) bitumen. B. Nodule surrounded by radiation halo, visible in ordinary light. Scales: A = 100 μm, B = 2 mm.

quartz pebbles in the Welsh borderland have halos in the quartz which may even be visible to the naked eye (Fig. 3B). The halos reflect a metamict state in the crystal structure of the quartz, as a consequence of radiation damage.

6. The mineralogy of metalliferous inclusions within the nodular carbon is closely comparable. The flyspeck nodules in the Witwatersrand contain predominantly uraninite, with some coffinite and also some uranium in the form of uraniferous titanates (brannerite and similar) (Schidlowski, 1981; Smits, 1984). Nodules of similar size to flyspeck in the Brazilian Moeda Formation contain a much more significant titanium component: most of the ~~uranium~~ occurs as uranium titanates and some nodules are exclusively titanate minerals without carbon (Fig. 6A). The thoriferous nodules contain inclusions of thorite, thorianite, or monazite. In the Welsh borderland, some nodules in the late Precambrian consist predominantly of titanium oxides, and like the titanate nodules of the Moeda Formation, may even be completely mineralized without carbon (Fig. 6B).

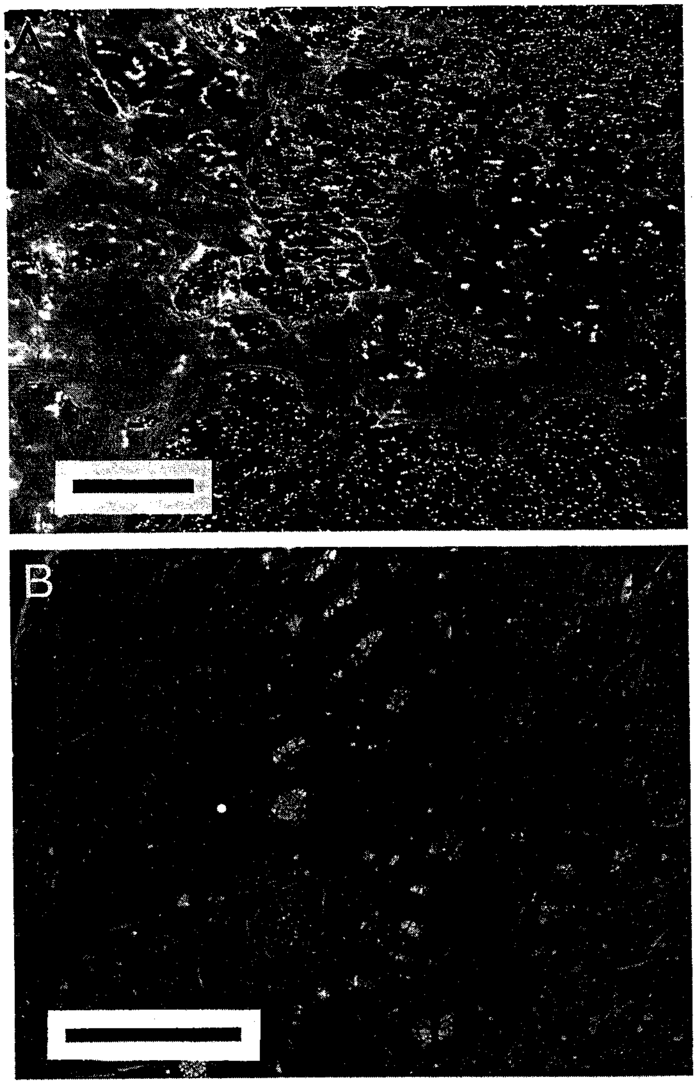

FIG. 4. Backscattered electron micrographs showing bitumen immediately around uraninite-thorite inclusions, distinct from background bitumen, probably due to effects of radiation immediately around inclusions. A. Uraninite-bearing bitumen, Oklo, Gabon. B. Thorite-bearing bitumen, Welsh borderland Silurian. Scales: A and B = 100 μm.

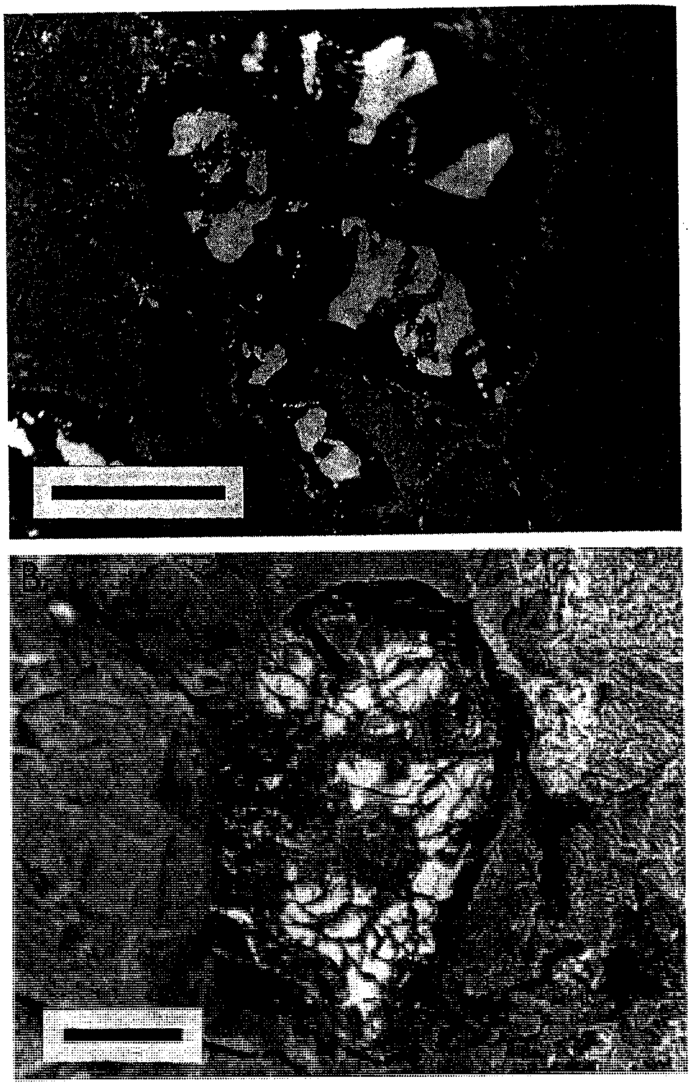

FIG. 5. Backscattered electron micrographs showing inclusions within bitumen exhibiting fragmentation and displacement of inclusion segments. A. Uraninite-bearing bitumen, Witwatersrand. B. Thorite-bearing bitumen, northwest Irish basin. Scales: A = 100 μm, B = 40 μm.

Discussion

Origin of Phanerozoic carbon nodules

An origin for the Phanerozoic carbon nodules from migrating hydrocarbons seems incontravertible. The occurrences of thoriferous bitumen nodules discussed here from the British Isles, and several occurrences in other countries, all occur in basins which are hydrocarbon-prospective today or have been in the geologic past (Parnell et al., 1990). In each case, the nodules occur in the vicinity of ordinary (pore-filling or fracture-bound) oil residues. In the Welsh borderland, the nodule-bearing sandstones are above a probable Precambrian-lower Paleozoic source rock, which also contains bitumen in crosscutting fractures (Parnell et al., 1991). Quartz crystals in veins cutting through the Llandovery nodule-bearing rocks and the overlying Wenlockian exposed to the south contain

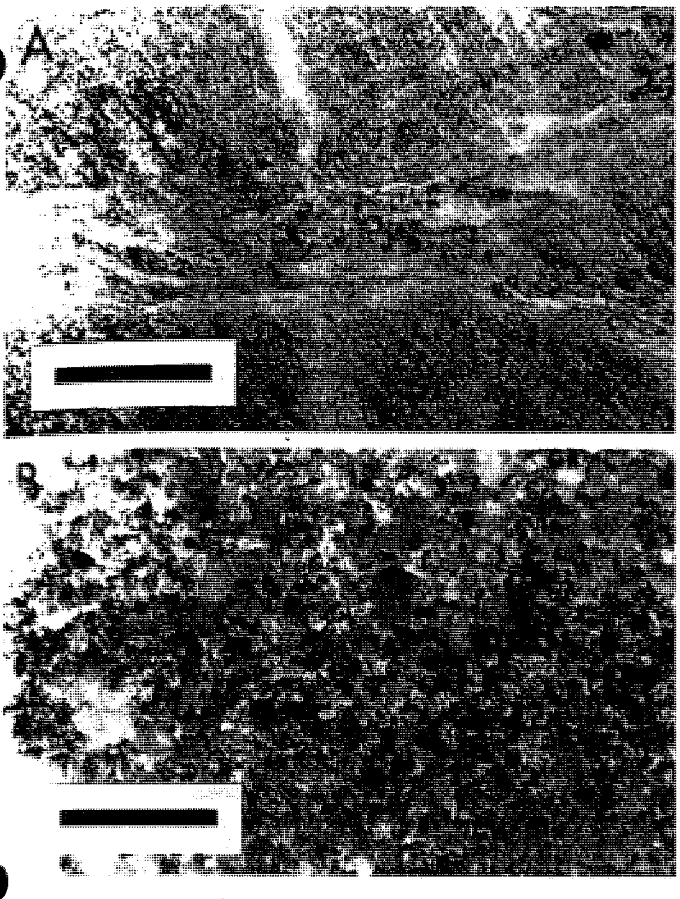

FIG. 6. Titanium-rich nodules. A. Seam of uranium titanate nodules (arrowed) in Moeda Formation, Brazil. B. Titanium oxide nodules in sandstone, Welsh borderland Precambrian. Scales: A = 4 mm, B = 2 mm.

abundant fluid inclusions which readily fluoresce in ultraviolet light due to their high content of fluid hydrocarbons (Fig. 7). In northwest Ireland the nodules occur in sandstones above and below a shale-bituminous limestone source rock, and there are, in addition, bitumens located nearby in hydrothermal fractures and in reservoir channel sandstones (Parnell and Monson, 1990). An example of the same phenomenon in Australia was shown by organic geochemical evidence to be probably related to oil elsewhere in the sequence (Rasmussen et al., 1989).

FIG. 7. Quartz crystal from crosscutting fracture in Welsh borderland Silurian, showing fluid inclusions fluorescing under ultra-violet light due to hydrocarbon content. Scale: 1 mm.

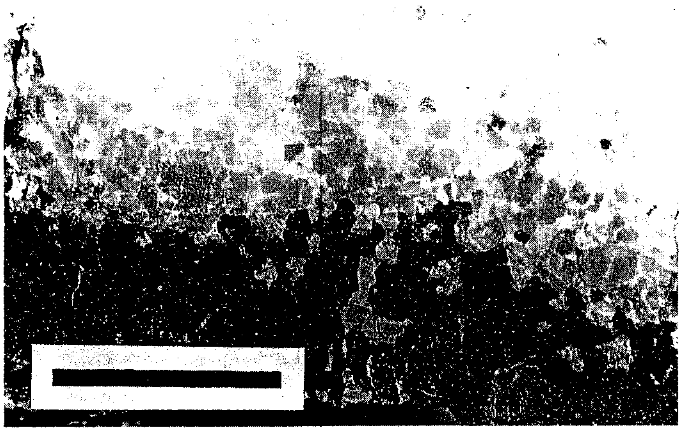

FIG. 8. Gradation from carbon (bitumen) seam to discrete bitumen nodules in Witwatersrand sample. Scale: 2 mm.

Morphology of carbon

In the Phanerozoic analogues described, carbon is in nodular form, with rare examples of coalescence and a preferred occurrence along bedding planes. In the Witwatersrand rocks, flyspeck nodules are common, as are seams of carbon. On detailed examination, the seams are seen to consist of closely packed nodules (Fig. 8). Where the nodules show a preferred orientation, they are elongate normal to bedding rather than bedding-parallel (Fig. 9A, B). This implies that the seam morphology is only due to coalescence of nodules, not growth of a carbon structure in a horizontal plane. Thus the concentration of Witwatersrand carbon along bedding planes is similar to that in Phanerozoic rocks but with a greater degree of coalescence. The elongation of the Witwatersrand nodules normal to bedding is due to the high lateral density of nodules (as seen in a plan view of a seam; Fig. 9A), which meant that expansion could only occur out of the bedding plane, to give the columnar morphology described by some workers (e.g., Hallbauer, 1975). Fragmentation of uraninite inclusions is a widely observed phenomenon in uraniferous organic matter (e.g., Parnell, 1988a; Eakin and Gize, 1992), explicable by the effects of irradiation. The phenomena associated with irradiation of organic matter are well discussed elsewhere (e.g., Curiale et al., 1983; Willingham et al., 1985; Rasmussen et al., 1993). In essence, alpha radiation (and to some extent beta and gamma radiation) induces condensation and polymerization reactions within fluid hydrocarbons, i.e., migrating oil and gas, which causes precipitation of viscous-solid hydrocarbon coatings around radioelement-bearing grains. Subsequent intense flux of alpha particles into the coating has a significant effect upon the polymeric hydrocarbon, causing progressive hardening (Charlesby, 1987). The polymer experiences a swelling effect as further fluid hydrocarbons enter the crosslinked structure. Volume increases of an order of magnitude are recorded in experimental studies (Bauman and Glantz, 1957). This enormous expansion ex- 5

Artificial Transmutation - The process of bombarding a nucleus with alpha particles, protons, or neutrons to give an unstable nucleus, which can then emit a proton or neutron in order to 110

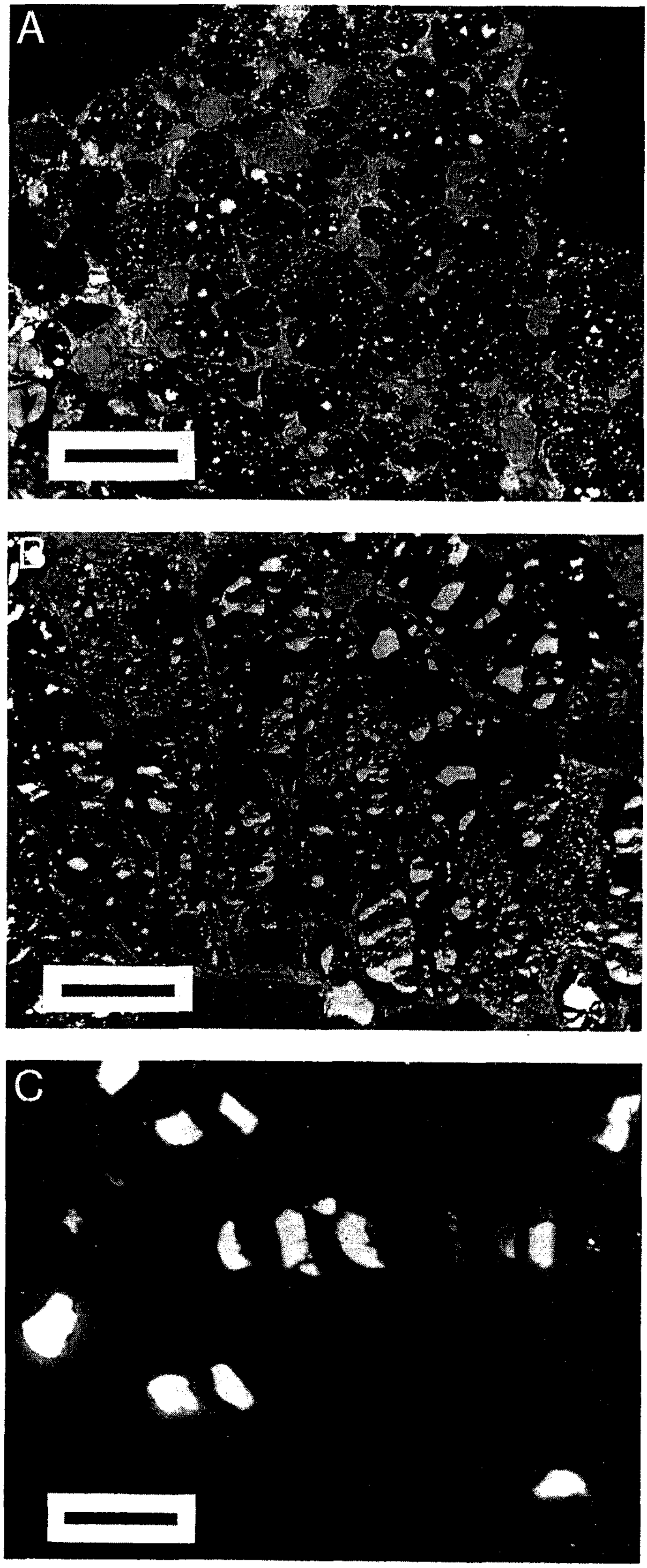

FIG. 9. Bitumen nodule morphology. A. Plan view of Witwatersrand seam showing it to consist of closely packed nodules. B. Cross section of Witwatersrand seam showing it consists of closely-packed nodules elongate normal to bedding, with fragments of uraninite inclusions displaced apart in this orientation. C. Analogous displacement of uraninite inclusion fragments in a consistent orientation in bitumen, Laxey mine, Isle of Man. Scales: A = 400 μm, B = 100 μm, C = 40 μm.

plains the observed displacement of the fragments of uraninite in the Witwatersrand nodules and the thorite-thorianite in the Phanerozoic nodules. The high degree of expansion of uraninite in one orientation (i.e., bedding-normal) in the Witwatersrand bitumen is also seen in Phanerozoic uraniferous bitumens (Fig. 9C shows an example from the Isle of Man; compare with Fig. 9B). A further effect of radiation is radiolysis of pore water to produce large amounts of free radicals, which may be responsible for the replacement of detrital grains.

Contrast in uranium and thorium enrichment

There are many known examples of solid bitumens which are highly enriched in radioelements and contain inclusions of radioelement minerals (Parnell, 1988a); however, in any one occurrence the mineral inclusions are either predominantly uraniferous or predominantly thoriferous. Bitumens are not comineralized by both uranium and thorium and fractionation of the two elements has clearly occurred at some stage. Fractionation is most likely to reflect differences in the mobility of the two elements as a function of prevailing pH-Eh conditions rather than a difference in metal-organic interaction. In Phanerozoic and late Proterozoic siliciclastic sequences, uraniferous bitumens tend to occur in red beds whereas thoriferous bitumens occur in white-gray beds, a feature which reflects the preferential mobility of uranium and thorium in high and low Eh conditions, respectively. In the north of Ireland, the white-gray Carboniferous sandstones in the west are thorium mineralized, whereas Permian and Triassic red sandstones and siltstones in the east are uranium mineralized (Parnell et al., 1990). However, the pale-colored Witwatersrand conglomerates are uranium mineralized rather than thorium mineralized. There is still debate about the content of oxygen in the atmosphere at the time of Witwatersrand sedimentation, but it is almost certain that the oxygen content was not at its present level and consequently red beds were not widely developed. As a result the potential for uranium to be oxidized and transported as the hexavalent ion, and consequently fractionated into red beds, was very limited, and it is not surprising that uranium occurs in paler (low Eh) beds. The Witwatersrand uraninite contains thorium (up to several percent), and unpublished observations by the author suggest that there is a limited content of thorium in the Witwatersrand carbon, within a titanate-silicate phase which is paragenetically later than the uraninite, indicating that fractionation was thus not as complete as in younger successions.

Origin of uranium-thorium minerals

As noted above, the uraninite and other metalliferous phases in the Witwatersrand have been interpreted as both detrital and authigenic in origin (Simpson and Bowles, 1977; Smits, 1984). It is not the purpose of this account to debate further the detailed evidence relating to this aspect of the Witwatersrand mineralization, but it is notable that there is similar ambiguity over the origin of the thoriferous phases in younger rocks. Thoriferous mineral cores to bitumen nodules were discovered independently by Parnell (1988b) and Rasmussen et al. (1989), who attributed an authigenic and detrital origin to their respective examples. The expansion-fragmentation process could cause such disruption to single detrital grains so that they appear to consist of an array of small authigenic crystals. There are numerous descriptions of how radioactive minerals in coals and shales, particularly uraniferous zircons, do act as nuclei for bituminous coatings (e.g., Stach, 1958; McKirdy and Kantsler, 1980). However, nodules in the Welsh borderland have been reported in crosscutting mineral veinlets and in the moldic porosity of fossils (Parnell and Eakin, 1989), indicating that at least some of the mineral inclusions have an authigenic origin. I and my colleagues have assumed that most of the thoriferous bitumen nodules which we have examined are diagenetically enriched in thorium (Parnell and Eakin, 1989; Parnell and Monson, 1990; Parnell et al., 1990; Monson and Parnell, 1993). This interpretation is similar to the model of uranium enrichment of hydrocarbons for the Witwatersrand deposits described by Phillips and Myers (1989), although most workers believe that a major portion of the uraninite is detrital (Robb and Meyer, 1991).

Relationships with granite

The uranium and thorium in the carbonaceous matter is probably of a predominantly plutonic provenance. The hinterland of the Witwatersrand basin includes several Archean granites (Robb et al., 1993), and the northwest Irish basin is adjacent to the Caledonian Barnesmore Granite (Parnell and Monson, 1990). The granites are updip from the sedimentary basins, and consequently, hydrocarbon-bearing fluids may have migrated through the upper (weathered, fractured) parts of the granites. In the Archean granites, Robb et al. (1993) have reported carbonaceous nodules nucleated about uraninite crystals in the granites themselves, a direct indication of hydrocarbon migration through the rocks. Carbonaceous matter has not been observed in the Barnesmore Granite, but weathered specimens of the granite contain numerous small crystals of the same thorium phosphosilicate (thorite var.) which occurs in the bitumen nodules found in the adjacent sediments (Monson and Parnell, 1993) and in Carboniferous sandstones in several other parts of the British Isles. The thorite crystals in the granite appear too small and delicate to have been the source, through erosion, of the thorite in the sediment-hosted bitumen nodules. It is also doubtful if so much thorite would occur as the primary thorium phase in the granite, which is more likely to be monazite or the thorium oxide mineral thorianite. Furthermore, the Barnesmore Granite is probably a fractionated I-type granite (I.G. Meighan, pers. commun.), which is unlikely to have contributed large amounts of detrital monazite or thorite. Rather, the thorite in the granite was probably precipitated from the same ground waters which interacted with migrating hydrocarbons to precipitate the thorite-bearing bitumen nodules. This implies that thorium precipitation was not completely dependent upon organic matter but may have been localized by it in the sandstones. The weathered granite is porous; the granite had been unroofed by Carboniferous times (Parnell and Monson, 1990) and probably experienced the deep oxidative weathering which affected northwest Europe in Permian times, so this porosity may date to the Paleozoic and have facilitated ground-water penetration. It should be noted, however, that we are relatively ignorant of the conditions under which thorium silicate could be precipitated, particularly at low temperatures.

Consequences for Witwatersrand mineralization

If the Phanerozoic thoriferous bitumen nodules can be regarded as an analogue for the Witwatersrand uraniferous carbon nodules, their genesis can help us to constrain the origin of the Witwatersrand carbon.

The unequivocal origin of the Phanerozoic carbon as a residue of migrating hydrocarbons strongly supports the school of thought that the Witwatersrand carbon is a migrated rather than an indigenous form. The concept that the Witwatersrand carbon may be derived from a microbial precursor is partly based upon so-called "filamentous" or "columnar" structures normal to the carbon seam orientations. These elongate structures in fact represent preferred displacement of fragmented uraninite inclusions within carbon nodules (see above), in an orientation normal to bedding (Fig. 9B). Fragmentation and displacement of thorite-thorianite can also be observed within thoriferous bitumen nodules, but displacement in a preferred orientation has not been noted.

The replacive thoriferous bitumen nodules appear to have grown late in the diagenetic sequences of the host sandstones. If the same timing can be applied to the Witwatersrand nodules (whose paragenetic context is difficult to assess directly due to the effects of metamorphism), this imposes some constraint on the timing of other mineralization within the Witwatersrand conglomerates. Petrographic evidence suggests that part of the gold mineralization is remobilized (Phillips et al., 1987), postdates the formation of carbon nodules, and therefore would have postdated the main diagenetic processes which were experienced by the conglomerates.

Conclusions

The thoriferous bitumen nodules found in Phanerozoic conglomerates and sandstones are a good analogue for the carbonaceous nodules which occur in Witwatersrand gold-uranium deposits. The analogy includes: (1) hosting in a quartz-pebble conglomerate-pebbly sandstone representing deposits of regional transgressions, (2) concentration of nodules along certain layers, (3) evidence for more than one phase of carbon, (4) disintegration and displacement of mineral inclusions within carbon, and (5) comparable mineralogy including oxides, silicates and titaniferous phases.

The source of the carbon in the Phanerozoic bitumen nodules was migrating hydrocarbons. The strong analogy with the Witwatersrand nodules suggests that the carbon in the Witwatersrand deposits was, similarly, migrating hydrocarbons. This is consistent with the views of some workers who claim a hydrocarbon origin on geochemical evidence (Schidlowski, 1981; Robb and Meyer, 1991), as opposed to a microbial origin favored by many other workers on petrographic evidence.

Acknowledgments

I am grateful to B. Nagy for providing samples from the Witwatersrand, and to the staff of the Queen's University electron microscopy unit for technical support. The manuscript benefited from reviews by *Economic Geology* referees. This paper is a contribution to IGCP project 357.

REFERENCES

Bauman, R., and Glantz, J., 1957, The effect of copolymer composition on radiation cross-linking: Journal of Polymer Science, v. 26, p. 397–399.

Charlesby, A., 1987, Radiation chemistry of polymers, *in* Farhataziz, and Rodgers, M.A.J., eds., Radiation chemistry—principles and applications: New York, VCH Publishers, p. 451–475.

Cortial, F., Gauthier-Lafaye, F., Lacrampe-Couloume, G., Oberlin, A., and Weber, F., 1990, Characterization of organic matter associated with uranium deposits in the Francevillian Formation of Gabon (Lower Proterozoic): Organic Geochemistry, v. 15, p. 73–85.

Curiale, J.A., Bloch, S., Rafalska-Bloch, S., and Harrison, W.E., 1983, Petroleum-related origin for uraniferous organic-rich nodules of southwestern Oklahoma: American Association of Petroleum Geologists Bulletin, v. 67, p. 588–608.

Dyer, B.D., Krumbein, W.E., and Mossman, D.J., 1988, Nature and origin of stratiform kerogen seams in Lower Proterozoic Witwatersrand-type paleoplacers—the case for biogenicity: Geomicrobiology Journal, v. 6, p. 33–47.

Eakin, P.A., and Gize, A.P., 1992, Reflected-light microscopy of uraniferous bitumens: Mineralogical Magazine, v. 56, p. 85–99.

Ebert, L.B., Robbins, E.I., Rose, K.D., Kastrup, R.V., Scanlon, J.C., Gebhard, L.A., and Garcia, A.R., 1990, Chemistry and palynology of carbon seams and associated rocks from the Witwatersrand goldfields, South Africa: Ore Geology Reviews, v. 5, p. 423–444.

Gauthier-Lafaye, F., and Weber, F., 1989, The Francevillian (Lower Proterozoic) uranium ore deposits of Gabon: ECONOMIC GEOLOGY, v. 84, p. 2267–2285.

Hallbauer, D.K., 1975, The plant origin of the Witwatersrand "carbon": Minerals Science and Engineering, v. 7, p. 111–131.

——1986, The mineralogy and geochemistry of Witwatersrand pyrite, gold, uranium and carbonaceous matter, *in* Anhaeusser, C.R., and Maske, S., eds., Mineral deposits of southern Africa: Johannesburg, Geological Society of South Africa, v. 1, p. 731–752.

Horscroft, F.D., 1986, The occurrence of gold in quartz-pebble conglomerate at Jacobina, Bahia, Brazil: Geocongress '86 Symposium, Johannesburg, Extended Abstract Volume, p. 259–262.

Landais, P., Dubessy, J., Robb, L.J., and Nouel, C., 1990, Preliminary chemical analyses and Raman spectroscopy on selected samples of Witwatersrand kerogen: University of the Witwatersrand Economic Geology Research Unit Information Circular 222, 8 p.

McKirdy, D.M., and Kantsler, A.J., 1980, Oil geochemistry and potential source rocks of the Officer basin, South Australia: APEA Journal, v. 20, p. 68–86.

Monson, B., 1993, Mineralogy of thoriferous bitumen nodules, northwest Irish basin, *in* Parnell, J., Kucha, H., and Landais, P., eds., Bitumens in ore deposits: Heidelberg, Springer-Verlag, p. 350–361.

Monson, B., and Parnell, J., 1993, Thoriferous bitumen nodules and hydrocarbon exploration in Carboniferous sandstones, British Isles: Preliminary results, *in* Parnell, J., Ruffell, A.H., and Moles, N.R., eds., Geofluids '93, Contributions to an International Conference on Fluid Evolution, Migration and Interaction in Rocks: Bath, Geological Society Publishing House, p. 439–442.

Mossman, D.J., 1987, Stratiform gold occurrences of the Witwatersrand type in the Huronian Supergroup, Ontario, Canada: South African Journal of Geology, v. 90, p. 168–178.

Parnell, J., 1988a, Mineralogy of uraniferous hydrocarbons in Carboniferous-hosted mineral deposits, Great Britain: Uranium, v. 4, p. 197–218.

——1988b, Metal enrichments in bitumen: A review: Mineralium Deposita, v. 23, p. 191–199.

Parnell, J., and Eakin, P., 1989, Thorium-bitumen mineralization in Silurian sandstones, Welsh borderland: Mineralogical Magazine, v. 53, p. 111–116.

Parnell, J., and Monson, B., 1990, Sandstone-hosted thorium-bitumen mineralization in the northwest Irish basin: Sedimentology, v. 37, p. 1011–1022.

Parnell, J., Monson, B., and Tosswill, R.J., 1990, Petrography of thoriferous hydrocarbon nodules in sandstones, and their significance for petroleum exploration: Geological Society of London Journal, v. 147, p. 837–842.

Parnell, J., Robinson, N., and Brassell, S., 1991, Discrimination of bitumen sources in Precambrian and lower Palaeozoic rocks, southern U.K., by gas chromatography-mass spectrometry: Chemical Geology, v. 90, p. 1–14.

Phillips, G.N., and Myers, R.E., 1989, The Witwatersrand gold fields: Part II. An origin for Witwatersrand gold during metamorphism and associated alteration: ECONOMIC GEOLOGY MONOGRAPH 6, p. 598–608.

Phillips, G.N., Myers, R.E., and Palmer, J.A., 1987, Problems with the placer model for Witwatersrand gold: Geology, v. 15, p. 1027–1030.

Pretorius, D.A., 1981, Gold and uranium in quartz-pebble conglomerate: ECONOMIC GEOLOGY 75TH ANNIVERSARY VOLUME, p. 117–138.

Rasmussen, B., Glover, J.E., and Alexander, R., 1989, Hydrocarbon rims on monazite in Permian-Triassic arenites, northern Perth basin, Western Australia: Pointers to the former presence of oil: Geology, v. 17, p. 115–118.

Rasmussen, B., Glover, J.E., and Foster, C.B., 1993, Polymerization of hydrocarbons by radioactive minerals in sedimentary rocks: Diagenetic and economic significance, *in* Parnell, J., Kucha, H., and Landais, P., eds., Bitumens in Ore Deposits: Heidelberg, Springer-Verlag, p. 490–509.

Reimer, T.O., and Mossman, D.J., 1990, The Witwatersrand controversy revisited: ECONOMIC GEOLOGY, v. 85, p. 337–343.

Renger, F.E., and Minter, W.E.L., 1986, Proterozoic placers of the Moeda Formation within the Gandarela syncline, Minas Gerais, Brazil: Geocongress 86 Symposium, Johannesburg, Extended Abstract Volume, p. 335–339.

Robb, L.J., and Meyer, F.M., 1991, A contribution to recent debate concerning epigenetic versus syngenetic mineralization processes in the Witwatersrand basin: ECONOMIC GEOLOGY, v. 86, p. 396–401.

Robb, L.J., Davis, D.W., and Kamo, S.L., 1990, U-Pb ages on single detrital zircon grains from the Witwatersrand basin, South Africa: Constraints on the ages of sedimentation and on the evolution of granites adjacent to the basin: Journal of Geology, v. 98, p. 311–328.

Robb, L.J., Landais, P., Meyer, F.M., and Davis, D.W., 1993, Nodular kerogen in granites: Implications for the origin of carbonaceous matter in the Witwatersrand basin, South Africa, *in* Parnell, J., Ruffell, A.H., and Moles, N.R., eds., Geofluids '93, Contributions to an International Conference on Fluid Evolution, Migration and Interaction in Rocks: Bath, Geological Society Publishing House, p. 446–449.

Roscoe, S.M., 1981, Temporal and other factors affecting deposition of uraniferous conglomerates. U.S. Geological Survey Professional Paper 1161, p. W1–W17.

Schidlowski, M., 1981, Uraniferous constituents of the Witwatersrand conglomerates: Ore-microscopic observations and implications for Witwatersrand metallogeny: U.S. Geological Survey Professional Paper 1161, p. N1–N29.

Simpson, P.R., and Bowles, J.F.W., 1977, Uranium mineralization of the Witwatersrand and Dominion Reef system: Royal Society of London Philosophical Transactions, v. A286, p. 527–548.

Smits, G., 1984, Some aspects of the uranium minerals in Witwatersrand sediments of the Early Proterozoic: Precambrian Research, v. 25, p. 37–59.

——1992, Mineralogical evidence for geochemical environment at the earth's surface during deposition of Witwatersrand reefs: Institution of Mining and Metallurgy Transactions, sec. B, v. 101, p. 99–107.

Snyman, C.P., 1965, Possible biogenetic structures in Witwatersrand thucholite: Geological Society of South Africa Transactions, v. 68, p. 225–233.

Stach, E., 1958, Radioaktive inkohlung: Brennstoff-Chemie, v. 39, p. 329–331.

Willingham, T.O., Nagy, B., Nagy, L.A., Krinsley, D.H., and Mossman, D.J., 1985, Uranium-bearing stratiform organic matter in paleoplacers of the lower Huronian Supergroup, Elliot Lake-Blind River region, Canada: Canadian Journal of Earth Sciences, v. 22, p. 1930–1944.

Ziegler, A.M., Cocks, L.R.M., and McKerrow, W.S., 1968, The Llandovery transgression of the Welsh borderland: Palaeontology, v. 9, p. 346–350.

Zumberge, J.E., Siglio, A.C., and Nagy, B., 1978, Molecular and elemental analyses of the carbonaceous matter in the gold and uranium-bearing Vaal reef carbon seams, Witwatersrand sequence: Minerals Science and Engineering, v. 10, p. 223–246.

8

American Mineralogist, Volume 76, pages 1964–1972, 1991

Occurrence and distribution of invisible gold in a Carlin-type gold deposit in China

SHUI HE MAO
Institute of Comprehensive Utilization of Mineral Resources, Emei, Sichuan 614200, People's Republic of China

ABSTRACT

From the results of EPMA on various minerals from the ore and from SEM observations and chemical dissolution experiments on pyrite in a Carlin-type gold deposit (Banqi gold deposit, Guizhou, China), the following conclusions are drawn:

Pyrite is the most important Au-bearing mineral. Most of the pyrite grains occur as anhedral granules consisting of earlier formed, euhedral crystal cores containing little or no Au and As and later formed rims that are rich in Au and As. The average tenor of Au is 257.6 ppm in pyrite, about 600 ppm in rims of anhedral grains, and less than 82 ppm in cores.

There is a positive correlation between the concentrations of Au and As, so the distribution of Au is similar to that of As in SEM images and EPMA data.

EPMA data show highly variable Au concentrations at different spots in a Au-rich rim within a pyrite grain. Moreover, in chemical dissolution tests on pyrite, most of the Au is not in the supernatant HNO_3 solution but remains in the undissolved residues and is available for leaching into KI + I_2 Au-leaching solution. All these facts illustrate that Au in pyrite occurs as ultramicrometer native gold inclusions, not as isomorphous substitution.

It is shown that more than 60% of the Au given by chemical assay of clay minerals occurs in submicrometer-size pyrite inclusions in which Au is remarkably enriched.

The Au contents in other minerals, such as arsenopyrite, quartz, calcite, or barite, are all below the detection limit of EPMA. Considering the results of chemical assays of these mineral separates, it is concluded that these minerals are not significantly Au bearing.

Knowledge of the mode of occurrence and distribution characteristics of invisible Au in Carlin-type deposits is beneficial to metallurgical process design for Au recovery. In this case, sufficient oxidation and leaching of the pyrite surface layer will produce satisfactory recovery at reduced cost in time, energy, and reagents.

INTRODUCTION

There is a type of Au-bearing ore in which the Au tenor is quite high—sometimes reaching tens of ppm—but the Au in the ore is not visible by reflected and transmitted light microscopy at high magnification. Generally, this Au is called invisible Au, ultramicrometer Au, or submicrometer Au.

Because ultramicrometer Au is invisible, it is extremely difficult to study its occurrence and distribution by conventional determinative means. Spending a great deal of time, the mineralogist can assay hand-picked mineral separates to obtain the average content of Au in each mineral. However, such analyses of mineral separates convey no information as to whether the Au is homogeneously distributed within and among the mineral crystals, is in solid solution, or is present as submicroscopic inclusions.

Assumptions and inferences have been made about the manner of occurrence of invisible Au (Boyle, 1979; Zhang et al., 1987; Cabri et al., 1989; Bakken et al., 1989; Cook and Chryssoulis 1990). However, there is some controversy about whether the Au is present in chemical combination in sulfide minerals such as pyrite and arsenopyrite (i.e., structurally incorporated Au) or whether the Au occurs as submicroscopic inclusions. But none of the studies provides direct and convincing evidence to confirm the inferences. Using an electron-probe microanalyzer (EPMA) and a scanning electron microscope (SEM), the author has investigated the distribution characteristics and concentration of invisible Au at different spots in Au-bearing minerals of various grain sizes, crystal forms, and paragenetic stages. Furthermore, the distribution of invisible Au is displayed by the distribution of As, which is positively correlated with Au in pyrite. Therefore, the present research work has provided a scientific basis for selecting an economical and effective treatment and extraction process for the ore from Banqi gold deposit, Guizhou, a Carlin-type gold deposit in China.

SAMPLE PREPARATION

The unoxidized (primary) ore sample consists of drill cuttings from many parts in the Banqi deposit, which is an epithermal disseminated gold deposit in China. The tectonic position of the Banqi gold deposit is in the syn-

---

taxis zo
graben
eralizat
in parti
Triassic
controll
arch di
and the
consisti
that are
and sul
The
selected
tions th
microsc
tigation
ground
to −20
Fe, Al,
used to
the oth
moving
separat
produc
chemic
The
total m
sample
estimat
accurat

Optical

Mine
examin
sections
Modal
pyrite v
and zor
optical

EPMA

The
mineral
equippe
(EDS) s
strumer
with be
eter abo
dards:
senopyr
routine
sured b
ing spe
metho
tromet
the co
od is n

taxis zone of the Youjing late Palaeozoic era–Triassic rift graben and late Precambrian Yangzi platform. The mineralization district emerges in Devonian-Triassic strata; in particular, the mineralized horizons are in the lower Triassic Ziyun formation. The ore bodies are multiply controlled by the vertical main fault of the anticline and arch districts, the fracture zones between the horizons, and the rock characteristics. The most rock is tectonite consisting of clastic rocks of terrigeneous sedimentation that are enriched in clayey, silty, and organic materials and sulfides.

The total ore sample weighs 2438 g. Ore blocks were selected for preparing the polished sections and thin sections that were used for mineralogical studies by optical microscopy and for SEM observation and EPMA investigations. The rest of the sample was crushed and then ground to −100 mesh; then a portion was further ground to −200 mesh for Au assay and chemical analyses of S, Fe, Al, and K. Most of the sample of −100 mesh was used to prepare two pyrite concentrates (one >0.074 mm, the other <0.074 mm) by sieving and panning, then removing impurities such as barite by use of a dielectric separator and by hand selecting under a microscope. This produced pure pyrite mineral separates for Au assay and chemical dissolution experiments.

The clay mineral separate with grain size <10 μm and total mass 860 mg was prepared using the pulverized ore sample and a precipitation method. The grain size was estimated according to the precipitation speed and not accurately measured.

EXPERIMENTAL METHODS

Optical microscopy

Mineralogical composition of the ore was obtained by examining quite a number of polished sections and thin sections with reflected and transmitted light microscopy. Modal analysis and the statistics of size distribution of pyrite were determined by point counting. Crystal forms and zoning characteristics of pyrite were investigated by optical microscopy.

EPMA and SEM analyses

The analyses of pyrite, As-bearing pyrite, and other minerals were performed on a JEOL 733 electron probe equipped with a TN 5500 energy-dispersive spectrometer (EDS) system and TN 5600 automation system. The instrument was operated at 25 kV (accelerating voltage) with beam current (cup reading) 20 nA and beam diameter about 1 μm, using the following X-ray lines and standards: Au$L\alpha$ (metal), Fe$K\alpha$ and S$K\alpha$ (pyrite), As$L\alpha$ (arsenopyrite). Fe, S, and As can be measured by EDS with routine procedure; the trace element Au can only be measured by wavelength-dispersive spectrometry (WDS) using special procedures and precautions. The common method for measuring background is to move the spectrometer to both sides of the peak position and measure the count rates, but in detecting trace elements this method is not suitable. In the present work, a pure pyrite crystal free of Au was employed as a standard for measuring background. The background count rate was measured at the Au$L\alpha$ peak position on the blank pyrite standard. One wavelength-dispersive spectrometer with a LiF crystal was dedicated to determine the Au concentration, so that during the entire procedure the spectrometer was not moved from the Au$L\alpha$ position. To reduce the detection limit and the counting statistics error, the counting time for detecting the trace Au was set at 100 s. Under the above conditions, the precision for detecting trace Au in pyrite was improved. The same method for background measurement was used to measure the Au concentrations in arsenopyrite, quartz, calcite, barite, etc. The TASK program provided by Tracor Northern is capable of doing EDS and WDS measurements simultaneously and then performing the quantitative corrections for atomic number, absorption, and fluorescence effects with the ZAF program included in TASK. If Au$M\alpha$ were chosen as the analyzed line and PET as the diffraction crystal, there would be the advantage of lower background count rate and therefore better sensitivity. Unfortunately, there is some overlap between Au$M\alpha$ (5.840 Å) and the third order line of Fe$K\alpha$ (5.812 Å). Therefore, Au$L\alpha$ is preferable as the analyzed line.

There are several expressions for calculating the detection limit (C_{DL}) by EPMA (Toya and Kato, 1983; Cox, 1983; Ziebold, 1967). In routine work, expression 1 is employed to calculate C_{DL} for a given element:

$$C_{DL} = \frac{3\sqrt{I_B t}}{(I_P - I_B)t} = \frac{3\sqrt{I_B}}{(I_P - I_B)\sqrt{t}} \qquad (1)$$

where I_P is the peak count rate, I_B is the background count rate both in counts per second (cps), and t is the counting time. Under the operating conditions mentioned above, I_P for Au is approximately 8900 cps, I_B is approximately 73 cps, t is 100 s, and the calculated value of C_{DL} by expression 1 is 0.029%. Considering uncertainties such as instrumental instability or sample polish imperfections, the practical C_{DL} value for detecting trace Au in pyrite is estimated to be 0.05%. Therefore, a Au concentration less than 0.05% in any analyzed spot is considered to be zero. If the invisible Au in pyrite is distributed homogeneously, it is almost impossible to be detected by EPMA under the operating conditions employed in this study. However, when the Au is relatively enriched in some areas within pyrite, it becomes possible to investigate the variation and enrichment characteristics of the invisible Au and the relationship between Au and other elements.

Chemical dissolution experiments

Chemical dissolution experiments on pyrite were carried out according to the flow chart shown in Figure 1 using a pyrite sample with the grain size <0.074 mm and total mass 400 mg. Au in solutions and in residue were concentrated by fire assay, then analyzed by atomic absorption spectrometry (AAS). Fe was analyzed by wet chemistry. In the experiments, pyrite is dissolved in HNO_3

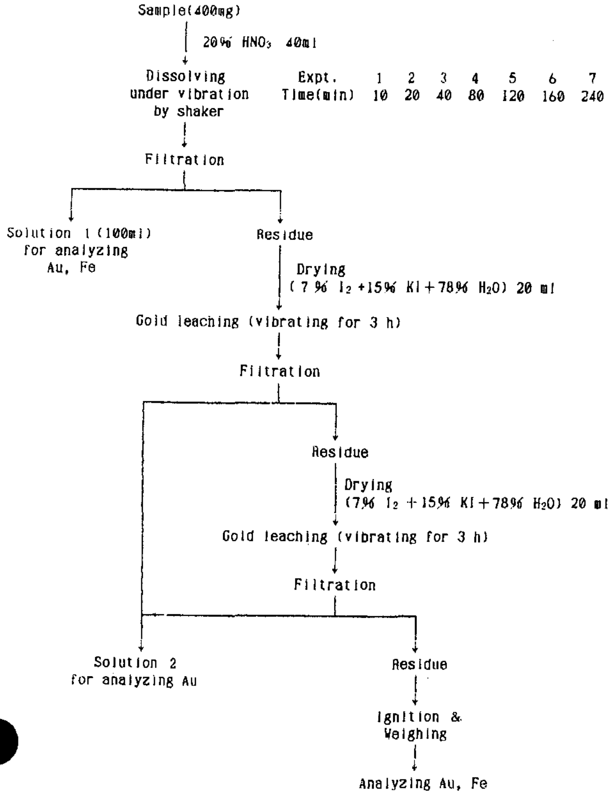

Fig. 1. Flow chart of dissolution experiment on pyrite.

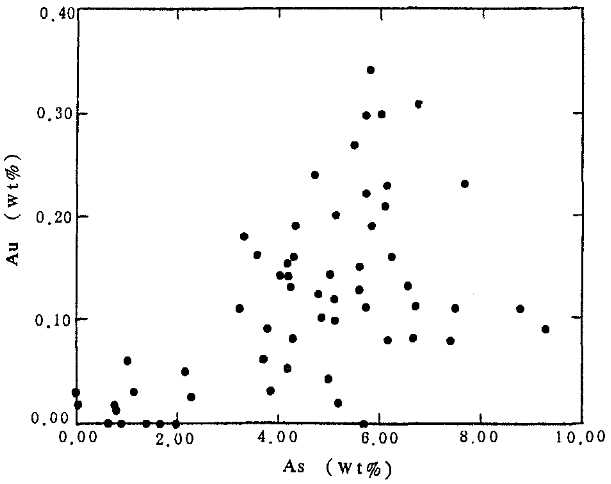

Fig. 2. Correlation between Au and As concentrations in tiny pyrite grains (<10 μm).

but particulate Au remains insoluble. The addition of a KI + I$_2$ solution can leach Au from the residue.

RESULTS

Mineralogical and chemical composition of the ore

Fire assay analysis yielded 31.02 ppm Au, and chemical analyses yielded 2.40% S, 3.41% Fe, 2.59% Al, and 1.63% K in bulk ore. The mineralogical study by optical microscopy showed that the sulfides in the ore sample are pyrite, arsenopyrite, marcasite, stibnite, pyrrhotite, chalcopyrite, realgar, orpiment, and pentlandite. The other common minerals present are quartz, illite, kaolinite, calcite, dolomite, apatite, and barite. Modal analysis and point-counting statistics gave 4.7% pyrite (including small quantity of some other sulfides), 68.7% quartz and some carbonates, 26.6% clay minerals.

The pyrite occurs as euhedral crystals and as anhedral granules. The size distribution of pyrite is as follows: pyrite <0.074 mm, 87.40%; pyrite >0.074 mm, 12.60%. More than 95% of the pyrite grains larger than 10 μm occur as anhedral granules; only 5% of these are euhedral and subhedral crystals. The concentrations of Au in different size fractions of pyrite in the ore differ considerably. According to the fire assay results, the Au concentration in pyrite <0.074 mm averages 275.0 ppm, whereas that in pyrite >0.074 mm is 137.1 ppm. Therefore, the pyrite averages 257.6 ppm Au.

Occurrence and distribution of Au in pyrite determined by EPMA and SEM in pyrite grains <10 μm

One hundred and twenty small pyrite grains (<10 μm) from multiple samples were selected for Au analysis by EPMA. In 28 grains the Au concentrations are below the detection limit (0.05%) and As concentrations are in the range 0–5.64% (average 2.05%). In the other 92 grains the Au concentrations are higher than the detection limit, ranging from 0.05% to 0.34% (average 0.15%); As concentrations range from 1.60% to 9.29% (average 5.22%) (Table 1). Figure 2 shows the positive correlation between Au and As concentrations.

TABLE 1. Concentrations of Au and As in minerals analyzed by EPMA

		Spots with Au conc. (>0.05%)					Spots with Au conc. (<0.05%)		
			Au (%)		As (%)			As (%)	
	Ana. sp.	sp.	Range	Ave.	Range	Ave.	sp.	Range	Ave.
[illegible]y. (<10 μm)	120	92	0.05–0.34	0.15	1.60–9.29	5.22	28	0–5.65	2.05
Int. of py.*	73	10	0.05–0.11	0.08	0–9.13	2.67	63	0–3.77	0.81
Rims of anh. py.*	57	44	0.05–0.46	0.18	0.85–7.37	5.61	13	0–4.51	0.76
Rims of euh. py.*	18	0					18	0–0.49	0.12

Note: Ana. = Analyzed, anh. = anhedral, Ave. = Average, conc. = concentration, euh. = euhedral, Int. = Interiors, Py. = Pyrite, Sp. = Spots.
* Pyrite grains >10 μm.

3

116

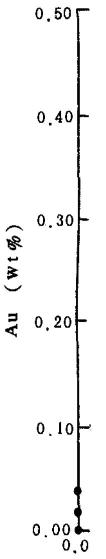

Fig. 3.
rims of

Interior

Rand
μm to
number
were an
Among
and As
(average
tions hi
to 0.11
range be
1).

In rims

The c
ral pyri
pyrite g
spots l
grains a
erywhe
tions ra
Fifty-
ral pyri
below t
from ze
the Au
ranging
As con
5.61%)
betwee
relation
cates t
qualitat
X-ra

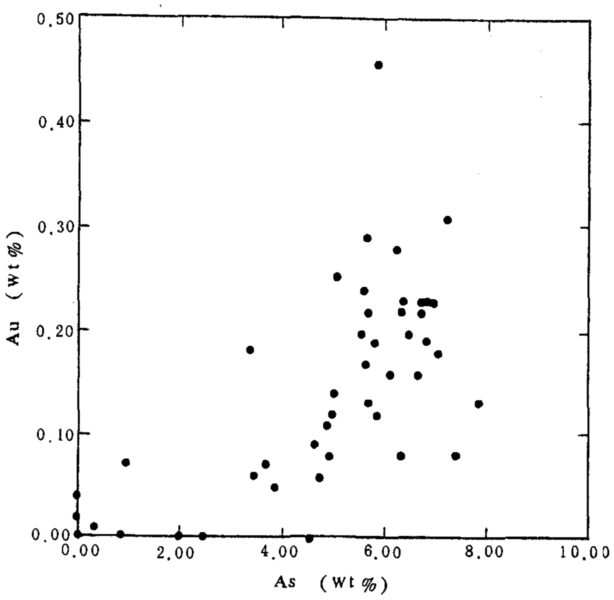

Fig. 3. Correlation between the Au and As concentrations in rims of anhedral pyrite grains >10 μm.

Interior of the pyrite grains >10 μm

Randomly chosen pyrite grains within the range of 10 μm to about 100 μm, with different crystal forms in a number of polished sections, were analyzed. Several spots were analyzed in each grain, yielding 73 spots in total. Among them, 63 spots had Au concentrations <0.05% and As concentrations ranging between zero and 3.77% (average 0.81%). Only in ten spots are the Au concentrations higher than the detection limit, ranging from 0.05% to 0.11% (average 0.08%); in the ten, As concentrations range between zero and 9.13% (average 2.67%) (see Table 1).

In rims of pyrite grains >10 μm

The concentrations of Au and As in the rims of euhedral pyrite grains are quite distinct from rims of anhedral pyrite grains. Data on Au and As concentrations in 18 spots located near the edges of several euhedral pyrite grains are shown in Table 1. Au concentrations are everywhere below the detection limit, and As concentrations range between zero and 0.49% (average 0.12%).

Fifty-seven spots were analyzed in a number of anhedral pyrite grains. In 13 spots, the Au concentrations are below the detection limit, and the As concentrations range from zero to 4.51% (average 0.76%). In the other 44 spots, the Au concentrations are higher than the detection limit, ranging from 0.05% to 0.46% (average 0.18%), and the As concentrations range from 0.85% to 7.37% (average 5.61%) (Table 1). Figure 3 shows the positive correlation between the concentrations of Au and As. The particular relation between the concentrations of Au and As indicates that the distribution of trace Au can be displayed qualitatively using the X-ray images of As in pyrite grains.

X-ray images in Figures 4 and 5 that were produced by electron beam scanning clearly show that As is conspicuously enriched in the rims of pyrite grains, and little or no As is contained in the interior of pyrite grains. Therefore, according to the positive correlation between the concentrations of Au and As, it is believed that Au must be enriched in the rims of pyrite grains. The secondary electron images (SEI) in Figures 4 and 5 show that there are boundary lines between the rims and interiors of pyrite grains. This indicates that anhedral pyrite grains in this gold deposit consist of earlier formed, euhedral crystal cores containing little Au and As and later formed rims containing remarkably rich Au and As, i.e., with a distinct zoning texture.

Au concentrations in arsenopyrite and other minerals determined by EPMA

Arsenopyrite. Au concentrations have been determined in 22 spots that are located at rims and interiors of arsenopyrite grains of different shapes and sizes, selected in several polished sections. Except one spot with a Au concentration equal to 0.15%, the Au concentrations are below the detection limit. In addition, the arsenopyrite is very sparsely disseminated in the ore.

Quartz. Within tens of quartz grains with different sizes, 59 spots were selected in different areas for Au analysis. In five spots the Au concentrations are just above the detection limit: 0.06, 0.05, 0.09, 0.07, 0.08%; the Au concentrations in the other 54 spots are below detection limit. Additionally, chemical assay shows that the average Au concentration in quartz is 0.08 ppm (Song and Diao, 1989).

Calcite. In 40 analyzed spots, only two have Au concentrations just above detection limit, 0.06% and 0.05%. The Au concentrations in the other 38 spots are below the detection limit. The chemical assay indicates that the Au concentration in carbonates averages 0.08 ppm (Song and Diao, 1989).

Barite. One spot had a Au concentration just at the detection limit (0.05%); Au concentrations are otherwise below the detection limit.

On the basis of the above results, it can be concluded that arsenopyrite, quartz, calcite, and barite are not significant Au-bearing minerals.

Clay minerals. The clay minerals are illite and kaolinite. Among 70 randomly selected spots in clay minerals, Au concentrations detected by EPMA are well above the detection limit in some spots. However, the EDS spectra of the corresponding spots show small peaks of S, As, and Fe, indicating that there may exist some very fine, As-bearing pyrite inclusions in the clay mixture. This inference is confirmed by the electron-beam scanning images for clay minerals. To determine whether the Au detected in some spots of clay by EPMA is contained in the clay mineral itself or in the micropyrite inclusions, the clay mineral separate with grain size <10 μm was prepared for chemical analysis of the concentrations of Au and S, and then the content of pyrite was calculated from

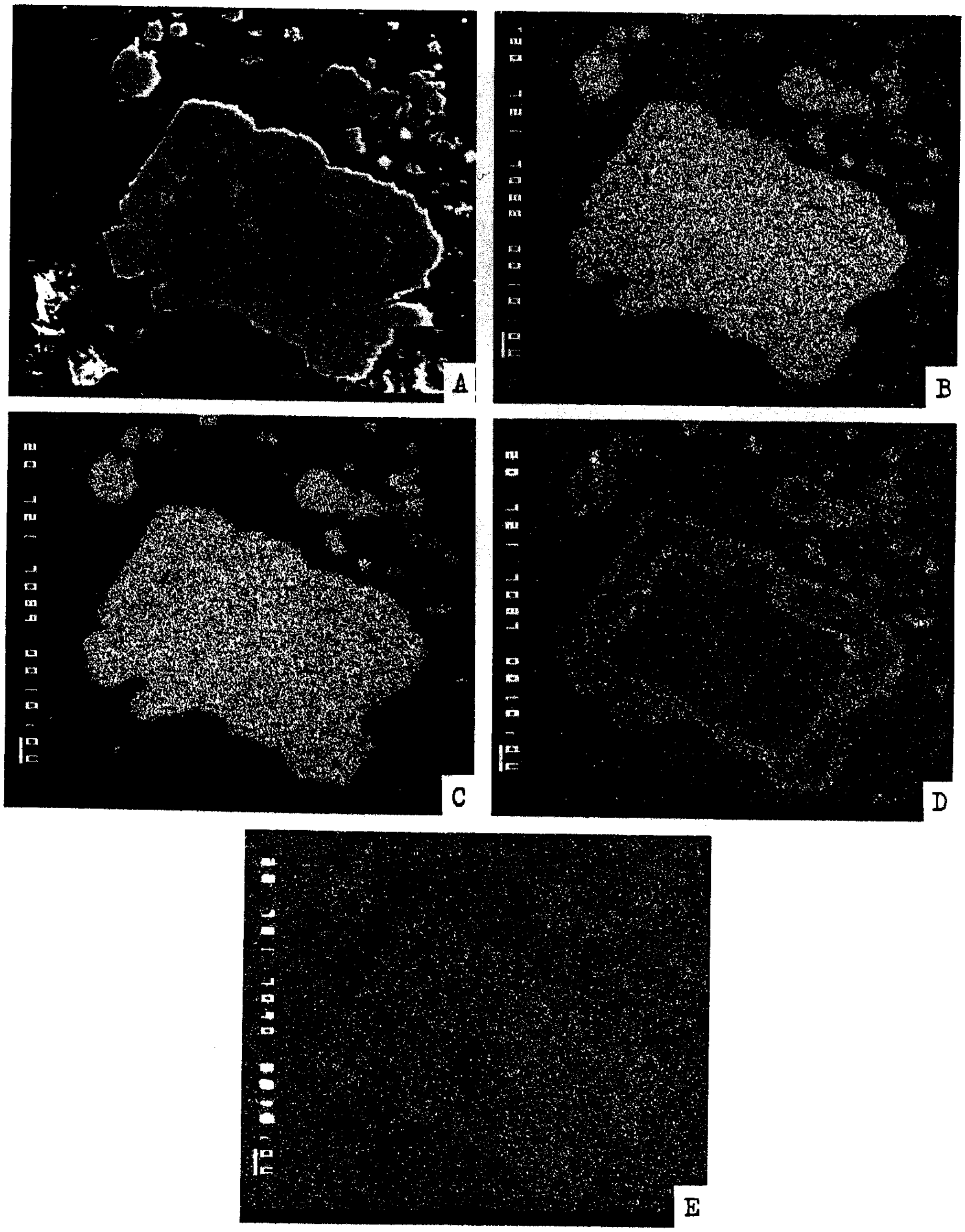

Fig. 4. Electron-beam scanning images on an anhedral pyrite grain. (A) SEI, (B) Fe*Kα*, (C) S*Kα*, (D) As*Lα*, (E) Au*Lα*.

the S concentration. Au assay of 860 mg of clay mineral separate of grain size <10 μm yielded 33.24 ppm Au and 1.75 wt% S, which can be recalculated as 3.27% pyrite as microscopic inclusions identified by SEM. The average Au concentration in clay minerals is far below the detection limit of EPMA, so it is believed that the Au detected in some spots of clay minerals is actually or mostly contained in micrometer-size pyrite inclusions that are remarkably enriched with Au. Another question of interest is what percentage of the Au content given by clay assays occurs in micropyrite inclusions vs. in the clay mineral structures. It is reasonable to consider that the Au concentration in micropyrite inclusions is probably at least equal to that in rims of the anhedral pyrite grains, i.e., 600 ppm or more (see below). Combining this with assay data of the clay mineral separate, we can make a rough calculation: the Au quantity contained in a 1-g clay sample is 33.24 μg, the quantity of pyrite inclusions is 0.0327 g, and these contain about 19.6 μg of Au at the 600 ppm level. Therefore, it is reasonably certain that about 60%

5

Fi

or mor
microp

Results

To c
SEM r
have b
results
ble 2, t
and th
due are

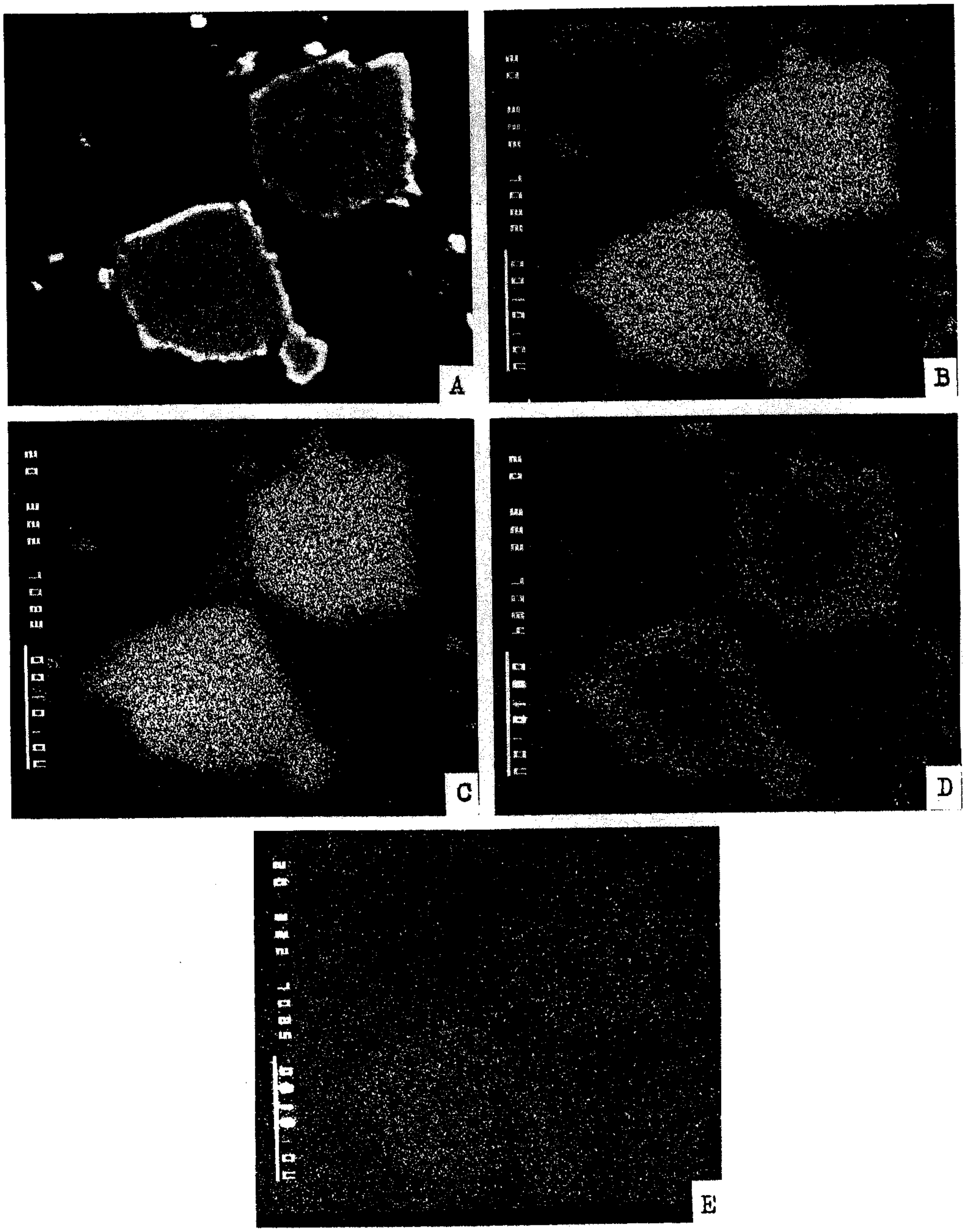

Fig. 5. Electron-beam scanning images on an anhedral pyrite grain. (**A**) SEI, (**B**) Fe*Kα*, (**C**) S*Kα*, (**D**) As*Lα*, (**E**) Au*Lα*.

or more of the Au in clay mineral assays occurs in the micropyrite inclusions.

Results of chemical dissolution experiments

To confirm the conjecture drawn from the EPMA and SEM results, chemical dissolution experiments on pyrite have been carried out, and a series of very meaningful results were obtained (Table 2). Using the data from Table 2, the correlations between the leaching time by HNO_3 and the Au concentrations both in solutions and in residue are shown in Figure 6. The correlations between the leaching time by HNO_3 and the Au concentrations both in dissolved pyrite and in undissolved pyrite remaining in the residue are shown in Figure 7.

In experiments lasting 10, 20, and 40 min, the Au concentrations in HNO_3 solution increase approximately linearly with time, so the solution is undersaturated with Au. There appears to be a large excess of NO_3^- ion relative to dissolved S species, so complete oxidation of dissolved S seems likely. In this case, the Au solubility would not be affected by formation of complexes with polysulfide, thiosulfate, sulfite, or other incompletely oxidized S an-

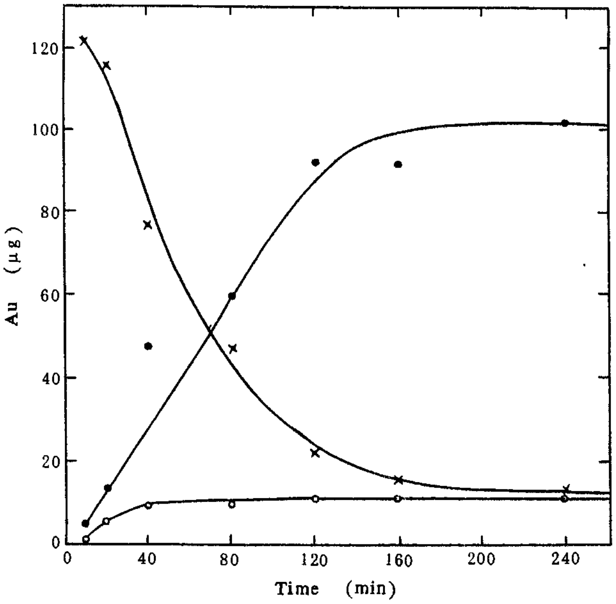

Fig. 6. Correlation between dissolution time (min) by HNO_3 and the Au contents (μg) in solutions and in residue. Open circles are in HNO_3 solution, solid circles in KI + I_2 solution, crosses in residue.

I_2 Iodine

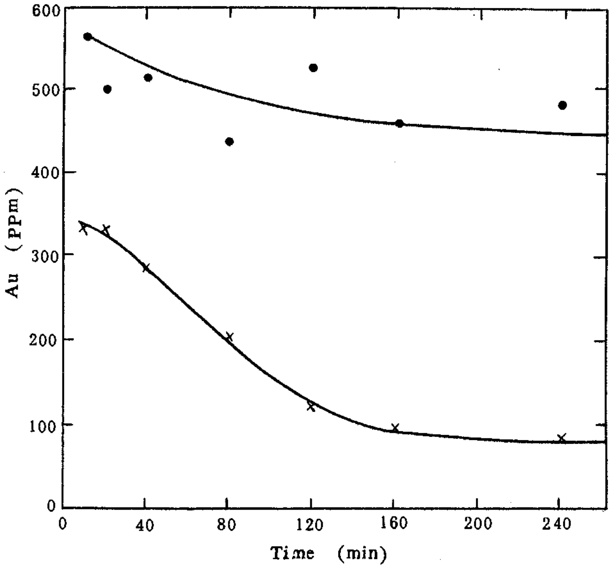

Fig. 7. Correlation between dissolution time (min) by HNO_3 and the Au concentrations (ppm) both in dissolved pyrite and in undissolved pyrite remaining in residue. Solid circles are in dissolved pyrite, crosses in undissolved pyrite.

ions that might enhance the solubility of crystalline Au as more pyrite dissolves in longer experiments (Webster, 1986). Therefore, the first three experiments did not precipitate Au that was liberated from pyrite during the dissolution of pyrite. On the other hand, the Au that was liberated from the dissolved pyrite and was not present in the HNO_3 solution was dissolved subsequently upon the addition of I_2 + KI. This must represent Au that occurred in pyrite as discrete metal particles, not as crystalline Au. Therefore, it is reasonable to conclude that most of the Au contained in pyrite occurs as ultramicrometer particulate native gold inclusions.

The Au concentration in the KI + I_2 solution increases dramatically with dissolution time up to 120 min, then increases very slowly (Fig. 6). After 160 min, the Au concentration reaches a plateau even though more pyrite is continuously dissolved by HNO_3, and the Fe concentration in HNO_3 solution increases up to 240 min. This suggests that in the period between 160 and 240 min the Au concentrated in pyrite rims has been dissolved out.

The concentration of Au in the residue decreases sharply over the interval between 10 and 120 min, and then it gradually slows down. After 160 min, little variation of Au concentration is detected in the residue. This result is in good agreement with the above description, i.e., the upper curve in Figure 6 and lower curve in Figure 7 are mirror images.

It is likely that when the dissolution time is less than 120 min, the dissolution is of pyrite rims in which Au is enriched. However, there is a wide range of size distribution for pyrite grains and of thickness for pyrite rims. It is likely that the rims of pyrite grains with smaller size and thinner rims have already been dissolved out in less than 120 min. Therefore, it is reasonable to assume that the Au concentration in pyrite dissolved by HNO_3 in 10

I_2 + Pottasim Iodine

TABLE 2. Results of chemical dissolution experiments on pyrite

No.	Disso. time (min)	Au cont. (μg) HNO$_3$ Sol. 1 (100 mL)	Au cont. (μg) KI + I$_2$ Sol. 2	Au cont. (μg) Resi.	Au cont. (μg) Total	Fe conc. in HNO$_3$ Sol. 1 (mg/mL)	Py. quan. in HNO$_3$ Sol. 1 (mg)	Resi. quan. (mg)	Fe cont. in resi. (%)	Py. quan. in resi. (mg)	Au conc. in dissd. Py. by HNO$_3$ (ppm)	Au conc. in undis. Py. (ppm)
1	10	0.95	5.17	121.26	127.38	0.05	10.74	329.5	51.02	361.12	569.8	335.8
2	20	5.79	13.72	115.74	135.25	0.18	38.67	319.0	50.65	347.15	504.5	333.4
3	40	9.36	48.38	77.22	134.96	0.52	111.71	265.0	47.26	268.96	516.9	287.1
4	80	9.83	60.50	47.11	117.44	0.74	158.97	227.8	47.44	232.22	442.4	202.9
5	120	11.04	92.76	24.01	127.31	0.91	195.49	200.3	45.34	195.06	531.0	123.1
6	160	11.28	92.28	15.86	119.42	1.04	223.42	180.5	44.84	173.79	463.5	91.3
7	240	12.34	102.00	12.70	127.04	1.09	234.16	167.5	43.08	155.10	488.3	81.9

Note: Disso. = Dissolving, Sol. = solution, cont. = content, Resi. = Residue, conc. = concentration, Py = Pyrite, quan. = quantity, undis. = undissolved, dissd. = dissolved.

7

---

min w
additic
of the
ment c
to cont
of anh
It is
of pyr
proxin
after d

Of t
most i
the py
of an e
tle Au
Au an
crystal
ppm.
hedral
rior of
Usu
invisit
(see Fi
invisit
amine
tive co
In c
liberat
solutic
dissol
by the
dicate
Au-ric
is con
pyrite
not as
The
senop
the de
the re
clear t
Moi
assay
rite in
The
that f
U.S.A
rence
the p
tions,
als, a
indica
mon
Romt
1989;
In

120

min was that in pyrite rims, i.e., 569.8 ppm (Table 2). In addition, microscopic observation shows that about 5% of the pyrite grains prepared for the dissolution experiment occur as euhedral crystals, which have been proved to contain little or no Au, so the Au concentration in rims of anhedral pyrite grains should be near 600 ppm.

It is apparent that the Au concentration in the interior of pyrite (euhedral core of anhedral pyrite grain) is approximately equal to or less than that in the pyrite residue after dissolving for 240 min, i.e., 82 ppm.

DISCUSSION AND CONCLUSIONS

Of the various minerals in the ore, pyrite is clearly the most important Au-bearing mineral. More than 95% of the pyrite grains occur as anhedral granules that consist of an earlier formed, euhedral crystal core containing little Au and As and later formed rims notably enriched in Au and As. There is little or no Au in euhedral pyrite crystals. The average Au concentration in pyrite is 257.6 ppm. The average Au concentration in the rims of anhedral pyrite grains is about 600 ppm, whereas the interior of the grains contains less than 82 ppm.

Usually there is no way of observing and displaying the invisible Au in pyrite grains because of its trace content (see Figs. 4E and 5E). The distribution characteristic of invisible Au in pyrite can however be displayed and examined by imaging arsenic by SEM because of the positive correlation between the concentrations of Au and As.

In chemical dissolution experiments on pyrite, the Au liberated from dissolved pyrite does not enter into HNO_3 solution but resides in the residue together with the undissolved pyrite. The Au in the residue can be dissolved by the Au-leaching solution. In addition, EPMA data indicate that Au concentrations at different points in the Au-rich rims of pyrite grains are remarkably different. It is confirmed from these facts that the invisible Au in pyrite occurs as ultramicrometer native gold inclusions, not as isomorphous substitution.

The Au concentrations in other minerals, such as arsenopyrite, quartz, calcite, or barite, are nearly all below the detection limit of EPMA (0.05%). In association with the results of chemical assays of mineral separates, it is clear that these minerals are not substantially auriferous.

More than 60% of the Au content given by chemical assay of clay minerals occurs in submicrometer-scale pyrite inclusions in which Au is remarkably enriched.

The ore in the Banqi gold deposit is very similar to that from the Carlin and Cortez gold mines, Nevada, U.S.A., in the following aspects: the manner of occurrence and distribution characteristics of the invisible Au, the positive correlation between Au and As concentrations, the microstructure of the main Au-bearing minerals, and the mineralogical composition of the ore. This indicates that the Carlin-type gold deposits have common and special features (Wells and Mullens, 1973; Romberger, 1986; Cathelineau et al., 1989; Bakken et al., 1989; Cook and Chryssoulis, 1990).

In hydrothermal ore-forming solutions, the $Au(HS)_2^-$ and $Au_2S_2^{2-}$ species are the most stable known inorganic complexes of Au^+ (Seward, 1989). Other species may also exist, such as AuS^- (Chen, 1987; Qin, 1987). In hydrothermal solutions containing appreciable As, a certain proportion of S may be complexed with As, and complexes consisting of Au, S, and As, such as $Au(S,As)_2^-$, may form. With changes in oxidizing and reducing conditions, temperature, pressure, or pH in the mineralizing environment, the Au complex may decompose leading to Au deposition. When Fe^{2+} and As are present in solution, the decomposition of Au complexes may take place as follows:

$$2AuS^- + Fe^{2+} = 2Au\downarrow + FeS_2 \quad (2)$$

$$Au(S,As)_2^- + Fe^{2+} = Au\downarrow + Fe(S,As)_2 \quad (3)$$

$$4Au(HS)_2^- + 4Fe^{2+} + O_2 = 4Au\downarrow + 4FeS_2 + 4H^+ + 2H_2O \quad (4)$$

$$2HAsS_2 + 3Fe^{2+} + 2H_2O = 3FeS_{1.33}As_{0.67} + 6H^+ + O_2 \quad (5)$$

$$4Au(HS)_2^- + 7Fe^{2+} + 2HAsS_2 = 4Au\downarrow + 7FeS_{1.714}As_{0.286} + 10H^+ \quad (6)$$

$$Au_2S_2^{2-} + Fe^{2+} = 2Au\downarrow + FeS_2. \quad (7)$$

Therefore, in various kinds of gold deposits, pyrite is commonly the most important Au-bearing mineral; Au concentration in pyrite is correlated very closely with As concentration; Au usually occurs as micrometer or ultramicrometer (submicrometer) native gold inclusions.

Knowledge of the special mode of occurrence and distribution characteristics of invisible Au in such ores is useful to metallurgical process design of oxidizing-roasting, chloridizing, and cyanide leaching. In this case, sufficient oxidization and leaching of the pyrite surface layer will produce satisfactory Au recovery.

ACKNOWLEDGMENTS

This work was supported by the Chinese Academy of Geological Sciences. I wish to thank my colleagues, G. Li, L. Bian, W. Lu, Z. Gong, S. Diao, and M. Liu, for giving valuable assistance and suggestions.

REFERENCES CITED

Bakken, B.M., Hochella, M.F., Marshall, A.F., and Turner, A.M. (1989) High-resolution microscopy of gold in unoxidized ore from the Carlin mine, Nevada. Economic Geology, 84, 171–179.

Boyle, R.W. (1979) The geochemistry of gold and its deposits. Geological Survey of Canada Bulletin, 280.

Cabri, L.J., Chryssoulis, S.L., de Villiers, J.P.R., Laflamme, J.H.G., and Buseck, P.R. (1989) The nature of "invisible" gold in arsenopyrite. Canadian Mineralogist, 27, 353–362.

Cathelineau, M., Boiron, M.C., Holliger, P., Marion, P., and Denis, M. (1989) Gold in arsenopyrite: Crystal chemistry, location and state, physical and chemical conditions of deposition. Economic Geology, Monograph 6, 328–341.

Chen, S. (1987) Geochemistry and mineralization of gold. Journal of Chengdu College of Geology, 16, 8–17 (in Chinese).

8

78-F. Behaviour during Processes Connected with Magmatism

(Pegmatites, Gas Transport, Ore Deposition)

I. Introduction

The major ore deposits of the platinum metals are associated with dunitic ultrabasic rocks and gabbroic rocks containing Cu—Ni sulfides, typically pyrrhotite, pentlandite and chalcopyrite. The association of platinum metals with sulfides, tellurides, selenides, arsenides and antimonides is well established. Survey studies of platinum metal abundances, mainly in sulfide minerals, are reported by I. and W. NODDACK (1931), GOLDSCHMIDT and PETERS (1932) and HAWLEY and RIMSAITE (1953). These data are condensed and summarized in Table 78-F-1.

The analytical uncertainties noted in Sections D and E are applicable to sulfide analysis, although the higher platinum metal concentrations probably permit better accuracy because sensitivity is not such a critical factor. The main features of platinum metal geochemistry in sulfide and related minerals and ore deposits indicated by these data include the following:

a) The extensive data of I. and W. NODDACK (1931) show that Pd and Pt are the principal platinum group metals in sulfides and that Pd is more abundant than Pt. However, exceptions do occur and are noted in 3) below.

b) Selenides and tellurides contain much higher platinum metal contents than sulfides. The occurrence of both high selenium-tellurium and platinum metal values in some Cu—Ni sulfide ore deposits, and the occurrence of platinum metal tellurides such as moncheite and kotulskite (GENKIN *et al.*, 1963) indicate a strong geochemical association of these metals with the platinum group.

c) Nickeliferous sulfides, as indicated by the survey of HAWLEY and RIMSAITE (1953) are generally higher in platinum metals than non-nickeliferous sulfides. In both types of deposits chalcopyrite, rather than pyrrhotite, is the major host for Pd and probably also Pt. In Cu—Ni sulfide deposits associated with gabbroic or ultrabasic rocks such as Insizwa, South Africa or Rankin Inlet, Canada, pyrrhotite is enriched in Ru, Os, Ir and possibly Rh, relative to chalcopyrite. As chalcopyrite is usually later than the bulk of the pyrrhotite in such deposits, it seems likely that Pt and Pd are more concentrated than Ru, Ir or Os in the late residual fluids of sulfur-rich magmas.

The distribution of platinum metals in a number of ore deposits including the Sudbury district, Canada (HAWLEY, 1962; HAWLEY and RIMSAITE, 1953), the Noril'sk deposit, U.S.S.R. (GINZBURG and ROGOVER, 1961), the Inaglinsk massif, South Yakutia, U.S.S.R. (RAZIN *et al.*, 1965) and the Bushveld Complex (WAGNER, 1929; SCHNEIDERHÖHN and MORITZ, 1931; HAGEN, 1954) has been investigated and is discussed below.

X ray spectrographic

II. Sudbury Complex, Canada

At Sudbury platinum metals are associated with pyrrhotite-pentlandite-chalcopyrite mineralization occuring as discrete minerals including sperrylite, michenerite and froodite and probably also in solid solution or as extremely fine disseminations in the major sulfides, particularly chalcopyrite, and in arsenides. The available data are given in Table 78-F-2 and 78-F-3, and were obtained largely by HAWLEY and RIMSAITE (1953) who used a fire assay-emission spectrographic method.

As indicated by the pyrrhotite and chalcopyrite data for the Falconbridge Mine, an extremely heterogeneous distribution of platinum metals may occasionally be found. This is probably due to sporadic inclusion of platinum minerals. Only tentative conclusions concerning relationships between major minerals and platinum metals can therefore be drawn from these data. Two generalizations, suggested particularly by the weight percentage data, are noted:

a) In pyrrhotite platinum is generally higher than palladium although the Falconbridge pyrrhotites do not appear to show this trend.

b) In general chalcopyrite and pentlandite are enriched in palladium relative to platinum.

One analysis indicated a marked enrichment of Pd in arsenides. HAWLEY (1962) regards the chalcopyrite mineralization as later than the bulk of the pyrrhotite and notes a consistent increase in palladium with the normal paragenetic order of these minerals. Ten year mine production figures suggest approximately equal Pt and Pd contents.

III. Noril'sk, U.S.S.R.

The distribution of Pt, Pd and Rh in the Noril'sk deposit was investigated by GINZBURG and ROGOVER (1961) using a spectrochemical method. Pyrrhotite, chalcopyrite and pyrrhotite-chalcopyrite concentrates were separated from the main ore-bearing rocks and from veins and encrustations. The results, summarized in Table 78-F-4 suggest that:

a) In disseminated sulfides from the main ore-bearing rocks (figures in parentheses in Table 78-F-4) Pd and Pt are concentrated in chalcopyrite whereas Rh is enriched in pyrrhotite.

b) There is an enrichment of Pd over Pt, with the Pd/Pt ratio for all data in Table 78-F-4 averaging 6.1. In the disseminated ores the enrichment of Pd relative to Pt is higher in chalcopyrite than in pyrrhotite.

c) In massive sulfides from veins and incrustations a Rh enrichment in pyrrhotite occurs as in the disseminated ores. The Pd/Pt ratio is more variable but the highest ratio, 9, is found in chalcopyrite as in the disseminated ore. However, total platinum metals are higher in pyrrhotite rather than chalcopyrite.

IV. Inaglinsk Massif, South Yakutia, U.S.S.R.

Platinum metals in the Inaglinsk Massif were studied by RAZIN *et al.* (1965). The Inaglinsk Massif is a complex pipe-like intrusive with a dunite core and a peripheral zone of alkali syenite rocks. The contact between these rocks, called apodunite, varies from peridotite at the inner contact with dunite through pyroxenite and alkalic gabbro to melanocratic alkali syenite on the outer contact.

Table 78-F-1. *Platinum metal concentrations in sulfide, selenide-telluride and arsenide minerals, ppm*

Sample description	Method and author[a]	Ru	Rh	Pd	Os	Ir	Pt
Sulfides: Mainly pyrrhotite, pyrite, chalcopyrite	(W/X)[5][b]	0.01—0.04[c] 0.014 (24)	0.02—2 0.2 (23)	0.2—9 3.7 (39)	0.9—2 0.4 (26)	0.2—1.0 0.5 (26)	0.2—5 0.95 (84)
Selenide-Tellurides	(W/X)[5]	—	2—12 7.0 (2)	5—90 46 (4)	0.05—0.1 0.075 (2)	0.6—15 5.5 (4)	10—50 27.5 (4)
Molybdenite	(FA/S)[3]	—	0.05—0.2 0.08 (4)	0.02—0.5 0.09 (8)	—	0.3	0.02—1 0.17 (9)
Molybdenite: Telemark, Norway	(W/X)[5]	0.006 (60)	—	—	0.01 (60)		0.06 (60)
Co and Ni sulfides and arsenides: Mainly cobaltite, niccolite, gersdorffite, linnaiete	(FA/S)[3]	—	—	0.1—0.5 0.3 (3)	—	—	0.1—0.5 0.2 (13)
Non-nickeliferous sulfide ore deposits, mainly from eastern Canada							
Chalcopyrite	(FA/S)[4]		0.003—0.13 0.06 (6)	0.004—1.8 0.45 (13)			0.09—0.41 0.15 (4)
Pyrrhotite			0.03—0.06 0.045 (2)	0.004—0.056 0.02 (6)			
Pyrite			0.003	0.012			

3

Nickeliferous sulfide ore deposits							
Pyrrhotite, Rankin Inlet, Northwest Territory, Canada	(FA/S)[4]	1.6—2.1 1.9 (2)	0.3—0.6 0.5 (3)	3.8—5.2 4.5 (3)	10	1.0—1.0 1.0 (2)	1.3—2.7 2.1 (3)
Pyrrhotite, Lynn Lake, Manitoba, Canada			0.018	1.36			0.18
Pyrrhotite, Duluth Gabbro, Minnesota, U.S.A.			0.07	1.47			0.11
Pyrrhotite-Pentlandite, Insizwa, South Africa		0.41	0.38	0.38	0.34	0.51	0.48
Chalcopyrite-Cubanite, Insizwa, South Africa		0.09	0.06	13.8			2.1
Chalcopyrite, Mosalani Mines, Bihar India	(FA/S)[2]						0.025—0.070 0.050 (4)
Almalyk ore region, Central Asia, U.S.S.R.							
Pyrite	(FA/S)[1]			0.014			
Chalcopyrite				0.21			0.02
Sphalerite				0.003			
Galena				0.032			
Molybdenite					2		

[a] 1. Badalov, S., and S. Terekhovich (1966). 2. Das Sarma, B., *et al.* (1966). 3. Goldschmidt, V., and Cl. Peters (1932). 4. Hawley, J., and Y. Rimsaite (1953). 5. Noddack, I., and W. Noddack (1931).

[b] Table I, Section 6 from Reference No. 4 excluding minerals from meteorites. Averages are weighed according to the number of samples of each mineral analysed.

[c] The data include the range (top), average (middle) and number of samples (in parentheses) if more than one.

4

Table 78-F-2. *Platinum metals in minerals from the Sudbury complex, Canada, ppm*

Sample description		Reference[a] and method	Ru	Rh	Pd	Os	Ir	Pt
Means from South range deposits	Pyrrhotite	(FA/S)[1]	0.04 to 0.35	0.28	0.60	0.37	0.2 to 0.33	0.52
	Chalcopyrite			0.27	1.17			1.30
Falconbridge mine	Pyrrhotite	(FA/S)[1]			34.2			15.6
					0.13			0.17
	Chalcopyrite				34.28			1.54
					1.61			3.77
	Pentlandite				17.50			29.8
					12.65			34.2
	Pyrite				0.31			0.37
	Arsenides				246.8			trace
Nickel-offsets	Pentlandite and Pyrrhotite	(FA/S)[1]	0.10		2.00			2.68
Creighton	Pyrrhotite	(N)[4]			0.10			0.48
	Chalcopyrite				0.013			0.72
	Pentlandite				6.3			0.2
Strathcona mine	Pyrrhotite, mafic norite	(N)[2] and (N)[3]	0.019		0.082	0.009	0.010	
	Pyrrhotite, xenolithic norite		0.054		0.025	0.023	0.053	
	Pyrrhotite, footwall		0.004		0.212	0.003	0.002	
	Chalcopyrite, footwall		0.014		0.962	0.003	0.001	

[a] HAWLEY, J., and Y. RIMSAITE (1953). 2. HSIEH, S. (1967). 3. KEAYS, R. (1968). 4. MORRIS, D., *et al.* (1963).

Platinum metals are found mainly in dunite as discrete minerals, minerals including native platinum (Pt, Fe), iridic platinum (Pt, Fe, Ir), nevyanskite (Ir, Os), sperrylite ($PtAs_2$) and cooprite (PtS), and in association with silicate and oxide minerals. The deposit is similar to the Urals type of platinum mineralization according to RAZIN *et al.*

Individual platinum metals were determined in whole rock samples by a quantitative spectrographic method following chemical enrichment. The data are presented in Table 78-F-5. High total platinum metal values occur in the dunite core carrying segregated chrome spinels. These rocks are particularily distinctive, since both Ir and Rh are higher than Pd. No other rocks noted in this survey had such high relative Rh and Ir values. The Pd/Pt ratios are low and vary from 0.13 to 0.20 in all the dunitic rocks.

Table 78-F-3. *Platinum metal ratios in common Sudbury ore minerals, percent.* (After HAWLEY, 1962)

Mineral and description	Number of samples	Rh	Pd	Pt	Total platinum metals in ppm
Pyrite	3	2.5	41.4	56.4	1.90
Pyrrhotite	37	7.8	32.7	61.6	1.36
Pentlandite	3	7.5	59.5	33.0	5.42
Chalcopyrite	7	0.9	81.4	17.7	7.69
Minerals from an offset deposit					
Pyrite		7.5	42.2	50.3	
Pyrrhotite		7.0	48.7	44.3	1.87
Pentlandite		10.3	64.6	25.1	10.52
Chalcopyrite		0.22	71.5	28.3	8.06
Mill average (6 months)		2.0	65.0	33.0	5.33
10 year production, Sudbury ores[a]		13	41	46	

[a] The Rh figure includes Ru + Ir.

Table 78-F-4. *Pt, Pd and Rh data for sulfides from the Noril'sk deposit, U.S.S.R.* (After GINZBURG and ROGOVER, 1961)

Sample Descriptions	Number of samples	Rh	Pd	Pt	Total platinum metals in ppm
		wt.-% and ppm/1 % Ni (in parentheses)			
Mineral concentrates from the main ore-bearing rocks[a]					
Chalcopyrite	27	1, (0.4)	86, (32)	13, (5)	
Chalcopyrite-pyrrhotite	29	4, (0.7)	83, (14)	13, (2)	
pyrrhotite	19	21, (1)	66, (4)	13, (0.9)	
Sulfides from veins and incrustations[b]					
Pyrrhotite, veins		37%	53%	11%	19
Pyrrhotite, incrustations		15%	73%	13%	20.6
Chalcopyrite, veins		—	83%	17%	4.5
Chalcopyrite, incrustations		0.8%	90%	10%	5.1

[a] Summarized from Table 1, p. 918. For each mineral weighed averages were calculated from the original data, expressed in grams/ton/1 % nickel, and converted to a weight percent basis.

[b] Summarized from Tables 4 and 5, p. 921 and 922.

Pure mineral separates were analysed for total platinum metals. The minerals were decomposed by heating with NH_4F or $HCl + H_2SO_4$ and the soluble platinum metals determined gravimetrically after purification from base metals. Chrome spinels were analysed colorimetrically after HCl decomposition. Platinum minerals occurring in intimate intergrowths with silicates did not dissolve, and were discarded after separation from host minerals. The total platinum values obtained are regarded as representing platinum metals in solid solution or adsorbed in silicates. The validity of this interpretation depends on whether the platinum minerals were

Table 78-F-5. *Platinum metal content in rocks of the Inaglinsk Massif. U.S.S.R., ppb.* (After RAZIN *et al.*, 1965)

Sampling point	Rock	No. of analyses	Pt	Pd	Ir	Rh	Os	Ru	Total average platinum metals
Core of massif	Dunite with accessory chrome-spinels	5	300 to 4,000[a] 500	40 to 600 100	2—40 17	1.7 to 80 50	7—60 8	2—30 5	680
Core of massif	Dunite with segregation chrome-spinels	6	300 to 600 400	20 to 60 50	200 to 900 400	20 to 700 270	5—9 7.5	3—6 4.5	1,132
Inner contact of the apodunite zone	Apodunite olivine-pyroxene rocks (analogues of pyroxenite)	4	30—90 80	9—20 12	0.4 to 40 15	0.4 to 5 2.5	2—8 4	0.9—4 2.2	96
Outer contact of the apodunite	Apodunite pyroxene biotite-K feldspar rock (analogue of mica shonkinite)	1	8	2	5	3	0.3	0.5	19
Periphery of massif	Pulaskites	1	2	3	2	5	traces (< 0.2)	0.2	12

[a] Range above and average below.

completely insoluble in the various reagents used to attack the silicates. Proof that no dissolution of platinum minerals occurred is lacking and, as noted by WRIGHT and FLEISCHER (1967), the extreme fine grain size of these minerals would favour solubility. The data are presented in Table 78-F-6 and indicate the following:

a) chrome-spinel is the principal concentrator of platinum metals. Olivine is the second major host, but, on the average, contains about 30 times less platinum than chrome-spinel;

b) in the dunites the weakly serpentinized rocks contain higher platinum metal contents than the medium serpentinized rocks. The authors suggest that while olivine accumulates large amounts of platinum metals during magmatic crystallization there is some loss during epigenetic alteration;

c) pyroxene, mica, magnetite and apatite contain very small amounts of platinum metals.

The association of platinum metals with chrome-spinel was further investigated by analysis of morphologically similar chrome-spinel with approximately the same degree of epigenetic alteration taken from the center and periphery of the dunite core.

The average value for total platinum metals in nine samples from the core of the intrusive is 30 ppm whereas two samples from the periphery average 96 ppm. The authors consider that the lower temperature chrome-spinels at the periphery are more active concentrators of the platinum metals than the higher temperature spinels from the center of the intrusive.

Table 78-F-6. *Total platinum metals in minerals of the Inaglinsk massif. U.S.S.R., ppm.* (After RAZIN *et al.*, 1965)[a]

Rock[c] type	Description and sample number	Whole rock	Olivine	Chrysotile	Chome-spinel	% total Pt metals present as Pt minerals
Dunite with accessory chrome-spinel	Fresh, slightly serpentinized; I-135	—	0.8	not detected	20	—
	Fresh, slightly serpentinized; I-130	4.7	2	0.15	10	—
	Fresh, medium serpentinized; I-105	1.0	0.4	0.3	20	64.8
	Intensively weathered, medium serpentinized, I-101	—	0.5	0.7	50	—
Apodunite	Mica-pyroxene-olivine rock[b], fresh, slightly serpentinized, I-111	0.11	0.06	0.28	20	53.7

[a] Data summarized from Tables 4 and 7, p. 123 and 126 respectively, RAZIN *et al.*

[b] Diopside and phlogopite from the apodunite, sample I-111, contained 0.002 and 0.004 ppm total platinum metals respectively.

[c] Platinum metals were detected in trace amounts only in magnetite and apatite in these rocks.

V. Bushveld Complex, South Africa

In the Bushveld, platinum metals are found in high concentration in the Merensky Reef (WAGNER, 1929; COUSINS, 1964) and the Mooihoek, Driekop and Onverwacht dunite pipes. Some data of geochemical significance on the Bushveld occurrences have been presented by SCHNEIDERHÖHN and MORITZ (1931) and HAGEN (1954).

The Merensky Reef, a pegmatitic pyroxenite normally bounded on top and bottom by thin chromite seams is characterized by high platinum metal values within or adjacent to the top and bottom chromite bands, although the chromite crystals themselves do not contain platinum (COUSINS, 1964). Platinum minerals found include ferroplatinum, braggite and cooprite with smaller amounts of laurite, stibiopalladinite and sperrylite. SCHNEIDERHÖHN and MORITZ (1931) analysed sulfide and silicate minerals from the Merensky Reef for platinum metals by microdrilling of polished sections, followed by direct analysis by emission spectrography. High values for silicate minerals suggest that some of their results (Table 78-F-7) may generally be high.

Pt and Pd are the most abundant sulfides with Pt in excess of Pd and the other metals present in approximately equal but much smaller amounts. The relative proportion of Merensky Reef platinum metals, computed from Cousins data (1964) are:

Pt = 63%, Pd = 28%, Ru = 5%, Rh = 2.7%, Ir = 0.7% and Os = 0.6%. In the samples examined by SCHNEIDERHÖHN and MORITZ no discrete platinum minerals were observed and they concluded that the platinum metals were in solid solution in sulfides. They also noted that the highest platinum metal contents were in the earliest sulfides, pyrite and pyrrhotite. The well-established occurrence of discrete platinum metal minerals in the Merensky Reef (WAGNER, 1929; RAMDOHR, p. 759, 1960) indicates, however, that only part of the total platinum metal content can be in solid solution in sulfides.

Table 78-F-7. *Platinum metal content of minerals from the Merensky Reef, Bushveld Complex, South Africa, ppm.* (After SCHNEIDERHÖHN and MORITZ, 1931)

Location	Mineral[a]	Ru	Rh	Pd	Ir	Pt
Klipfontein-[b]	Pyrite	0.5—1	1	5—10	0.5—1	10—50
Krondaal,	Pyrrhotite					
Rustenburg	Pentlandite	0.5		0.5—1	5	0.5—1	5—10
District	Bronzite	—	0.1—0.5	0.5—1	0.1—0.5	1—5
Schildpadnest,[c]	Pyrite	0.1—1	0.1—1	10—100	0.1—1	10—100
Rustenburg	Pyrrhotite					
District	Pentlandite	0.1—1	0.1—1	1—10	0.1—1	1—10

[a] Platinum metal concentrations in chalcopyrite from both localities were below the detection limit.

[b] Olivine, diallage and plagioclase were also analysed in the Klipfontein sample. In olivine 1 and 0.5 ppm Pt and Pd respectively were found and in diallage 1—5 ppm Pt was obtained.

[c] In the Schildpadnest sample chromite, olivine, diallage and serpentine + millerite were analysed. No platinum metals were detected.

SCHNEIDERHÖHN and MORITZ also determined platinum metals in minerals from the Mooihoek and Driekop dunite pipes and a few determinations for the Mooihoek and Onverwacht pipes were reported by HAGEN (1954). The highest platinum metal concentrations are found in the iron-rich hortonolite cores of the Mooihoek and Onverwacht pipes whereas in the Driekop pipe, which lacks concentric structure and marked fractionation of iron, the distribution of high platinum metal values is more irregular. The platinum metals occur as discrete minerals including mainly ferroplatinum, sperrylite and, at Driekop, geversite, according to STUMPFL (1961). In addition small quantities of braggite, cooprite, laurite, stibiopalladinite, osmiridium and osmite are associated with the major platinum group minerals. Using an electron microanalyser STUMPFL (1961) identified eight additional new platinoid-rich minerals, principally compounds of antimony, arsenic and bismuth, in mine concentrates from Dreikop.

Data for whole-rock samples from dunite pipes are given in Table 78-F-8. An increase in platinum metal content in the hortonolite facies of the Mooihoek and Onverwacht pipes is apparent. In the Driekop mine where the degree of iron enrichment is small, little difference is found in the olivine and hyalosiderite facies. WAGNER regards the hortonolite cores of the pipes as later than the forsterite mantle because of both the lower temperature indicated by the iron-rich composition and the presence of mineralizers suggested by the association of phlogophite, hornblende and fluorapatite with the hortonolitic rocks. The platinum metals are therefore

Table 78-F-8. *Platinum metal content of dunite pipes from the Bushveld Complex, South Africa, ppm*

Pipe	Rock type and description	Author[a] and method	Ru	Rh	Pd	Ir	Pt
Mooihoek	Medium grained hortonolite dunite	S[2]	0.5	0.5—1	1—5	0.5	5—10
	Coarse grained hortonolite dunite in the vicinity of pegmatitic veins	S[2]	0.5—1	1—5	5—10	1	10—50
	Chromite band in hortonolite dunite	S[2]	0.5—1	1—5	5	1	0—50
	Hortonolite, inner core, No. 8	Fa/S[1]		0.29	0.65		12.3
	Hortonolite, inner core, No. 106	FA/S[1]			0.02		0.3
	Olivine, outer rim, No. 31[b]	FA/S[1]			0.07		0.07
Driekop	Olivine dunite, surface	S[2]		0.1—0.5	1		1—5
	Hyalosiderite dunite, surface	S[2]		0.5	1—5		1—5
	Hyalosiderite dunite, 400 foot level	S[2]		0.5	1—5		1—5
	Weathered dunite, surface	S[2]		0.5—1	1—5	0.5	5—10
Onverwacht	Olivine, outer rim, No. 16	FA/S[1]			0.004		0.02
	Hortonolite, inner core, No. 17	FA/S[1]			0.013		3.2

[a] 1. HAGEN, J. (1954). 2. SCHNEIDERHÖHN, H., and H. MORITZ (1931).

[b] VINCENT and SMALES (1956) obtained 0.123 Pd for this sample

considered to be fractionated and concentrated in late or residual fluids which gave rise to the hortonolite cores.

As in the Merensky Reef, Pt and Pd are the most abundant metals with Pt in excess of Pd. Rh is the third most abundant metal and Os and Ru minerals are known to be present.

SCHNEIDERHÖHN and MORITZ also found platinum metal contents up to 5 ppm Pt in silicate minerals such as hornblende, mica and diallage from the Mooihoek and Driekop pipes. Such high platinum values were regarded as resulting from the presence of inclusions of platinum minerals. The large difference between Hagen's Pd values for two hortonolite samples from the inner core of the Mooihoek pipe suggest non-uniform distribution of this metal.

VI. Discussion

A summary of some of the properties of the platinum metal distributions and mineral associations for the ores discussed above is presented in Table 78-F-9. The platinum metals of highest concentration in these ores are Pt and Pd followed by

Table 78-F-9. *Summary of platinum metal distribution in the Sudbury, Noril'sk. Inaglinsk and Bushveld deposits*

Deposit	Pd/Pt	Sulfide, silicate or oxide minerals with highest platinum metal content		
		Rh	Pd	Pt
Sudbury	1	Pyrrhotite Pentlandite	Chalcopyrite Pentlandite	Chalcopyrite Pentlandite
Noril'sk	6	Pyrrhotite	Chalcopyrite	Chalcopyrite
Inaglinsk (whole rock samples)	0.25	Total platinum metals highest in chrome-spinels		
Bushveld Merensky Reef	0.4		Pyrite Pyrrhotite	Pyrite Pyrrhotite
Bushveld Dunite Pipes	0.2	Pt and Pd highest in hortonolitic facies		

Rh with Ru, Os and Ir occurring at considerably lower concentration levels. In Cu-Ni sulfide deposits associated with gabbroic rocks Pd equals or exceeds the Pt content on the average, whereas in deposits associated with dunitic rocks Pt is the more abundant of the two metals. The Merensky Reef ores, which are associated with significant quantities of Cu—Ni sulfides and in this sense are comparable with Sudbury and Noril'sk, are an exception. However, they do show some analogy with the dunitic deposits in that platinum metals are concentrated in the chromite layers immediately above and below the pyroxenitic facies of the Reef.

In the Cu—Ni sulfide ores of Sudbury and Noril'sk Pt and Pd are dominantly associated with chalcopyrite and pentlandite whereas Rh is distinctly higher in pyrrhotite, particularly at Noril'sk. The Merensky Reef, however, is different in that pyrite and pyrrhotite rather than chalcopyrite are richest in Pt and Pd according to SCHNEIDERHÖHN and MORITZ's data. Although distinctive platinum metal — sulfide mineral associations are apparent, it is by no means clear whether the platinum metals are in solid solution or are mechanically admixed as discrete minerals with the sulfides. STUMPFL (1962) has discussed the genesis of platinum ore deposits pointing out that discrete platinum metal minerals have been recognized in all these deposits. He concluded (p. 622) that while the "possibility that traces of Pt-metals enter the lattice of sulfides" cannot be disregarded, "the bulk of the Pt-metals in the above deposits is fixed in independent Pt-minerals".

While the presence of platinum minerals in Cu—Ni sulfide ores is well established-it is unlikely that the strong association of Pt and Pd with copper but Rh with iron sulfides is accidental. Two possible reasons for the existence of these relationships follow.

a) Because of favourable crystallochemical factors Pt and Pd form dilute solid solutions with chalcopyrite, cubanite and pentlandite. If solubility is favoured at high temperatures exsolution may occur on cooling with the formation of cooprite or braggite. Rh, again because of crystallo-chemical factors, may be capable of substitution only in the pyrrhotite lattice.

b) Pt and Pd may form complex ions, possibly with S, As or Sb and with square coplanar stoichiometry (by analogy with known low temperature S complexes of Pd)

11 132

which inhibit solid solution of these metals but increase solubility in S-rich melts. These Pt metals therefore tend to occur in highest concentration in residual or late magmatic solutions as discrete minerals, and in association with the youngest major sulfide in the paragenetic sequence, usually chalcopyrite. If Rh does not form a species of high solubility in a sulfur-rich melt, it may be adsorbed, coprecipitated or otherwise enter into solid solution with the earliest major sulfide in the paragenesis, pyrrhotite.

Accurate data on the platinum metal concentrations in individual sulfide minerals from Cu—Ni sulfide ores are required to test the validity of these hypotheses.

The occurrence of platinum metals in dunitic rocks is characterized by two important features including enrichment in spinels, particularly in massive or segregation type chromite, and in the youngest dunitic rocks. High platinum metal values are found in the chromite layers marking the upper and lower boundaries of the Merensky Reef (COUSINS, 1964), and in chrome -spinel of the Inaglinsk Massif. The occurrence of high platinum metal values in the youngest facies of dunitic rocks is particularly apparent in the Mooihoek and Onverwacht pipes where a core of hortonolitic olivine is present. Also at Inaglinsk the dunitic core, which presumably crystallized later than the dunite on the periphery, is highest in platinum metals. A suggested explanation is that low solubility of platinum metals in silicate lattices has led to concentration in residual magmatic fluids or melts where they have finally crystallized as native metals, sulfides, arsenides or antimonides depending on the availability of these elements. RAZIN *et al.* (1965) maintain that in the Inaglinsk Massif, silicates do carry platinum metals. However, the interpretation of their data is open to some doubt as previously noted. The reason for the association of platinum metals with chrome spinels is unclear. RAZIN *et al.* appeal to substantial solid solution or adsorption of platinum metals, whereas COUSINS (1964) and WAGNER (1929) maintain that Merensky Reef and other Bushveld chromite is free of platinum metals although supporting analytical data are not presented.

Revised manuscript received: March 22nd, 1968

12

METALLOGENY OF HEAVY OILS, NATURAL BITUMENS, AND OIL SHALES

[illegible]

Richard F. Meyer [illegible]

[illegible]

METALLOGENY OF HEAVY OILS, NATURAL BITUMENS, AND OIL SHALES

ISBN 0-7732-1316-3

PUBLISHED BY

ALBERTA OIL SANDS TECHNOLOGY AND RESEARCH AUTHORITY
500 HIGHFIELD PLACE
10010 – 106 STREET
EDMONTON, ALBERTA, CANADA
T5J 3L8

5.1 ACCUMULATION AND COMPOSITION OF THE SHALES

In the Phanerozoic section, a fairly distinct periodicity has been found in the accumulation of the sapropelic carbonaceous rock facies termed oil shales, black shales, domanikites, and the like. Many of these are enriched in Mo, U, Re, V, Se, Cd, Bi, Tl, Ag, Au, As, Sb, and other rare and disseminated elements. Against a relatively high overall geochemical background in carbonaceous rocks, groups of formations are distinguished which are characterized by a certain combination of rare elements. The content of the elements is several orders of magnitude higher than their clarkes and may reach the levels of economic ore concentrations. On the basis of current ideas concerning the concentrating function of organic matter, sapropelic carbonaceous formations as a source of metals should reflect the conditions of accumulation and fossilization of the organic matter and the environment of deposition. The difference in the environments in which black shales of different genetic types are formed is manifested not only in the distribution and concentration of rare and disseminated elements, but also in the mineral composition of the rocks, which enables us to correlate their composition and metal potential. A proposed compositional classification (Goldberg, Mitskevich, and Lebedeva, 1991) was based on a combination of methods, including X-ray, silicate and carbonate-chemical, and petrographic, with the chemical methods of principal importance. The chemical analyses were recalculated to the complete mineral composition, bringing out the main components of these rocks: free authigenic silica; carbonates; and clastic components, which consist mainly of clay minerals. On the basis of processing about 500 analyses of black shales from various basins with respect to these components, five types of rocks were distinguished. The first three types — siliceous, clayey-siliceous, and siliceous-carbonate — can be classified as sediments of the domanik type on the basis of the details of their formation, distribution, and composition. These rocks always contain an elevated, often high, amount of free authigenic silica which most investigators believe to be planktonogenic. Domanikites are the sediments of uncompensated ("starved"), relatively deep-sea basins, accumulated at an extremely low rate (up to 6 m/Ma) with an oxygen deficit in the bottom water and extensive hydrogen sulfide contamination. The decisive factors in the accumulation of organic matter in these sediments are the low sedimentation rates, with very slight inorganic dilution, and a high degree of fossilization of organic matter, mainly due to the formation of organo-montmorillonite compounds. At the same time, these factors promoted long-term processes of absorption of the metals by active organic matter from the sea water during early diagenesis, which led to the formation of strong geochemical anomalies. It is well known that functional groups with coordination saturation of oxygen and nitrogen atoms rise to the surface of organic matter and take part in binding metals in compounds of the chelate type.

Another variety of carbonaceous deposit is oil shale proper, which is composed of clastic and clay-carbonate rocks practically devoid of authigenic silica. Most of the richest oil shale deposits, containing up to 20–50 percent organic matter, are related to these. The main factor controlling the accumulation of large masses of organic matter apparently was the abruptly increased primary bioproductivity (the P factor of Yudovich and Ketris, 1988).

Because oil shales, as a rule, were formed in shallow marine or continental basins, the accumulation and preservation of organic matter is guaranteed only if the sedimentation rate is high, leading to rapid burial of the sediment. In addition, a considerable amount of organic matter (including humic) was introduced with the clastic material, as is indicated, particularly, by the presence of highly carbonaceous rocks in the purely clastic sections of intermontane basins. It is noteworthy that, in contrast to domanikites, the predominant clay minerals of oil shales proper are hydromicas and

2 135

kaolinite, which do not form organomineralic compounds and do not preserve organic matter. The separation of organic matter from the inorganic components of oil shales determines their distinctive qualitative parameters: the output of shale resin and the heating capacity. In addition, the specifics of the formation of oil shales did not foster the concentration of these elements in oil shales. These factors include a high sedimentation rate, a brief period of diagenesis and rapid separation of the sediment from the bottom water layer, and, frequently, accumulation in closed freshwater bodies which were impoverished in rare elements in the aqueous environment.

Table 5.1 summarizes the most important indices for distinguishing the environment of formation as well as the mineralogic, lithologic, and geochemical characteristics of domanikites and oil shales proper.

5.2 ORE SPECIALIZATION OF THE SHALES

The classification of domanikite and oil shale facies that has been worked out on the basis of composition and genetic criteria is tied in with the distribution of included rare and disseminated elements.

The material on which these formulations were based includes numerous data on the trace element composition of black shales published in our own and in the foreign literature, as well as results of analytical investigations of shales made by neutron activation, X-ray fluorescence, and emission spectral analyses. The various basins studied include, among others, the Baltic, West Siberian, Olenek, Timan-Pechora, Volga, and Central Asian.

In dealing with the problems of classification, most attention has been paid to study of the patterns of distribution of rare elements in carbonaceous facies of various types as the basis for the prediction of their metal potential. On the basis of calculations made for the concentrations of a number of elements in black shales, we were able to ascertain the nature of the association of organophilic elements and, on that basis, to classify the principal Phanerozoic carbonaceous facies of the world. These metallogenic facies were determined on the basis of a series of elements that had stable maximum values of concentration coefficients (C_c) for the type of facies in question: the ratio of the elemental content of a rock enriched in organic matter (≥ 5 wt%) to its clarke for clays. In addition, the next series of elements which considerably exceeds the clarke level was taken into account in the classification In some black shale facies, secondary mineralization has been superposed on the primary geochemical background of the facies. This is related to the introduction and deposition of metals at geochemical barriers, as a rule in mineral form. In addition, in zones of old upwelling, strong geochemical anomalies appear, mainly in P, U, and V, which blur the main series of rare and disseminated elements accompanying the planktonogenic sapropelic organic matter of black shales.

Table 5.2 gives the main metallogenic types of domanikite and oil shale that have been distinguished, and the concentration coefficients of elements defining these types. The combination of elements accompanying sapropelic organic matter in domanikites on the one hand, and in oil shales on the other, remains fairly constant. In the various associations, mainly domanikite, only redistribution of the elements in the concentration order is observed, with the formation of typical metallogenic associations of a relatively small number of elements (Mo, Re, U, Se, V, Zn, Cd, Bi, Ag, Tl, and others).

TABLE 5.1

Comparative characteristics of oil shales and domanikites

Indicators	Oil shales	Domanikites
Regime of deposition/rate of deposition (m/Ma)	Compensated, relatively high, up to 50–100	Uncompensated low, up to 1–6
Facies setting	Shallow sea, lagoons, lakes	Relatively deep sea (up to 500–1000 m); extensive hydrogen sulfide contamination of water above bottom
Tectonic setting	Intraplatform syneclises, shallow depressions on platform structures, intermontane basins	Platforms, chiefly regions of pericratonic subsidence; geosynclinal regions
Area of occurrence (km^2)	Isolated basins, tens to hundreds, rarely thousands	Continuous over areas of tens to hundreds of thousands to a few million
Host rocks	Sandstones, siltstones, conglomerates, effusives, clayey rocks, rarely carbonates; coal is found	Clayey and clay-carbonate rocks, limestones
Type of rocks enriched in organic matter	Clayey and carbonate-clayey oil shales, usually silty	Siliceous, clayey-siliceous, clayey and siliceous-carbonate domanikites
Rock-forming minerals	Hydromicas, kaolinite, montmorillonite, calcite, dolomite, pyrite; considerable silt admixture	Montmorillonite, calcite, dolomite, opal, chalcedony, pyrite; slight admixture of silt
Thickness of sequence containing rocks rich in organic matter (m)	Hundreds, sometimes a few thousand	A few tens
Number of intercalations (beds) rich in organic matter	Tens	Isolated; one or two economically ore-bearing
Amount of organic matter at end of diagenesis (%)	15–50	5–20, rarely up to 35
Type of organic matter	Humite-sapropelite, sapropelite	Mainly sapropelite
Heating capacity (Kcal/kg)	1000–4500 (usually 2000–2500)	800–2500 (usually about 1000)
Yield of shale tars (%)	3.5–32.5 (usually 10–15)	1.5–8 (usually 3–4)
Content of elements	About clarke; above clarke: Mo, Re, sometimes P, U, Se, Cd, Au, Ag, As, Cu	Everywhere 1–4 orders above clarke: Re, Mo, Se, Cd, Bi, Ag, Au, As, Tl, Sb, U, V, Zn; often P, Ni; sometimes Cu, Pb, Co, Cr

ikites
d low, up to
p sea (up to
; extensive
ie contamina-
ove bottom
ly regions of
subsidence;
gions
r areas of tens
housands to a
ay-carbonate
s
ey-siliceous,
ceous-carbo-
s
ite lcite,
chalcedony,
admixture of
two econo-
ing
o 35
ite
ually about
-4)
orders above
, Se, Cd, Bi,
l, Sb, U, V,
; sometimes

Among domanikites of clayey-siliceous (siliceous-clayey) composition, two main metallogenic types are distinguished: Mo-U-V (Re, Bi) and Mo-Se-Zn (Table 5.2).

Classic examples of the first metallogenic type are the Cambrian Alum Shale and Ordovician Dictyonema shales, underlying the territory from northern Norway to southern Sweden. The accumulation of the Alum shales corresponded to the stage of maximum transgression with minimal sedimentation rates (1 to 2 m per Ma). In the stratigraphic section of the Alum shales, which is from 1219 m (Nyarke) to 50 m thick (Skane), three members with different contents of organic matter, sulfur, and metals are distinguished. A general tendency is observed toward an increase in concentration of C_{org}, S, U, Mo, and Ni upward in the section. Numerous inclusions of concentrated organic matter (up to 80 percent), the so-called "kolms," containing up to 10 percent FeS_2 and 2000–5000 g/t U, are confined to the Peltura zone of the upper Renstad member (Andersson *et al.*, 1985); the background concentrations are 15–30 percent C_{org}, 135–337 g/t U, and 240–340 g/t Mo. In the Tremadocian Dictyonema shales, a very high concentration of V is observed, despite a decrease in the organic matter content to 68 percent.

On the basis of concentration coefficients, the disseminated and rare elements in shales form the following series (the first figure is the minimum C_c value, the second, the maximum): Mo (35–230), U (4.5–105), V (3.4–28), As (2.5–24), Cd (7.3–23), Ag (3–14), (Sb 3–10), Zn (1.6–3.3), and Cu (1.3–3.3); in individual samples, Bi (130) and Pb (46) have been found. A fairly clear relationship of the shales richest in rare and disseminated elements, especially U and Mo, to the zones with minimum thickness of the shale-bearing member is found. It is to these zones that the shale deposits of Sweden, containing large reserves of U, Mo, and other elements, are confined (the Nyarke, Billingen-Falbigden, Renstad, and Ostergotland). For instance, the uranium reserves in the Billingen-Falbigden deposit are estimated at 1.7 million tons and those of the Nyarke deposit, 0.28 million tons (Andersson *et al.*, 1985). The source of the uranium in the shales is believed to be the weathered mantles overlying basement granites of the Baltic shield, as well as associated deposits of the uranium-albite association (Yudovich and Ketris, 1988). In addition, the strict stratification of the uranium mineralization throughout the section and its areal persistence may indicate biogenic accumulation of uranium, if its concentration in the paleo-basin is relatively high.

The kerogen mudstones of the Tremadocian Tyurisalus formation in northern Estonia may be an analog of the Dictyonema shales of Scandinavia. According to Pukkkonen (1989), the order of decreasing average values of rare and disseminated element concentration coefficients in shales is as follows: Re (143), Bi (111), Mo (69), U (15), Tl (10), Ag (10), Au (10), Cd (9.5), V (7), Sb (7), As (5), Se (5), and Cu (2.5). In some sections a high concentration of Zn (up to 7100 g/t) is observed. With the decreasing thickness of the shale layer from west to east and toward the south, from 7 to 1 m, there is an increase in the concentration of Re, V, Mo, U, P, S, Ag, As, and Ni and a decrease in the content of C_{org}, Nb, Al, and others. For instance, from the central part of northern Estonia to the Toolse deposit, the V content increases from 760 to 1040 g/t, Mo from 133 to 406 g/t, and Re from 0.05 to 0.17 g/t (Maremäe, 1989).

Black shales such as the Chattanooga (Hathaway member), which extends parallel to the Appalachians from New York to northern Texas, belong to the first metallogenic type. The Chattanooga shales were deposited in a vast (more than 650,000 km^2), relatively deep, stagnant epicontinental basin with extremely slow sedimentation rates. Conant and Swanson (1961) pointed out the similarity of the Chattanooga shales to the Alum shales of Scandinavia, with respect to their conditions of formation and composition. Analysis of data on the trace-element composition also

5

TABLE 5.2
Metallogenic types of domanikite and oil shale associations

Basin	Country	Age of horizon, formation	Type of association	Predominant rock composition	Organic matter, range/average (%)	Metallogenic associations (in order of decreasing C_c)		Elements forming their own minerals	Examples of deposits (metal content, g/t)	Reference
						Main	Secondary			
Type I. Mo-U-V (Re, Bi)										
Baltic	Sweden	0_1, Dictyonema	Domanikite	Siliceous-clayey	6–15/–	(Bi), Mo, U, V	As, Au, Ag, Zn, Cu	Fe	Ostergotland (Mo-135; U-140–190; V-2000)	
		$\mathrm{Є}_2$–$\mathrm{Є}_3$ "alum shales"	Domanikite	Siliceous-clayey	5–30/12	(Bi), Mo, U, V	As, Ag, Au, Cd, Zn, Cu	P, Fe	Nyarke (Mo-270; U-135–245 V-1000); Billingen-Falbigden (Mo-270–340; U-155–337; V-780)	Andersson and others (1985); Anderson and Bjerle (1988)
	Estonia	0_1, Pakerort, Tyurisalu	Domanikite	Siliceous-clayey	5–14/11	Re, Bi Mo, U, V	Au, Ag, Cd, Sb, As, Se	P, Pb, Zn, Fe	Toolse (V-1040; Mo-406; Re-0.17)	Pukkonen (1989); Märemäe (1989); author's data
Chattanooga	USA	D_3–C_1^1	Domanikite	Siliceous-clayey	5–25/22	Mo, U, V	Ag, Zn, Cu, Th	P, Fe (Mo-100;	Chattanooga (Mo-100; U-80–120; V-500; (Mo-200; V-1500)	Conant and Swanson (1961); Landis (1962); Vine (1964)
Type I. Mo-U-V (Re, Bi)										
Illinois	USA	C_2–C_3	Domanikite	Siliceous-carbonate	4–24/–	P, U, V, Mo, Se, Zn	Cu, Ni, Pb, Cd	P, Pb, Mo Zn, Fe	Logan Quarry (P_2O_5-1%; U-240; V-1430; Se-300); Mecca Quarry (U-160; V-5850; Mo-1160; Se-250)	Davidson and Lakin (1961); Coveney and Martin (1983)

6

									Mecca Quarry (U-160; V-5850; Mo-1160; Se-250)	

Table 5.2 cont'd ...

Basin	Country	Age of horizon, formation	Type of association	Predominant rock composition	Organic matter, range/average (%)	Metallogenic associations (in order of decreasing C_c) Main	Metallogenic associations (in order of decreasing C_c) Secondary	Elements forming their own minerals	Examples of deposits (metal content, g/t)	Reference
Type II. Mo-Se-Zn										
West Siberian	Russia	J_3v-K_1v, Bazhenovo	Domanikite	Siliceous-clayey	6–15/10	Mo, Se, Zn, U, As, Sb	Au, Ag, V, Ni, Cu	Fe	–	Gayshin and Bobrov (1982); Gurari and others (1988); author's data
Type III. U										
California (Ventura Los Angeles)	USA	N_1, Monterey, Sisquoc	Domanikite	Siliceous & clayey siliceous	4–14/5.4	U	Mo, Cr, Be, Y V, Cu, Ni	P	Temblor Range (U-240)	Durham (1987)
Type IV. P-U-V (Mo, Se, Zn)										
Phosphoria (old upwelling zone)	USA	P_1, Phosphoria (Meade Peak horizon) "vanadium zone"	Domanikite	Siliceous-carbonate	7–10/5	P, V, U, Mo, Se, Zn	Ni, Cu, Cd, Pb	P, Zn, Pb, Fe	(P_2O_5-30.5%; U-120; V-500-4000 Se-680; Mo-500; Zn-3500)	Love (1961); Sheldon (1959);
Type V. Mo-V (Cd, Bi, Ag)										
Olenek	Russia	Є$_1$–Є$_2$ Kuonamka	Domanikite	Siliceous-carbonate	6–33/14	Mo, V, Ag Bi, Cd	Zn, Au, Se As, Sb, Ni	P, Fe	–	Bakhturov, Yevtushenko and Pereladov (1988); Gavshin & others (1984); author's data
Eromanga	Australia	K_1, Tooleback	Domanikite	Siliceous-carbonate	4–26/13	Mo, Bi, Cd Se, V	Zn, U, Ni As, Ag, Sb	Fe	Julia Creek (Mo-270; V-2000; Cd-25; Se-30; Au-5; U-30)	Glikson and others (1985); Patterson & others (1985); Riley and Saxby (1982)

Table 5.2 cont'd ...

Basin	Country	Age of horizon, formation	Type of association	Predominant rock composition	Organic matter, range/average (%)	Metallogenic associations (in order of decreasing C_c)		Elements forming their own minerals	Examples of deposits (metal content, g/t)	Reference
						Main	Secondary			
Type VI. Ag-Mo-Zn (Cd, Bi, Tl)										
Atlantic Ocean		K	Domanikite	Siliceous-carbonate	–/(6)	Bi, Cd, Tl, Ag Mo, Zn, V	Cu, Cr, Ni, Co	Fe	–	Brumsack (1980); Brumsack and Lew (1982)
Type VII. Re-Mo-Se (Cu, Zn, Pb, Ag)										
Edinburgh	Great Britian	P_2 Merle Slate	Domanikite	Siliceous	4–11/–	Re, Mo	Ag, V, Ni, Cu, Co	Fe	Merle Slate (Re-0.1–30; Mo-20–800)	
Central European	Germany	P_2, Kupferschiefer "Copper schists"	Domanikite	Siliceous	7–15/–	Cu, Zn, Pb Ag, Re, Se, Mo	Au, As, V, Ni Co, Cd, Ge, U	Cu, Pb, Zn (Cd), Ag, Fe	Mansfeld (Cu-2.5%; Zn-0.7%; Pb-0.44%; Re-0.7%; Se-300; Mo-65–920); Sangerhausen (Cu-2.95%; Zn-1.25%; Pb-0.64%; Ag-106; Re-21; Mo-201)	Wedpohl (1967); Lur'ye (1983)
	Germany	P_2 Kupferschiefer	Domanikite	Siliceous	7–15/–	Cu, Zn, Pb Ag, Re, Se, Mo	Au, As, V, Ni Co, Cd, Ge, U	Cu, Pb, Zn (Cd), Ag, Fe	Richelsdorf (Cu-1–3%; Zn-0.6–1.0% Pb-0.5–0.7%)	
	Poland	P_2 Kupferschiefer	Domanikite	Siliceous	10–13/–	Cu, Zn, Pb Ag, Se, Re, Mo, Au, Pt, Pd	Au, V, Ni Bi, Ir, Os	Cu, Pb, Zn Ag, Fe	Lubin-Serozzovice (Cu-4.5%); Zechstein (Se-300; Mo-80–310)	Kucha (1985)
Syr Dar'ya Upper Amur	Tadzhikistan, Uzbekistan	P_2 Suzak	Domanikite	Siliceous-carbonate	12–31/–	Re, Mo, Se, Cd	Tl, Bi, V, Ag Ni, Sb, Cu, Zn	Fe, P	Baysun (Mo-1500; (Mo-1500; V-1262; Se-78; Re-5.6; Tl-6.3; P-5250); Urtabulak (Mo-1500; Re-6.2)	Kler and others (1987); Poplavko and others (1977);

8

141

Upper Amur	Uzbekistan	Suzak		carbonate			Ni, Sb, Cu, Zn		Baysun (Mo-1500; (Mo-1500; V-1262; Se-78; Re-5.6; Tl-6.3; P-5250); Urtabulak (Mo-1500; Re-6.2)	Kler and others (1987); Poplavko [illegible] others (1977);

Table 5.2 cont'd …

Basin	Country	Age of horizon, formation	Type of association	Predominant rock composition	Organic matter, range/average (%)	Metallogenic associations (in order of decreasing C_c)		Elements forming their own minerals	Examples of deposits (metal content, g/t)	Reference
						Main	Secondary			
					Type VIII. Re-Mo					
Volga and Timan-Pechora	Russia	J_3v_1,	Oil shale	Clayey-carbonate	7–15/– 15–40/–	Re, Mo	Se, Cd, Bi, Au Ag, As, V, Ni, Sb, Zn, Tl	Fe	Kashpir; Ayyuva, etc.	Kler and others (1987); author's data
					Type IX. Mo					
West European	G. Britain Spain, France Germany Switzerland and others	J_1, "Posidonia shales"	Oil shale	Clayey-carbonate	10–30/–	Mo	V, Ni, Co, Cu, Cr	Fe, (Li), Sr	Stowell Peak (Mo-60); Corset (Mo-15–260); Wurtenberg (Mo-80); Mons Terri (Mo-40)	Bitterli (1960); Kunz and Bauss (1975); Tourtelot (1970)
Piceance Creek Green River, Uinta, Washiki	USA	P_2, Green River	Oil shale	Clayey-carbonate	8–50/14	Mo,P, U	As, Zn, Cu V, Au	Na, Ba, Sr Fe, P, U	Wilkins Peak (Mo-200); (Mo-30); P_2O_5-2.2–18% U-0.005–15%	Yudovich & Ketris (1988); Meddaugh & Salotti (1983); Saelher *et al.* (1984); Saether, Runnells, & Meglen (1984)

indicates that the content of rare and disseminated elements in these facies is of much the same type (Landis, 1962; Vine, 1964). According to data on the concentration coefficients, the principal elements in the Hathaway shales form the following series (minimum and maximum C_c): Mo (50–115), U (25.0–37.5), V (4.0–11.5), Ag (2–20), and Zn (2–11). In Tennessee alone, the in-place uranium reserves in the shales are estimated to be 4.2–5.1 million tons.

The unique conditions under which the metals accumulated in the black shales are observed in the Illinois basin, where maximum concentrations of Mo, U, V, Se, and Zn are confined to shales that were deposited on the eastern littoral zone of the basin, near the old shoreline, at the boundary between reducing and oxidizing environments (Davidson and Lakin, 1961). This single region of concentration at a geochemical barrier occupies an area of several thousand square kilometers in Indiana and Illinois, in which rare and disseminated elements form the following series with respect to C_c values (minimum and maximum C_c): Mo (360–580), Se (400–500), Zn (37–111), U (50–75), V (11–45), and so on. Coveney and Charon (1983) found that Mo in the shales is bound mainly in organic matter, V in hydromicas, and U in organic matter and phosphates, whereas Zn, Cd, Cu, Pb, and, in part, Mo are in mineral form and consist of sphalerite, chalcopyrite, covellite, molybdenite, and other sulfides.

The second metallogenic type is typical of the siliceous-shaly Volgian-Valanginian domanikites (Bazhenovo formation) of the West Siberian Basin, with stable anomalous concentrations of Mo, Se, Zn, As, Sb, and other rare and disseminated elements (Table 5.2). The bituminous mudstones (20–35 m thick) accumulated in a vast (0.8–1.0 million km^2), relatively deep, uncompensated marine basin under conditions of widespread hydrogen sulfide contamination of the bottom water (Gurari, Vayts, Moskvin *et al.*, 1988). The average organic matter content in the rocks of the Bazhenovo formation is eight percent, reaching 12–15 percent in the central part of the basin. According to Gavshin and Bobrov (1982), the elements that accumulated in the organic matter are, in descending order of average values of concentration coefficients: Mo (61), U (10.5), As (7.3), Sb (6.9), Zn (5.9), V (4.6), Ni (4.1), Au (4.0), Ag (3.9), Cu (3.3), and Ba (2.8). An increase in concentration of organophilic elements from the periphery to the center of the basin is observed, with maximum values in the Salym, Surgut, and Krasnolininsk areas. According to the results of our activation analyses, the average rare and disseminated element concentration coefficients in the bituminous mudstones of the Salym area have the following values: Se (170), Mo (104), Au (25), Zn (17.5), As (16), Ag (14), V (8), Sb (5), Ni (4), and Co (2).

The main reason for the relative enrichment in rare earths of the rocks of the Bazhenovo Formation probably was the very slight mineral dilution due to the extremely low sedimentation rates. This conclusion is deduced particularly from the observed relationship between the rare and disseminated element concentrations and the ratio between the contents of organic matter and clay minerals in the rocks. From the clayey-siliceous rocks of the Bol'shoy Salym area to the siliceous-clayey rocks in the eastern part of the Shirotnoye Priob'ye ["Latitudinal Ob'"] area, to the clayey domanikites of the Nadym and Tazovsk areas, as the ratio of organic matter to clay mineral content changes from 0.5–0.4 to 0.4–0.2 and then to less than 0.1, the content of Mo, for instance, drops from 160–100 g/t to 75–50 g/t and 15–3 g/t, respectively. That same trend is traceable for other organophilic elements (U and Zn). In addition, the concentration of elements bound to the clastic components of the rock (Zn, Sr, Cr, and others) increases substantially from the central part to the perimeter of the basin.

10

143

h the same type
incipal elements
o [illegible]115), U
-place uranium

are observed in
d to shales that
t the boundary
ingle region of
e kilometers in
with respect to
, U (50–75), V
ound mainly in
Zn, Cd, Cu, Pb,
olybdenite, and

ian domanikites
ions of Mo, Se,
dstones (20–35
d marine basin
(Gurari, Vayts,
vo formation is
o Gavshin and
nding order of
(5[illegible]V (4.6),
of organophilic
s in the Salym,
he average rare
the Salym area
(8), Sb (5), Ni

he Bazhenovo
nentation rates.
n the rare and
natter and clay
the siliceous-
, to the clayey
nineral content
ice, drops from
able for other
l to the clastic
tral part to the

In the third metallogenic type, essentially siliceous, diatomaceous formations enriched in uranium are distinguished, related to the bathyal regions of the ocean basins. In particular, the black shale-diatomites in the Miocene-Pliocene Monterey and Sisquoc Formations in southern California are of this type. According to Durham (1987), the U concentration in the shales ranges from 2.5 to 1985.0 g/t. Most of the U is in organic matter and biogenic opal; the U contained in phosphate, which forms numerous inclusions in the "nodular shales," is not more than 510 percent of the total U in the rock. The extremely low concentrations of elements other than Mo in the shales are noteworthy. The order of decreasing values of their concentration coefficients is as follows (minimum and maximum C_c): Mo (5–60), Cr (0.2–1.5), Be (0.6–1.1), U (0.2–1.0), Cu (0.3–0.8), Ni (0.1–0.7), Ga (0.3–0.5), and Co (0.1–0.4). The uranium content is not accompanied by a relatively high content of Mo or other elements. Similar uraniferous diatomite deposits have also been found on the continental slope of southwest Africa.

A geochemical phenomenon among domanikites of siliceous-carbonate composition is the Permian Phosphoria Formation (type IV) (Table 5.2), unique in concentration of P, U, and V; it occurs over a vast area of the western United States. In the lower part of the Formation, in the Mead Peak horizon, there are phosphate layers containing up to 30.5 percent P_2O_5 and 0.012 to 0.024 percent U_3O_8 (Sheldon, 1959). The accumulation of phosphorus is attributed by many investigators to an ancient upwelling zone. In Wyoming, there is a highly carbonaceous carbonate-phosphate shale member ("vanadiferous zone"), with a content of 2 percent P_2O_5, 0.56 percent V_2O_5 and 0.001–0.060 percent U. The reserves of vanadium pentoxide in this member are estimated to be 18–25 million tons (Love, 1961). Besides P and V, a broad combination of rare and disseminated elements has been found in the Phosphoria formation, among which the following predominate, on the basis of C_c: Se (660), Mo (250), Zn (87), U (37), Ni (7), and Cu (7). It is significant that redistribution of the metals throughout the formation is observed, with the formation of ore concentrations in limestone intercalations. For instance, in the Mead Peak Phosphatic deposit, individual carbonate intercalations contain up to 0.4 percent V and 0.068 percent Se.

Siliceous-carbonate domanikites with geochemical anomalies of Mo, V, Cd, Bi, Ag, and other rare and disseminated elements belong to the fifth metallogenic type (Lower to Middle Cambrian Kuonamka Formation of the Siberian platform and the Lower Cretaceous Tulebak Formation of the Australian platform). The similarity of the geologic environments in which these facies accumulated is striking: (1) area of occurrence, 700,000–750,000 km^2, with a thickness of 40–75 m; (2) occurrence of the shales in the form of isolated intercalations and members up to a few meters thick in rocks poor in organic matter; and (3) zoned distribution of deposits with different concentrations of organic matter, with a maximum content of as much as 10–34 percent in the interior of the paleobasins.

In the oil shales of the Kuonamka formation, Bakhturov, Yevtushenko, and Pereladov (1988) report that the following elements have the highest concentration coefficients (minimum and maximum C_c): Mo (19–180), Cd (13–163), Bi (30–110), V (1.5–13.0), and Ag (5–9). However, the concentrations of the elements are unevenly distributed vertically and horizontally in the basin. On the whole, the highest concentrations of V, Mo, Ag, Cd, Se, Sb, and other organophilic elements are confined to the lower shale member and to zones of the Kuonamka sedimentary basin, where the rates of deposition were minimal. Our calculations show that in these zones, the sedimentation rates during Lena and Amga time were 0.6–1.7 m/Ma, and for the lower shale member, probably even lower. According to the data of our detailed sampling, one or two ore-bearing layers of oil shale, 0.5–2.6 m thick and with average concentrations of 3000 to 5100 g/t of vanadium and 200 to 340 g/t of

11

molybdenum, are distinguished in the lower member, with maximum contents of 6500 g/t of V and 660 g/t of Mo. Study of the composition of the ore-bearing shales showed that they have a high content of the clay fraction (more than 77.5 vol% minus authigenic minerals), a C_{org} content of 12.5 to 34.5, and a lack of correlation between the concentrations of C_{org} and V, Se, and, in part, Mo. This last is probably governed by the fact that in early diagenesis, chemically active organic matter can bind only part of the elements sorbed from sea water, the rest being sorbed by clay minerals.

By analogy with the Olenek Basin, it can be assumed that in many basins of black shale sedimentation, the ore potential of the entire volume of oil shales is controlled by just one or two horizons, which accumulated under conditions of slower and more prolonged deposition.

In the sapropelic shales of the Tulebak formation, the concentration coefficients of organophilic elements, calculated from the data of Glikson *et al.* (1985) and Riley and Saxby (1982), have the following values: Mo (29.5–150.0), Bi (100), Cd (83), Se (50), V (6.5–25.0), Zn (7.5–10.0), U (3.5), and Ni (1.1–4.0). In individual samples, relatively high contents of Ag, Sb, and As are observed.

In the Julia Creek deposit, with oil shale reserves of 4 billion tons (220 million tons of shale resins), the content of V is 1600–2700 g/t, Ni, 140–320 g/t, and Mo, up to 270 g/t. Deep-sea drilling data are very important for interpreting the origin of black shales and determining the sources of their enrichment in metals. In recent years, much work has appeared on the composition and metal potential of oceanic black shales. As an example, we can cite data from Brumsack (1980) and Brumsack and Lew (1982) on the distribution and concentration of rare and disseminated elements in the Cretaceous black shales of the Atlantic Ocean, which correspond to siliceous-carbonate domanikites with regard to their conditions of sedimentation and composition. Calculations have shown that, first, the usual level of bio-productivity of ocean waters is sufficient for high concentrations of C_{org} to arise in black shales if sedimentation is slow, and second, the order of enrichment of black shales in Pb, Co, Cr, Ni, Cu, V, Zn, Mo, and Ag relative to clays is, except for Ag, the order of increasing concentrations of elements in normal sea water, which is the main source of heavy metals. The presence of high concentrations of Cd, Tl, and Bi in black shales also is noteworthy.

The seventh metallogenic type (Table 5.2) includes siliceous-carbonate domanikites with relatively high and anomalous primary concentrations of Re, Mo, Se, Cd, Tl, Cd, and other chalcophilic rare and disseminated elements. The so-called copper schists (Kupferschiefer) of the Central European Zechstein basin and the Lower Eocene Suzak shales of the Scythian-Turanian platform (Syr Dar'ya and Upper Amu Dar'ya Basins) are of this type. The distinguishing feature of these facies is the fact that the shales occur in them mainly in the form of single thin layers (0.25–2.20 m thick in Western Europe and 0.05–2.0 m thick in Central Asia) that persist over areas tens or hundreds of thousands of km^2. Analysis of published data (Wedepohl, 1967; Kucha, 1985; Ivanov and Poplavko, 1982) on the Kupferschiefer shows that, aside from the Cu-Zn-Pb-Ag mineralization, they contain the following set of rare and disseminated elements, listed in order of decreasing C_c values: Re (100–37,500), Se (170–500), Mo (10–460), As (13–450), Cd (15–330), Au (up to 2–50), V (2.5–35.0), and Ni (1–10). In the basal layer of the black shales, there are exceptionally high concentrations of Au and platinum-group elements (Pt, Pd, Os, and Ir). In Kucha's (1985) opinion, the concentration of gold and platinoids was the result of self-oxidation and desulfatization of organic matter. The platinum-group elements, which acted as catalysts for the oxidation process, were concentrated at a redox barrier. The radioactivity of the shales, especially that related to thucholites, intensified the process.

There are differing points of view concerning the source of the nonferrous metals in the Kupferschiefer. Wedepohl (1967) proposes a terrigenous source for the Cu, Zn, and Pb. Lur'ye (1983)

12

145

00 g/t of V and
ley have a high
ontent of 12.5 to
rt, [illegible] This last
matter can bind

of black shale
ust one or two
ı.

of organophilic
982), have the
-10.0), U (3.5),
bserved.

ı tons of shale
ep-sea drilling
ources of their
netal potential
Brumsack and
he Cretaceous
es with regard
irst, the usual
arise in black
b, Co, Cr, Ni,
centrations of
ence of high

uni[illegible] with
d, and other
iiefer) of the
ian-Turanian
ng feature of
rs (0.25–2.20
ıreas tens or
; Ivanov and
ization, they
$_c$ values: Re
$^{\prime}$ (2.5–35.0),
ations of Au
ition of gold
ıe platinum-
l at a redox
process.

etals in the
ır'ye (1983)

---

relates the formation of the mineralization to discharge of ground water from the red molasse of the "dead red [lezhnya]" into the sedimentary basin and concentration of the copper and associated metals at the shale geochemical barrier.

In the Suzak shales of the basins of Central Asia, the following elements have the highest concentration coefficients (minimum and maximum C_c): Re (880–4470), Mo (730–1450), Se (810–1000), Cd (435–790), Bi (22–100), V (15–56), Tl (20–35), Ag (11–21), and Ni (6.5–20.0) (Kler, Volkova, Gurvich *et al.*, 1987; Poplavko, Ivanov *et al.*, 1977). In the face of considerable fluctuations in the element contents for the individual areas, the order of their concentration over the whole area of occurrence of the Suzak shales remains fairly constant. In individual sections, different relationships between the organic matter content and the elements (Mo, Se, V, As, and others) are found for different concentration levels of the elements. For instance, anomalously high Mo concentrations (from 500 to 2500 g/t) fall within a relatively narrow range of variation of organic matter content (from 40 to 60 vol%), which indicates the patterns of accumulation of metals in the ore-bearing horizons established for the shales of the Olenek basin. The Suzak shales were formed in a relatively deep sea basin during the initial phase of a transgression, when rapid subsidence was not compensated by sedimentation.

Compared to domanikites, oil shale facies are acutely impoverished both in their combination of rare and disseminated elements and in the concentration of the individual elements. In clayey-carbonate oil shales (Upper Jurassic shales of the Volga and Timan-Pechora Basins, Eocene Green River Formation), mainly the rare elements Mo or Mo plus Re are found in above-clarke concentrations (Table 5.2). In some oil shale formations, locally elevated concentrations of Se, As, Au, Ag, V, and other rare elements have been found, bound in both the organic and inorganic fractions.

In the Posidonia oil shales, developed over most of the European countries (Great Britain, France, West Germany, *etc.*), the average Mo concentration is 40–80 g/t, and the concentration coefficients of other rare and disseminated elements are low: V (0.5–3.0), Ni (0.4–2.7), Co (0.6–2.0), and Cu (0.2–1.6) (Bitterli, 1960; Kunz and Bauss, 1975; Tourtelot, 1970). In the Volga oil shales, according to the data of neutron activation analysis, the order of decreasing C_c values of the elements is as follows: Mo (11–34), Se (12–15), Au (4–7), Ag (46), As (0.2–2.4), V (0.6–2.1), Ni (0.4–1.5), Sc (0.6–1.5), Sb (0.2–1.5), Co (0.5–0.6), Ce (0.5–0.6), Cr (0.3–0.5), La (0.3–0.5), and Rb (0.2–0.5). According to Kler, Volkova, Gurvich *et al.* (1987), the shales contain from 0.5 to 2 g/t Re.

In the Green River shales, with unique reserves, a low concentration of rare and disseminated elements is observed despite the high organic matter content (up to 50 percent), except for individual intercalations containing U (0.005–0.15 percent) in association with phosphates (2.2–18.2 percent P_2O_5). The presence in some oil shale deposits, for example, the Wilkins Peak Member of the Green River Formation of Colorado, of relatively high contents of Mo (30–200 g/t), as well as of Se, As, and Au is related the heavy mineral fractions of the shales, which are enriched in pyrite (Meddaugh and Salotti, 1983; Saether, Runnells, and Meglen, 1984). The impoverishment of the Green River shales in rare and disseminated elements is governed by the conditions under which they were formed, that is, in a continental (lacustrine) sedimentary environment with high rates of accumulation of the oil shales (up to 50–100 m/Ma).

To a considerable extent, also in connection with the specifics of its generation and composition, the Middle Ordovician carbonate-kukersite facies of the Baltic area has extremely low concentrations

13

of rare and disseminated elements. As a result of our investigations, the trace elements in the shales are in the following order of concentration: Mo (0.9), Ce (0.6), U (0.5), Sb (0.5), Sc (0.5), As (0.3), Ni (0.25), V (0.2), Co (0.2), Th (0.2), Hf (0.2), and Rb (0.1). According to published data (Kler, Volkova, Gurvich *et al.*, 1987), Re (0.05 g/t) and Mo (up to 12 g/t) have also been reported.

In clayey oil shales (late Devonian-early Permian of the Kenderlyk Basin; Eocene of the Boltysh depression; Permo-Carboniferous torbanite and tasmanite of New South Wales and Tasmania; Oligocene shales of the Fu-Shun Coal Basin; and others), the combination of rare elements and their concentration levels is governed largely by the composition of the surrounding rocks, which are the source of the clastic material. But on the whole, the content of ore elements in this type of oil shale is at the clarke level, except for some formations enriched in Mo, Be, Sc, and other rare and disseminated elements.

The above data on the distribution of rare and disseminated elements in black shales of various composition make it possible to draw the following conclusions:

1. The accumulation of rare and disseminated elements in association with organic matter and their levels of concentration are governed by the setting in which Phanerozoic black shales were formed, mainly the depositional environment and sedimentation rate. The conclusion is confirmed that the concentration of organophilic elements arose during slow absorption of an accumulation of elements from organic matter in the layer of sea water above the bottom, rather than as a result of biological activity. On the whole, the tracing of the same type of metallogenic associations at different stratigraphic levels from Cambrian to Neogene indicates that the trace-element composition of sea water was fairly constant throughout the Phanerozoic. The highest rare and disseminated element concentrations are typical of domanikite formations, which were deposited in deep-sea basins in zones that were not compensated by accumulating sediments and, correspondingly, exhibit a reduced thickness of the shale-bearing members.
2. The horizons of ore-bearing shales with economic concentrations of Mo, V, U, Ag, Re, and other rare elements were formed only in stages of extremely slow sedimentation (probably less than 1 m/Ma), with prolonged exposure of the sediments on the basin floor. Here, not only complete bonding of rare elements by chemically active organic matter occurred, but also the accumulation of the excess elements in the inorganic part of the rock, in particular, in hydromicas, phosphates and similar components, to the actual production of mineral forms. Such conditions could have been created, in particular, at the time of the initial phase of a transgression, when rapid subsidence was not compensated by sedimentation.
3. In siliceous-clayey domanikites, a close relationship is observed between organic matter and clay minerals, which even in diagenesis form single organo-montmorillonite compounds, which sorb most metals. This determines the high average concentrations of Mo (up to 135–400 g/t), U (140–340 g/t), V (up to 1500–2000 g/t), Se (up to 300 g/t), and other rare and disseminated elements and their relatively even areal distribution, with strict stratification of the mineralization throughout the stratigraphic section.
4. Because of the low content of clay material in siliceous carbonate domanikites, most of the organic matter in the domanikites remains crystallochemically unbound to the rock, which makes it possible for ore material to be redistributed and form ore concentrations in the oil shale host rocks. Moreover, the distribution of rare and disseminated elements in these siliceous-carbonate domanikites is less uniform over the area of a basin than in siliceous-clayey domanikites, and

14

147

locally high concentrations of Mo (up to 800–2600 g/t), Re (up to 5–30 g/t), V (up to 4500–6200 g/t), Se (up to 200–400 g/t), and other elements may be formed at sorption barriers, which are chiefly clayey.

5. In siliceous domanikites, with a low content of organic matter partly bound in organosilica compounds, the sorption properties of the rocks are slight, which governs the relatively low concentration of metals.
6. Domanikite facies should be considered a potential source of gold and elements of the platinum group, the concentration of which can occur at the boundary between oxidizing and reducing environments (Kucha, 1985; Shalamov, Popova, and Savitskaya, 1991).
7. In oil shale facies, the concentration of rare and disseminated elements associated with organic matter is much higher than the clarke level. This is a result of the high rates of shale accumulation, the brief period of diagenesis, and the rapid separation of the sediment from the bottom water layer. In addition, many oil shales accumulated in continental basins, and therefore lacked sea water, the main source of rare and disseminated elements.

92-8-W4

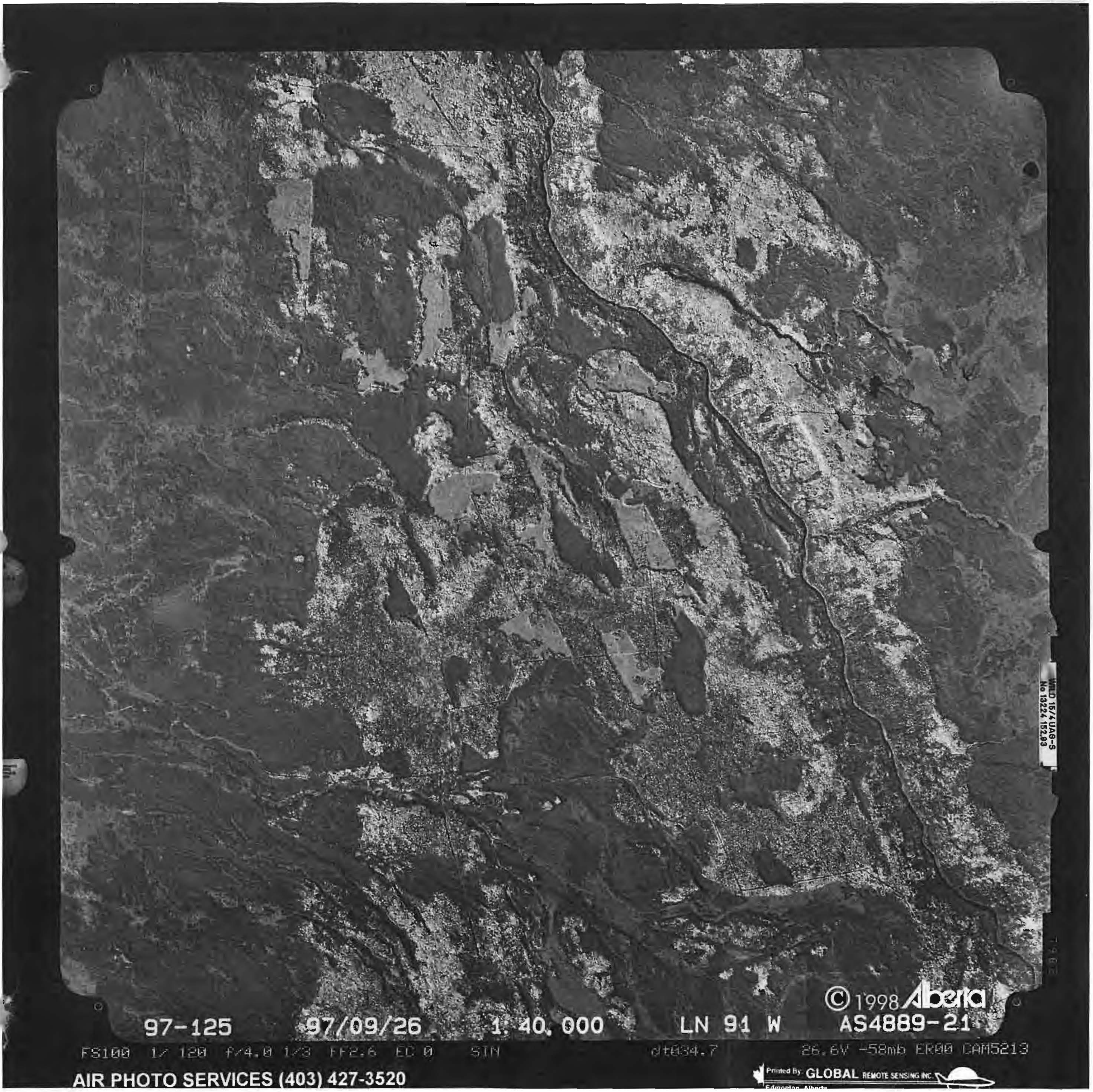

South

Map 1#

92-8-W4

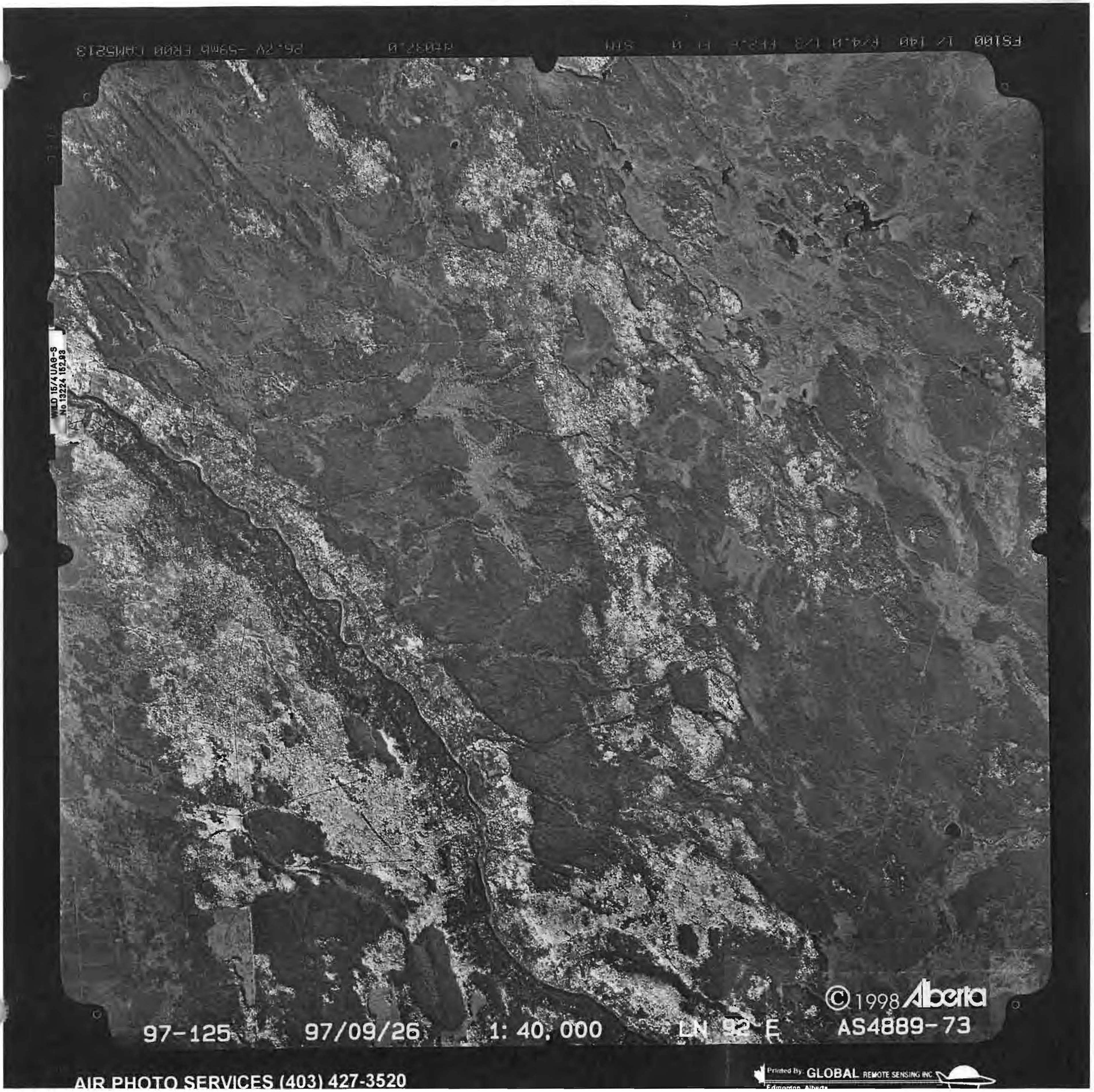

AIR PHOTO SERVICES (403) 427-3520

Printed By: GLOBAL REMOTE SENSING INC
Edmonton, Alberta

North

Map 2#

74 D/14 1:50,000

CANADA

EDITION 3 74 D/14

Military users, refer to this map as: Référence de cette carte pour usage militaire:	
SERIES A 741 SÉRIE	
MAP 74 D/14 CARTE	
EDITION 3 MCE ÉDITION	

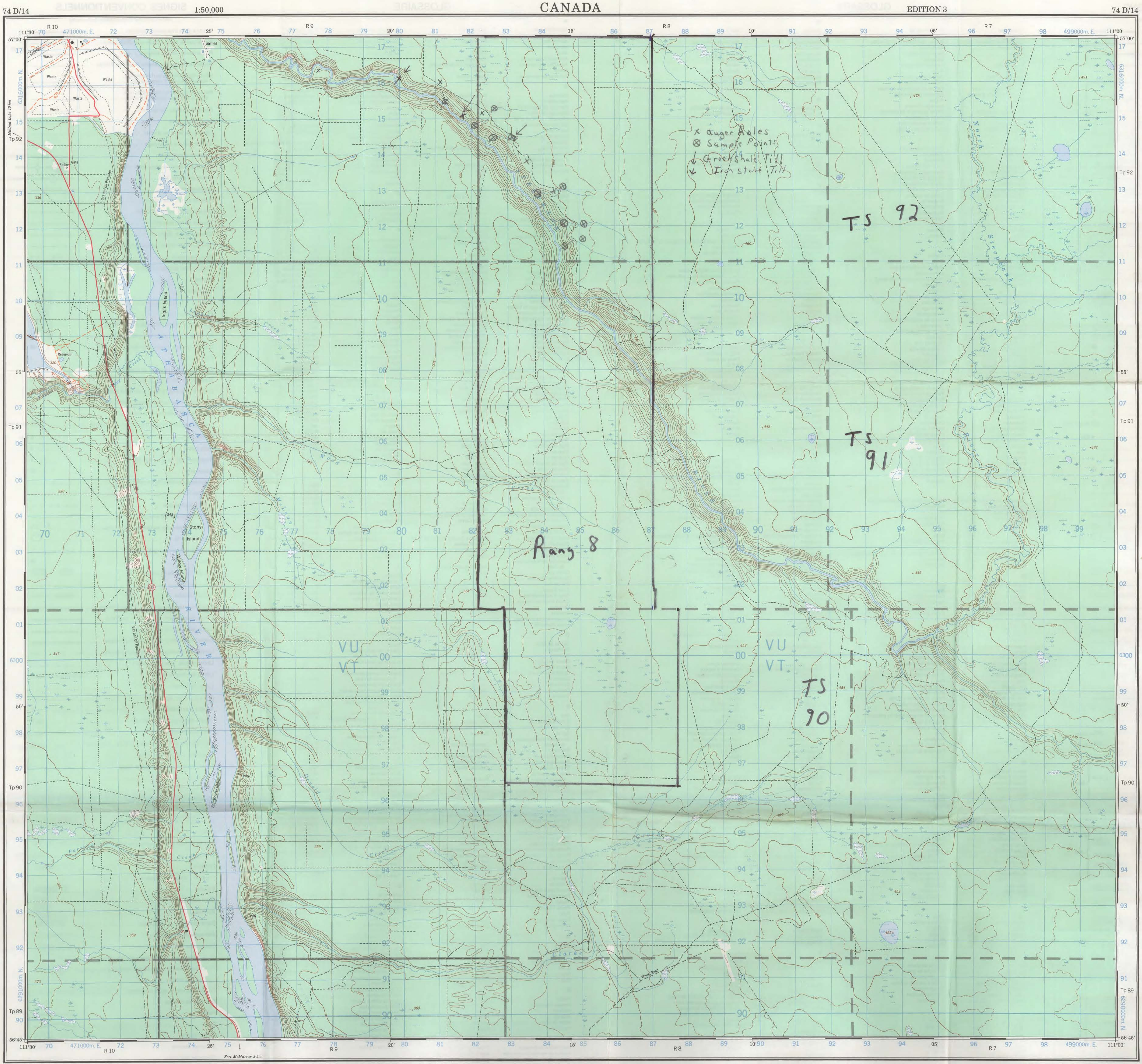

GLOSSARY GLOSSAIRE

Airfield	Terrain d'aviation
Arena	Aréna
City Limits	Limites de ville
Customs	Douane
Ditch	Fossé
Dugout	Abreuvoir
Dump	Dépotoir
Filtration Plant	Usine de filtration
Gas	Gaz
Golf Course	Terrain de golf
Junk Yard	Ferraille
Kiln	Four
Lookout	Belvédère
Mine Waste	Déblai de mine
Oil Wells	Puits de pétrole
Park	Parc
Rink	Patinoire
Senior Citizens Home	Foyer de l'âge d'or
Ski Area	Station de ski
String Bog	Fondrière à filaments
Surveyed Line	Ligne arpentée
Tank	Réservoir
Water	Eau
Winter Road	Chemin d'hiver

For a complete glossary see reverse side
Pour un glossaire complet, voir au verso

ABBREVIATIONS ABRÉVIATIONS

Aband	Abandoned	Abandonné, ée
C	Cemetery	Cimetière
CO	County	Comté
E	Elevator	Élévateur
Fy	Ferry	Traversier
IR	Indian Reserve	Réserve indienne
H	Hospital	Hôpital
L	Lot	Lot
Micro	Microwave	Micro-ondes
Mun	Municipality	Municipalité
P	Post Office	Bureau de poste
PH	Power House	Centrale électrique
RCMP	Royal Canadian Mounted Police	Gendarmerie Royale Canadienne
Res	Reservoir	Réservoir
Trans Sta	Transformer Station	Poste de transformateurs
TFL	Tree Farm Licence	Licence de sylviculture

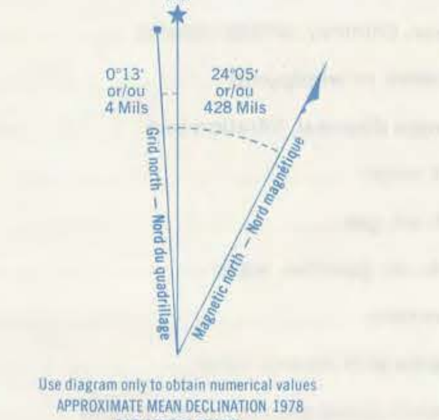

Use diagram only to obtain numerical values
APPROXIMATE MEAN DECLINATION 1978
FOR CENTRE OF MAP
Annual change decreasing 6.9′

N'utiliser le diagramme que pour obtenir les valeurs numériques
DÉCLINAISON MOYENNE APPROXIMATIVE
AU CENTRE DE LA CARTE EN 1978
Variation annuelle décroissante 6,9′

ONE THOUSAND METRE
UNIVERSAL TRANSVERSE MERCATOR GRID
ZONE 12
QUADRILLAGE DE MILLE MÈTRES
TRANSVERSE UNIVERSEL DE MERCATOR

GRID ZONE DESIGNATION: DÉSIGNATION DE LA ZONE DU QUADRILLAGE:	100,000 M. SQUARE IDENTIFICATION IDENTIFICATION DU CARRÉ DE 100,000 M.
12 V	VU VT 63 5

EXAMPLE OF METHOD USED
TO GIVE A REFERENCE TO NEAREST 100 METRES
EXEMPLE DE LA MÉTHODE EMPLOYÉE
POUR FIXER DES REPÈRES À 100 MÈTRES PRÈS

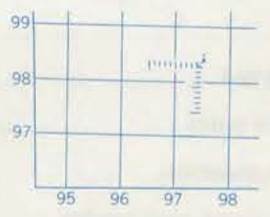

REFERENCE POINT / POINT DE REPÈRE — CHURCH - ÉGLISE (as above) (ci-dessus)

EASTING: Read number on grid line immediately to left of point:
LONGITUDE EST: Noter le chiffre de la ligne du quadrillage immédiatement à gauche du repère: 97
Estimate tenths of a square from this line eastward to point:
Estimer le nombre de dixièmes du carré entre cette ligne et le repère en direction est: 5
975

NORTHING: Read number on grid line immediately below point:
LATITUDE NORD: Noter le chiffre de la ligne du quadrillage immédiatement en-dessous du repère: 98
Estimate tenths of a square from this line northward to point:
Estimer le nombre de dixièmes du carré entre cette ligne et le repère en direction nord: 4
984

GRID REFERENCE: / RÉFÉRENCE AU QUADRILLAGE: 975984

Nearest similar grid reference 100,000 metres (about 63 miles)
La prochaine référence similaire est à 100,000 mètres (environ 63 milles)

Coordinate Conversion NAD 27 to NAD 83 (WGS 84)
Mean values for this map

Geographic:	Latitude -	add	0.4"
	Longitude -	add	3.3"
Grid:	Northing -	add	225m
	Easting -	subtract	55m

Conversion des coordonnées NAD 27 à NAD 83 (WGS 84)
Valeurs moyennes pour cette carte

Coordonnées géographiques :	Latitude -	additionner	0,4"
	Longitude -	additionner	3,3"
Quadrillage :	Ordonnée (N) -	additionner	225m
	Abscisse (E) -	soustraire	55m

TABLEAU D'ASSEMBLAGE DU SYSTÈME NATIONAL DE RÉFÉRENCE CARTOGRAPHIQUE

112°00′ 57°15′		110°30′ 57°15′
74 E/4	74 E/3	74 E/2
74 D/13	74 D/14	74 D/15
74 D/12	74 D/11	74 D/10
56°30′ 112°00′		56°30′ 110°30′

INDEX TO ADJOINING MAPS OF THE NATIONAL TOPOGRAPHIC SYSTEM

Produced by the SURVEYS AND MAPPING BRANCH, DEPARTMENT OF ENERGY, MINES AND RESOURCES, from information provided by the SURVEYS AND MAPPING BRANCH, ALBERTA TRANSPORTATION. Aerial photography 1974 and 1976. Culture check 1977. Information current as of 1976.

Copies may be obtained from the Canada Map Office, Department of Energy, Mines and Resources, Ottawa, or your nearest map dealer.

Roads:	Routes:		
hard surface, all weather	pavée, toute saisom	dual highway 2 chaussées séparées	more than 2 lanes plus de 2 voies
hard surface, all weather	pavée, toute saisom	2 lanes 2 voies	less than 2 lanes moins de 2 voies
loose or stabilized surface, all weather	gravier, aggloméré, toute saison	2 lanes or more 2 voies ou plus	less than 2 lanes moins de 2 voies
loose surface, dry weather	de gravier, temps sec		
unclassified streets	rues hors classe		
cart track	de terre		
trail, cut line or portage	sentier, percée ou portage		

FOR COMPLETE REFERENCE SEE REVERSE SIDE POUR UNE LISTE COMPLÈTE DES SIGNES, VOIR AU VERSO

WOOD CREEK

IMPROVEMENT DISTRICT 18

ALBERTA

WEST OF FOURTH MERIDIAN - OUEST DU QUATRIÈME MÉRIDIEN

Scale 1:50,000 Échelle

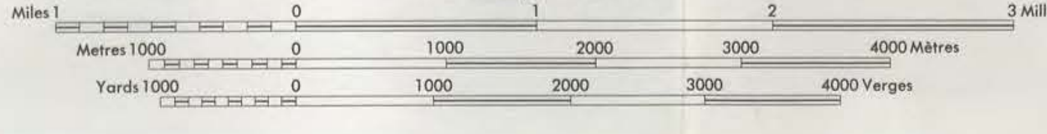

Information concerning location and precise elevation of bench marks can be obtained by writing to the Geodetic Survey, Surveys and Mapping Branch, Ottawa.

On peut obtenir des renseignements sur le lieu et l'altitude exacte des repères de nivellement en écrivant aux Levés géodésiques, Direction des levés et de la cartographie, Ottawa.

CONVERSION SCALE FOR ELEVATIONS ÉCHELLE DE CONVERSION DES ÉLÉVATIONS

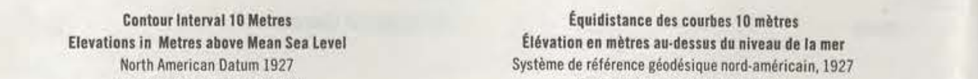

Contour Interval 10 Metres
Elevations in Metres above Mean Sea Level
North American Datum 1927
Transverse Mercator Projection

Équidistance des courbes 10 mètres
Élévation en mètres au-dessus du niveau de la mer
Système de référence géodésique nord-américain, 1927
Projection transverse de Mercator

Établie par la DIRECTION DES LEVÉS ET DE LA CARTOGRAPHIE, MINISTÈRE DE L'ÉNERGIE, DES MINES ET DES RESSOURCES, à partir des renseignements fournis par la DIRECTION DES LEVÉS ET DE LA CARTOGRAPHIE, TRANSPORT ALBERTA. Photographies aériennes prises en 1974 et 1976. Vérification des ouvrages en 1977. Renseignements à jour en 1976.

Ces cartes sont en vente au Bureau des Cartes du Canada, ministère de l'Énergie, des Mines et des Ressources, Ottawa, ou chez le vendeur le plus près.

WOOD CREEK
74 D/14
EDITION 3

STeep Bank River

149

CONVENTIONAL SIGNS

(Black unless otherwise stated)

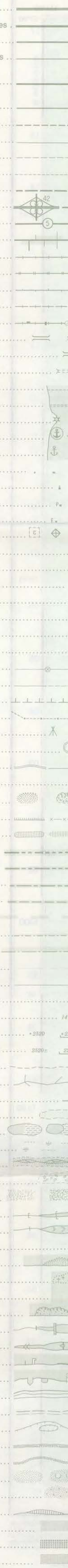

Dual highway	Red
Road, hard surface, all weather, more than 2 lanes	
Road, hard surface, all weather, 2 lanes	
Road, hard surface, all weather, less than 2 lanes	
Road, loose or stabilized surface, all weather, 2 lanes or more	Orange
Road, loose or stabilized surface, all weather, less than 2 lanes	
Road, loose surface, dry weather	
Unclassified streets	
Cart track or winter road	
Trail, cut line or portage	
Road under construction	Orange or red
Highway interchange with number; traffic circle	Red
Highway route marker	Orange or red
Built up area	Red screen
Railway, single track	
Railway, multiple track	
Railway, narrow gauge	
Railway, abandoned	
Railway station; stop; turntable	
Bridge; footbridge	
Bridge: swing, draw, lift	
Tunnel	
Ferry	
Ford	
Navigation light	
Seaplane base; seaplane anchorage	
Vessel anchorage: large, small	
House; barn; large building	
Church; school	
Post office; telegraph office	
Elevator; greenhouse	
Cemetery; historic site; historic battlefield	
Tower, chimney, similar objects	
Windmill or windpump	
Sewage disposal, filtration bed	Black & Blue
Well: water	Blue
Well: oil, gas	
Tank: oil, gasoline, water	
Gasometer	
Pipeline with control valve	
Pipeline: above ground, underground	
Telephone line	
Power transmission line	
Campsite; picnic site	
Sports track	
Retaining wall: large, small	
Mine	
Gravel or sand pit; quarry	
Dyke; fence	
Cutting; embankment	
International boundary with monument	Red screen
Province, territory, or state boundary	
County or district boundary	
Township, parish boundary	
Township boundary, unsurveyed	
City, town, settlement boundary	
Reserve, park boundary	
Section line	
Surveyed line, lot line	
Horizontal control point	
Bench mark with elevation	
Spot elevation: precise, non-precise	Brown
Water elevation: precise, non-precise	Brown
Stream or shoreline, indefinite	Blue
Irrigation canal, drain, ditch	
Direction of flow	
Lake intermittent, slough	
Flooded land; inundated land, seasonal	
Marsh or swamp	
Dry river bed with channels	Blue & Brown
String bog	Blue
Tundra ponds; tundra polygons	
Falls	
Rapids	
Reservoir, dugout, swimming pool	
Foreshore flats	
Submerged reef	
Rocks	
Rocky ledge, rocky reef	
Dams: small, large	
Locks: small, large	
Wharf, breakwater, pier, dock; seawall	
Ferry slip; dry dock; ramp	
Contours	Brown
Approximate contours	
Depression contours	
Cliff	
Esker	
Sand; sand dunes	
Moraine, scree	
Glacial crevasse	Blue
Wooded area	Green
Orchard	
Vineyard, hop field	

144 Stony Bush River

GLOSSARY

A

Abandoned	Abandonné, ée
Aerial Cableway	Téléphérique
Agricultural Research Station	Station de recherches agricoles
Air Beacon	Aérophare
Airfield	Terrain d'aviation
Airport	Aéroport
Airport Limits	Limites d'aéroport
Alkali	Alcali
Amusement Park	Parc d'attractions
Animal Farm	Ferme d'animaux
Animal Research Farm	Ferme de recherche animale
Aqueduct (underground)	Aqueduc (souterrain)
Arena	Aréna
Armoury	Manège militaire
Ash Disposal Lagoon	Dépôt lagunaire de cendres
Asphalt Plant	Usine d'asphalte
Auto Depot	Cour d'automobiles
Automobile Plant	Usine d'automobiles

B

Ball Park	Terrain de baseball
Ballast Pit	Ballastière
Barrier	Barrière
Bible Camp	Colonie biblique
Bird Sanctuary	Sanctuaire d'oiseaux
Boat House	Hangar à bateaux
Boom Piers	Jetées d'estacade
Boys Camp	Colonie de vacances pour garçons
Boy Scout Camp	Camp de scouts
Brewery	Brasserie
Brick Factory	Briqueterie
Brick Plant	Briqueterie
Brick Yard	Dépôt de briques
Bunker	Soute
Burner	Brûleur
Butts	Buttes

C

Cabin	Cabine
Cable Car Crossing	Croisement de tramways
Cable House	Station de téléphérique
Cannery	Conserverie
Cattle Feeder Station	Poste d'alimentation du bétail
Causeway	Chaussée
Cave	Caverne
Cement Plant	Usine de ciment
Cemetery	Cimetière
Chair Lift	Télésiège
Cheese Factory	Fromagerie
Chemical Plant	Usine de produits chimiques
Chimney	Cheminée
Church Camp	Colonie d'appartenance religieuse
Cinema	Cinéma
City Hall	Hôtel de ville
City Limits	Limites de ville
Clay Pit	Glaisière
Coke Plant	Usine de coke
Community Centre	Centre communautaire
Community Hall	Salle communautaire
Compressor Station	Station de compression
Concrete Plant	Usine de béton
Conservation Area	Zone de conservation
Conservation Park	Parc de conservation
Control Dam	Barrage de régulation
Control Gate	Barrière de contrôle
Control Tower	Tour de contrôle
Convent	Couvent
Conveyor	Convoyeur
Correctional Institute	Institut de réhabilitation
Court House	Palais de justice
Covered Bridge	Pont couvert
Crane	Grue
Crib	Caisson
Cricket Club	Club de cricket
Crippled Childrens Camp	Colonie d'enfants handicapés
Crushing Plant	Installation de broyage
Curling Club	Club de curling
Customs	Douane

D

Department of National Defence	Ministère de la Défense Nationale
Detention Home	Maison de détention
Disposal Area	Décharge
Disposal Bed	Lit d'épuration
Distillery	Distillerie
Ditch	Fossé
DND	MDN
Dolphin(s)	Pieu(x) d'amarrage
Drawbridge	Pont roulant
Driver Training Centre	Centre de formation des automobilistes
Dugout	Abreuvoir
Dump	Dépotoir

E

Electronics Plant	Usine de matériel électronique
Elevator	Élévateur
Equestrian Centre	Centre équestre
Exhibition Grounds	Terrain d'exposition
Experimental Farm	Ferme expérimentale
Exposed Wreck	Épave visible

F

Factory	Fabrique
Fairgrounds	Champ de foire
Feed Mill	Moulin à grain de provende
Ferry	Traversier
Fertilizer Plant	Usine d'engrais
Fiberglass Plant	Usine de fibre de verre
Filtration Bed	Lit de filtration
Filtration Plant	Usine de filtration
Fire	Feu
Fire Guard	Coupe-feu
Firing Range	Zone de tir
First Aid Post	Poste de premiers soins
Fish Hatchery	Centre de pisciculture
Fish Ladder	Échelle à poissons
Fish Packing Plant	Usine de mise en baril du poisson
Flour Mill	Moulin à farine
Flume	Canal d'amenée
Ford	Gué
Foundry	Fonderie
Fur Farm	Animaux à fourrures
Furniture Factory	Fabrique de meubles

G

Game Bird Farm	Élevage d'oiseaux pour la chasse
Game Preserve	Parc à gibier
Game Reserve	Réserve de gibier
Garment Factory	Fabrique de vêtements
Gas	Gaz
Gas Field Limits	Limites de champ de gaz
Gas Pipeline	Gazoduc
Gas Plant	Usine de gaz
Gas Pumping Station	Station de pompage de gaz
Gas Wells	Puits de gaz
Gate	Barrière
Gauging Station	Station d'enrégistrement du niveau de l'eau
Girl Guide Camp	Camp de guides
Girls Camp	Colonie de vacances pour jeunes filles
Glass Factory	Verrerie
Glider Club	Club de planeur
Go-cart Track	Piste de karting
Golf Course	Terrain de golf
Golf Range	Pratique de golf
Granite Plant	Usine de granit
Grist Mill	Meunerie
Gun Club	Club de tir
Gypsum Plant	Usine de gypse

H

Hall	Salle
Health Camp	Colonie de plein air
Heliport	Héliport
Hopper	Trémie
Hops	Houblon
Hospital	Hôpital

I

Icefield	Champ de glace
Ice Shelf	Corniche de glace
Illuminated Cross	Croix illuminée
Indian Summer Camp	Camp d'été des indiens
Indian Village	Village indien
Industrial Centre	Centre industriel
Iron Works	Ferronnerie

J

Jail	Prison
Junk Yard	Ferraille

K

Kelp	Varech
Kiln	Four
Knitting Mill	Filature

L

Lift	Levant
Log Chute	Glissoire de billots
Lookout	Belvédère
Lumber Camp	Camp de bûcherons
Lumber Depot	Dépôt de bois
Lumber Mill	Scierie
Lumber Yard	Cour à bois

M

Marine	Marin
Medical Centre	Centre médical
Meter Station	Station de comptage
Metis Colony	Colonie de métis
Microwave	Micro-ondes
Mile Post	Borne milliaire
Mine Dump	Halde
Mine Waste	Déblai de mine
Monastery	Monastère
Municipal Hall	Salle municipale
Museum	Musée

N

Nature Camp	Camp de naturalistes
Nursing Home	Maison de repos

O

Observatory	Observatoire
Oil	Pétrole
Oil Pipeline	Oléoduc
Oil Refinery	Raffinerie de pétrole
Oil Wells	Puits de pétrole
Open Pit	Fosse à ciel ouvert
Oratory	Oratoire
Orphanage	Orphelinat

P

Packing Plant	Usine d'empaquetage
Paint Works	Fabrique de peinture
Palsa Bog	Fondrière de palse
Paper Mill	Papeterie
Park	Parc
Parliament Buildings	Édifices du Parlement
Peat Bog	Tourbage
Peat Cutting	Tourbière
Peat Plant	Établissement de transformation de la tourbe
Penitentiary	Pénitencier
Penstock	Conduite forcée
Pile	Pieu
Plant	Usine
Plastic Factory	Manufacture de plastiques
Pollution Sensing Tower	Tour de détection de la pollution
Position Approximate	Position approximative
Poultry Farm	Ferme avicole
Power House	Centrale électrique
Private	Privé, ée
Private Road	Route privée
Proposed	Projeté, ée
Pulp Mill	Usine de pâte à papier
Pumphouse	Usine de pompage
Pumping Station	Station de pompage

R

Radio Telescope	Télescope radioguidé
Raised Beaches	Plages surélevées
Ranger Station	Poste de garde
R C M P	G R C
Recreation Centre	Centre récréatif
Refinery	Raffinerie
Rehabilitation Centre	Centre de réadaptation
Religious Camp	Colonie religieuse
Religious Colony	Colonie religieuse
Research Station	Station de recherches
Reservoir	Réservoir
Residue Pond	Étang de résidu
Rifle Range	Champ de tir
Rink	Patinoire
Roundhouse	Rotonde
Ruins	Ruines

S

Salt	Sel
Salt Domes	Remises de sel
Sand Domes	Remises de sable
Sand Hills	Collines de sable
Satellite Tracking Station	Station de détection de satellites
Sawmill	Scierie
Seed Processing Plant	Usine de traitement de la semence
Seminary	Séminaire
Senior Citizens Home	Foyer de l'âge d'or
Service Centre	Centre de service
Settling Pond	Étang de sédimentation
Settling Tank	Réservoir de sédimentation
Sewage	Égout
Sewage Pipeline	Tuyau d'égout
Sewage Pumping Station	Station de pompage des eaux d'égout
Shipyard	Chantier naval
Shopping Centre	Centre commercial
Shrine	Chapelle
Sink Hole	Puits d'écoulement
Skeet Club	Club de tir aux pigeons
Skeet Range	Champ de tir aux pigeons
Ski Area	Station de ski
Ski Club	Club de ski
Ski Jump	Saut de ski
Ski Lift	Téléski
Ski Lodge	Chalet de ski
Ski Tow	Télésiège
Slag Heap	Crassier
Sluice	Canal de décharge
Sluice Gate	Vanne
Snowshed	Paraneige
Space Research Institute	Institut de recherche spaciale
Spillway	Déversoir
Sportsplex	Centre sportif
Spring	Source
Stadium	Stade
Stand Pipe	Château d'eau
Steam Power House	Centrale à vapeur
Steel Mill	Usine sidérurgique
Stockpile	Réserves
Stockyards	Parc à bestiaux
String Bog	Fondrière à filaments
Strip Mine	Mine à ciel ouvert
Sub Station	Sous-station
Submarine Cable	Câble sous-marin
Sugar Camp	Sucrerie
Summer Camp	Camp d'été
Sunken Wreck	Épave submergée
Surge Pipe	Tuyau de déversement
Surge Tank	Réservoir d'équilibre
Surveyed Line	Ligne arpentée
Suspension	Suspendu
Swing	Pivotant

T

Tailrace	Canal d'aval
Tanks	Réservoirs
Telecommunication	Télécommunication
Television	Télévision
Textile Mill	Usine de textile
Tile Factory	Fabrique de tuiles
Tobacco Plant	Manufacture de tabac
Toll	Péage
Town Hall	Hôtel de ville
Town Limits	Limites de ville
Township Hall	Bureau administratif de township
Trading Post	Poste de traite
Trailer Factory	Usine de roulottes
Trailer Park	Parc de roulottes
Transformer Station	Poste de transformateurs
Tree Nursery	Pépinière
Trout Farm	Centre d'élevage de truites

U

Under Construction	En construction
Underground Reservoir	Réservoir souterrain
Underground Stream	Cours d'eau souterrain
University	Université
University Grounds	Terrains de l'université

V

Valve Station	Poste de valve
Vehicle Testing Track	Piste d'essai de véhicules
Village Limits	Limites de village

W

Wall	Mur
Warden's Station	Station du gardien
Waste	Déchets
Water	Eau
Watermill	Moulin à eau
Water Pipeline	Conduite d'eau
Water Pollution Control	Contrôle de la pollution de l'eau
Water Pumping Station	Station de pompage des eaux
Water Purification Plant	Usine de filtration des eaux
Water Treatment Plant	Usine d'épuration des eaux
Weigh Scale	Balance
Weir	Barrage-déversoir
Wildlife Park	Parc de la faune
Wildlife Sanctuary	Sanctuaire de la faune
Windmill	Moulin à vent
Windpump	Pompe éolienne
Winery	Producteur de vin
Winter Road	Chemin d'hiver

Y

Yacht Club	Club de yacht
Y M C A Camp	Camp Y M C A
Youth Hostel	Auberge de jeunesse

Z

Zoological Gardens	Jardins zoologiques

GLOSSAIRE

A

Abandonné, ée	Abandoned
Abreuvoir	Dugout
Aérophare	Air Beacon
Aéroport	Airport
Alcali	Alkali
Animaux à fourrures	Fur Farm
Aqueduc (souterrain)	Aqueduct (underground)
Aréna	Arena
Auberge de jeunesse	Youth Hostel

B

Balance	Weigh Scale
Ballastière	Ballast Pit
Barrage de régulation	Control Dam
Barrage-déversoir	Weir
Barrière	Barrier, Gate
Barrière de contrôle	Control Gate
Belvédère	Lookout
Borne milliaire	Mile Post
Brasserie	Brewery
Briqueterie	Brick Factory, Brick Plant
Brûleur	Burner
Bureau administratif de township	Township Hall
Buttes	Butts

C

Cabine	Cabin
Câble sous-marin	Submarine Cable
Caisson	Crib
Camp de bûcherons	Lumber Camp
Camp de guides	Girl Guide Camp
Camp de naturalistes	Nature Camp
Camp de scouts	Boy Scout Camp
Camp d'été	Summer Camp
Camp d'été des indiens	Indian Summer Camp
Camp Y M C A	Y M C A Camp
Canal d'amenée	Flume
Canal d'aval	Tailrace
Canal de décharge	Sluice
Caverne	Cave
Centrale à vapeur	Steam Power House
Centrale électrique	Power House
Centre commercial	Shopping Centre
Centre communautaire	Community Centre
Centre de formation des automobilistes	Driver Training Centre
Centre d'élevage de truites	Trout Farm
Centre de pisciculture	Fish Hatchery
Centre de réadaptation	Rehabilitation Centre
Centre de service	Service Centre
Centre équestre	Equestrian Centre
Centre industriel	Industrial Centre
Centre médical	Medical Centre
Centre récréatif	Recreation Centre
Centre sportif	Sportsplex
Chalet de ski	Ski Lodge
Chapelle	Shrine
Champ de foire	Fairgrounds
Champ de glace	Icefield
Champ de tir	Rifle Range
Champ de tir aux pigeons	Skeet Range
Chantier Naval	Shipyard
Château d'eau	Stand Pipe
Chaussée	Causeway
Chemin d'hiver	Winter Road
Cheminée	Chimney
Cimetière	Cemetery
Cinéma	Cinema
Club de cricket	Cricket Club
Club de curling	Curling Club
Club de planeur	Glider Club
Club de ski	Ski Club
Club de tir	Gun Club
Club de tir aux pigeons	Skeet Club
Club de yacht	Yacht Club
Collines de sable	Sand Hills
Colonie biblique	Bible Camp
Colonie d'appartenance religieuse	Church Camp
Colonie de vacances pour jeunes filles	Girls Camp
Colonie de métis	Metis Colony
Colonie d'enfants handicapés	Crippled Childrens Camp
Colonie de plein air	Health Camp
Colonie de vacances pour garçons	Boys Camp
Colonie religieuse	Religious Colony, Religious Camp
Conduite d'eau	Water Pipeline
Conduite forcée	Penstock
Conserverie	Cannery
Contrôle de la pollution de l'eau	Water Pollution Control
Convoyeur	Conveyor
Corniche de glace	Ice Shelf
Coupe-feu	Fire Guard
Cour à bois	Lumber Yard
Cour d'automobiles	Auto Depot
Cours d'eau souterrain	Underground Stream
Couvent	Convent
Crassier	Slag Heap
Croisement de tramways	Cable Car Crossing
Croix illuminée	Illuminated Cross

D

Déblai de mine	Mine Waste
Décharge	Disposal Area
Déchets	Waste
Dépôt de bois	Lumber Depot
Dépôt de briques	Brick Yard
Dépôt lagunaire de cendres	Ash Disposal Lagoon
Dépotoir	Dump
Déversoir	Spillway
Distillerie	Distillery
Douane	Customs

E

Eau	Water
Échelle à poissons	Fish Ladder
Édifices du Parlement	Parliament Buildings
Égout	Sewage
Élevage d'oiseaux pour la chasse	Game Bird Farm
Élévateur	Elevator
En construction	Under construction
Épave submergée	Sunken Wreck
Épave visible	Exposed Wreck
Établissement de transformation de la tourbe	Peat Plant
Étang de résidu	Residue Pond
Étang de sédimentation	Settling Pond

F

Fabrique	Factory
Fabrique de meubles	Furniture Factory
Fabrique de peinture	Paint Works
Fabrique de tuiles	Tile Factory
Fabrique de vêtements	Garment Factory
Ferme avicole	Poultry Farm
Ferme d'animaux	Animal Farm
Ferme de recherche animale	Animal Research Farm
Ferme expérimentale	Experimental Farm
Ferraille	Junk Yard
Ferronnerie	Iron Works
Feu	Fire
Filature	Knitting Mill
Fonderie	Foundry
Fondrière à filaments	String Bog
Fondrière de palse	Palsa Bog
Fossé	Ditch
Fosse à ciel ouvert	Open Pit
Four	Kiln
Foyer de l'âge d'or	Senior Citizens Home
Fromagerie	Cheese Factory

G

Gaz	Gas
Gazoduc	Gas Pipeline
Glaisière	Clay Pit
Glissoire de billots	Log Chute
G R C	R C M P
Grue	Crane
Gué	Ford

H

Halde	Mine Dump
Hangar à bateaux	Boat House
Héliport	Heliport
Hôpital	Hospital
Hôtel de ville	City Hall, Town Hall
Houblon	Hops

I

Installation de broyage	Crushing Plant
Institut de recherche spaciale	Space Research Institute
Institut de réhabilitation	Correctional Institute

J

Jardins zoologiques	Zoological Gardens
Jetées d'estacade	Boom Piers

L

Levant	Lift
Ligne arpentée	Surveyed Line
Limites d'aéroport	Airport Limits
Limites de champ de gaz	Gas Field Limits
Limites de village	Village Limits
Limites de ville	City Limits, Town Limits
Lit de filtration	Filtration Bed
Lit d'épuration	Disposal Bed

M

Maison de détention	Detention Home
Maison de repos	Nursing Home
Manège militaire	Armoury
Manufacture de plastiques	Plastic Factory
Manufacture de tabac	Tobacco Plant
Marin	Marine
MDN	DND
Meunerie	Grist Mill
Micro-ondes	Microwave
Mine à ciel ouvert	Strip Mine
Ministère de la Défense Nationale	Department of National Defence
Monastère	Monastery
Moulin à eau	Watermill
Moulin à farine	Flour Mill
Moulin à grain de provende	Feed Mill
Moulin à vent	Windmill
Mur	Wall
Musée	Museum

O

Observatoire	Observatory
Oléoduc	Oil Pipeline
Oratoire	Oratory
Orphelinat	Orphanage

P

Palais de justice	Court House
Papeterie	Paper Mill
Paraneige	Snowshed
Parc	Park
Parc à bestiaux	Stockyards
Parc à gibier	Game Preserve
Parc d'attractions	Amusement Park
Parc de conservation	Conservation Park
Parc de la faune	Wildlife Park
Parc de roulottes	Trailer Park
Patinoire	Rink
Péage	Toll
Pénitencier	Penitentiary
Pépinière	Tree Nursery
Pétrole	Oil
Pieu	Pile
Pieu (x) d'amarrage	Dolphin (s)
Piste de karting	Go-cart Track
Piste d'essai de véhicules	Vehicle Testing Track
Pivotant	Swing
Plages surélevées	Raised Beaches
Pompe éolienne	Windpump
Pont couvert	Covered Bridge
Pont roulant	Drawbridge
Position approximative	Position Approximate
Poste d'alimentation du bétail	Cattle Feeder Station
Poste de garde	Ranger Station
Poste de premiers soins	First Aid Post
Poste de traite	Trading Post
Poste de transformateurs	Transformer Station
Poste de valve	Valve Station
Pratique de golf	Golf Range
Prison	Jail
Privé, ée	Private
Producteur de vin	Winery
Projeté, ée	Proposed
Puits d'écoulement	Sink Hole
Puits de gaz	Gas Wells
Puits de pétrole	Oil Wells

R

Raffinerie	Refinery
Raffinerie de pétrole	Oil Refinery
Remises de sable	Sand Domes
Remises de sel	Salt Domes
Réserve de gibier	Game Reserve
Réserves	Stockpile
Réservoirs	Reservoirs, Tanks
Réservoir d'équilibre	Surge Tank
Réservoir de sédimentation	Settling Tank
Réservoir souterrain	Underground Reservoir
Rotonde	Roundhouse
Route privée	Private Road
Ruines	Ruins

S

Salle	Hall
Salle communautaire	Community Hall
Salle municipale	Municipal Hall
Sanctuaire de la faune	Wildlife Sanctuary
Sanctuaire d'oiseaux	Bird Sanctuary
Saut de ski	Ski Jump
Scierie	Lumber Mill, Sawmill
Sel	Salt
Séminaire	Seminary
Source	Spring
Sous-station	Sub Station
Soute	Bunker
Stade	Stadium
Station de compression	Compressor Station
Station de comptage	Meter Station
Station de détection de satellites	Satellite Tracking Station
Station d'enrégistrement du niveau de l'eau	Gauging Station
Station de pompage	Pumping Station
Station de pompage de gaz	Gas Pumping Station
Station de pompage des eaux	Water Pumping Station
Station de pompage des eaux d'égout	Sewage Pumping Station
Station de recherches	Research Station
Station de recherches agricoles	Agricultural Research Station
Station de ski	Ski Area
Station du gardien	Warden's Station
Station de téléphérique	Cable House
Sucrerie	Sugar Camp
Suspendu	Suspension

T

Télécommunication	Telecommunication
Téléphérique	Aerial Cableway
Télescope radioguidé	Radio Telescope
Télésiège	Chair Lift, Ski Tow
Téléski	Ski Lift
Télévision	Television
Terrain d'aviation	Airfield
Terrain de baseball	Ball Park
Terrain de golf	Golf Course
Terrains de l'université	University Grounds
Terrain d'exposition	Exhibition Grounds
Tourbage	Peat Bog
Tourbière	Peat Cutting
Tour de contrôle	Control Tower
Tour de détection de la pollution	Pollution Sensing Tower
Traversier	Ferry
Trémie	Hopper
Tuyau de déversement	Surge Pipe
Tuyau d'égout	Sewage Pipeline

U

Université	University
Usine	Plant
Usine d'asphalte	Asphalt Plant
Usine d'automobiles	Automobile Plant
Usine de béton	Concrete Plant
Usine de ciment	Cement Plant
Usine de coke	Coke Plant
Usine de fibre de verre	Fiberglass Plant
Usine de filtration	Filtration Plant
Usine de filtration des eaux	Water Purification Plant
Usine de gaz	Gas Plant
Usine de granit	Granite Plant
Usine de gypse	Gypsum Plant
Usine de matériel électronique	Electronics Plant
Usine de mise en baril du poisson	Fish Packing Plant
Usine d'empaquetage	Packing Plant
Usine d'engrais	Fertilizer Plant
Usine de pâte à papier	Pulp Mill
Usine de pompage	Pumphouse
Usine de produits chimiques	Chemical Plant
Usine d'épuration des eaux	Water Treatment Plant
Usine de roulottes	Trailer Factory
Usine de textile	Textile Mill
Usine de traitement de la semence	Seed Processing Plant
Usine sidérurgique	Steel Mill

V

Vanne	Sluice Gate
Varech	Kelp
Verrerie	Glass Factory
Village indien	Indian Village

Z

Zone de conservation	Conservation Area
Zone de tir	Firing Range

SIGNES CONVENTIONNELS

(Noir à moins d'indication contraire)

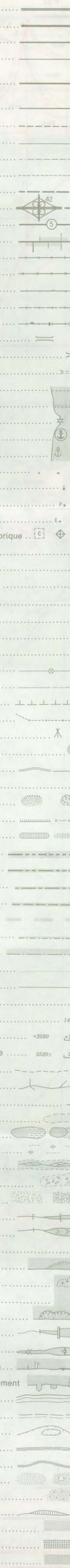

Route à deux chaussées séparées	Rouge
Route pavée, toutes saisons, plus de 2 voies	
Route pavée, toutes saisons, 2 voies	
Route pavée, toutes saisons, moins de 2 voies	
Route de gravier ou surface durcie, toutes saisons, 2 voies ou plus	Orange
Route de gravier ou surface durcie, toutes saisons, moins de 2 voies	
Route de gravier, temps sec	
Rues hors classe	
Chemin de terre ou d'hiver	
Sentier, percée ou portage	
Route en construction	Orange ou rouge
Échangeur avec numéro; rond-point	Rouge
Signalisation routière	Orange ou rouge
Agglomération	Trame rouge
Chemin de fer, voie unique	
Chemin de fer, voies multiples	
Chemin de fer, voie étroite	
Chemin de fer abandonné	
Gare; arrêt sur signal; plaque tournante	
Pont; passerelle	
Pont mobile: pivotant, roulant, levant	
Tunnel	
Traversier	
Gué	
Feu de navigation	
Base d'hydravions; ancrage d'hydravions	
Ancrage pour gros navires; petits navires	
Maison; grange; grand bâtiment	
Église; école	
Bureau de poste; bureau de télégraphe	
Élévateur; serre	
Cimetière; lieu historique; champ de bataille historique	
Tour, cheminée, constructions semblables	
Moulin à vent, pompe éolienne	
Lit d'épuration des eaux d'égout, lit de filtration	Noir & Bleu
Puits d'eau	Bleu
Puits: pétrole, gaz	
Réservoir: pétrole, essence, eau	
Gazomètre	
Pipeline avec valve de contrôle	
Pipeline sur terre; sous terre	
Ligne téléphonique	
Ligne de transport d'énergie	
Terrain de camping; terrain de pique-nique	
Piste de sports	
Mur de soutènement: grand, petit	
Mine	
Gravière ou sablière; carrière	
Digue; clôture	
Déblai; remblai	
Frontière internationale avec bornes-repères	Trame rouge
Limite de province, de territoire, ou d'état	
Limite de comté ou de district	
Limite de township ou canton, de paroisse	
Limite de township ou canton non arpentée	
Limite de cité, ville, établissement	
Limite de réserve, de parc	
Ligne de section	
Ligne arpentée, ligne de lot	
Repère planimétrique	
Repère de nivellement avec cote	
Point coté: précis, imprécis	Brun
Altitude de la surface de l'eau: précise, imprécise	Brun
Cours d'eau ou rive; imprécis	Bleu
Canal d'irrigation, de décharge, fossé	
Direction du courant	
Lac intermittent, bourbier	
Terrain inondé, inondé en saison	
Marais ou marécage	
Lit de cours d'eau tari avec chenaux	Bleu & Brun
Fondrière à filaments	Bleu
Étangs de toundra; polygones de toundra	
Chutes	
Rapides	
Réservoir, abreuvoir, piscine	
Estrans	
Récif submergé	
Roches	
Barre rocheuse, récif rocheux	
Barrages: petits, grands	
Écluses: petites, grandes	
Quai, brise-lame, jetée, bassin; mur de protection	
Cale pour traversier; cale sèche; rampe de chargement	
Courbes de niveau	Brun
Courbes de niveau approximatives	
Courbes de cuvette	
Falaise	
Esker	
Sable; dunes	
Moraine, éboulis	
Crevasse glaciaire	Bleu
Région boisée	Vert
Verger	
Vignoble, houblonnière	